AMERICAN UNIVERSITY OF BEIRUT

THE EFFECT OF DRAINAGE CONDITIONS ON THE LOAD RESPONSE OF SOFT CLAYS REINFORCED WITH GRANULAR COLUMNS

by
HANI ELIAS BOU LATTOUF

A thesis
submitted in partial fulfillment of the requirements
for the degree of Master of Engineering
to the Department of Civil and Environmental Engineering
of the Faculty of Engineering and Architecture
at the American University of Beirut

Beirut, Lebanon
May 2013

AMERICAN UNIVERSITY OF BEIRUT

THE EFFECT OF DRAINAGE CONDITIONS ON THE LOAD RESPONSE OF SOFT CLAYS REINFORCED WITH GRANULAR COLUMNS

by

HANI ELIAS BOU LATTOUF

Approved by:

Dr. Shadi Najjar, Assistant Professor — Advisor
Civil and Environmental Engineering

Dr. Salah Sadek, ~~Professor~~ — Co-Advisor
Civil and Environmental Engineering

Dr. Issam Srour, Assistant Professor — Member of Committee
Engineering Management

Date of thesis defense: May 17, 2013

AMERICAN UNIVERSITY OF BEIRUT

THESIS RELEASE FORM

I, Hani Elias Bou Lattouf

☐ authorize the American University of Beirut to supply copies of my thesis to libraries or individuals upon request.

☐ do not authorize the American University of Beirut to supply copies of my thesis to libraries or individuals for a period of two years starting with the date of the thesis/dissertation/project deposit.

_____
Signature

_____
Date

ACKNOWLEDGMENTS

First and foremost, my recognition and gratitude are addressed to my advisors Dr. Shadi Najjar and Dr. Salah Sadek for their relentless and vital support. I thank them for sharing their theoretical and technical expertise which helped and enriched my research and master studies.

The success of this research study was greatly influenced by Mr. Helmi Al Khatib who was always keen to provide his critical input when problems arise. I express my deep gratitude and thankfulness to him.

Special thanks are directed to Mrs. Zakia Deeb for her administrative assistance.

Finally, deep thanks are dedicated to my parents and close friends for their indispensable support and encouragement.

AN ABSTRACT OF THE THESIS OF

Hani Elias Bou Lattouf for Master of Engineering
Major: Civil Engineering

Title: The effect of drainage conditions on the load response of soft clays reinforced with granular columns

Various techniques have been used to improve weak and soft clays. A common method of ground improvement consists of the construction of columnar inclusions in the clay matrix. These columns are normally used to accelerate the rate of consolidation, increase the bearing capacity, and reduce settlements. Numerous experimental laboratory-scale studies have investigated the main characteristics of the soil/column interaction and response. Recently, experimental studies have shifted towards reliance on triaxial testing, where the drainage conditions and loading rates could be controlled. Almost all of the published studies involving triaxial testing of such systems are based on fully drained or fully undrained tests conducted on samples reinforced at area replacement ratios in the range of 5 to 20%. In the field, clay/granular column systems are expected to exhibit partial drainage. In addition, the typical area replacement ratios are typically in the range of 30 to 35%. The objectives of this thesis are to (1) conduct conventional drained and undrained triaxial tests to study the performance of clay specimens that are reinforced at a relatively high area replacement ratio (about 30%,) (2) devise a triaxial test/setup where clay specimens that are reinforced at an intermediate area replacement ratio (about 18%) could be tested under partially drained conditions, and (3) compare the results obtained from the partially drained tests with those from conventional drained and undrained tests, respectively. To achieve the objectives, triaxial tests were conducted on back-pressure saturated, normally consolidated, Kaolin specimens that are prepared from slurry. For the tests with the high area replacement ratio, the parameters that were varied are the height of the column relative to the height of the clay specimen, the type of the sand column (ordinary sand column or geotextile-encased sand column), and the drainage conditions (drained versus undrained). For the partially drained tests, the varied parameter was the rate of loading (3.5%, 40%, and 80% strain per hour). All tested samples were consolidated and tested at confining pressures of 100 kPa, 150 kPa, and 200 kPa to study the effect of confinement on the load response.

CONTENTS

ILLUSTRATIONS

TABLES

CHAPTER 1

INTRODUCTION AND SCOPE OF WORK

1.1. Introduction

The in-situ improvement of weak soils and the development of practical and effective solutions and approaches to address such conditions have been the subject of interest for a significant number of researchers. Among the explored options is the reliance on sand drains to accelerate the rate of consolidation of weak clays in response to loading and/or preloading. However, as observed by Najjar et al. (2010), the potential reinforcing and strengthening effects of these columns on both the short and long term response of the composite clay/sand system are typically neglected in design.

The behavior of clayey soils is generally governed by their undrained strength; nevertheless, the assumption of fully undrained conditions may not apply for the case of clays with granular column inclusions since those will act as drains facilitating the pore pressure dissipation and water movement in the composite system. As such, considering the behavior of the composite as either fully drained or undrained may be an inaccurate idealization. In general, the fully drained strength of soft clays is expected to be higher than the undrained strength, and could provide an upper bound for the shear strength of the composite. The actual behavior of the system is expected however to be partially drained with a shear strength that is intermediate between undrained and drained conditions.

Najjar et al. (2010) and Maakaroun et al. (2009) conducted a series of undrained triaxial tests with pore pressure measurements on soft consolidated Kaolin samples reinforced with partial or full penetrating single sand columns. The authors varied the area replacement ratios represented by the diameter of the sand columns, the depth of the penetrating columns, the effective confining pressure and the nature of the reinforced column which was either encased with a geotextile fabric or not encased. The results reported by Najjar et al. (2010) indicated an improvement in the undrained shear strength of the clay for all the area replacement ratios. These results are aligned with the results of undrained triaxial tests conducted by Black et al. (2007) who state that the relative increase in undrained shear strength is function of the area replacement ratio. Furthermore, Najjar et al. (2010) stated that this increase in strength was coupled with a decrease in pore pressures and an increase in stiffness. These results are also in alignment with the test results obtained by Sivakumar et al. (2004) who reported this decrease in pore pressure when sand columns were used as reinforcement. The testing conditions and methods used by all the above authors are very similar, which enhances the credibility of the results and their repeatability.

Maalouf (2012) conducted a series of drained triaxial tests which were identical counterparts to the undrained triaxial tests conducted by Maakaroun(2009) and Najjar et al (2010). The author found that the inclusion of 2cm non encased columns (7.9% area replacement ratio) did not result in improvements in strength. However tests with encased 2cm columns, and both encased and non-encased 3cm columns (17.8% area replacement ratio) resulted in significant improvements in the drained shear strength of the clay. This improvement in strength was coupled with a reduction in the contractive volumetric strains of the specimens, with the specimens reinforced with

fully penetrating columns yielding the biggest reductions. Maalouf (2012) also compared the results of the drained and undrained tests and found that although the drained strength was consistently higher than the undrained strength, the use of sand columns in clay would increase the undrained strength more effectively than the drained strength.

For typical construction applications, sand/gravel columns in the field are expected to act as drains that will facilitate partial drainage of the surrounding clay during loading. The degree of partial drainage will depend on the rate of loading, the permeability of the clay, the spacing and diameter of the sand/gravel columns, and the possibility of smearing of the clay around the column during installation. The rate and extent of partial drainage from the clay to the sand/gravel columns could play a significant role in defining the load response of the clay-sand-gravel column system. This is particularly true for applications involving relatively low area replacement ratios and medium dense columns (ex. sand drains), where the clay is expected to carry a significant portion of the total load. Current design procedures for problems involving foundations on soft clay deposits that are reinforced with sand/gravel columns lack a systematic approach for quantifying the effect of partial drainage and accounting for it in design.

In fact, studies pertaining to the investigation of partially drained behavior are scant. In what follows a brief summary of two such studies is provided: The first investigation was conducted by Juran and Guermazi (1988) and the second by Andreou et al (2008). Juran and Guermazi (1988) studied the effect of partial drainage of a silty soil sample reinforced with river sand using a modified triaxial cell. The authors conducted tests at a specified rate of shearing while allowing the sand column to drain

freely. They also conducted another series of tests in which both the sand column and the surrounding soil were not allowed to drain. The stress-strain response of the reinforced soil was greatly affected by the drainage of the column. Juran and Guermazi (1988) reported results indicating that the drainage of the column notably improved the resistance of the reinforced soil to the applied strain and that the freely drained column had a maximum load carrying capacity of about twice that of the undrained column. These findings further reinforce the hypothesis that allowing partial drainage of the composite system, which is more in line with actual field conditions, will improve the undrained shear resistance compared to the case where the columns are undrained. Andreou et al. (2008) conducted triaxial compression tests on reinforced kaolin clay samples. Three (3) series of tests were conducted. These included drained, undrained, and partially drained setups. The comparison of the results from the three series provided indications of the influence of drainage conditions and rate of loading on the load response. Andreou et al. (2008) measured a reduction in strength when the rate of loading was "accelerated" with drainage allowed (partially drained) relative to slower rates of loading (fully drained). In spite of this decrease in resistance, the measured strength remained higher than that of the reinforced undrained sample.

The limited results obtained by Juran and Guermazi (1987) and Andreou et al. (2008), suggest that the assumption of undrained conditions in the clay surrounding sand/gravel columns would lead to an underestimation of the degree of improvement in the shear strength of the clay-sand column system which would be obtained in the field. In addition, the limited data shows that the more realistic case of partial drainage through the sand column may lead to an added improvement in the short-term bearing capacity of the clay/sand column composite.

It is clear from the above that further work is necessary to further explore and understand the behavior of clay-sand column systems under partially drained conditions. Moreover, the response of these systems at relatively high area replacement ratios, which represent typical field applications, is neither fully established nor quantified. In fact, most of the published triaxial studies are based on fully drained or fully undrained tests conducted on samples reinforced at area replacement ratios in the range of 5 to 20%. In the field, clay/granular column systems may be executed at area replacement ratios reaching 30 to 35%.

The objectives of this thesis are to (1) conduct conventional drained and undrained triaxial tests to study the performance of clay specimens that are reinforced at a relatively high area replacement ratio (about 30%,) (2) devise a triaxial setup where clay specimens that are reinforced at an intermediate area replacement ratio (about 18%) could be tested under partially-drained conditions, and (3) compare the results obtained for the partially drained tests with those for conventional drained and undrained tests, respectively.

1.2. Significance of Stone Columns

The wide-spread development of urban cities and the expansion of industrial projects have urged investors and developers to look for available land for future construction. However, the majority of available future expansion sites are generally located in areas where the ground conditions are not favorable for carrying typical structural loads. Examples of soft lands include water front sites, recently deposited alluvium areas, and filled ground locations. In spite of the unfavorable ground

conditions for these sites, a considerable number of projects are being constructed on weak soils provided that ground improvement techniques are implemented to improve the mechanical properties of the soil. Typical ground improvement techniques include installation of vibro-stone columns, preconsolidation using prefabricated or sand column vertical drains, drilling or driving piles into competent strata, and preloading of fill with/out vacuum. Soil improvement techniques that involve the use of stone/sand columns were adopted in European countries in the early 1960's and their use spread thereafter following their successfully implementation in different countries.

Contrary to pile foundations which are designed to bypass weak layers of soil to transfer superstructure loads into competent strata, the use of stone/sand columns in clayey soils will take advantage of the surrounding weak soil and improve its load carrying capacity. Upon application of load, stone columns generally expand and bulge, thus exerting lateral pressure to the weak surrounding clay. In addition, and contrary to conventional piles, stone columns will reduce the dissipation of excess pore water pressure during loading.

The positive effect of the stone columns can be improved by encasing the columns with geotextiles to provide additional lateral support to the stone column. The installation of geosynthetics around the perimeter of the stone column can reduce the bulging of the sand column during loading, thus increasing the stiffness and bearing capacity of the sand column. This will in turn increase the ability of the hybrid clay sand column system to sustain the applied loads. Murugesan and Rajagopal (2006) recommend encasing stone columns with geogrids especially when the clay is very soft with undrained shear strength that is below 20 kPa.

Finally, vibro stone columns are seen as environmentally friendly (McKelvey et al. 2000). The stone column is possibly the most “natural” foundation system in existence. They are also more durable than any other foundation system that would involve the use of cement or steel. As a result, reinforced sand columns can be considered as one of the vital ground improvement techniques that can be adopted for improving and enhancing the load carrying capacity of the weak clayey soils. Sand columns have been successfully used in different structures such as under liquid storage tanks, earthen embankment, low rise buildings, industrial ware houses, and under raft foundations.

1.3. Methods of Construction of Stone Columns

Stone columns construction necessitates a partial replacement (10% to 35%) of unsuitable surface soil with a compacted vertical column of granular material that usually fully penetrates the weak soil. Typical column lengths range from 3m to 15m with diameters ranging from 0.5m to 1.5m. Stone columns can support loads up to 300 kN (Hughes and Withers 1970). There are two methods for constructing stone columns: 1) Wet method, known as top feed method or vibro-replacement method, and 2) Dry method, known as bottom feed method, or vibro-displacement method. The term vibroflot or poker is used to describe the probe which penetrates the weak soil (Figure 1.1.a). Rotation of the eccentric weight within the body of the probe causes lateral vibration at the tip of the probe, thus inducing a lateral force varying approximately from 12 to 28 tons (Figure 1.1.b). The probe usually varies in diameter from 0.3m to 0.5m with a length of 2m to 5m. The vibrator is suspended from the boom of crane where a 10 m probe can easily be handled with a 40 ton crane with a 12m boom length.

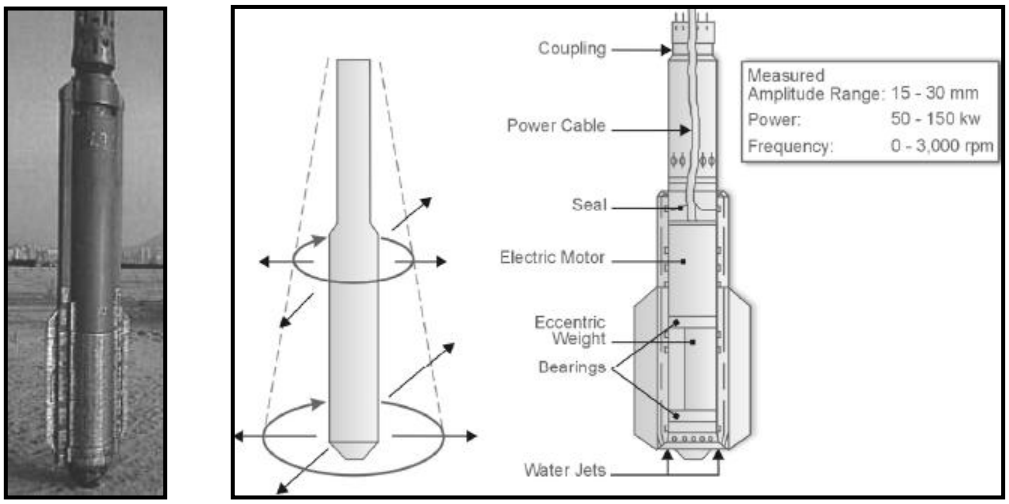

(a) (b)

Figure 1.1. (a) Vibroflot/poker (b) Vibroflot motion with vibrator parts

1.3.1. Top Feed Construction / Wet Vibro Replacement Method

In the vibro replacement (wet) method (Figure 1.2.a). A hole is formed in the ground by jetting a probe down to the desired depth. Jetting water is used to remove soft material, stabilize the probe hole, and guarantee that the stone backfill reaches the tip of the vibrator. The uncased hole is flushed out and then crushed stones with diameter ranging from 20 mm to 100 mm are added from the top in increments of 0.3m to 1.2m. The stones are then densified by means of a vibrator that is located near the bottom of the probe. Successive lifts are placed and densified until a column of stone is formed up to the ground surface.

The wet process is generally used when the borehole stability is questionable, and it is used for sites with a high water table. This method is the currently the most commonly used technique. Special consideration must be given to the construction of stone columns in silts and sensitive clays which undergo large strength losses when

subjected to vibrations during stone column construction. According to Baumann and Bauer (1974), all contractors indicated that saturated silty soils tend to lose strength during stone column construction due to a build-up in pore pressure.

1.3.2. Bottom Feed Construction / Dry Vibro Displacement Method

The main difference between the vibro-replacement and vibro-displacement methods (Figure 1.2.b) is the absence of jetting water during the initial formation of the hole in the vibro-displacement method. This method uses the same vibrator probe as in the wet vibro-replacement method but with the addition of a hopper at the top of the probe and a supply tube along the length of the probe to bring the crushed stone directly to the tip of the poker. This dry technique is suitable for partially saturated soils which can remain stable as the probe penetrates the ground. Sometimes air is used as a jetting medium in order to facilitate the extraction of the probe since the probe will occasionally adhere to the walls of the hole. The lack of flushing water in this method eliminates the generation of flushing fluid, and this in turn will widen the range of the sites that can be improved with dry-displacement method.

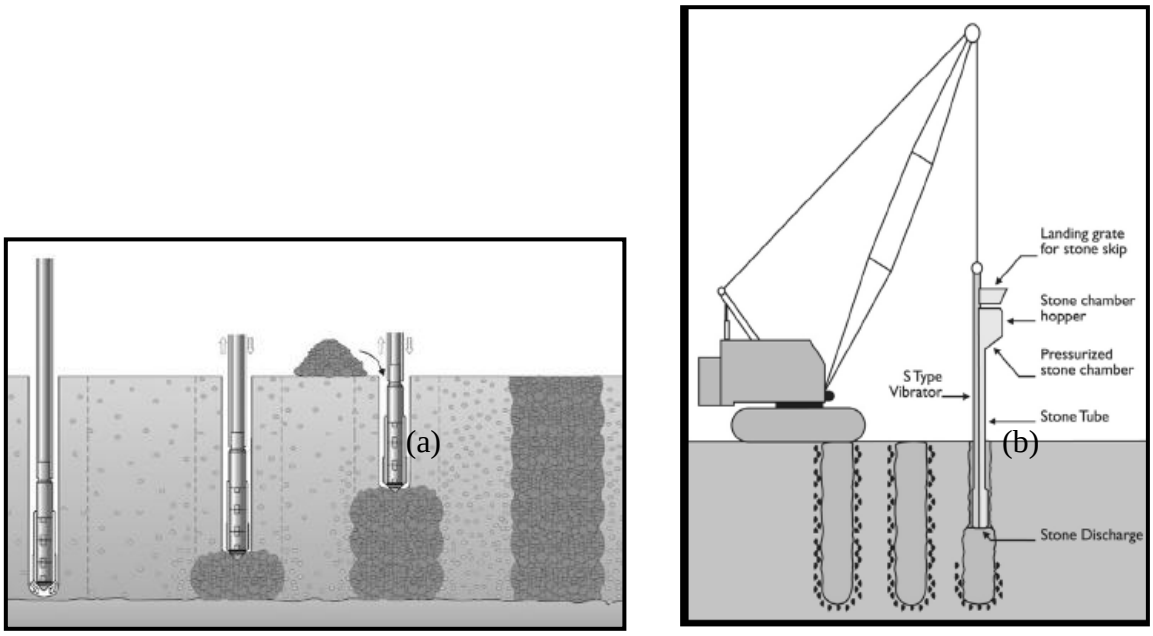

Figure 1.2. (a) Top feed construction (wet method), (b) bottom construction (dry method)

1.4. Scope of Work

The study involves conducting two series of triaxial tests on kaolin specimens that are reinforced with sand columns.

In the first series of tests, drained and undrained triaxial tests were conducted on 7.1-cm diameter clay specimens that are reinforced with 4cm-diameter sand columns that are installed in encased and non-encased states. This represents an equivalent area replacement ratio of ~30%. Both fully penetrating and partially penetrating columns were used to investigate the effect of column height on the improvement in the drained and undrained shear strength. The triaxial tests were performed on slurry-consolidated, back-pressure saturated kaolin specimens at confining pressures ranging from 100 to 200 kPa. The objective of this first series of test is to explore the behavior of clay-sand

columns systems at high area replacement ratios under triaxial conditions. A detailed representation of the first series of tests is shown in Table 1.1.

In the second series of tests, partially drained triaxial tests were conducted on 7.1-cm diameter clay specimens that are reinforced with 3cm-diameter sand columns that are installed to full penetration in a non-encased state (representing an area replacement ratio of ~18%). The partial drainage was enforced by prohibiting drainage from the bottom of the clay specimen and allowing it through the top cap of the triaxial cell only. Partially penetrating tests with different shearing rates were conducted to represent relatively quick loading (a strain rate of 80% per hour) and relatively slow loading (strain rate of 3.5% per hour). All tests were performed on slurry-consolidated, back-pressure saturated, kaolin specimen at confining pressures ranging from 100 to 200 kPa. In addition to these tests, a series of fully undrained tests that are implemented at a strain rate of 80% per hour will also be conducted to isolate any effect of the high rate of loading on the results of the partially drained test. Finally, one additional test was conducted at a very high strain rate of 120 % per hour to provide an upper bound of any realistic loading rate that could be achieved using a laboratory triaxial setup. The objective of this second series of tests is to compare the behavior of partially drained samples to that of fully drained and fully undrained samples under similar conditions. The results of the undrained and drained triaxial tests that were conducted on similar kaolinite samples that were reinforced with sand columns are presented in Najjar et al. (2010) and Maalouf (2012). A detailed representation of the second series of tests is shown in Table 1.2.

The experimental tests involve normally consolidated Kaolin samples with a diameter of 7.1cm and a length of 14.2cm prepared from slurry conditions. Sand columns of different diameters are then installed in the Kaolin specimens to model different area replacement ratios (area of sand column/area of specimen). The two diameters of sand columns which were used in this study are 3-cm and 4-cm. The first diameter (3cm) will result in an area ratio of 17.8% and the second diameter (4cm) will result in an area ratio of 31.7%. A procedure for specimen preparation was implemented to obtain normally consolidated kaolin specimens that are close to 100% saturation. Initially, dry Kaolin clods will be mixed with water at a water content of 100% using an electric mixer. The resulting slurry will then be poured into each of four prefabricated consolidometers that consist of 4 PVC pipe segments, each with a height of 35cm, an external and internal diameter of 7.3cm and 7.1cm respectively, and a wall thickness of 0.1cm. The pipe segments are designed to function as a split mold, thus eliminating the need for extruding the soil sample after consolidation. The soil specimen is consolidated from slurry using a loading system with dead weights placed sequentially, similar to the approach used in 1-D consolidation tests. The dead weights are seated on a circular steel plate that transfers the load to the top of the soil specimen through a circular steel rod with a diameter of 1cm. A perforated circular steel piston with a diameter of 7.1cms (same as inner diameter of PVC pipe) is fixed to the bottom of the steel rod to act as a loading plate and transmit the load to the Kaolinite slurry. The soil is separated from this loading plate with a porous stone and a filter paper to provide a freely draining boundary at the top of the soil specimen. At the end of consolidation, the Kaolin PVC specimen will be removed from the apparatus.

For test specimens that require the installation of sand columns, a hole with a diameter that is equivalent to the respective diameter of the sand column is augured gently into the specimen using a fabricated hand augur apparatus. The sand is then installed into the pre-drilled hole in layers. In the case where the sand column will be encased with a geotextile, the sand material is filled in layers into the fine geosynthetic material that has the shape of the respective column. The sand column is then inserted into the predrilled hole.

Finally, the specimen will be installed in an automated triaxial machine "TruePath" to be back-pressure saturated, consolidated under the specified confining pressures (100 kPa, 150 kPa, or 200 kPa), and then sheared under drained, undrained, or partially drained conditions. The variation of the deviatoric stress, excess pore water pressure, and volume change with the axial strain will be measured and analyzed to investigate the advantages of inserting sand columns of different characteristics in soft clays, particularly with regards to increasing the load carrying capacity during the different loading conditions.

Table 1.1. Triaxial soil testing program for Series 1

Test No.	Confining pressure σ_3, (kPa)	Diameter of sand column (cm)	Drained/ Undrained	Area replacement ratio: A_c/A_s (%)	Height of sand column (cm)	Column height penetration ratio, (H_c/H_s)	Column height diameter ratio, (H_c/D_c)
1	100	0	D	0	0	0	-
2		0	U	0	0	0	-
3		4	D	31.7	10.75	0.75	2.69
4		4	U	31.7	10.75	0.75	2.69
5		4 (ESC)	D	31.7	10.75	0.75	2.69
6		4	D	31.7	14.2	1	3.55
7		4	U	31.7	14.2	1	3.55
8		4 (ESC)	D	31.7	14.2	1	3.55
9	150	0	D	0	0	0	-
10		0	U	0	0	0	-
11		4	D	31.7	10.75	0.75	2.69
12		4	U	31.7	10.75	0.75	2.69
13		4 (ESC)	D	31.7	10.75	0.75	2.69
14		4	D	31.7	14.2	1	3.55
15		4	U	31.7	14.2	1	3.55
16		4 (ESC)	D	31.7	14.2	1	3.55
17	200	0	D	0	0	0	-
18		0	U	0	0	0	-
19		4	D	31.7	10.75	0.75	2.69
20		4	U	31.7	10.75	0.75	2.69
21		4 (ESC)	D	31.7	10.75	0.75	2.69
22		4	D	31.7	14.2	1	3.55
23		4	U	31.7	14.2	1	3.55
24		4 (ESC)	D	31.7	14.2	1	3.55

Note: (ESC) indicates geosynthetic-encased sand columns

Table 1.2 Triaxial soil testing program for Series 2

Test	Confining pressure σ_3, (kPa)	Diameter of sand column (cm)	Rate of loading (%strain /hr)	Partially drained/ Undrained	Area replacement ratio: A_c/A_s (%)	Height of sand column (cm)	Column height penetration ratio, (H_c/H_s)	Column height diameter ratio, (H_c/D_c)
1	100	3	3.5	PD	17.8	14.2	1	3.55
2		3	40	PD	17.8	14.2	1	3.55
3		3	80	PD	17.8	14.2	1	3.55
4		3	80	U	17.8	14.2	1	3.55
5	150	3	3.5	PD	17.8	14.2	1	3.55
6		3	40	PD	17.8	14.2	1	3.55
7		3	80	PD	17.8	14.2	1	3.55
8		3	80	U	17.8	14.2	1	3.55
9		3	120	PD	17.8	14.2	1	3.55
10	200	3	3.5	PD	17.8	14.2	1	3.55
11		3	40	PD	17.8	14.2	1	3.55
12		3	80	PD	17.8	14.2	1	3.55
13		3	80	U	17.8	14.2	1	3.55

Note: U is undrained and PD is partially drained

1.5. Organization of Thesis

The thesis consists of 9 chapters. A literature review which includes the major experimental and analytical studies related to the reinforcement of soft clays with stone columns is presented in CHAPTER II. In CHAPTER III, the properties of the materials used in the testing program are presented together with the methodology used in the clay sample preparation and construction of the reinforced and unreinforced sand columns. A step by step procedure for operating the automated triaxial equipment is discussed and presented in a detailed manner in CHAPTER IV. The results of drained and undrained tests are presented and analyzed in CHAPTERS V and VI, respectively. A comparison between the results of drained and undrained tests is done and presented in CHAPTER VII. The results of partially drained tests are presented and analyzed in

CHAPTER VIII. Finally, conclusions and recommendations are presented in CHAPTER IX.

CHAPTER 2

LITERATURE REVIEW

2.1. Introduction

This chapter includes a literature review of the major experimental and theoretical studies conducted to investigate the behavior of stone or sand columns in clays. The response of clays improved with granular inclusions has interested researchers since the 1970s. The initial work focused mainly on the use of stone columns that would increase the bearing capacity and the rate of settlement of weak clays. One of the earliest experimental studies on soft kaolin clay was conducted by Hughes and Withers (1974). They used sand columns as reinforcement for the clay and their tests were conducted under fully drained conditions. Later, experimental studies evolved to include different drainage conditions and test setups. Examples include the work done by Charles and Watts (1983), Bachus and Barksdale (1984), Juran and Guermazi (1988), NarasimhaRao et al. (1992), Muir Wood et al. (2000), Sivakumar et al. (2004), McKelvey et al. (2004), Ayadat and Hanna (2005), Black et al. (2006, 2007), Ambily and Ghandi (2007), Andreou et al (2008), Black et al (2011) and Sivakumar et al (2011). Other studies involved the use of finite element modeling to examine the effect of sand/stone columns on the stress-strain load response of the reinforced clay. Numerical studies include the work of Elshazly et al (2008) and Chen et al (2009).

Most of the studies mentioned above were conducted in one dimensional loading chambers which do not allow for the control of drainage in the soil specimens

during loading. Recently, experimental studies have shifted towards reliance on triaxial testing, where the drainage conditions and loading rates could be controlled. Published studies involving triaxial testing of such systems are based on fully drained or fully undrained tests conducted on samples reinforced at area replacement ratios in the range of 5 to 20%. Sivakumar et al. (2004) and Black et al. (2006, 2007) performed tests under full triaxial conditions in which the loading rate and the drainage conditions were controlled during shear. In some tests, the reinforced clay samples were sheared slowly to establish drained conditions, but more generally, soil specimens were sheared undrained.

For typical construction applications, sand/gravel columns in the field are expected to act as drains that will facilitate partial drainage of the surrounding clay during loading. The degree of partial drainage will depend on the rate of loading, the permeability of the clay, the spacing and diameter of the sand/gravel columns, and the possibility of smearing of the clay around the column during installation. In fact, studies pertaining to the investigation of partially drained behavior are scant. In what follows a brief summary of two such studies is provided: The first investigation was conducted by Juran and Guermazi (1988) and the second by Andreou et al (2008). Juran and Guermazi (1988) studied the effect of partial drainage of a silty soil sample reinforced with river sand using a modified triaxial cell. Andreou et al. (2008) conducted triaxial compression tests on kaolin clay samples reinforced with single columns of Hostun (HF) sand and gravel. Three (3) series of tests were conducted, these included drained, undrained, and partially drained setups. The limited results obtained by Juran and Guermazi (1987) and Andreou et al. (2008) suggest that the assumption of undrained conditions in the clay surrounding sand/gravel columns would lead to an

underestimation of the degree of improvement in the shear strength of the clay-sand column system which would be obtained in the field.

Results of the experimental and finite element investigations listed above indicate that the mode of failure of clay specimens that are reinforced with circular single sand/stone columns is characterized by lateral bulging of the sand column. This bulging occurs generally in the top 4 to 5 diameters along the height of the column and depends on the method of construction and virgin soil characteristics.. Specimens with short partially-penetrating columns appeared to fail below the reinforced portion of the clay, causing no significant improvement in the load carrying capacity of the specimen. Based on the above observations, several researchers proposed the idea of the "critical column length" that is between 4 to 8 times the diameter of the column beyond which the sand column will not improve the capacity of the clay (Hughes and Withers 1974; NarasimhaRao et al. 1992; Muir Wood et al. 2000; and McKelvey et al. 2004).

In some field applications involving sand drains, geosynthetic filter materials are used to separate the sand columns from the surrounding clay. Ayadat and Hanna (2005) and Najjar et al (2010) studied the effect of encapsulating sand columns with geofabrics of different strengths and stiffnesses. The results obtained indicated that encasing the columns with geotextiles or geogrids provided additional lateral support to the granular column and reduced the bulging of the column during loading, with the degree of improvement depending on the area replacement ratio and column penetration ratio.

Below is a summary of the research studies which targeted the behavior of clays that were reinforced with granular columns in a laboratory setting under 1-g and triaxial conditions.

2.2. Studies Involving 1-g Tests:

Historically, experimental research studies have been designed to investigate the behavior of sand/stone column-reinforced clay systems in the laboratory using 1-g tests that are conducted in one dimensional loading chambers (Hughes and Withers 1974, Charles and Watts 1983, Bachus and Barksdale 1984, Narasimha Rao et al. 1992, Muir Wood et al. 2000, 2004, McKelvey et al. 2004, Ayadat and Hanna 2005, Ambily & Gandhi 2007, Murugesan & Rajagopal 2008, Murugeson & Rajagopal 2010). In these studies, tests were conducted on clay specimens reinforced with partially or fully penetrating, encased or ordinary, stone or sand columns that were installed as single columns or as column groups. The loading mechanisms involved either direct column loading or foundation/plate loading at loading rates that varied from "slow" to "quick", in an attempt to simulate drained or undrained loading, respectively.

2.2.1. Hughes and Withers (1974)

Hughes and Withers (1974) conducted one of the earliest experimental studies on soft Kaolin clay reinforced with single sand columns. The clay specimens had a length of 225 mm and a width of 160mm. Using a one-dimensional loading apparatus, the specimens were consolidated under a constant stress of 100kPa. The single sand columns were later installed in the clay, with a length of 150 mm and a diameter

ranging from 12.5 mm to 38 mm. To ensure having a fully drained behavior, the columns were loaded in stages to ensure the complete dissipation of excess pore water pressure during loading. Observations of the mode of failure indicated that vertical and lateral distortions occurred at the top of the columns. Moreover, only the clay within a radial distance of 2.5 column diameters was laterally strained by loading, indicating that stone columns in groups can be assumed to act without interaction if the spacing between the columns was greater than 2.5 diameters. Furthermore, the vertical displacement of the columns did not extend below four diameters. The presence of sand columns accelerated the rate of settlement by four times and reduced the vertical displacement by a factor of about six.

Hughes and Withers (1974) state that as "the column expands, the radial resistance of the soil reaches a limiting value at which indefinite expansion occurs." They conclude that stone columns in soft ground would act like a column in a triaxial chamber where the cell pressure is limited. They propose the following expression to determine the maximum vertical stress that the column can carry as the sand/stones in the top region reach the critical state of stress:

$$\sigma'_v = \frac{(1+\sin\phi')}{(1-\sin\phi')}(\sigma_{ro} + 4c - u) \qquad (1)$$

Where *c* and *u* are the undrained strength and the pore water pressure, respectively while ϕ' is the angle of internal friction of the column material, σ'_v is the vertical capacity of the columns, and σ_{ro} is the initial radial total stress in the soil prior to column construction. Hughes and Withers (1974) showed that any increase in the column length beyond a column depth to diameter ratio of 6.3 will not increase the load

carrying capacity of the column. Finally, the authors state that in practical application, the loads are generally applied and distributed on both the column and the surrounding clay. This load distribution will consolidate the clay and lead to an increase in radial stiffness. However, this increase will not add appreciable strength to the load carrying capacity of the sand column.

2.2.2. Charles and Watts (1983)

Charles and Watts (1983) used large scale instrumented laboratory tests to assess the effectiveness of granular columns in reducing the vertical compressions of soft clay. The authors state that a group of columns loaded by a foundation loading causing a long term drained behavior, can be modeled by a granular column surrounded by a cylindrical mass area of soft clay. Therefore, the authors conducted five drained tests using 0.6m in height and 1m in diameter clay specimen, reinforced with granular columns of different diameters to study the effect of the area replacement ratio. The diameters of the granular columns used were 45, 350, 455, 500 and 572mm which are equivalent to area replacement ratios of 0.2, 12, 21, 25, and 33 %, respectively. Remolded Boulder clay (plasticity index of 12 % and liquid limit of 27 %) was used as the surrounding soil. The undrained shear strength of the clay which was compacted to a water content of 19 % was 30 kPa. A sample consolidated under a cell pressure of 100 kPa and sheared under drained conditions, yielded an angle of shearing resistance of 33.6˚. Similarly, drained triaxial tests done at cell pressures of 50, 100 and 200 kPa, yielded frictions angles of 53, 51 and 47˚ respectively. Polythene sheets were placed on the top and bottom of the clay to restrict drainage to the sand column only. The ring was instrumented with earth pressure cells with small cells placed in the soft clay and much

larger cells used in the granular columns. The small cells were calibrated using samples of soft clay subjected to known stress conditions in a triaxial cell, and it was noted that errors in the order of 12% were expected in all stress measurements. Pore water pressures were measured using piezometers and LVDT's were used to measure displacement.

Loading of the samples was done in four stages with each load being double the value of the previous load, until reaching an average vertical stress of 360kPa. The sample was allowed to dissipate all the pore pressures generated by keeping the load constant for a sufficient time and thus a test took more than one month to finish.

The authors report that for a given vertical stress the granular column was ten times less compressible than the soft clay, and soft clay specimens reinforced with granular columns showed less vertical compression compared to the control clay specimen. Furthermore, the vertical compression of the reinforced specimen decreases as the area replacement ratio increases. The results show that in order to reduce the vertical stress on the clay and thus reduce the vertical compression, an area replacement ratio of over 25% must be used. Also, it was noted that only for the 33% area replacement ratio did the authors measure a significant volume reduction in the column. The measured stress concentration ratios ranged from 2.2 to 4.

2.2.3. Bachus and Barksdale (1984)

Bachus and Barksdale (1984) conducted tests on single and group columns using an experimental setup consisting of a Plexiglas unit cell with a diameter of 10.8 cm and a height of 30.5 cm for the single tests and a box with dimensions of 17.3 cm x

50.5 cm x 30.5 cm for the group tests. The columns were made of fine quartz sand, had diameters of 2.9 and 5.3cm, and were installed using a replacement method. The clay used was kaolinite clay (plasticity index of 15 % and a liquid limit of 42). The specimens were prepared by mixing the clay as slurry and then one dimensionally consolidated to shear strengths of 14.4–19.1 kPa. Loading was done using a loading plate instrumented with pressure cells to measure stresses in the clay and sand column.

For the single column tests, load increments were applied to the specimen with enough time intervals to complete primary consolidation. The area replacement ratios were 0, 0.07, 0.25 and 1. The results indicate that as the area replacement ratio increases, the reduction in settlement increases as well. Furthermore, the authors state that to achieve a 50% reduction in settlement in the field, an area replacement ratio of 40% is required. The authors also studied the effect of L/D with results showing that for an area replacement ratio of 0.07, most of the movement was vertical with almost no lateral bulging occurred, and as the ratio increases the lateral movement increases. The authors measured stress concentration factors between 2.8 and 4.2.

For the group tests, pressure cells were mounted at five elevations in either the center of the end walls or the side faces of the box to measure lateral pressures developed between adjacent columns. Loading of the specimen was done using a rigid footing that was sized such that the column center-to footing-edge distance was 1 column diameter. Both stress and deformation controlled tests were conducted with the displacement rate of deformation controlled tests being 0.030mm/min. For the stress controlled tests, stress increments were added approximately every 4 h (until stabilization of load occurred). Results of the group tests showed that bulging occurred along the whole length with more prominent bulging at the top where the highest lateral

stresses were measured. Stress concentration factors varied between 1.5 and 5.0 at low stress levels and converged to between 2.5 and 4.0 upon loading to failure. However, the stress concentration factors were higher for the stress controlled tests which allowed for complete dissipation of pore pressures compared to the strain controlled tests which did not allow the completion of primary consolidation.

2.2.4. Narasimha Rao et al. (1992)

The authors used rectangular tanks of dimensions 1m x 0.8m and a height of 1m to prepare clay beds at different consistencies. Narasimha Rao et al (1992) conducted load tests on stone columns that reinforced the clay beds. The columns had diameters of 25mm, 50mm, and 75mm with column height to diameter ratios of 5, 8 and 12. The load was directly applied to the column through a circular steel plate of 1.5 times the diameter of the column. A PVC pipe with outer diameter corresponding to the column diameter was inserted in the middle of the tank, and then the tank was filled with clay up to the required column height. The PVC pipe was then slowly removed, and the gap was gradually filled in layers with granite chips ranges from 25mm to 30mm in size through tamping the material with a rod. The angle of friction for the granite chips was 38º.

The authors observed that the load applied to the columns is transferred to the clay by the bulging action of these columns. This bulging helps the mobilization of the passive resistance of the clay that surrounds and confines the stone columns. The area replacement ratio for the different columns was 44.44%. Furthermore, results indicated that the rate of increase in the ultimate load carrying capacity of the columns decreases for columns with length to diameter ratio greater than 8. This suggests that obtaining an

effective load transfer would require an optimum length of between 5 to 8 times the diameter of the column.

2.2.5. Muir Wood et al. (2000)

Muir Wood et al. (2000) performed load tests on stone column groups under a footing. The authors varied the spacing, diameter, and length of columns. The model tests were performed in a loading tank having a diameter of 300 mm using Kaolin clay which was consolidated under a maximum vertical stress of 120 kPa and allowed to swell back under a stress of 30 kPa to a final thickness of 300 mm. The drained angle of the shearing resistance of the Kaolin clay was 23º and the average undrained shear strength was equal to 12 kPa based on vane shear tests. Sand columns with diameters equal to 11 mm and 17.5 mm were constructed from fine quartz sand with a mean particle diameter (D_{50}=0.21mm) and installed into the clay tank by means of a replacement (auguring) method. The sand columns were distributed on a square grid with a spacing that ranges from 17.6 mm to 31.5 mm This range of column spacing yields area ratios (A_s) that are between 10 % and 30%.

The reinforced clay beds were loaded at a penetration rate of 0.061mm/min through a rigid circular footing with a diameter of 100 mm, and loading was terminated when the displacement reached a value of 30 mm. The load was applied in increments with sufficient time to allow the completion of primary consolidation t_{95} after every load increment. The duration of the test was around 24 t_{95}. Consequently, this time was enough to ensure drained conditions during loading stages. An investigation of the

different modes of failure for the sand columns was conducted leading to the following observations:

- If the column is loaded and not prohibited from expanding radially by near columns, then the average stress in the column increases and the column bulges.
- If the column is subjected to high stress ratios with small lateral restraint, then a diagonal shear failure plane may form through the column.
- If the column is adequately short, then the column will punch and penetrate the underlying clay material. As the length of the column increases the penetration of the column into the clay is reduced since a smaller load will reach the base of the column.

The variation of average footing pressure, normalized with initial undrained strength, with footing settlement, normalized with footing diameter was analyzed for the different tests. Results indicated that as the area ratio increases, both stiffness and strength increase; moreover, the column length is significant up to a certain point beyond which increasing the column length will not lead to an increase in strength. Muir Wood et al. (2000) indicate that this critical length increases as the area ratio increases, since the failure mechanism is pushed deeper below the footing.

2.2.6. McKelvey et al. (2004)

McKelvey et al. (2004) investigated the load deformation behavior of a small group of sand columns under strip, pad, and circular footings. Two types of material were used in the experimental work, the first being Kaolin clay and the second being a

transparent clay-like material that had almost the same properties as Kaolin clay. Kaolin slurry was consolidated under a vertical pressure of 140 kPa for 8 days. The internal diameter of the loading chamber was 413 mm and its length was 1200 mm. After the completion of the 1-dimensional consolidation the length of sample was around 500mm and the undrained shear strength was estimated at 32 kPa. At the end of consolidation, the pressure was removed and columns having a diameter of 25 mm were augured into the clay bed and filled with sand poured through a wire mesh. After constructing the columns, a loading plate was installed at the top of the columns. For the Kaolin specimens, 4 sand columns with a square pattern were installed under the pad footing with column length to diameter ratios of 6 (length of column = 150mm) and 10 (length of column = 250mm) and an area replacement ratio of 24%. The model footing was subjected to a strain controlled loading at a rate 0.0064mm/min using a 9x9cm footing. The loading was terminated when the vertical displacement of the footing reached 40 mm. The consolidation pressure of 142 kPa was removed prior to loading the footing.

The insertion of sand columns with a length of 150 mm and an area ratio of 24% increased the maximum load carrying capacity by 130 % increase. Increasing the length of the column to 250mm increased the improvement by 5%. The authors concluded that increasing the column length to diameter ratio to a value above 6 does not lead to any significant improvement in the load carrying capacity. However, the undrained stiffness for column lengths of 150 mm and 250 mm was 4 times and 5.7 times higher than that of unreinforced clay, respectively.

The authors reported in their observations that the failure of the specimens was characterized by bulging, bending or shearing. In long columns, deformations were concentrated in the upper zones of the column while for shorter columns, the columns

tended to bulge and bend outward away from the neighboring columns and punched a distance of 10 mm into the soft clay bed. Using miniature pressure transducers the authors were able to calculate that the stress concentration ratio (n) was found to be less than 2 for short columns and greater than 4 for long columns, immediately after the load application on the footing. At higher loading stages, the stress concentration ratio approached a value of 3 regardless of the column length.

2.2.7. Ayadat and Hanna (2005)

Ayadat and Hanna (2005) studied the effect of encapsulating sand columns with four geofabric material on the load carrying capacity of a collapsible soil (78% concrete sand, 10% Leighton Buzzard sand, and 12% Kaolin clay) that was tested in a loading chamber with a diameter of 39cm and a height of 52cm. Single sand columns with diameters equal to 2.3 cm and lengths equal to 25, 30, and 41 cm were constructed at a relative density of 80% (ϕ'=44^o) in the middle of a soil specimen with a diameter of 39 cm and a height of 41 cm. Axial loads were applied to the column through a rigid circular plate with a diameter of 4 cm. Results of stress controlled tests indicated that the load carrying capacity of the composite material increased with increases in the stiffness of the geofabric. This increase in the axial capacity of the sand column can be explained by the higher lateral restraint provided by the reinforcement. Furthermore, increasing the length of the column also played a role in increasing the axial capacity.

Ayadat and Hanna (2005) developed an equation to calculate the ultimate carrying capacity of encased stone columns inserted in soft cohesive soils. The vertical stress that could be supported by an encased stone column is given by:

$$\sigma'_{vlim} = \tan^2(\frac{\Pi}{4} + \frac{\phi'}{2})(\sigma'_{ho} + kc' + \alpha \frac{\tau_a t}{r_o}) \quad (2)$$

Where σ'_{vlim} is the maximum effective vertical stress acting on the column, ϕ' is the angle of shearing resistance of the column material, $\sigma'_{ho} = K_o(q + \frac{\gamma L}{2})$ is the effective lateral stress of the soil before installing the column, k is a constant that is equal to 4, c' is the drained cohesion of the collapsible soil, K_o is the coefficient of earth pressure at rest, q is the surcharge applied on the ground surface, γ is the unit weight of the surrounding soil, L is the length of the stone column, τ_a is the tensile strength of the geofabric material, *t* is the thickness of the geofabric material, and r_o is the initial radius of the column. The factor (α) is a reduction factor that should be applied to the additional lateral stress provided by the geofabric material, on the premise that the columns may bulge (and thus fail) before the stress in the fabric reaches the ultimate stress. The authors have proposed that α is to be evaluated as a function of the modulus of deformation of the stone column E_p as: $\alpha = 3.2x10^5 E_p^{-1.37}$, where the modulus E_p of the stone column should be obtained from triaxial tests conducted on the sand column alone.

2.2.8. Ambily and Gandhi (2007)

Ambily and Gandhi (2007) used the results of an experimental program coupled with FEM numerical analyses to develop a design procedure for stone columns considering the load sharing between the stone and the surrounding soft clay. The experimental program involved tests that were conducted on single and group 100mm-

diameter stone columns in triangular pattern that were installed to full depth in a 450 mm thick soft clay specimen. The clay was prepared in a cylindrical tank with a height of 50 cm and a diameter ranging from 21 cm to 83.5 cm. Clays with undrained shear strengths of 7, 14, and 30 kPa were used in the experiments. For single stone columns, the diameter of the clay tank ranged from 21 to 42 cm, while for sand columns in groups of 7, the diameter of the tank was 83.5cm. The height of the columns was 45cm.

The clay sample was prepared by compaction. The columns were constructed using crushed stones of size 2 to 10 mm using the replacement method, prepared at a density of 16.62 kN/m^3 and resulting in a friction angle of 43^o. Entire area loading and column loading were adopted. The load was applied at a displacement rate of 0.0625mm/min and monitored at equal time intervals till a settlement of 10 mm was exceeded. The authors observed that if the entire area was loaded, the columns didn't show signs of bulging, while for loaded column, bulging was observed at a distance of 0.5D from the top of the column. Based on the experimental test results and FEM analysis, the ratio of the limiting axial stress to the corresponding shear strength of surrounding clay was found to be independent of the shear strength of soil and is a constant for a given (s/d) ratio and a given angle of internal friction of column material.

Using FEM analyses, the authors developed the design chart shown in Figure 2.1. The authors argue that part of the stresses that are applied to the column will be shared by the surrounding clay. This will add a "surcharge" (q) to the clay which in turn improves the limiting axial capacity σ_{su} of the column. Based on FE analyses involving surcharge, an expression for the limiting axial capacity including surcharge was developed as:

$$\sigma_{suq} = \sigma_{su} + (0.0088\phi^2 - 0.5067\phi + 10.86)q \quad (3)$$

Where σ_{suq} is the limiting axial stress with a surcharge (q) on the surrounding clay and ϕ is the friction angle of column.

In tests where the entire area was loaded, failure of the column didn't occur due to the confinement effect of the boundary of the unit cell and this can be linked to the fact that the columns did not bulge. However, the stiffness of the reinforced composite was improved significantly. The authors define the stiffness improvement factor (β) which is the ratio of the stiffness of the reinforced ground to the stiffness of the unreinforced ground. Curves showing the variation of (β) with (s/d) for different values of ϕ were derived using the FE analysis. The stiffness factor (β) was found to be independent of the strength of the surrounding soil. For triangular column groups' pattern, the behavior of the reinforced samples was found to be similar to the specimens reinforced with a single column. This indicates that the single column behavior with a unit cell concept can simulate the behavior of an interior column when a large number of columns are simultaneously loaded. As the shear strength of the clay decreases, more load will be taken by the stone column (stress concentration factor between 4 and 6) as indicated in Figure 2.2. Finally, the authors proposed a design method for stone columns in soft clays.

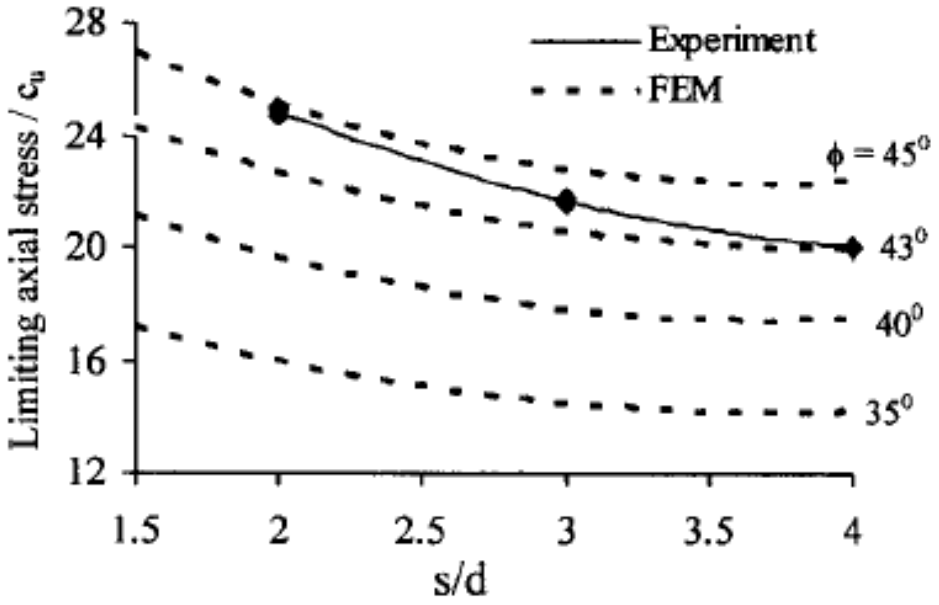

Figure 2.1. Effect of s/d and Ø on axial capacity of stone column (Ambily and Ghandi 2007)

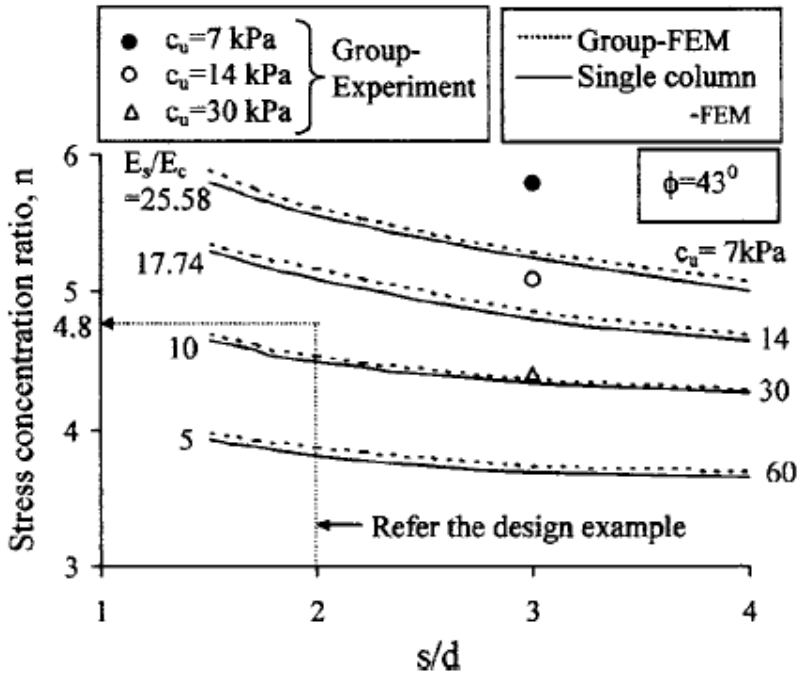

Figure 2.2. Effect of s/d and cu on stress concentration ratio (n) (Ambily and Ghandi 2007)

2.2.9. Murugesan and Rajagopal (2008)

Murugesan and Rajagopal (2008) investigated the performance of encased stone columns through 1-g laboratory tests consisting of column loading of granite chips with a unit weight =15.7 kN/m^3, and a friction angle of ϕ'=41.5^o. The columns were installed in lucastrine clay in a tank with a diameter of 210mm and a height of 500mm. In the experimental program, different parameters were varied including the diameter of the columns (D=5cm, 7.5cm, and 10cm) and the type of encasement (4 different types). The columns were loaded at a rate of 1.2mm per minute which results in an undrained loading. The ordinary stone columns showed a catastrophic failure, whereas the encased columns showed an elastic behavior. The load carrying capacity of individual stone columns for a settlement of 10 mm was increased by 3 to 5 times. Encasing the columns with geosynthetics proved to minimize the bulging of the columns in contrast with the ordinary columns which underwent large settlements because of the excessive bulging, whereas bulging was minimized for encased columns. Results indicated that for ordinary columns, the load capacity is almost the same for all diameters, whereas for the encased columns as the diameter increases, the load capacity of encased stone column decreases. Similar trends were reported by Murugesan and Rajagopal (2006) based on the numerical analysis. The authors used these results to provide guidelines developed for the design of geosynthetic encased stone columns. The bearing support from the soft soil was conservatively ignored in the proposed methodology.

2.2.10. Murugesan and Rajagopal (2010)

Murugesan and Rajagopal (2010) investigated the performance of encased stone columns through 1-g laboratory tests. The stone columns were prepared using granite chips that were installed in lacustrine clay. The lacustrine clay was consolidated under a pressure of 10 kPa in a large tank with dimensions of 1.2x1.2x0.85m to a final height of 0.6m. The displacement method was used to install single and group columns having diameters of 5.0, 7.5, and 10cm, at a density of 16 kN/m^3. In order to simulate an undrained behavior, the single columns were loaded with a plate having a diameter that is twice the diameter of the columns at a rate of 1.2mm/min. The column group was comprised of 12 columns with a diameter of 7.5cm placed in a triangular grid at a spacing of 15cm. The group was loaded through a loading plate that inscribed three central columns (diameter of plate is 24.82cm). Four different types of encasements were used in the testing program.

Results of tests with ordinary columns exhibited a clear failure while encased columns did not show signs of failure. The pressure on the encased column at a settlement of 10mm was found to be three to five times greater than the non-encased column. The authors noted that the pressures developed in the encased columns were found to decrease as the diameter of the columns increased, since the additional confinement provided by the encasement is inversely proportional to the diameter of the columns.

Results of the load tests on the groups indicated that encased columns showed a linear increase in pressure even at high settlements which indicate an elastic behavior, while the group of ordinary columns showed clear signs of failure. The load carrying capacity increases 3 to 5 folds due to the encasement effect of the geosynthetics. The

stress concentration factor on the encased columns was found to be about 5. The clay carried only 0.1 to 0.6 of the total pressure on the loading plate, with the clay in the encased group carrying less stress than that in the ordinary group. The stress concentration factor is only 2 for the ordinary columns at failure. Design charts are presented at the end of the paper as a guideline for the design of encased columns in clays.

2.3. "Undrained" Triaxial Tests

Sivakumar et al. (2004), and Najjar et al. (2010) performed conventional consolidated undrained triaxial tests on Kaolin specimens that were reinforced with partially and fully penetrating sand columns.

2.3.1. Sivakumar et al. (2004)

Sivakumar et al. (2004) performed consolidated undrained triaxial tests on model sand columns with a diameter of 3.2 cm and height penetration ratios (ratio of column height to height of specimen) of 0.4, 0.6, 0.8, and 1 in soft Kaolin specimens having a diameter of 10 cm and a length 20 cm. Two types of loading were used to test the kaolin specimens. In the first type, the entire area of the Kaolin specimen was loaded while in the other type, the specimen was subjected to "foundation loading" where the Kaolin specimen was loaded at its middle through a rigid circular footing having a diameter of 4 cm. Furthermore, the authors used geo-grid reinforcement to encase the columns and study the effect of increasing the lateral confinement of the sand.

Kaolin specimens were prepared from a slurry at a water content of 105% (1.5 times its liquid limit of 70%) and initially consolidated using air pressure that subjected the samples to a vertical pressure of 200 kPa in a one dimensional consolidometer. After 3 days, the consolidation stage was completed, air pressure was removed. The sand columns were installed by auguring into the clay specimen to form a column with a 3.2 cm diameter. The void ratio of the clay was 1.43±0.05. Four different lengths of columns were used which are 8, 12, 16 and 20 cm. Having saturated the specimens at a 300 kPa backpressure, the specimens were isotropically consolidated at an effective confining pressure of 100kPa. Finally, the samples were sheared in the triaxial cell at a strain rate of 4 % per day.

Sand columns were prepared using two methods: a wet compaction method and a frozen method. In the wet method, each layer was constructed by tamping the wet sand having a water content of 18% to form the column. The wet compaction method yielded sand columns with a bulk density ranging from 2300 to 2450 Kg/m^3. In the frozen method, wet sand at a water content of 18% was compacted in layers into a plastic tube and frozen. After freezing, the tube was cut along its length and the frozen column was inserted into the predrilled augured hole. For the encased sand column, geo-grid fabric enclosed the wet sand material prior to installing the plastic tube. The bulk density of the frozen column was about 1930±30 Kg/m^3. The authors state that although freezing of sand columns is not adopted in the field, the method is used in the laboratory because it results in a consistent sand column diameter, leading to little variations in the density of the column.

After failure, samples that were sheared with uniform loading were cut vertically to investigate the failure mechanism. Short columns bulged below the

reinforced portion of the clay, while fully penetrating columns bulged relatively uniformly along their length. Analysis of stress strain curves for the different types of loading and different method of column insertion indicated that the generation of excess pore water pressure was smaller in the case of Kaolin specimens with sand columns. Furthermore, the percentage of reduction of the excess pore water pressure was higher for fully penetrating columns compared with partial penetrating columns.

The deviatoric stress increased by 40 % for fully penetrating columns that were installed using the wet compaction method and which were subjected to uniform loading, compared with untreated Kaolin specimen. For partially penetrating columns, the deviatoric stress was reduced in comparison to unreinforced specimens. The authors explained this behavior to be dependent on the column preparation method, which in this case is the wet compaction method. On the other hand, frozen column that were fully penetrating into the clay resulted in 30% increase in the deviatoric stress. Similarly pore water pressures were reduced due to possible dilatation of the compacted sand column during undrained shearing. Furthermore, the authors noted that kaolin specimens reinforced with frozen sand column of height penetration ratios under 0.6 showed no increase in the load carrying capacity of the sand-clay composite (Figure 2.3).

For foundation loading, the unreinforced specimen carried 280N which is equivalent to a bearing pressure of 220 kPa. Fully penetrating wet and frozen sand columns carried 450 kPa and 400 kPa respectively. The authors used the method by Hughes and Withers (1974) to predict the ultimate capacity of the tested sand columns. For $\phi' = 35$, $\sigma_{ro} = 100$ kPa, $c = 28$ kPa, and $u = 44$ kPa, the predicted σ'_v turned out to be

equal to 613 kPa. As a result, the estimated pressure on the footing was calculated to be equal to $\sigma'_v - (\sigma'_3 - \Delta u)$ =613-(100-44) =557 kPa. The measured value for the bearing capacity of wet fully penetrating sand columns was equal to 450 kPa. The authors state that this indicates good agreement with the values predicted using the model by Hughes and Withers (1974).

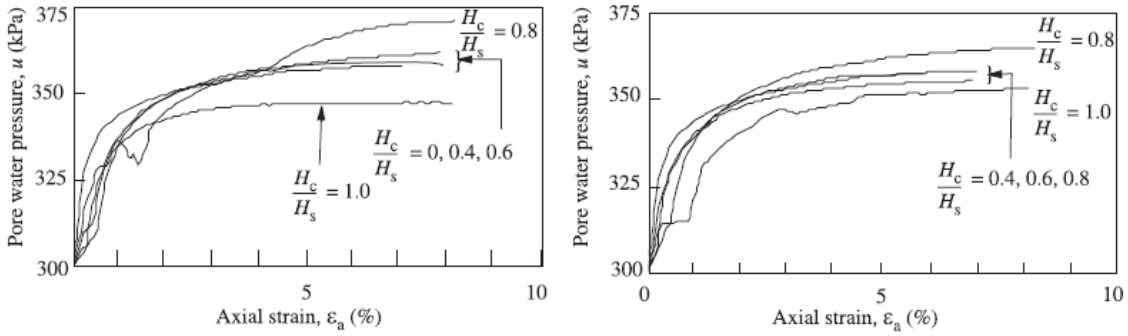

Figure 2.3. Stress-strain relationship for uniform loading: (a) wet compaction; (b) previously frozen sand column.

In the case of uniform and foundation loading, the presence of a geo-grid sleeve around the sand column increased the load carrying capacity of the composite sand-column system by 70% and 60% respectively, in comparison to the unreinforced frozen sand columns. Moreover, settlement was reduced significantly in the case of reinforced stone columns. These findings are clearly shown in Figure 2.4. Similarly, excess pore water pressures were reduced for reinforced sand columns.

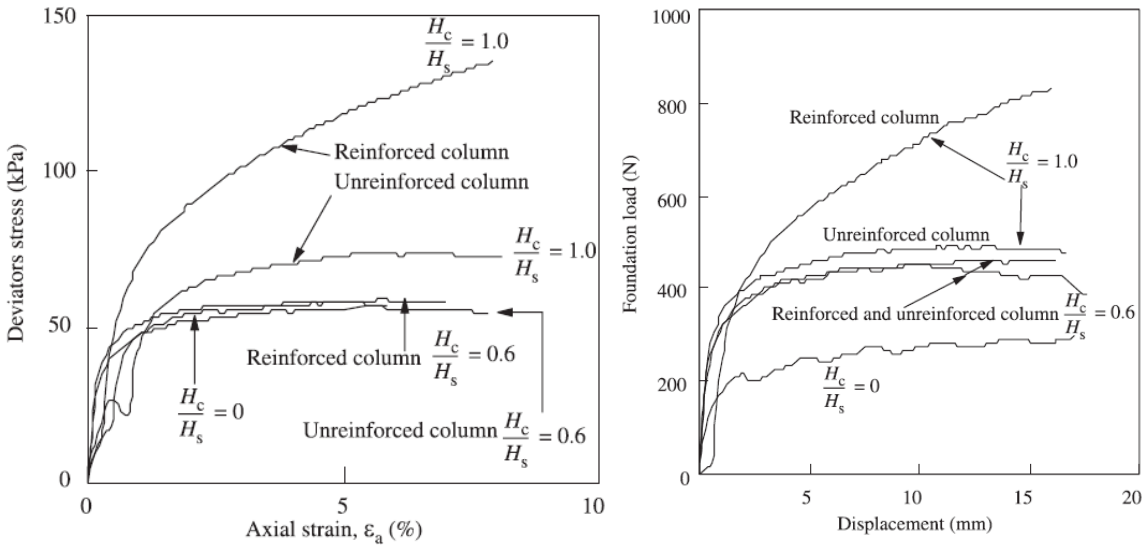

(a) (b)

Figure 2.4. Stress-strain and load-settlement behavior, comparison between reinforced and unreinforced columns (a) uniform loading, (b) foundation loading

2.3.2. Najjar et al. (2010)

Najjar et al. (2010) implemented a comprehensive testing program to assess the impact of sand columns on the undrained load response of soft clays in practical application involving the use of sand drains or sand columns in clayey soils. The experimental program involves performing 32 isotropically consolidated undrained triaxial tests on one-dimensionally consolidated kaolin specimens having a diameter of 7.1cm and a length of 14.2cm with pore pressure measurement on soft clay specimens that were reinforced with sand columns. The parameters that were varied in the program were:

- The area replacement ratio, A_c/A_s, defined as the ratio of the cross sectional area of the sand column A_c to the cross-sectional area of the specimen A_s (7.9% and 17.8% for the 2cm and 3cms sand column diameter respectively)
- The column penetration ratio, H_c/H_s, defined as the ratio of the height of the sand column H_c to the height of the specimen H_s (0.5, 0.75 and 1)
- The confinement of the sand column with a geosynthetic fabric.

The tests were conducted at three effective confining pressures (100kPa, 150kPa and 200kPa) to isolate the effect of confinement on the degree of improvement in the mechanical properties of the sand column-clay system including undrained strength and Young's modulus, but more importantly to characterize and compare the effective Mohr-Coulomb failure envelopes for control clay specimens and specimens that were reinforced with sand columns. The program of testing is summarized in Table 2.1.

Table 2.1. Laboratory Testing Program and Results (Najjar et al. 2010)

Test number	Effective confining pressure $(\sigma_3')_o$ (kPa)	Diameter of sand column (cm)	Area replacement ratio A_c/A_s (%)	Height of sand column (cm)	Column penetration ratio (H_c/H_s)	Column height to diameter ratio (H_c/D_c)	Undrained shear strength (kPa)	Excess pore-water pressure (kPa)	$(E_{sec})_{1\%}$ at 1% axial strain (kPa)	Increase in undrained shear strength (%)	Reductio in exces pore pressure (%)
1	100	0	0	0	0	—	32.3	61.3	4,150	—	—
2		2	7.9	7.1	0.50	3.55	32.5	59.9	4,166	0.6	2.9
3		2	7.9	10.65	0.75	5.32	35.2	57.3	4,220	9.0	6.5
4		2	7.9	14.2	1	7.10	36.6	51.2	4,390	13.3	16.5
5		2 (ESC)	7.9	7.1	0.5	3.55	32.8	58.8	4,187	1.5	4.1
6		2 (ESC)	7.9	10.65	0.75	5.32	37.2	58.0	4,762	15.1	5.4
7		2 (ESC)	7.9	14.2	1	7.10	52.0	58.9	5,132	61.0	3.9
8		3	17.8	10.65	0.75	3.55	38.9	48.9	4,597	20.4	20.2
9		3	17.8	14.2	1	4.73	56.7	42.7	5,853	75.5	30.3
10		3 (ESC)	17.8	7.1	0.5	2.36	36.0	59.2	4,280	11.5	3.5
11		3 (ESC)	17.8	14.2	1	4.73	64.8	42.8	7,150	100.6	30.2
12	150	0	0	0	0	—	42.1	95.1	6,092	—	—
13		2	7.9	10.65	0.75	5.32	48.2	88.9	6,100	14.5	6.5
14		2	7.9	14.2	1	7.10	50.3	87.8	6,368	19.5	7.7
15		2 (ESC)	7.9	7.1	0.5	3.55	42.3	89.4	4,920	0.5	6.0
16		2 (ESC)	7.9	10.65	0.75	5.32	50.9	85.4	6,402	20.8	10.2
17		2 (ESC)	7.9	14.2	1	7.10	58.5	76.8	6,093	39.0	19.2
18		3	17.8	7.1	0.5	2.36	46.0	87.2	6,101	9.3	8.3
19		3	17.8	10.65	0.75	3.55	56.8	78.1	6,697	34.9	17.9
20		3	17.8	14.2	1	4.73	73.9	65.2	8,624	75.5	31.4
21		3 (ESC)	17.8	7.1	0.5	2.36	46.8	92.7	6,574	11.1	2.5
22		3 (ESC)	17.8	14.2	1	4.73	79.4	67.8	8,045	88.7	28.7
23	200	0	0	0	0	—	55.1	130.9	7,637	—	—
24		2	7.9	10.65	0.75	5.32	60.1	120.3	7,904	9.1	8.1
25		2	7.9	14.2	1	7.10	65.8	112.1	7,996	19.4	14.4
26		2 (ESC)	7.9	7.1	0.5	3.55	58.4	119.2	7,788	6.0	8.9
27		2 (ESC)	7.9	10.65	0.75	5.32	61.9	121.1	8,144	12.4	7.5
28		2 (ESC)	7.9	14.2	1	7.10	70.9	115.7	8,228	28.6	11.6
29		3	17.8	10.65	0.75	3.55	71.2	107.8	8,983	29.2	17.6
30		3	17.8	14.2	1	4.73	92.3	89.4	10,103	67.5	31.7
31		3 (ESC)	17.8	7.1	0.5	2.36	58.2	119.7	8,121	5.6	8.5
32		3 (ESC)	17.8	14.2	1	4.73	103.3	86.5	11,407	87.4	33.9

The mode of failure of the specimens with fully penetrating sand columns showed minimal and uniform bulging throughout the height of the sand column as indicated in Fig. 2.5 (a). Whereas for partially penetrating sand columns, bulging was significant and concentrated at the lower portion of the column which indicates that the stresses at the base of the column generally exceeded the bearing capacity of the soil leading to premature bearing capacity failure in the unreinforced lower portion of the specimen (Figure 2.5 (b) and (c)). The use of encasement reduced the degree of bulging compared to the control specimen and specimens that were reinforced with non-encased columns (Figure 2.6).

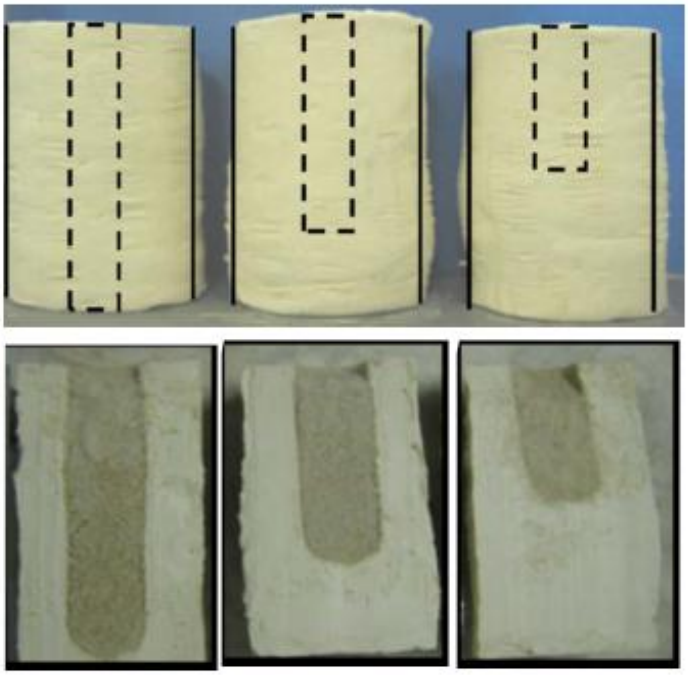

Figure 2.5. Modes of failure of clay specimens (upper part) and sand columns (lower part) reinforced with (a) fully penetrating column; (b) column with penetration ratio of 0.75; and (c) column with penetration ratio of 0.5

Figure 2.6. Modes of failure of clay specimens with (a) fully penetrating unreinforced column; (b) fully penetrating reinforced column; (c) unreinforced column with penetration ratio of 0.5; and (d) reinforced column with penetration ratio of 0.5

The stress-strain curves and the pore pressure versus strain curves are presented in

Figure 2.7 and 2.8 for ordinary and encased sand columns, respectively. The sand

columns improved the undrained shear strength on average by a factor of 17.4% and 72.8% for an area replacement ratio of 7.9% and 17.8% respectively. The encasement of the sand columns showed an increase in the average improvement in the undrained shear strength by a factor of 2.5 and 1.3 for an area replacement ratio of 7.9% and 17.8% respectively. Table 2.1 indicates that for samples that were reinforced with fully penetrating non-encased sand columns with area replacement ratios of 7.9 and 17.8%, the average reduction in the excess pore-water pressure was 12.9 and 31.3%, respectively. The reduction in the generation of excess pore-water pressure is due to the dilatational tendency and the higher stiffness of the sand columns. For partially penetrating columns with H_c/H_s=0.75, the average reductions of excess pore-water pressure were reduced to about 7 and 17% for area replacement ratios of 7.9 and 17.8%, respectively. Hence, the insertion of sand columns reduces the excess pore-water pressure generation during undrained loading, and their effectiveness in reducing the water pressure increases with increasing the column height and area replacement ratio. The insertion of fully penetrating encased sand column with area replacement ratios of 7.9 and 17.8% lead to an average reduction of 11.6 and 30.9% in the excess pore-water pressure, respectively.

With regards to the effective shear strength envelops (Figure 2.9), the effective friction angle (ϕ ') and the apparent cohesion (c') of clay specimens that were reinforced with non-encased sand columns were not significantly affected by the presence of the sand column. However, for samples that were reinforced with fully penetrating sand columns with an area ratio of 17.8%, c' increased from 0 kPa (for unreinforced specimen) to 12 kPa.

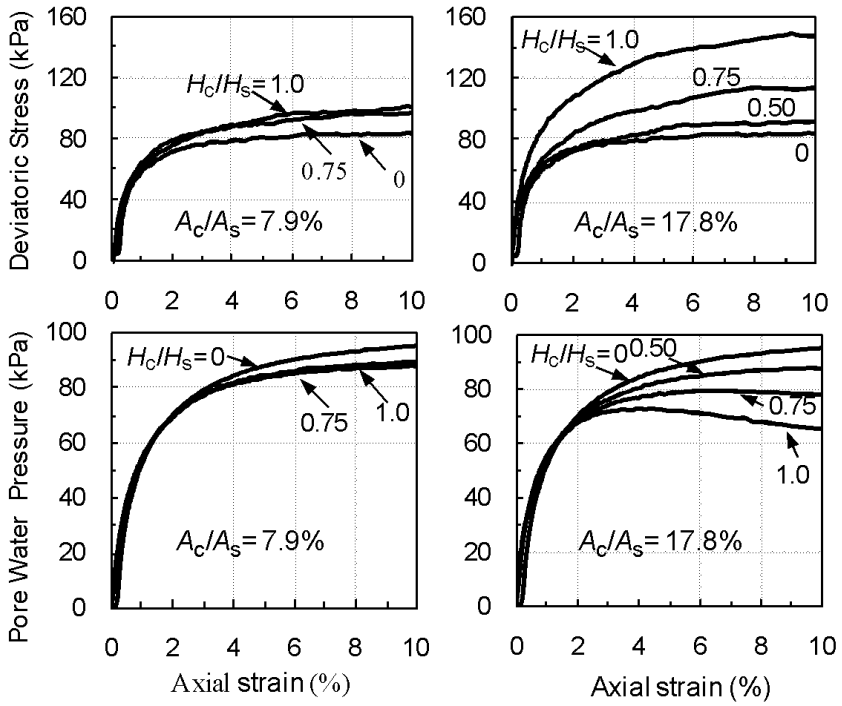

Figure 2.7. Deviatoric stress and excess pore water pressure versus axial strain for kaolin specimens reinforced with non-encased sand columns ($(\sigma'3)_o$=150 kPa)

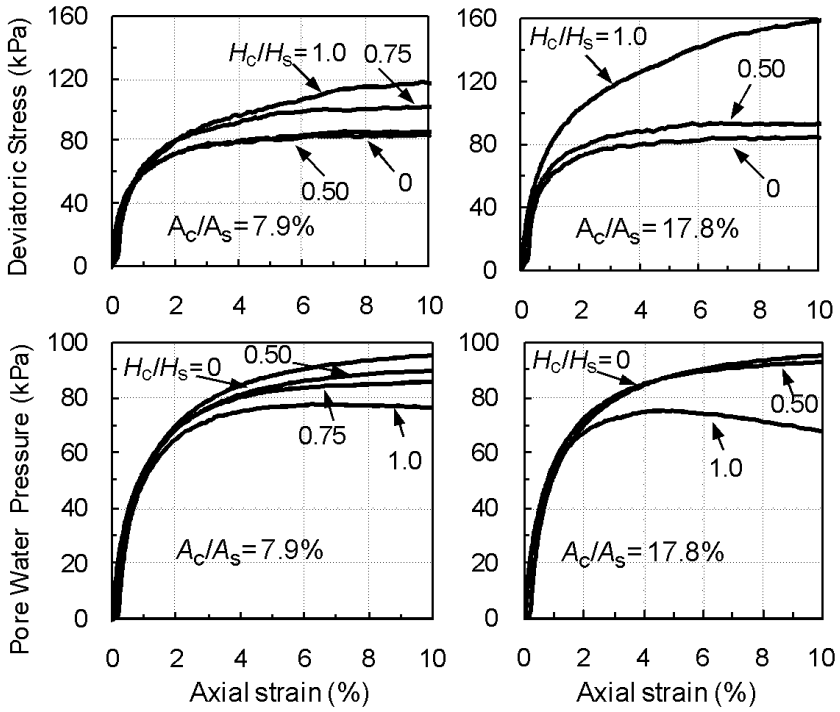

Figure 2.8. Deviatoric stress and excess pore water pressure versus axial strain for kaolin specimens reinforced with encased sand columns ($(\sigma'3)_o$=150 kPa)

As a result, it can be concluded based on the data that was collected in this study that reinforcing soft normally consolidated clays with sand columns with a friction angle of about 33 degrees, will not have a significant impact on the effective shear strength parameters of the reinforced clay, except if fully penetrating columns with relatively high area ratios (greater than 17%) were used to reinforce the clay. The encasement of sand columns with a geotextile fabric improved the apparent cohesion of the composite, particularly for small area replacement ratios (Ac/As=7.9%) and fully penetrating columns. However, the increase in c' was accompanied by a reduction in the effective angle of friction. For an area replacement ratio of 17.8%, the increase in c' was not as significant.

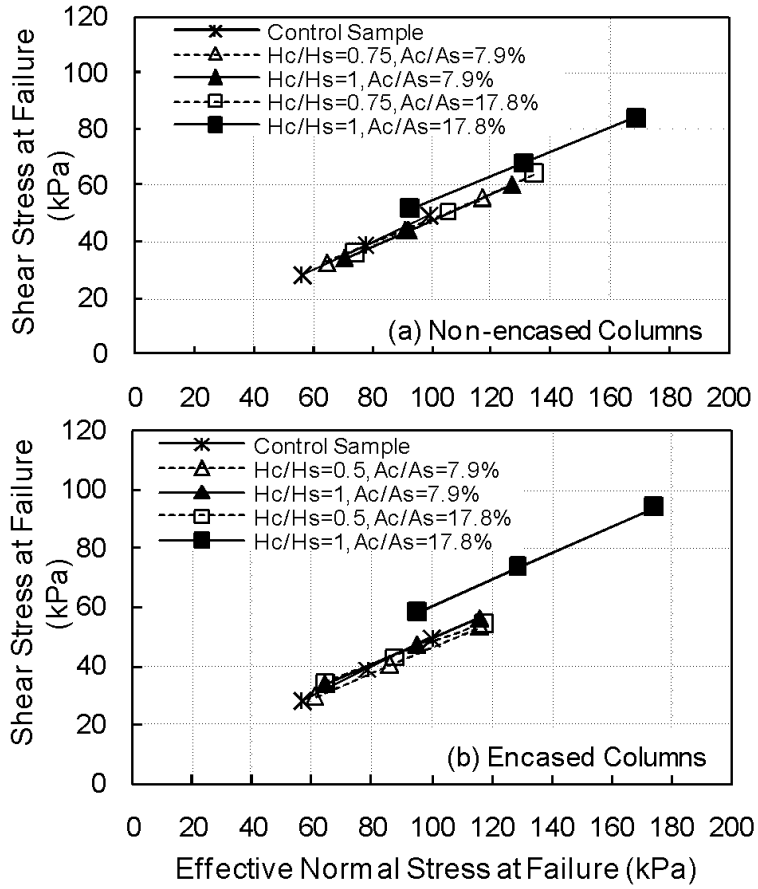

Figure 2.9. Effective failure envelops for unreinforced and reinforced kaolin specimens

2.4. "Drained" Triaxial Tests

Black et al. (2006), El Shazly et al (2008), Chen et al (2009), Black et al. (2011), Sivakumar et al. (2011) and Maalouf (2012) conducted tests that involved drained loading of isotropically and K_o-consolidated kaolin samples.

2.4.1. Black et al. (2006)

Black et al. (2006) built and assembled a triaxial testing machine that has the capability of testing Ko-consolidated samples having a diameter of 30 cm and a height of 40 cm.

Kaolin clay was used in this study. The specimens were first mixed in slurry form and then consolidated under a 1-dimensional vertical stress of 75 kPa. The Sand columns had a diameter of 25mm and were prepared by the wet compaction method using the procedure described in Sivakumar et al. (2004). The specimen was then placed into the triaxial test chamber and initially subjected to an isotropic effective confining pressure of 75 kPa. This was then followed by Ko loading where the vertical stress (σ_1') and horizontal stress (σ_3') where raised slowly to reach values of 125 kPa and 100 kPa respectively. In order to maintain saturation of the specimen, a back pressure of 200 kPa was maintained all the time. To achieve fully drained loading conditions, the authors loaded the specimen with a stress rate of 0.8kPa/hr. In the proposed test setup, the load is independently applied to the sample via a circular plate with a diameter of 60 mm. The test took 2-3 week to reach a settlement of 15 to 20 mm.

For a footing displacement of 10 mm, the capacity of the unreinforced column was 1.25 kN. The curves on Figure 2.10 indicate that reinforcing the specimen with sand columns of 6 and 10 height to diameter ratio increased the capacity by 12% and 28%, respectively. The area replacement ratio was 17%. Pressure cells installed in the sand column and in the surrounding clay allowed for measurements that indicated that for samples reinforced with long columns, the pressure in the column at a settlement of 10 mm was equal to 1100 kPa, while the pressure in the clay was equal to 600 kPa. This translates into a stress concentration factor of about 1.83. Undrained loading conditions and higher area replacement ratios will typically yield higher values of stress concentration.

Observations of the modes of failure revealed that short columns suffered no distinctive bulging, while long columns showed crucial deformation in the top regions.

These findings are in line with the observations of Hughes and Withers (1974) who stated that long columns fail by bulging while short columns penetrate in the underlying clay. The authors finally conclude that the optimum column length to diameter ratio is confined in the range of 6 to 10.

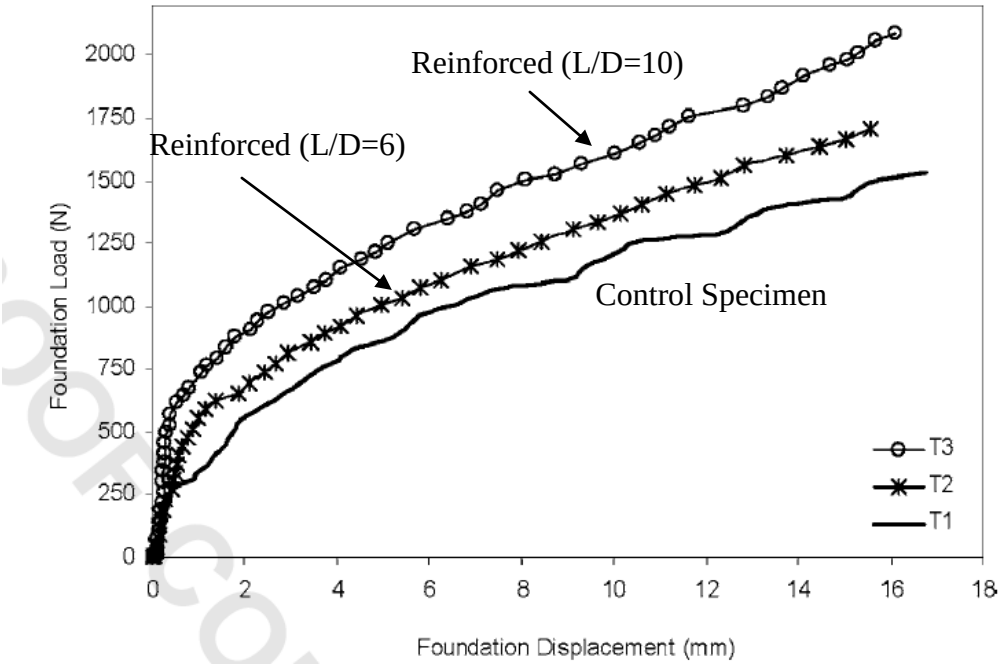

Figure 2.10. Load-settlement behavior for control and reinforced specimens (L/D = 6 and 10)

2.4.2. El Shazly et al (2008)

Elshazly et al (2008) conducted an FEM analysis using PLAXIS to test the unit cell idealization concept by comparing its results against "trusted" settlement values. A settlement correction factor is introduced and computed for different conditions.

The authors placed a lot of emphasis on the model calibration, which would eventually be the main element that provides reliability. This calibration was done using real settlement records from a full-scale test in the field, and by using back analysis, a set of modeling parameters were determined. The authors used the well documented case history by Mitchel and Huber (1985) and adopted the same set of parameters for their own study. The below tables summarizes the post-installation parameters used for the case of layered soil.

Soil classification	Estuarine cohesive	Estuarine cohesionless	Marine cohesive	Marine cohesionless	Gravel
γ_d (kN/m^3)	15.0	15.0	17.0	17.0	18.6
γ_{sat} (kN/m^3)	19.0	19.0	20.0	20.0	21.6
ϕ' (°)	34	38	34	37	41
E (kPa)	8,500	17,000	8,700	12,600	22,200
M	0.65	0.69	0.65	0.90	0.59
R_f	0.87	0.69	0.67	0.67	0.86

Figure 2.11. Post-installation parameters (case of layered soil)

However, the post-installation ratio of horizontal to vertical stress K* which was simply assumed by Mitchel and Huber (1985) did not lead to a match between the model deformations and the field measurements. An inverse approach was adopted by the authors to evaluate K*, i.e. the initial soil stresses were determined based on the knowledge about the settlements and post-installation parameters. Having conducted this inverse approach and an iterative procedure, the authors concluded that K* ranged from 1.1 to 2.5 with a best estimate of 1.5.

Various foundation dimensions were used in the analysis, the diameters B ranged from 5 to 50 m and the size ratios B/L ranged from 0.5 to 4.7. Pressures of 30,

90, and 150 kPa were used in the analysis. An axisymmetrical model was used in the FE analysis of the column groups, with a single column surrounded by concentric rings of columns. The thickness of these rings was determined such that the area replacement ratio in the model is kept constant as in the field. Also, the center-to-center distance between rings is kept equal to the spacing between columns in the field. Flexible loadings with different diameters were applied through blankets having the same material properties as those of the stone column material.

Using an advanced hyperbolic stress dependent model satisfying the Mohr–Coulomb criterion, namely the Hardening model, the stress–strain behavior of the natural soils and the stone columns was modeled. Compared to the (bilinear) elasto-perfectly plastic model (Mohr–Coulomb model in PLAXIS), the Hardening model provides better simulation for soil behavior under small stress levels due to the fact that soil curvilinear behavior starts at low stress levels.

Two cases were studied, the first with a layered soil and the second with a soft clay layer. In both cases, two numerical simulations were required to develop an understanding on the subject. The first simulation is the axisymmetrical model which mimics the full geometry of the foundation-soil system and the second simulation is the idealized unit cell concept which simulates an interior single column of an indefinite grid of stone columns. To compare the results a settlement factor correction was defined as follows:

$$f = \frac{S}{S_{uc}} \qquad (4)$$

With S being the calculated settlement of the axisymmetrical model which represents the “trusted settlement” that was back calculated from true full scale field testing, and S_{uc} being the settlement obtained by the unit cell model.

The authors plotted this settlement correction factor (f) against the foundation size ratio B/L. The curves on Figure 2.12 summarize the results obtained for the first case, the layered soil model.

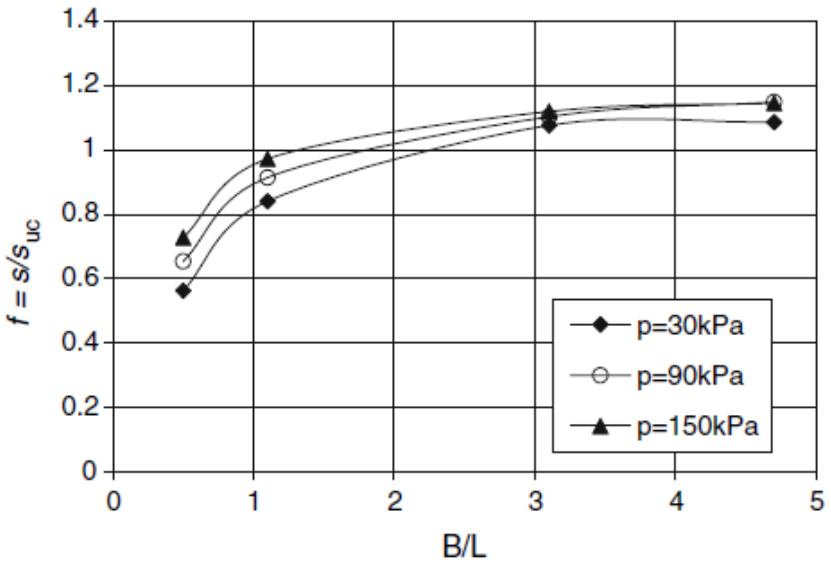

Figure 2.12. Settlement correction factor versus size ratio (case of layered soil)

It can be inferred from Figure 2.12 that as the size ratio of the foundation increases so does the settlement correction factor. Furthermore, if the unit cell is assumed to represent a given foundation with finite extent and with B/L<2, then the "trusted" settlement estimate would be smaller than the unit cell settlement. However, if B/L> 2 then the "trusted" settlement would be larger than the real field behavior, and therefore the unit cell concept is not an upper bound for settlement prediction in this case.

The correction factor for the soft clay case is represented in Figure 2.13. In this case, the settlement correction factor is always larger than 1, even for small foundations.

The authors explained this to be caused by the relative weakness of the soft clay, which provides reduced lateral support at the edges and thus causes larger settlements in the axisymmetrical model in comparison with the unit cell model which has a rigid boundary. However, as the foundation size increases, the edge effect becomes less dominant and therefore a reduction in the correction factor is observed for B/L>1.

Generally, the authors deduce that the settlement correction factor depends on both the foundation size and the virgin soil characteristics.

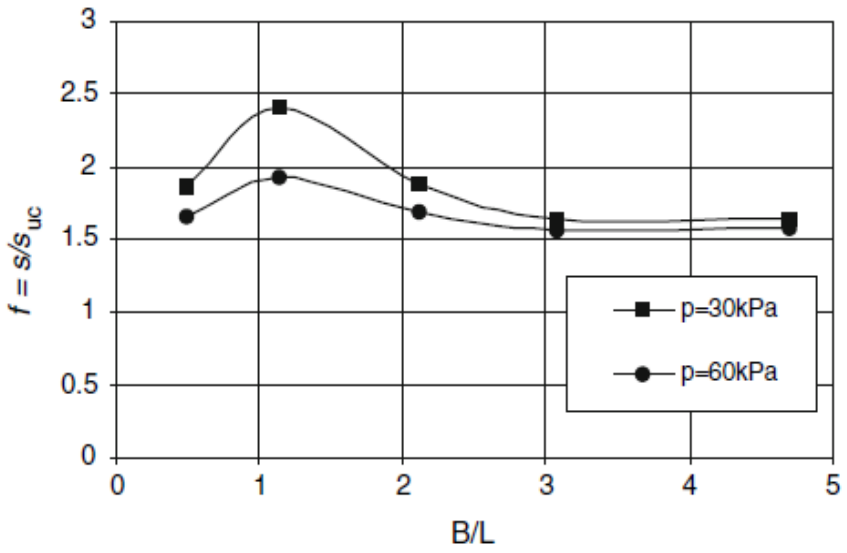

Figure 2.13. Settlement correction factor versus size ratio (case of soft clay)

2.4.3. Chen et al (2009)

Chen et al (2009) conducted a three dimensional numerical analysis simulating the effect of installation of a single rammed aggregate pier (RAP). The authors used the computer program FLAC 3D and verified the results by comparing it with measured values in the field. To establish the effect of installation (cavity expansion), another

model was constituted to model an un-rammed aggregate pier (UAP). Both piers had a nominal diameter of 0.76m and a nominal length of 5.05m and were installed in a 13m layer of soft alluvial clay with groundwater table 2m below the surface.

The 3D numerical model was square in a plan view and formed by brick and shell elements. The edge length of the model was 16 m and the thickness was 14 m. Thin solid continuum elements were used along the pier-soil boundary in lieu of interface elements. On top of the pier, a concrete cap was placed and modeled as a linear elastic solid material. Fully drained conditions were assumed with the modified Cam-Clay model used to model the soil matrix and the Mohr-Coulomb model used to model the aggregate pier. Verification of the parameters used in the Cam-Clay model was carried out by comparing the stress–strain curves obtained from the Cam-clay model with the measured data obtained from CD triaxial tests at confining pressures of 22.5, 41, and 60 kPa, respectively. The parameters used in the model were adjusted to yield an improved match between the measured and calculated values. Figure 2.14 summarizes these parameters.

Parameter		Desiccated soil	Alluvial clay
Dry density, γ	(kN/m^3)	13.9	13.9
Max. bulk modulus, K_{max}	(MPa)	1000	1000
Shear modulus, G	(MPa)	11.3	3.75
Poisson ratio, υ	–	0.2	0.2
Slope of url, κ	–	0.00543	0.01083 (0.009*)
Slope of ncl, λ	–	0.02171	0.04343 (0.036*)
Slope of csl, M	–	1.42	0.94 (0.98*)
Ref. pressure, p_{ref}	(Pa)	25500	25500
Initial specific volume, v	–	2.00	2.00

Figure 2.14. Modified Cam-clay model parameters for the matrix soil

It is important to note that the rammed pier in the field increased by length and diameter and had final dimensions of 0.84m diameter and 5.13m of length. This increase in dimension was also modeled by the authors; however, the UAP (0.76m diameter & 5.05m length) was assumed to have the same unit weight and bulk and shear modulus as the RAP to isolate the effects of installation.

The results of the numerical model will be discussed in the following paragraphs. The bulging of the piers was observed to be at depth 2xdiameter for the RAP and 4xdiameter for the UAP, and the magnitude of the bulging was significantly lower for the RAP compared to the UAP. The authors explained this difference due to the densification and pre-stressing of the soil matrix surrounding the RAP during the installation, which led to a higher confining pressure near the ground surface.

The axial load increase in the piers is defined as the difference at the same depth between the axial loads before and after the compressive stresses were applied. The authors noted that axial load increase in the RAP decreases rapidly with depth and almost no load reaches the tip. However in the UAP, this decrease in axial load is less rapid and thus at a certain depth more load is measured in UAP than in the RAP. This difference was explained by the lower side resistance of the soil acting on the UAP and that the UAP is not subjected to cavity expansion. It is important to note that the reduction in axial load for the RAP was observed in the bulging region (2D), where the higher side resistance is acting.

The shortening of the pier shaft was assessed by introducing a settlement ratio R_b which is defined as follows:

$$R_b = \frac{S_{top} - S_{tip}}{S_{tip}} \qquad (5)$$

Where S_{top} is the settlement at the top of the pier and S_{tip} is the settlement at the tip of the pier.

When R_b is larger than 1, the governing settlement results from the shortening of the pier i.e. bulging and compression of the pier shaft. When R_b is less than 1, the governing settlement results from the compression of the soil below the tip of the shaft. The analysis was conducted for different l/d ratios and for two clays, one relatively soft, and the other relatively stiff.

The R_b value generally increases with an increase in l/d ratio in all the cases. For the RAP, the shortening of the pier is dominant when l/d ≥3 in the stiff clay and when l/d≥6 or l/d≥4 with the compressive load ≥ 240 kN in the soft clay. However for the UAP, the shortening of the pier is dominant until l/d≥ 4 in the stiff clay and until l/d≥ 5 in the soft clay.

Finally, the authors recommend that the critical length to diameter ratio is equal to 4 for the RAPs and equal to 5 for the UAPs.

2.4.4. Black et al. (2011)

Black et al. (2011) used a large triaxial cell to test clay samples with diameters of 30cm and depths of 40cm, that were consolidated under Ko conditions. Kaolin clay was used in this study. The specimens were first mixed in slurry form and then consolidated under a 1-dimensional vertical stress of 150 kPa resulting in clay specimens with an undrained shear strength of 35 kPa. Gravel columns with diameters of 2.5cm, 3.2cm, and 3.8cm (area ratios of 17, 28, and 40% when loaded with a 6cm wide footing) were installed using the replacement method. The columns were constructed in layers by compaction using 10 blows of a 1.0 kg rod that was raised a

distance of 5cm. The resulting density of the columns was about 15.5 kN/m^3. The authors state that 6% increase in cavity volume occurred during the installation of the columns. For group loading, three columns of 1.8cm and 2.2cm diameters were adopted to produce area ratios of 28% and 40%, respectively. The study also tested three column lengths (12.5cm, 25cm, and 40cm) representing column penetration ratios of 0.31, 0.62, and 1.0 respectively. The samples were then consolidated under an effective cell pressure of 75 kPa followed by Ko consolidation with a Ko of 0.71. The Ko consolidation was assumed to represent the unit cell concept where zero lateral displacement is maintained at the boundaries. The final step which is the shearing stage consisted of applying a foundation with a controlled stress rate of 1 kPa/hour. This stress rate insured drained conditions.

Monitoring of settlement versus stress during Ko consolidation indicated that the strains measured for the reinforced samples were 0.77%, 0.72%, and 0.54%, for area ratios of 0.7%, 1.1%, and 1.6%, respectively (total area reinforced with single columns), compared with a strain of 1.5% for the unreinforced clay. Comparison of settlements for partially penetrating columns indicated that settlements reduce as the depth of treatment increases as indicated in Figure 2.15. Foundation loading indicated that the settlement improvement factors increase as 11 the L/D ratio increases for a given area ratio, although the improvement seems to level off at L/d between 8 and 10. The settlement improvement factor also increased with increase in the area replacement ratio, but the improvement seems to decrease at a threshold of about 30% to 40% area replacement. For foundations supported on column groups, the pressure-settlement response was found to be similar to the individual columns at the same area replacement ratio.

.

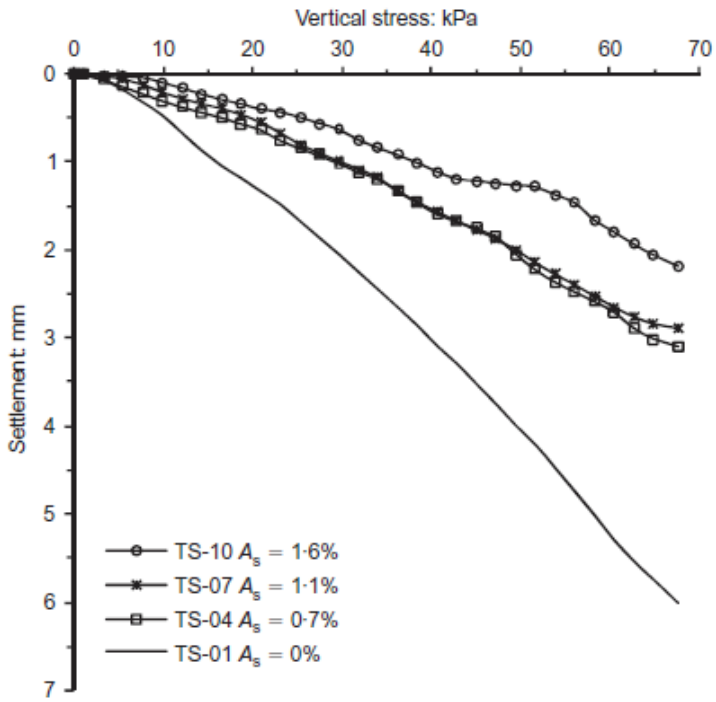

Figure 2.15. Settlement under unit cell consideration with increasing area replacement ratio

The results indicated that the settlement improvement factor were 3.2 and 3.8 for area replacement ratios of 28% and 40% respectively. The settlement improvement factors for the corresponding single columns were about 6.5 to 7.5 indicating that the performance of the group is not as good as that of the single columns. Furthermore, the limited results for pressures recorded in the column and in the clay in the group indicate a stress concentration factor in the order of 1.5 which reinforces the findings of Black et al (2006).

2.4.5. Sivakumar et al. (2011)

Sivakumar et al. (2011) used a large triaxial cell to test clay samples with diameters of 30cm and depths of 40cm, reinforced with columns of compacted crushed basalt. First the samples were saturated and then consolidated under a confining pressure of 50 kPa followed by a shearing stage which consisted of a foundation loading at a stress controlled rate of 1 kPa/hour. Loading of the specimen was done using a loading plate with a 6cm diameter. The crushed basalt column diameters were 4, 5, and 6cm. During consolidation, the stone columns settled with time due to consolidation of the surrounding clay. However, negative skin friction was generated on the columns due to the fact that the clay consolidated more than the columns. In the control clay test, the footing settled 15 mm at a pressure of 300 kPa. For the 6cm columns, the pressure under the footing increased by 500 kPa. The authors placed the critical length of the columns in the range of about 5 column diameters. Furthermore, for a pressure of 150 kPa, a comparison of the settlements indicated improvement factors of 1.7, 1.7, and 4.8 for the 4, 5, and 6cm columns respectively as presented in Figure 2.16. Priebe (1995) and Black et al (2011) measured larger improvement factors than those presented in this study. This is probably due to the fact that Priebe (1995) assumed a unit cell whereby zero lateral strains are imposed and Black et al. (2011) had rigid boundary conditions which increased the confinement.

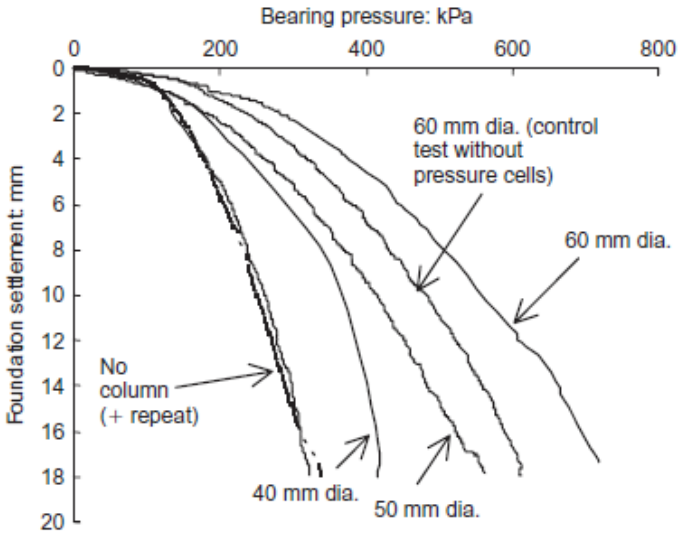

Figure 2.16. Bearing Pressure-settlement characteristics

2.4.6. Maalouf (2012)

Maalouf (2012) conducted a series of drained triaxial tests on 7.1-cm diameter clay specimens that are reinforced with 2cm or 3cm-diameter sand columns which translates into 7.9% and 17.8% area replacement ratios respectively. The author also varied the penetration ratio of the columns and studied the effect of encasing the columns with a geotextile on the drained shear strength.

The clay used was kaolin clay which was mixed to create a slurry. The clay slurry is then consolidated using a custom made one dimensional consolidation frame under a pressure of 100 kPa. The normally consolidated samples will then be trimmed to a height of 14.2cm, and afterwards the sand column is installed by auguring into the sample and inserting a prepared frozen column into the augured hole. The sand column is prepared in layers of Ottawa sand using dry pluviation, then water is added before the

column is set to freeze. The consolidated drained triaxial tests will be performed on slurry-consolidated back-pressure saturated kaolin specimens at confining pressures ranging from 100 to 200 kPa. The table below summarizes the proposed testing program.

Table 2.2. Summary of testing program.

Test No.	Confining pressure σ_3, (kPa)	Diameter of sand column (mm)	Area replacement ratio: A_c/A_s (%)	Column Penetration Ratio: H_c/H_s	Height of Sand Column: Hs (cm)	Deviatoric stress @ failure (kPa)	Volume strain (%)	E_{sec} @ 1% axial strain (kPa)	Increase in deviatoric stress (%)
1	100	0	0	0	-	112.0	-4.41	4260	-
2		20	7.9	0.75	10.65	116.4	-4.21	3800	3.9
3		20	7.9	1.0	14.2	131.7	-3.93	4050	17.6
4		20 (ESC)	7.9	0.75	10.65	119.0	-4.15	3420	6.3
5		20 (ESC)	7.9	1.0	14.2	160.0	-3.91	2580	42.9
6		30	17.8	0.75	10.65	133.0	-3.64	3754	18.8
7		30	17.8	1.0	14.2	169.7	-2.34	7630	51.5
8		30 (ESC)	17.8	0.75	10.65	154.0	-3.63	4230	37.5
9		30 (ESC)	17.8	1.0	14.2	206.0	-3.07	5300	83.9
10	150	0	0	0	-	165.0	-4.15	4780	-
11		20	7.9	0.75	10.65	163.3	-4.67	3190	-1.0
12		20	7.9	1.0	14.2	173.6	-4.17	4360	5.2
13		20 (ESC)	7.9	0.75	10.65	169.2	-4.04	4380	2.5
14		20 (ESC)	7.9	1.0	14.2	204.0	-4.02	4150	23.6
15		30	17.8	0.75	10.65	193.0	-3.92	3765	17.0
16		30	17.8	1.0	14.2	237.0	-3.57	8580	44.2
17		30 (ESC)	17.8	0.75	10.65	198.0	-4.05	4469	20.0
18		30 (ESC)	17.8	1.0	14.2	269.0	-3.15	8100	63.0
19	200	0	0	0	-	210.0	-4.93	5240	-
20		20	7.9	0.75	10.65	209.0	-5.21	4725	-0.5
21		20	7.9	1.0	14.2	203.0	-5.02	3600	-3.3
22		20 (ESC)	7.9	0.75	10.65	223.0	-4.50	6220	6.2
23		20 (ESC)	7.9	1.0	14.2	266.0	-4.95	5480	26.7
24		30	17.8	0.75	10.65	262.6	-3.72	6100	25.0
25		30	17.8	1.0	14.2	311.9	-3.27	7030	48.5
26		30 (ESC)	17.8	0.75	10.65	250.0	-3.70	7932	19.0
27		30 (ESC)	17.8	1.0	14.2	319.0	-3.12	7320	51.9

The results of 27 consolidated drained triaxial tests that were conducted in this experimental research study were also compared with the undrained triaxial tests presented by Najjar et al (2010). The following conclusions can be drawn with regards to the effect of sand columns on the drained load response of soft clay, volumetric strains during drained loading, and effective shear strength parameters:

- Using an area replacement ratio of 17.8% led to a reduction in the contractive volumetric strains of the clay specimens, with the reduction being more significant for tests involving fully penetrating sand columns, which are expected to be more dilative compared to partially penetrating columns. In contrast, the 7.9% area replacement ratio proved to have no significant effect in reducing the high volumetric strains. For cases involving ordinary columns, a correlation was observed between reductions in volumetric strains and increases in deviatoric stresses at failure. Such a correlation was not present in samples with encased columns.
- Similarly, using non-encased 2-cm diameter sand columns did not result in a significant increase in the deviatoric stress at failure except for the case of fully penetrating columns with a confining pressure of 100 kPa which yielded an increase of 17.6%. However, encasing the 2-cm columns increased the improvement at 100 kPa to 41.3%, while improvements in the order of 25% were observed for confining pressures of 150 and 200 kPa. For the 3cm columns, the improvements ranged from 31.2% to 51.5% for samples reinforced with fully penetrating ordinary columns and from 17% to 25% for partially penetrating ordinary columns. Again, encasing the columns led to additional improvements in the deviatoric stress at failure, with the

improvement ranging from 51.9% to 83.9% for specimens reinforced with fully penetrating columns and from 19% to 37.5% for partially penetrating columns.

- The effective friction angle ϕ' and the apparent cohesion c' were not significantly affected for clay specimens that were reinforced with partially penetrating 2-cm sand columns. For fully penetrating 2-cm columns, non-zero c' values were observed and were associated with unchanged or slightly reduced ϕ' values compared to the control clay specimens. The notable improvement in deviatoric stresses at 100kPa confining pressure compared to the 150 and 200kPa confining pressures led to these non-zero c' values.
- For the larger area replacement ratio of 17.8% improvements in ϕ' were observed for ordinary columns (ϕ' increased from 21º for the control clay to 23º for partially penetrating columns to 26º for fully penetrating columns), while improvements in c' were observed for encased columns (c' values increased from 0 kPa for control samples to 15 kPa for partially penetrating columns to 34 kPa for fully penetrating columns). These results of encased columns are in line with previous research which shows that encasing sand columns with geosynthetics results in non-zero cohesive intercepts (Wu and Hong 2009), with the increases in c' being associated with no improvements in the friction angle ϕ'.
- The author compared the results of the drained and undrained tests. Results show that the degree of improvement of the undrained strength of clay reinforced with granular inclusion is better than the measured improvement of the drained strength. However, at any confining pressure the drained strength

was found to be consistently greater in magnitude than the undrained strength.

- The above observation indicates that in field applications, the undrained strength of the composite system will likely govern the bearing capacity of the reinforced clay.

The author also observed that differences in the failure envelops from drained and undrained tests tend to become smaller as the differences in the mean effective stresses between drained and undrained tests become smaller.

2.5. "Partially Drained" Triaxial Tests

Juran and Guermazi (1987) and Andreou et al. (2008) studied the effects of partial drainage and rate of loading on the improvement brought by the addition of sand columns to soft soils in a triaxial framework.

2.5.1. Juran and Guermazi (1988)

Juran and Guermazi used a modified triaxial cell to investigate the effect of partial drainage of a soft silty soil. Their study consisted of using silty soil specimens with a 10cm diameter reinforced with compacted river-sand columns (RD=80%, ϕ'=38°) at an area replacement ratio of 4 and 16% which translate into 2cm and 4cm diameter columns respectively. Two types of tests were conducted by the authors. The first series of tests were conducted tests at a rate of 0.05mm/min while allowing drainage of the sand columns, and thus getting a partially drained behavior. In the second series of tests both the sand column and the surrounding soil were not allowed to

drain, resulting in an undrained test. Results presented in Figure 2.17 indicated that the drained column had a positive effect on the system and improved the resistance of the soil. Moreover, results indicated that the maximum load carried by the "drained" column was about twice that carried by the undrained column. The stress concentration ratio was equal to about 6 for samples that were reinforced with the drained column compared to 3 for samples reinforced with undrained columns.

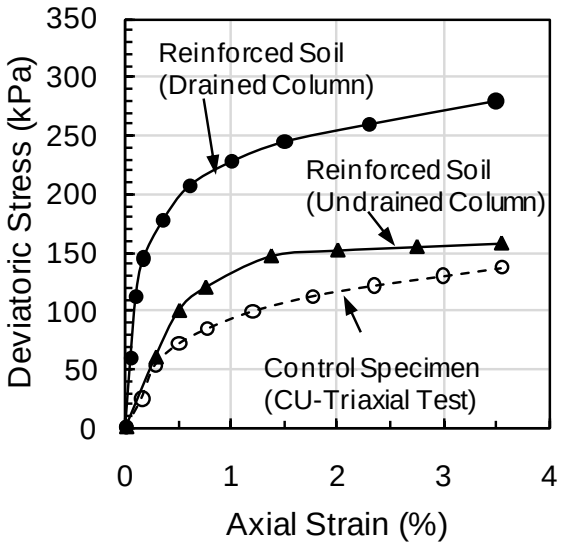

Figure 2.17. Effect of drainage on response of reinforced soil specimens to triaxial compression

2.5.2. Andreou et al. (2008)

Andreou et al. (2008) conducted triaxial compression tests on kaolin clay reinforced with single columns consisting of Hostun (HF) sand and gravel. In order to highlight the influence of the drainage conditions and rate of loading, the authors conducted drained, undrained, and partially drained tests. The kaolin clay specimens had a diameter of 10cm and were reinforced with columns with a diameter of 2cm and a

height of 20cm, leading to an area replacement ratio of 4%. The samples were consolidated under confining pressures of 50 to 200kPa. Results in Figure 2.18 indicated that the strength increase in the reinforced specimens is dependent on both the drainage condition and the loading rate. The maximum deviatoric stress carried by the reinforced sample under drained conditions is twice that of the undrained condition. In the partially drained tests the authors increased the rate of shearing (from 0.003 to 0.3mm/min) while allowing drainage. These conditions lead to a reduction in the strength of the reinforced sample compared to the fully drained case; however, the measured strength remained higher than that of the reinforced undrained sample. The undrained tests results indicated that as the confining pressure increased from 50 to 200kPa the improvement in undrained strength decreased from 45 to 20%. Furthermore, the effective friction angle increased slightly compared to unreinforced samples (23^o to 24^o).

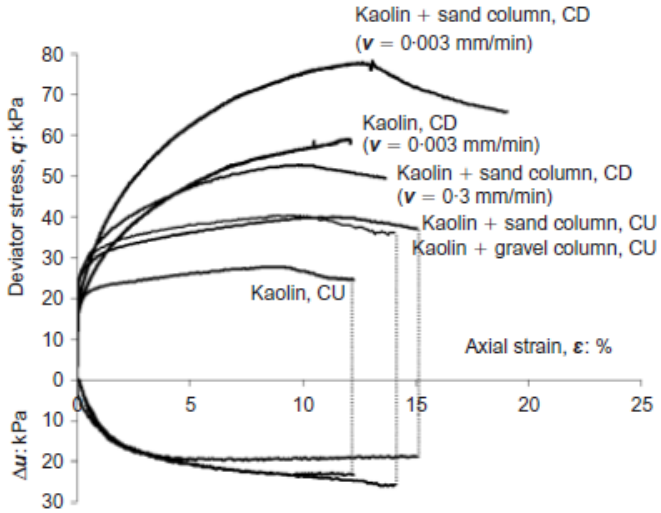

Figure 2.18. Variation of deviator stress and excess pore pressure with axial strain

2.6. Summary

In the course of the last 30 years, results from laboratory and field tests and numerical modeling/analyses have converged to certain conclusions.

The mode of failure observed was mainly characterized by bulging and deformations concentrated in the upper 0.5 to 3 column diameters for long columns. Short columns tended to fail by punching into the lower layers of soft clays. Bulging of columns is significantly reduced when encased with a geotextile, and tends to be distributed along the whole length of the column rather than be concentrated in the upper or lower portion.

The improvement in bearing capacity and stiffness is significantly dependent on the area replacement ratio used.

Hughes and Withers (1974) were the first to propose the concept of a "critical column length". This approach suggests that the column length is only significant up to a certain depth, and further increasing its length will not result in an increase in its load bearing capacity. However, the increased length causes an increase in stiffness and thus reduces settlement which indicates that long columns are efficient in controlling settlements. Studies have put the critical length in the range of 5 to 8 times the diameter of the column.

Encasing the columns was shown to increase the stiffness of the columns and decrease pore pressure generation. The improvement however is not the same for all diameters and column densities. Smaller columns showed greater levels of improvement than larger diameter columns, and looser specimens gain more strength than dense

specimens. It is interesting to note here that some results of FEM analyses and laboratory testing have indicated that encasing the column could have a negative effect on strength, depending on the stiffness of the geotextile. This decrease in strength is attributed to the restricted bulging which utilizes the passive resistance of the surrounding soil.

CHAPTER 3

TEST MATERIALS AND SAMPLE PREPARATION

3.1. Introduction

This chapter describes the properties of the materials used in the testing program. These materials include Kaolin clay, Ottawa sand, and the geotextile fabric. Atterberg limits, specific gravity, hydrometer analysis, and 1-dimensional consolidation tests were performed using Kaolin clay. The results of the consolidation tests were used to determine the coefficient of consolidation of the clay using the log time method and the square root of time method. For Ottawa sand, sieve analysis, triaxial, and relative density tests were performed. The geotextile fabric was subjected to pull out tests for the purpose of determining the tensile strength and the stiffness of the material, with the fabric oriented in both the lateral and the vertical directions.

Furthermore, a detailed description of the process of sample preparation is presented. The process includes the preparation of Kaolin specimens form a slurry, 1-dimensional consolidation of the slurry in custom-fabricated consolidometers, and installation of encased and frozen sand columns in pre-augured holes in the specimens.

3.2. Test Materials

3.2.1. Kaolin Clay

Kaolin clay was brought to the laboratory in sealed bags with a weight of 25kg from Uniceramic, a local tile manufacturer. A large percentage of the clay was composed of round clodded particles with an approximate length of 2cm and a diameter of about 0.4cm. The clay clods were crushed with a rubber tipped hammer and stored in a tightly closed plastic drum in order to preserve their water content. Index properties for the Kaolin clay were determined in the laboratory and are presented in Table 3.1.

Table 3.1. Index properties of Kaolin clay

Liquid limit (%)	Plastic limit (%)	Plasticity index	Specific gravity	Percent finer than 10 μm (%)	Percent finer than 2 μm (%)
55.7	33.3	22.4	2.52	85	53

The consolidation properties of the Kaolin slurry were obtained from a one-dimensional consolidation test that was conducted on a clay sample with a diameter of 5.08cm and a height 1.91cm. The test specimen was trimmed from a larger specimen which was consolidated from a slurry in a 1-dimensional prefabricated consolidometer under a vertical effective stress of 100 kPa as will be explained in section 3.3.2. The specific gravity, initial water content, and initial void ratio of the slurry-consolidated specimen are presented in Table 3.2.

Maalouf (2012) conducted the consolidation test in accordance with

requirements of ASTM 2435, with the results are presented in Table 3.3 and 3.4. For further information refer to Maalouf (2012).

Table 3.2. Initial properties of 1-dimensional consolidation test specimen of Kaolin clay

Specific gravity	2.52
Initial water content (%)	61
Initial void ratio	1.53
Initial saturation (%)	100 (assumed)

Table 3.3. One-Dimensional consolidation pressure test results

Cosolidation pressure (kPa)	Final dial reading (cm)	Change in specimen height (cm)	Final specimen height (cm)	Height of void (cm)	Final void ratio	Average height during consolidation (cm)
0	0		1.905	1.153	1.534	
		0.144				1.833
10	0.144		1.761	1.009	1.342	
		0.033				1.7445
20	0.177		1.728	0.976	1.298	
		0.05				1.703
49	0.227		1.678	0.926	1.232	
		0.068				1.644
98	0.295		1.61	0.858	1.141	
		0.08				1.57
196	0.375		1.53	0.778	1.035	
		0.09				1.485
383	0.465		1.44	0.688	0.915	
		0.097				1.3915
775	0.562		1.343	0.591	0.786	
		0.103				1.2915
1550	0.665		1.24	0.488	0.649	
		-0.044				1.262
383	0.621		1.284	0.532	0.708	
		-0.07				1.319
98	0.551		1.354	0.602	0.801	
		-0.062				1.385
20	0.489		1.416	0.664	0.883	

Table 3.4. Coefficient of consolidation obtained from t50 and t90

Consolidation pressure (kPa)	Coefficient of consolidation, C_v (cm^2/min)	
	From t_{90}	From t_{50}
10	0.055	0.103
20	0.101	0.156
49	0.104	0.156
98	0.112	0.175
196	0.136	0.182
383	0.147	0.231
775	0.152	0.214
1550	0.030	0.013

3.2.2. Ottawa Sand

The soil used in the reinforced columns was Ottawa sand which is a well-known laboratory tested material. Grain size distribution analyses conducted on Ottawa sand indicate that the particles have a mean diameter, D_{50} of 0.34mm, a uniformity coefficient, U_c of 2.3, and a coefficient of curvature, C_c of 0.82. The sand classifies as poorly graded sand (SP) according to the Unified Soil Classification System (USCS). The index properties for Ottawa sand and the sieve analysis results are shown in Table 3.5. and 3.6, respectively, while the particle size distribution curve is shown in Figure 3.1.

Table 3.5. Index properties of Ottawa sand

D_{10} (mm)	0.22
D_{30} (mm)	0.3
D_{60} (mm)	0.5
Coefficient of uniformity (D_{60}/D_{10})	2.3
Coefficient of curvature $(D_{30})^2/(D_{60}*D_{10})$	0.82
Soil classification (USCS)	SP
Maximum void ratio (e_{max})	0.49
Minimum void ratio (e_{min})	0.75
Specific gravity	2.65
Drained angle of internal friction (Ø')°	33

Table 3.6. Sieve analysis results for Ottawa sand

Sieve No.	Diameter (mm)	Weight of retained soil (gm)	Cumulative percent retained (%)	Cumulative percent finer (%)
20	0.84	0	0.0	100.0
40	0.42	223.8	28.0	72.0
60	0.25	464.4	86.2	13.8
100	0.15	87.2	97.1	2.9
140	0.105	18.5	99.5	0.5
200	0.075	1.5	99.6	0.4
pan		2.8	100.0	0.0

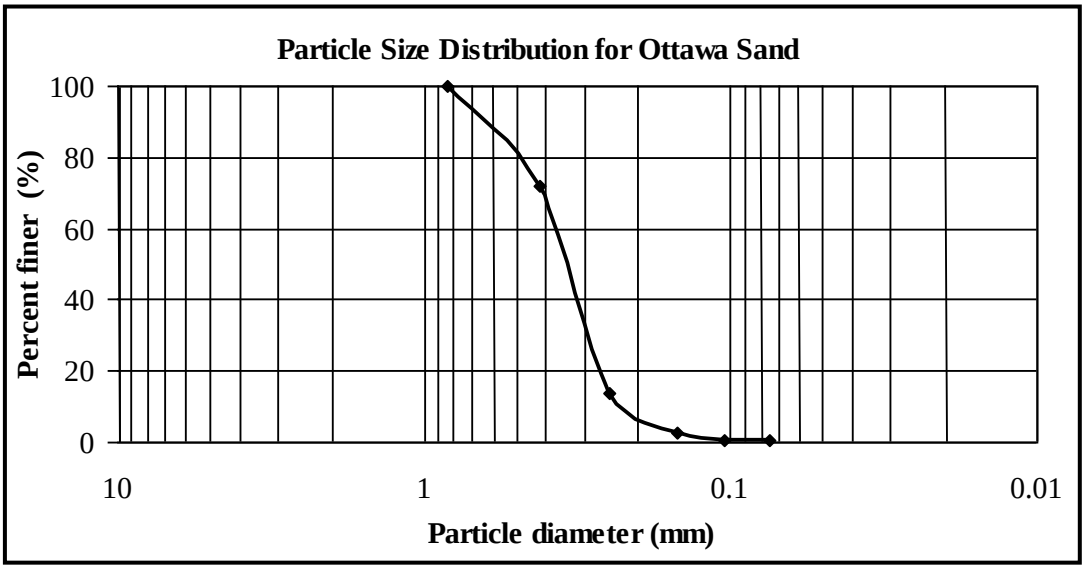

Figure 3.1. Sieve analysis curve for Ottawa sand

Consolidated drained (CD) and undrained (CU)triaxial tests were conducted on Ottawa sand at confining pressures of 100, 150, and 200 kPa. Ottawa sand triaxial specimens with a height of 14.2cm and a diameter of 7.1cm were prepared at a dry density of 16.2 kN/m^3 (corresponding to a relative density of 44%, and a void ratio of 0.604). This density corresponds to the dry density of the sand column that was used to reinforce the Kaolin clay specimens in the testing program. Variation of deviatoric stress and volumetric strain with axial strain for the Ottawa sand during CD testing at the different confining pressures is shown on Figure 3.2.a. As indicated by the Mohr Coulomb effective stress failure envelop for the Ottawa sand (Figure 3.2.b), the drained angle of friction (Ø') corresponds to a value of about 35º and a cohesion of zero. Results for the undrained tests are documented in Najjar et al (2010).

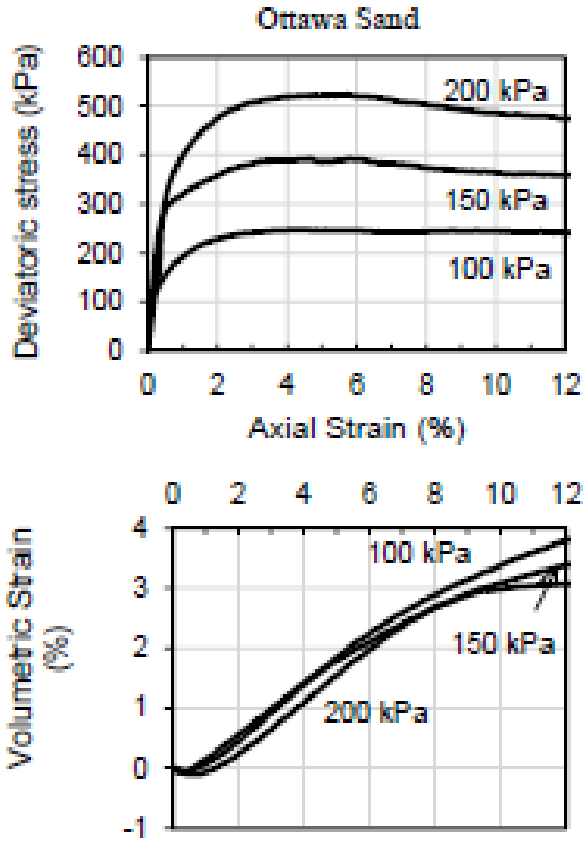

Figure 3.2.a. Deviatoric stress and Volumetric strain versus axial strain for Ottawa sand at confining pressures (σ'_3) of 100 kPa, 150 kPa, and 200kPa

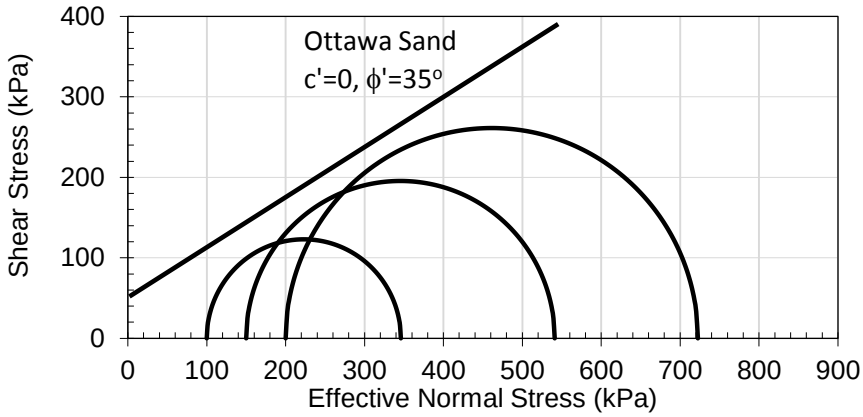

Figure 3.2.b. Mohr Coulomb effective stress failure envelop for Ottawa sand

3.2.3. Geotextile Fabric

The selection of the type of the geotextile fabric was made based on several criteria. First, the fabric had to ensure a moderate lateral support for the encased Kaolin specimen during loading. Second, the geotextile fabric had to provide proper drainage of pore water during isotropic consolidation. Finally, the fabric had to prevent the mixing of the sand column material with the surrounding clay during insertion of the column into the Kaolin specimen. Based on these criteria, the geotextile fabric was selected and brought from a tailor supplier. The width of the geotextile fabric roll was 0.8m and its length was 5m. At the tailor shop, the geotextile fabrics were cut and sewed to provide a cylindrical shape having a length of 19cm and diameters of 4cm as shown in Figure 3.3. The fabrics were sewed along the weak longitudinal direction, which represents the orientation of the weak fabric for the geotextile material. The orientation of the strong fabric was in the lateral direction.

The tensile strength of the geotextile fabric was determined in the laboratory using a digital force gauge. A piece of fabric with a length of 30cm, a width of 10cm, and a thickness of 0.11mm was subjected to a pullout force by fixing one end of the geotextile and applying a tensile force to the other end. In the test, the fabric was fixed at each end to two steel plates by wrapping the fabric into multiple layers between the plates, which were attached to each other using two bolts (Figure 3.4). From one end, the steel plates were connected to a fixed plate through a steel ring, while from the other end the plates were connected to the digital force gauge through a hook as shown in Figure 3.4. The peak rupture force was recorded on the screen of the digital force gauge.

Figure 3.3. Preparation of cylindrical geotextile fabric of 4cm diameter

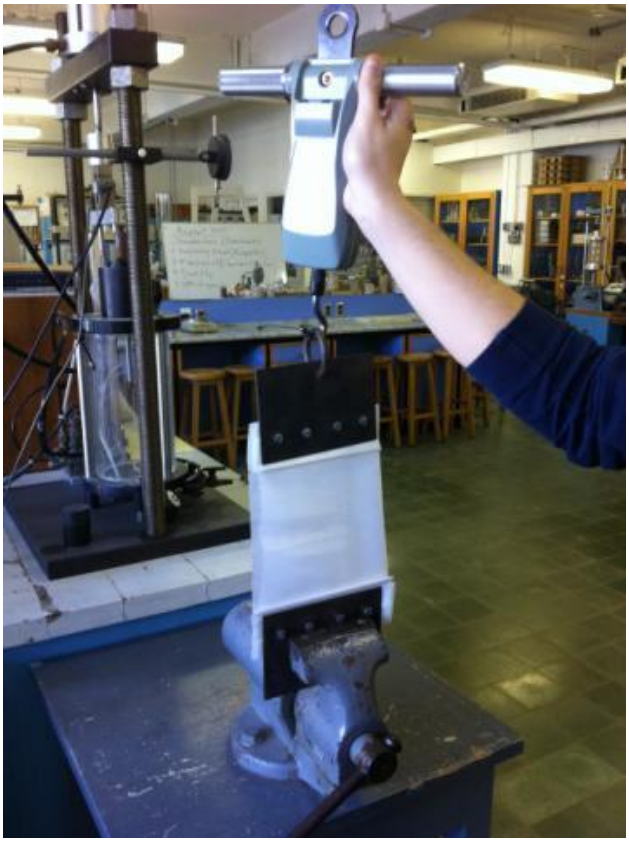

Figure 3.4. Performing pull out test on geotextile fabric

The fabric was tested in dry and soaked conditions and along the strong and weak fabric orientations. Each test was repeated twice to confirm the results and to obtain average values for the tensile force. The average values for the tensile strength of both dry and soaked geotextiles are presented in Table 3.7. Soaking the fabric with water led to a 25% decrease in the value of the tensile strength, which was determined to be about 5.8 MPa and 3 MPa for strong and weak fabric orientations, respectively. Moreover, the secant modulus of elasticity for the dry and the soaked geotextile fabrics was determined at a strain of 1% as shown in Table 3.7.

Table 3.7. Results of pullout tests on geotextile fabrics

Test#	Fabric orientation	Geotextile condition		Tensile force (N)	Average tensile strength (KPa)	Secant modulus of elasticity at 1% strain (KPa)
		Dry	Soaked			
1	Along strong fabric orientation	X		61	5770	35400
2		X		66		
3			X	47	4410	22600
4			X	50		
5	Along weak fabric orientation	X		31	3000	14300
6		X		35		
7			X	22	2300	10000
8			X	28		

3.3. Preparation of Normally Consolidated Kaolin Samples

3.3.1. Preparation of Kaolin Slurry

Kaolin clay powder was mixed with water at a water content of 100% (i.e. 1.8 times its liquid limit). A mass of 0.5kg of Kaolin material was initially mixed with 0.5

liters of water by means of an electric mixer with a capacity of 1.5 liters (Figure 3.5). To ensure proper mixing and homogeneity of the slurry material, the slurry was mixed at a constant rate of 200 rounds per minute for a period of one minute.

Figure 3.5. Electric Mixer for preparing Kaolin slurry

3.3.2. One-Dimensional Consolidometers

Four 1-D consolidometers were fabricated for the purpose of consolidating the Kaolin slurry (Figure 3.6). Each consolidometer consisted of a PVC pipe segment with a height of 35cm, an external and internal diameter of 7.3cm and 7.1cm respectively, and a wall thickness of 0.1cm. The PVC pipe segment was cut longitudinally in the vertical direction into two halves to function as a split mold (Figure 3.7. a), thus eliminating the need for extruding the soil sample after consolidation. The two PVC sections were held in place using high-strength duct tape (Figure 3.7. b) which was wrapped around the two cylindrical PVC sections to prevent leakage of slurry and to

ensure that lateral strains are negligible during 1-D consolidation under the desired axial load. The advantage behind using a split PVC pipe was to ensure that an undisturbed, relatively soft, normally consolidated clay specimen can be obtained and removed with minimal disturbance after consolidation was achieved.

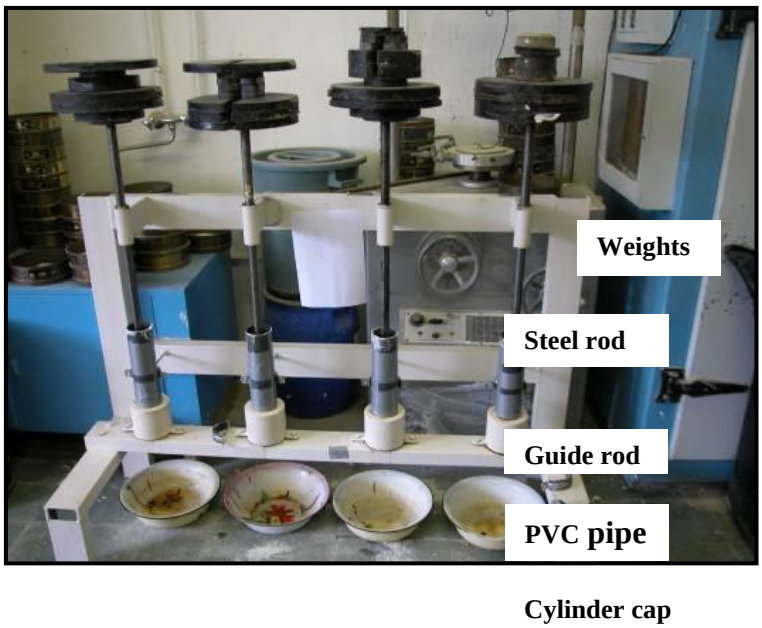

Figure 3.6. Picture for custom fabricated 1-dimensional consolidometers

Figure 3.7. Photo for Split PVC pipe and Wrapped PVC pipe with duct tape

At its lower end, the PVC pipe segment was fixed in place by means of a hollow steel cylinder with a height of 9cm as shown in Figures 3.6 and 3.8. The stiff and heavy cylinder wraps tightly around the bottom of the PVC segment to provide additional lateral confinement and support to the PVC segment during slurry consolidation. The inner walls of the steel cylinder were coated with a thin layer of oil to facilitate the removal of the PVC segment once consolidation was achieved. Moreover, the circumference of the steel rod was coated with a thin layer of grease at the location of the steel rod guide to reduce friction between the steel rod and the guide rod. A porous stone and a filter paper were used to provide a freely draining boundary at the lower end of the soil specimen.

At its upper end, the soil specimen was loaded with a loading system consisting of dead weights similar to those used in 1-D consolidation tests. The dead weights were seated on a circular steel plate that transferred the load to the top of the soil specimen through a circular steel rod having a diameter of 1cm. A perforated circular steel piston with a diameter of 7.1 cm (same as inner diameter of PVC pipe) was fixed to the bottom of the steel rod to act as a loading plate which transmitted the load to the slurry. The soil was separated from the loading plate with a porous stone and a filter paper to provide a freely draining boundary at the top of the soil specimen. To reduce friction between the perforated loading plate and the PVC segment, the outside periphery of the loading plate was also coated with a thin layer of oil.

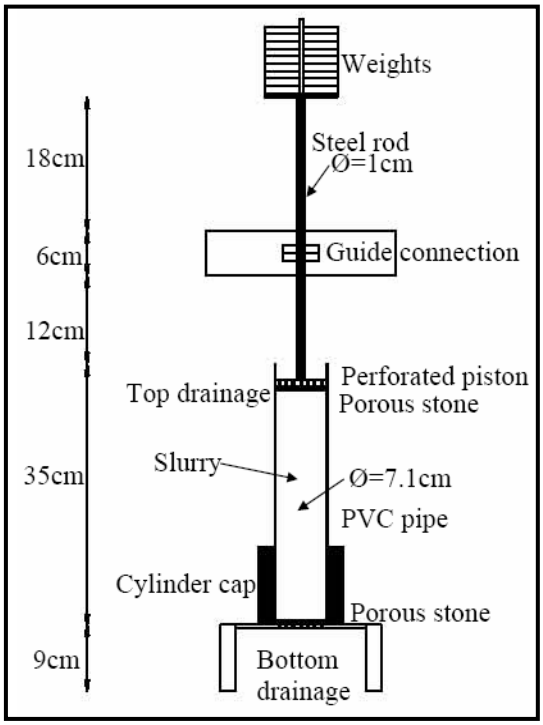

Figure 3.8. Custom fabricated 1-dimensional consolidometer

3.3.3. One Dimensional Consolidation of Kaolin Slurry

The slurry was poured into the appropriate consolidometer and consolidated under K_o conditions using a vertical effective stress of 100 kPa. With four consolidometers, four clay samples could be prepared simultaneously, three of which were used for testing while the fourth sample was kept on reserve. Each consolidometer could handle a volume of slurry that is equivalent to two mixed batches of kaolin slurry, i.e. one kg of Kaolin with one liter of water. After pouring the slurry in the appropriate consolidometer (initial specimen height was 35cm), the clay was allowed to consolidate under its own weight for a period of 4 hours. During 1-D consolidation, drainage was allowed from both ends of the sample through the top and bottom porous stones. Dead

weights were then added in stages to the top of the sample, with each weight applied for a specified time period according to the loading sequence shown in Table 3.8.

Table 3.8. Loading sequence during 1-D consolidation of Kaolin slurry

Accumulated weights (Kg)	0.5	1	2	4	8	12	20	30	40
Applied pressure (kPa)	1.25	2.5	5	10	20	30	50	75	100
Duration (Hr)	4	4	24	24	24	24	24	24	24

The consolidation time periods that were allocated to each loading increment were estimated based on the results of the 1D consolidation test and were adjusted using trial and error. The objective was to develop a loading sequence which was repeatable, and which resulted in Kaolin specimens that were uniform. A typical time duration that is required to fully consolidate a clay sample under an effective normal stress of 100 kPa is approximately 7.5 days.

The water content after consolidation was found to be relatively uniform (about 53%) throughout the depth of the sample. The variations of the water content and the void ratio with depth were determined by slicing a consolidated clay sample into 7 pieces and determining the void ratio and water content for each slice. The variation of the void ratio and water content with depth for a typical sample is shown in Figure 3.9. The variations are relatively small indicating a relatively uniform degree of

consolidation in the sample. As expected, the void ratio was found to be the smallest at the upper and lower ends of the sample where the sample is completely drained during consolidation.

Additional measures were taken to further reduce disturbance during sample preparation. These measures included spreading a thin layer of oil over the inner surfaces of the PVC pipes to reduce friction between the kaolin specimen and the inner surface of the pipe. This allowed for dismantling the pipe and removing the soil specimen from the consolidometer with minimal disturbance to the soil specimen.

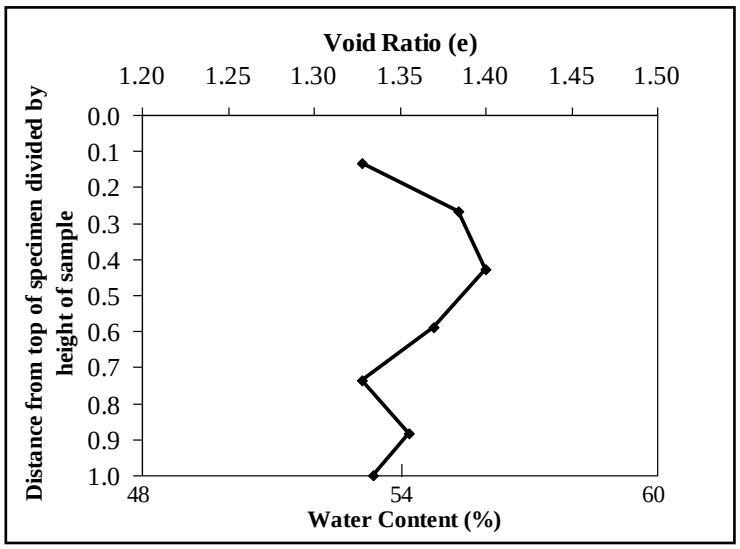

Figure 3.9. Water content and void ratio along the height of the sample after consolidation

3.3.4. Sample Preparation Prior to Placement in the Triaxial Cell

At the end of primary consolidation under a pressure of 100 kPa, the dead weights were removed and the PVC cylinder was slowly pulled out from the cylindrical

cap of the consolidometer. The duct tape surrounding the periphery of the PVC cylinder was unwrapped and the two PVC pieces were dismantled. The consolidated Kaolin specimen is shown in Figure 3.10 along with the above two steps. The clay specimen was then trimmed to a final height of 14.2cm (initial height is about 18 cm) by means of a sharp spatula. Two presoaked porous stones were then placed on the top and bottom of the Kaolin specimen and the sample was prepared for triaxial testing. Finally, the sample was wrapped with a presoaked filter paper that has longitudinal perforations in order to speed up the process of consolidation in the triaxial cell. Figure 3.11 illustrates the above explained process.

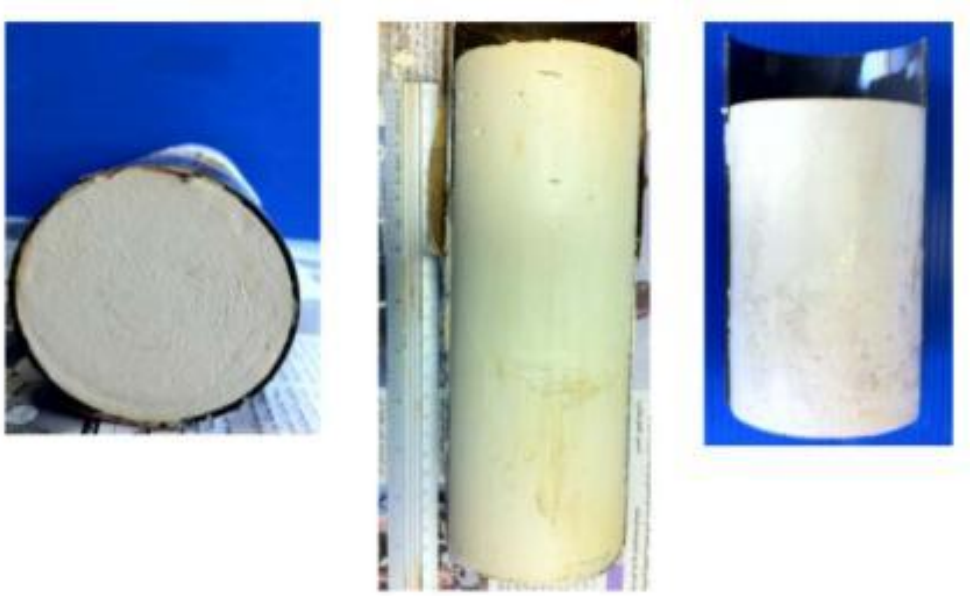

Figure 3.10. Kaolin specimen after removal from custom fabricated consolidometer, dismantling of PVC pipe, and Kaolin specimen after removal form PVC pipe

Figure 3.11. Kaolin specimen after trimming, installation of porous stones, and installation of filter paper around Kaolin specimen.

A thin rubber membrane with a diameter of 7.1cm was then placed on the inside of a cylindrical brass membrane stretcher. To facilitate the placement of the membrane into the stretcher, a thin layer of powder was sprayed over the membrane. Vacuum was then applied to ensure that the membrane adhered well to the inner walls of the stretcher. The stretcher was then positioned around the soil specimen and the vacuum was released. Rubber bands were used to fasten the membrane tightly around the specimen. The specimen was then attached to the base of the triaxial cell and the top drainage tubes were inserted into the holes of the top cap. The triaxial cell was then assembled and the seating piston positioned over the top cap. Figure 3.12 illustrates the above mentioned procedure. Finally, the triaxial cell was placed in the "TruePath" system in preparation for saturation, consolidation, and shear as will be explained in Chapter#4.

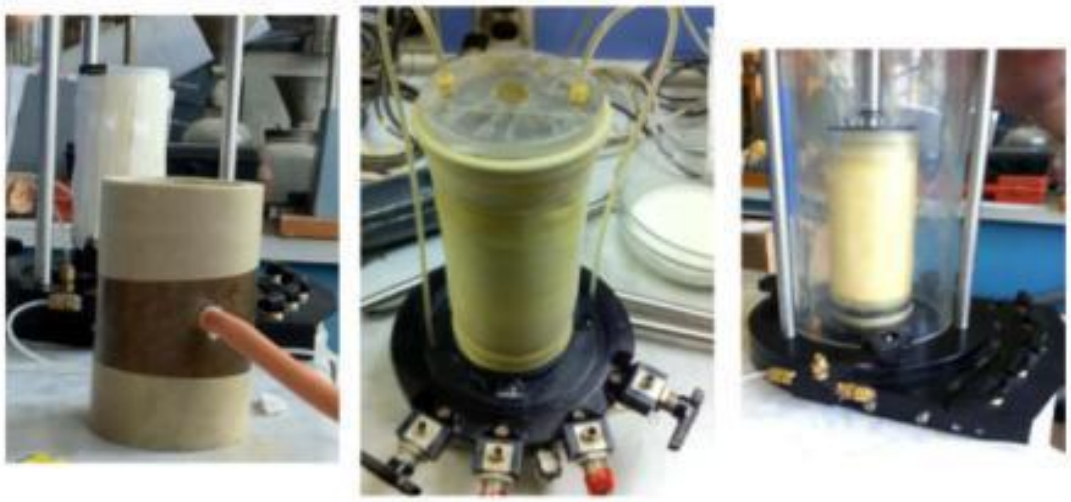

Figure 3.12. Brass tube with the rubber membrane. installation of Kaolin specimen on the cell chamber, and insertion of glass cover around cell chamber.

3.4. Preparation of Sand Columns

The first step in the preparation of clay specimens that were reinforced with single sand columns involved the formation of a hole with a diameter of 3cm or 4cm, in the middle of the clay specimen. For this purpose, a custom-fabricated hand auguring apparatus was manufactured in the machine shop. The auguring apparatus was used to drill holes with different penetration depths in the clay specimen. The procedure followed in drilling holes is presented below.

After dismantling the cylindrical Kaolin specimen from the PVC pipe and trimming it to a final height of 14.2cm, the specimen was wrapped with two lubricated plastic cylindrical PVC tubes which were in turn wrapped with duct tape around their circumference as shown in Figure 3.13. The wrapped specimen was then placed on the auguring apparatus that is shown in Figure 3.14. Augurs with diameters of 3cm or 4cm were connected to the auguring machine. During drilling, the vertical alignment of the

rotating rod is maintained through the presence of plastic guide plates that are connected to the top and bottom of the steel rod. The penetration of the augur into the specimen is continued in stages till the required penetration length is achieved.

Figure 3.13. Wrapping the Kaolin specimen with PVC tubes prior to auguring

Figure 3.14. Custom fabricated auguring machine, 4cm -diameter auger, auguring of specimen by 4cm diameter augur, Removal of Kaolin material by 4 cm diameter auger

For sand columns with heights of 10.65cm (partially penetrating column), a mark was made on the steel rod to indicate the required penetration distance of the augur. Auguring was continued in stages until the depth of the augured hole reached the marked length. The maximum penetration distance of the augur into the Kaolin specimen in each stage is 3cm for the purpose of reducing the suction pressure that is generated as the augur is retrieved from the Kaolin specimen.

3.4.1. Encased Sand Columns with Geotextile Fabric

For both encased and frozen sand columns, geotextile fabrics that were prepared to the desired diameter and length as discussed in Section 3.2.3 were used to construct a column using Ottawa sand. The empty cylindrical geotextile fabric was

inserted in a glass tube of the same diameter, which was in turn placed in a plastic tube. Ottawa sand was placed in the geotextile column in three layers, and every layer was vibrated for a period of 1 minute. Prior to placing sand in the empty geotextile column, the required column heights of 14.2cm, 10.65cm were marked on the geotextile by means of a pen and the calculated weight of sand that was required to reach the desired density was poured into the column. The dry density of the sand columns after vibration for the different column heights was 16.2 kN/m^3± 0.22. The same density was maintained for the two column diameters of 3 cm and 4 cm.

After ensuring that the target dry density is achieved, the sand column is saturated with water which is permeated slowly from the top of the column to its bottom. It was found that the sand columns generally get saturated at a water content of about 20%. The water content was measured after removing the sand column from the glass tube. Measurement of the total weight and the dimensions of the sand column indicated that the total weight corresponded to the saturated weight at a water content of about 20%. The bulk density of the vibrated sand column after adding 20% water was 19.4 kN/m^3± 0.22.

In clay specimens that were reinforced with encased sand column, the columns were inserted in the pre-drilled holes and any extra height of the geotextile fabric that remained protruding from the soil specimen was cut using a sharp cutter. Figure 3.15 shows the sequence of installing encased sand column into the Kaolin specimen.

Figure 3.15. Installation of 4-cm diameter encased sand column with geotextile fabric

3.4.2. Frozen Sand Columns

Sand columns that were encased with geotextile fabrics were also used to prepare frozen columns. After saturating the sand column with water, the column was inserted into a flask and placed inside the freezer. After freezing, the geotextile fabric was detached from the frozen sand column by cutting the geotextile fabric along its vertical stitching using a sharp cutter. To prevent thawing of the sand column while cutting the geotextile fabric, the cutting operation was performed on a tray filled with frozen water. The unreinforced sand column (Figure 3.16) was then inserted in the predrilled hole (Figure 3.17) and left to thaw. It is worth noting that while preparing frozen sand columns, the fabric was initially overturned so that stitches of the geotextile were on the outer face. This facilitated the process of removing the fabric prior to installing the frozen columns in the clay specimen. The uniformity and the vertical alignment of the inserted frozen sand column are revealed in Figure 3.18 where a kaolin specimen was cut vertically along its length directly after inserting the frozen sand column of diameter 4cm and height of 10.65cm.

Although freezing of sand columns is not usually implemented in the field, the idea behind using frozen sand columns in this research is to be able to construct columns with mechanical properties that are repeatable and uniform across the different samples. The friction angle of Ottawa sand depends on the initial density of the column material, which in turn depends on the column diameter. Thus, any variation in the column diameter form one sample to another will lead to variations in the column density and the friction angle of the column material. By constructing frozen columns in which sand particles are compacted outside the Kaolin specimen, the column diameter and density will be uniform and repeatable.

Figure 3.16. 3cm frozen sand column

Figure 3.17. Predrilled 3-cm diameter hole, Insertion of frozen sand column in clay, and reinforced Kaolin specimen with frozen sand column

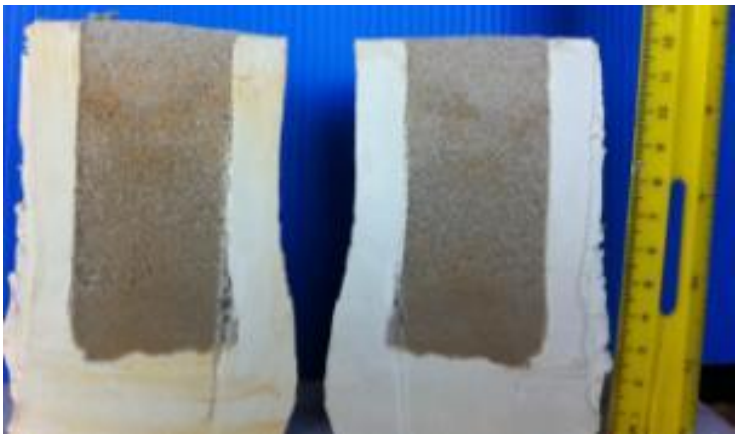

Figure 3.18. Photograph of vertical cross section of Kaolin specimen with frozen sand column of diameter 4cm and height 10.65cm after column insertion

3.5. Summary

Index and compressibility characteristics for the Kaolin clay were presented in a comprehensive way in this chapter; moreover, the engineering properties, particle size distribution, and shear strength of Ottawa sand were also presented in this chapter. Through using a digital pullout tensile machine, the tensile strength of the geotextile fabric in both directions, strong and weak fabric orientation, was determined using a digital force gauge. Kaolin was prepared from slurry and consolidated in a prefabricated one dimensional consolidometer after which Kaolin specimen was arranged for testing. Step by step methods for preparing encased and frozen sand columns were discussed in a simple way enriched with pictures and photos for the purpose of clarifying the preparation process and making it plain and easy for tracking the details for the method of sand column preparation.

CHAPTER 4

TRIAXIAL TESTING

4.1. Introduction

This chapter describes the method and steps to be followed in performing consolidated drained tests using the automated triaxial "TruePath" equipment. The step by step approach which describes the process from the initial stage of seating the test specimen to the final stage of shearing the specimen under drained conditions is designed to be a guide for future users of the "TruePath" equipment.

4.2. General Steps in Performing Consolidated Drained (CD), Consolidated Undrained (CU) and Consolidated Partially Drained (PD) Tests

After preparing the Kaolin specimen as described in section 3.3.4, the triaxial cell (with the sample inside it) is placed in the automated triaxial "TruePath" system. The main components of the system are presented in Figure 4.1. The "TruePath" system consists of four main parts which are the load frame with pressure transducer and the deformation sensor, the cell pump which provides the confining cell pressure to the cell chamber, the back/pore pump which provides the back pressure for the specimen and measures the pore water pressure through connecting a pressure transducer to valve#3 (as will be explained in a later stage), and the operating system which allows the user to

perform the test and monitor its progress through the screen that displays all the stages of the test.

The triaxial test consisted of four stages which include seating, back pressure saturation, consolidation, and shearing. Each stage is characterized by a series of commands that appear on top of the screen and guide the user throughout the test. The four tabs, which represent each stage, become active after specimen and test data files are created. A specific tab representing a specific stage will become active only after the previous stage is completed. The following steps describe the detailed procedure to be followed in performing consolidated drained tests (CD) on normally consolidated clay samples.

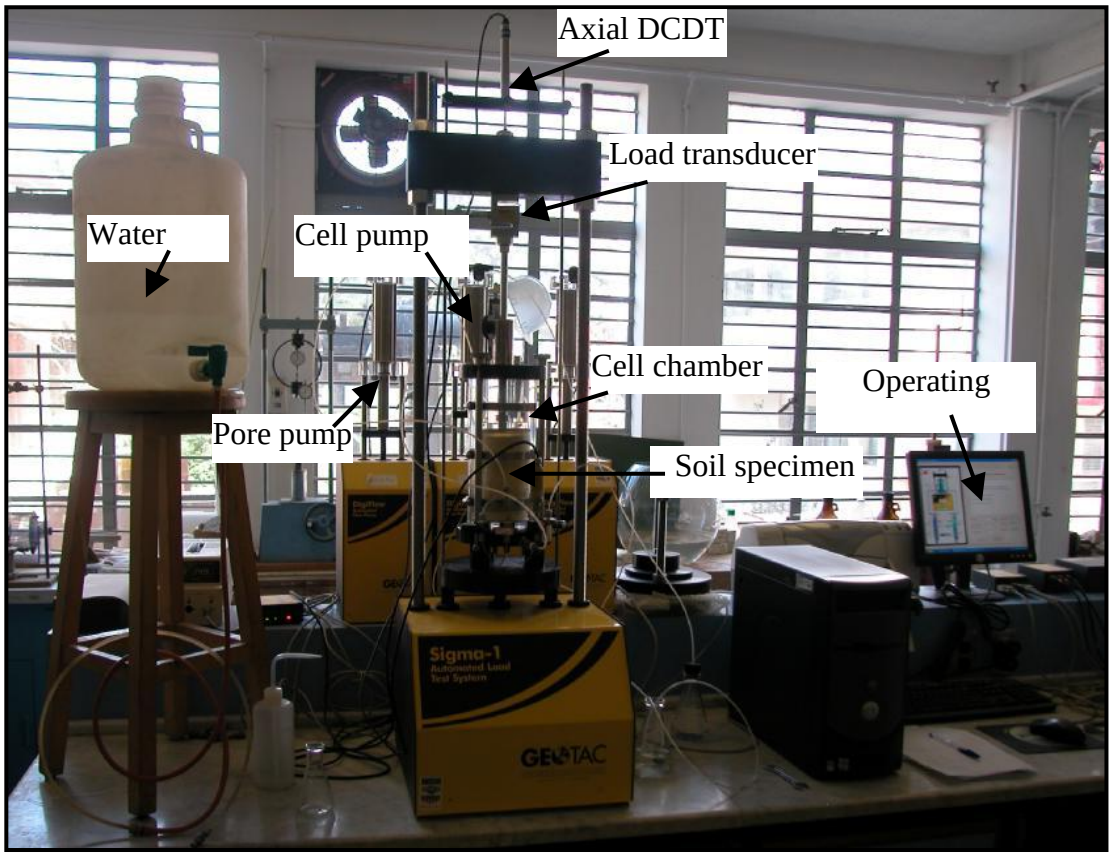

Figure 4.1. Automated triaxial equipment “TruePath

4.3. Creating Specimen and Test Data Files

In order to view the test results while performing the test, the file called “graph initiative” should be deleted prior to the start of the test from the “TruePath” folder which is located under the “program files” folder. The first step in performing the CD test involved setting all the sensors and load transducer readings to zero. This can be achieved by entering the “Set Up” menu and selecting “Sensor”. After highlighting the required sensor or transducer and pressing “Test”, a window will appear for the selected sensor. On this window, the “Take Zero” button should be pressed so that the sensor reading will indicate the average of ten consecutive readings that are almost zero. This process should be repeated for all the sensors, i.e. pore pressure, back pressure, cell pressure sensors, external load cell and axial DCDT. Figures 4.2 to 4.4 show a step by step procedure for setting the sensors to zero readings.

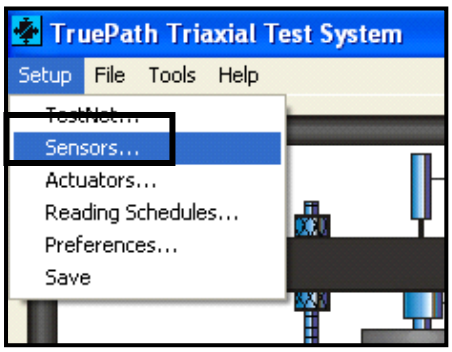

Figure 4.2. Selection of sensor button

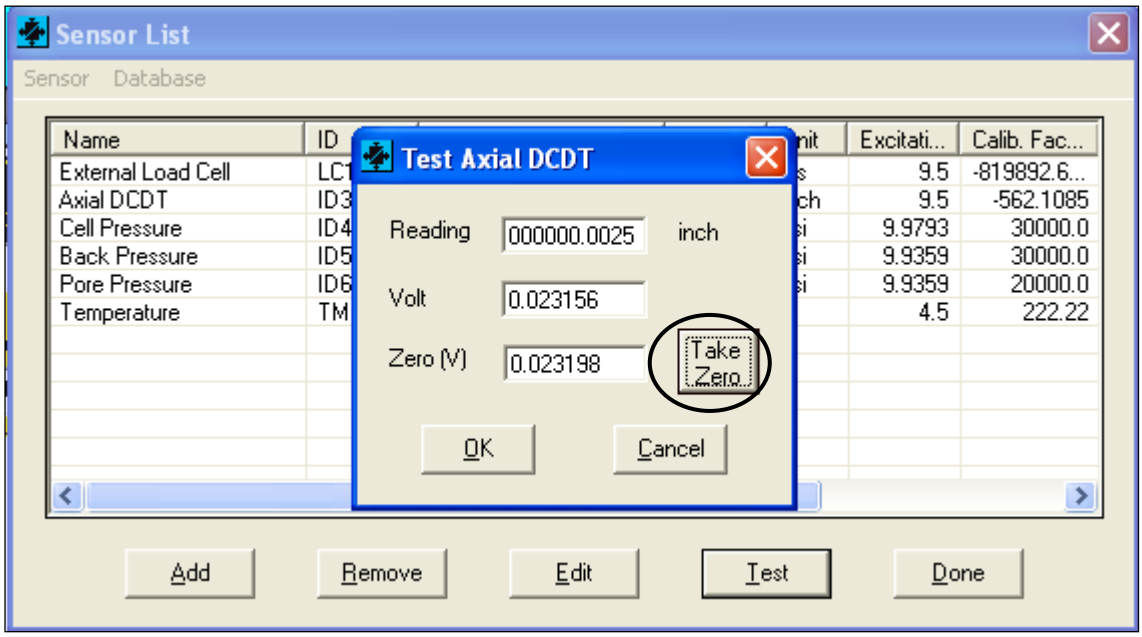

Figure 4.3. Selection of the cell pressure sensor

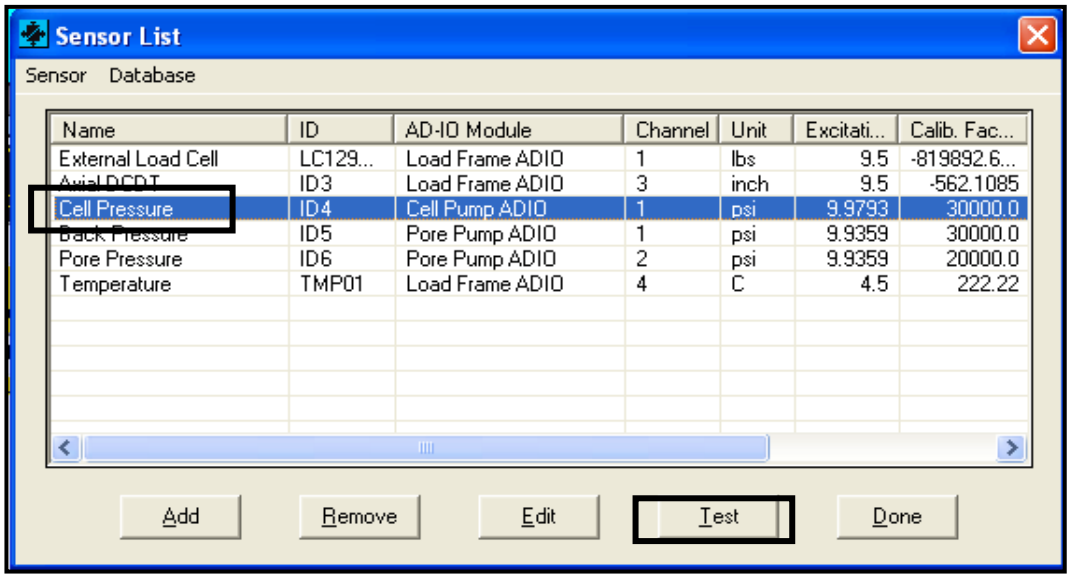

Figure 4.4. Initializing readings for the selected sensors

The second step involved accessing the “File” menu and choosing “Specimen Data” as shown in Figure 4.5. Then the “specimen data” window will appear as shown

in Figure 4.6 where the user has to click each box to fill the appropriate information which includes the sample height (5.79 inch), sample diameter (2.5 inch), and the sample number and project number. The third step is also initiated from the "File" menu by selecting "Test Data" as shown in Figure 4.5. A window will appear as shown in Figure 4.7 where the user has to enter the control test parameters in the empty spaces.

The input data for the test consists of four categories that are included in one window. The user has to enter the following:

- The value of the target seating pressure which is defined as the seating confining pressure needed to keep the membrane pressed against the specimen during the flushing of the drain lines. A pressure of 5 Psi (35kPa) is used for the samples in the testing program.
- The value of the saturation/back pressure that is needed to saturate the sample. A pressure of 45 Psi (310 kPa) is chosen for the Kaolin sample to ensure proper saturation.
- The type of consolidation (isotropic in this test program) and the value of the target effective stress that is needed to consolidate the sample. Since the test program involved three different confining cell pressures, an initial cell pressure of 14.5 Psi (100 kPa) was applied to the Kaolin sample, and then in the consolidation stage, the confining pressure was raised to the required values of either 21.75 Psi (150 kPa) or 29 Psi (200 kPa). The stress rate for the target effective stress was chosen to be 300 Psi (2073 kPa) per hr to guarantee instantaneous application of the consolidation pressure.
- The drainage conditions which were defined in this testing program to be either "consolidated drained" (CD) for CD and PD tests or CU' for

undrained (CU) tests, the loading direction which was chosen to be "compression", the maximum vertical effective stress which was taken as 150 Psi (1036 kPa), the maximum strain which was taken as 18%, and the strain rate which was taken as 0.25%/hr for the drained tests, ranging from 3.5%/hr to 120%/hr for the partially drained tests and 1%/hr for the undrained tests . It was also chosen that shearing will be terminated when either the maximum stress or the maximum strain is reached.

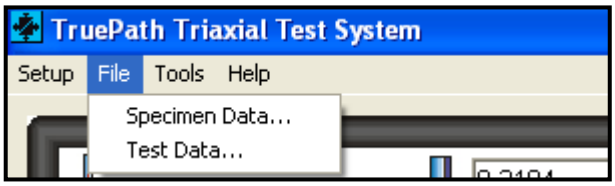

Figure 4.5. Entering file menu to select Specimen Data

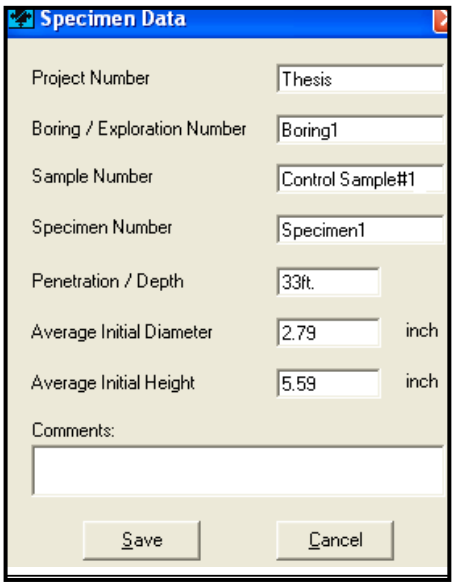

Figure 4.6. Writing the specimen data information

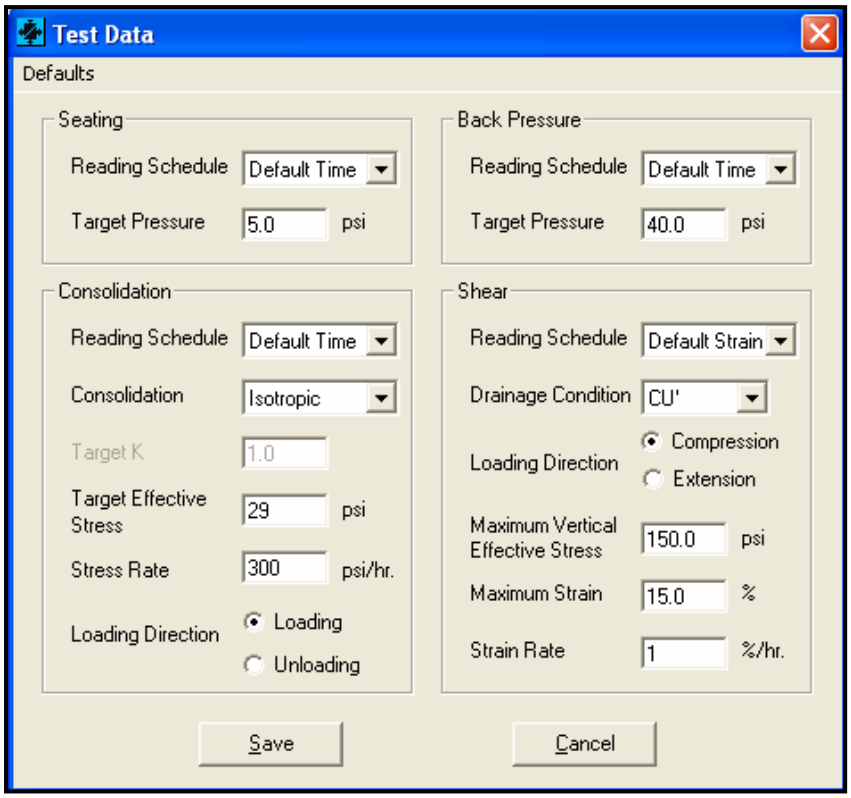

Figure 4.7. Entering the control test parameters

4.4. Seating Stage

After entering the specimen data, the "Seating" tab becomes active. The seating process involves seating the piston, adjusting the external load transducer, filling the cell with water, selecting the cell pressure, flushing the drains, and maintaining the volume of the sample.

4.4.1. Seating the Piston

The process of seating the piston involves locking the piston and minimizing the gap between the piston and the load button using manual control. This is achieved by entering the "Tools" menu, selecting "Manual Mode", pressing on the "Load Frame" and then pressing on the 1st upward button. When the "Start" button is pressed, the platen will move upward till it reaches the load button. Figures 4.8 through 4.9 show the sequence followed for reducing the gap between the piston and the load button.

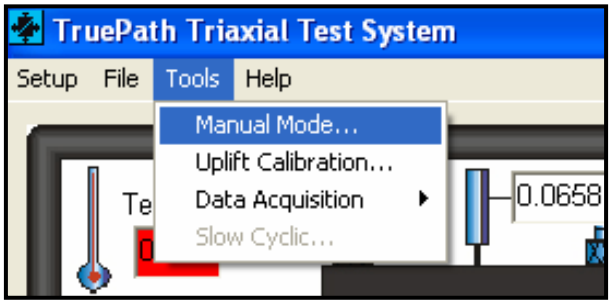

Figure 4.8. Selection for the manual mode

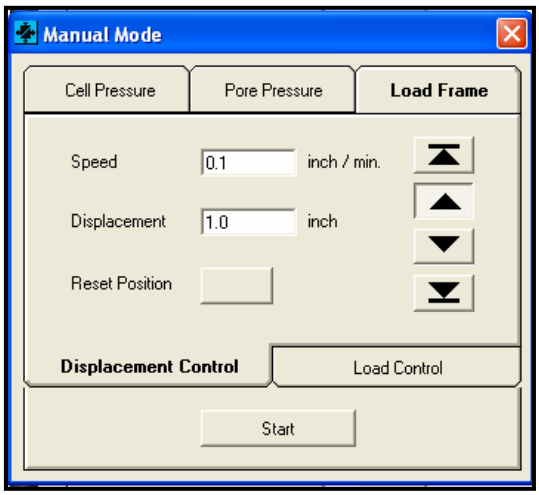

Figure 4.9. Reduction of gap between the piston and the load button

After reducing the gap, the “start” button is pressed as shown in Figure 4.10 and another window will appear. In this window, the “Start” button has to be pressed again and the platen will move upward till it reaches the load button and the platen stops automatically when the load button is seated on the piston.

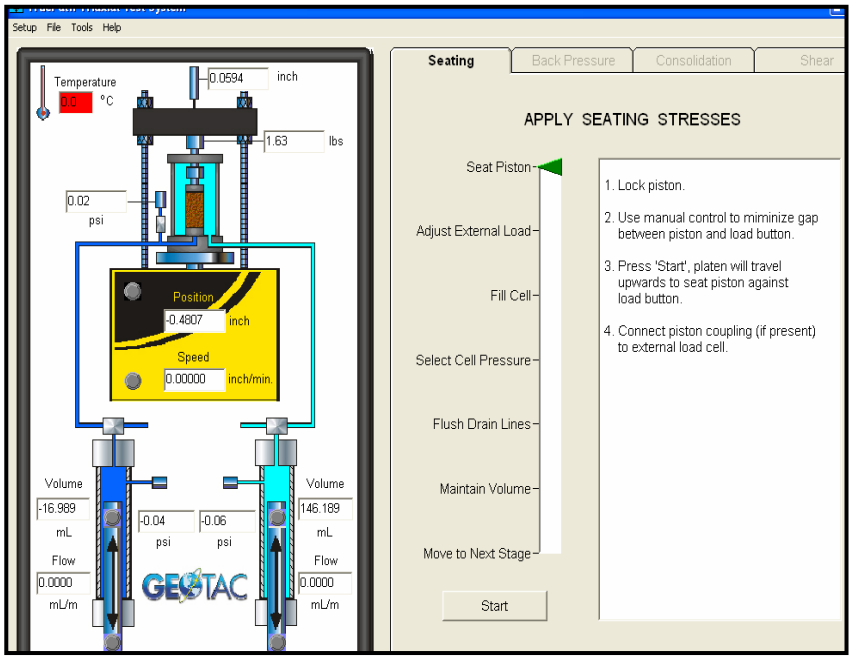

Figure 4.10. Window for seat piston

4.4.2. Adjust the External Load Sensor

When the "Adjust external load" button is pressed followed by pressing the "Start" button, the reading of the load cell becomes almost zero. The piston should be unlocked when the load cell reading approaches zero. Figure 4.11 shows the procedure for adjusting the load.

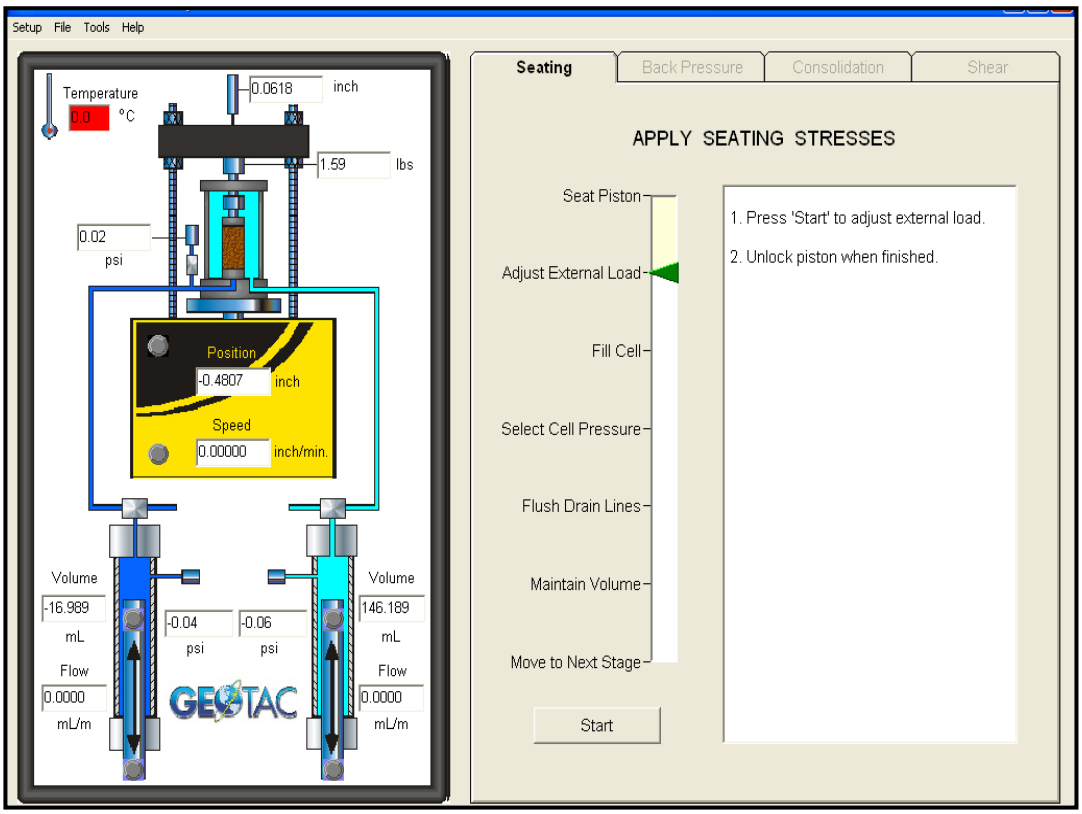

Figure 4.11. Adjustment for the external load transducer

4.4.3. Fill the Cell Chamber with Water

To fill the cell chamber with water, the “Fill Cell” button needs to be clicked and the ventilation air valve should be inserted into the top of the cell as shown in Figure 4.12. Then water should be supplied from an elevated water tank to the bottom quick connect of the cell through a plastic hose with a fitting on its top to allow entrance of the hose into the cell. The air in the cell is displaced by the water and is allowed to escape through the vent port. After filling the cell, water is allowed to flow out from the air vent port to ensure that all the air was driven out of the cell. The elevated water source should then be closed and the water hose is removed together with the air vent valve. The user can follow the step by step instructions that are displayed on the screen for the purpose of filling the cell with water as shown in Figure 4.13.

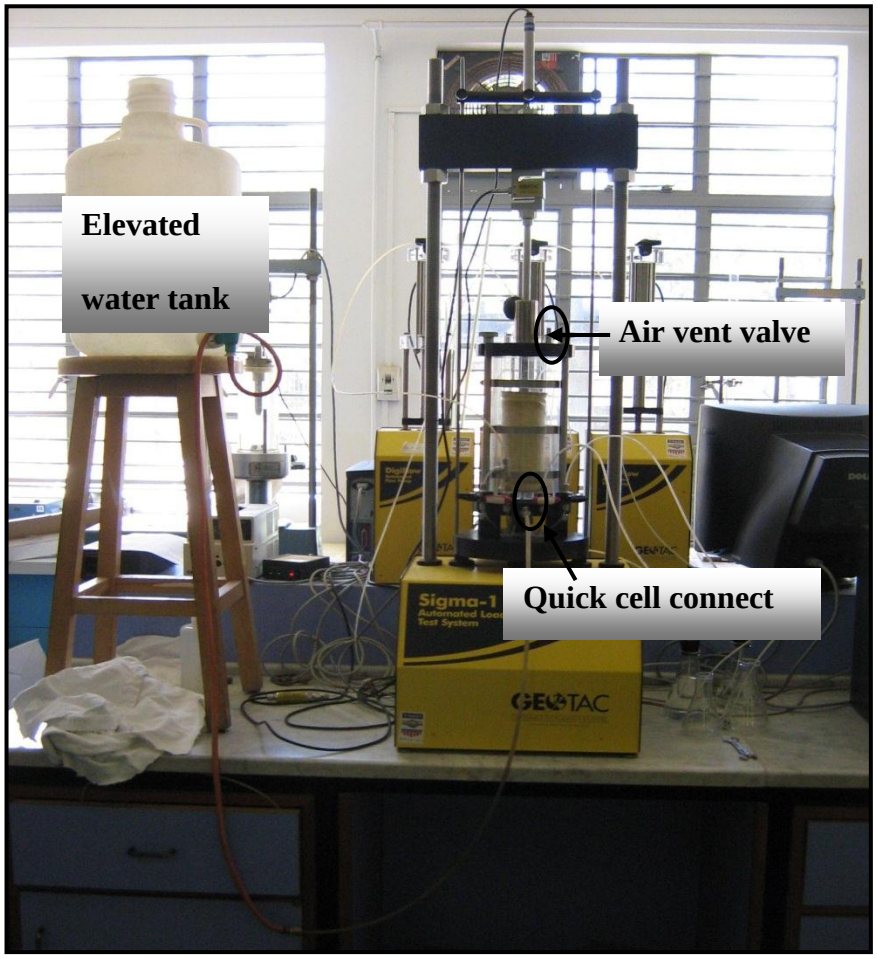

Figure 4.12. Filling the cell chamber with water

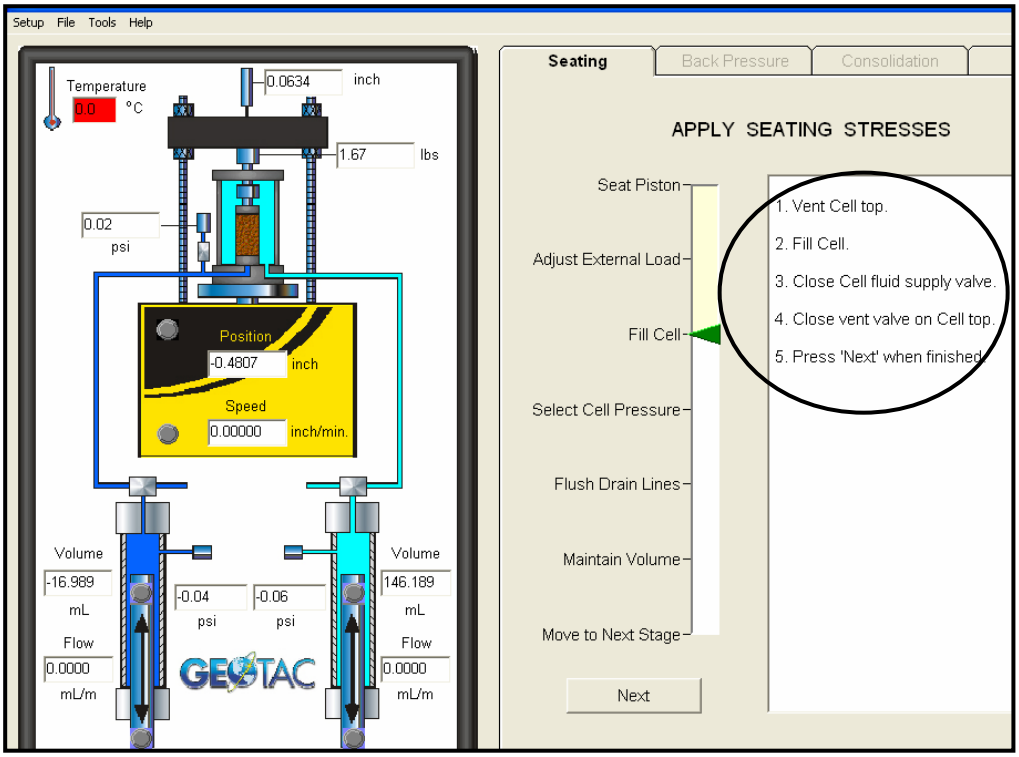

Figure 4.13. Steps for filling the cell chamber with water

4.4.4. Cell Pressure Selection

For the purpose of keeping the membrane pressed against the Kaolin sample during the drain line flushing, a small confining pressure of 5 Psi (34 kPa) is applied to the specimen. This can be achieved by opening the port valve of the cell pressure and connecting the cell pump pressure line to the cell bottom quick connect as shown in Figure 4.14. The “Start” button should then be pressed to produce a window in which a pressure of 5 Psi should be entered. After about 2 minutes, the cell pressure will reach the required value and become stable. When this is achieved the user should press the “Done” button to complete the operation.

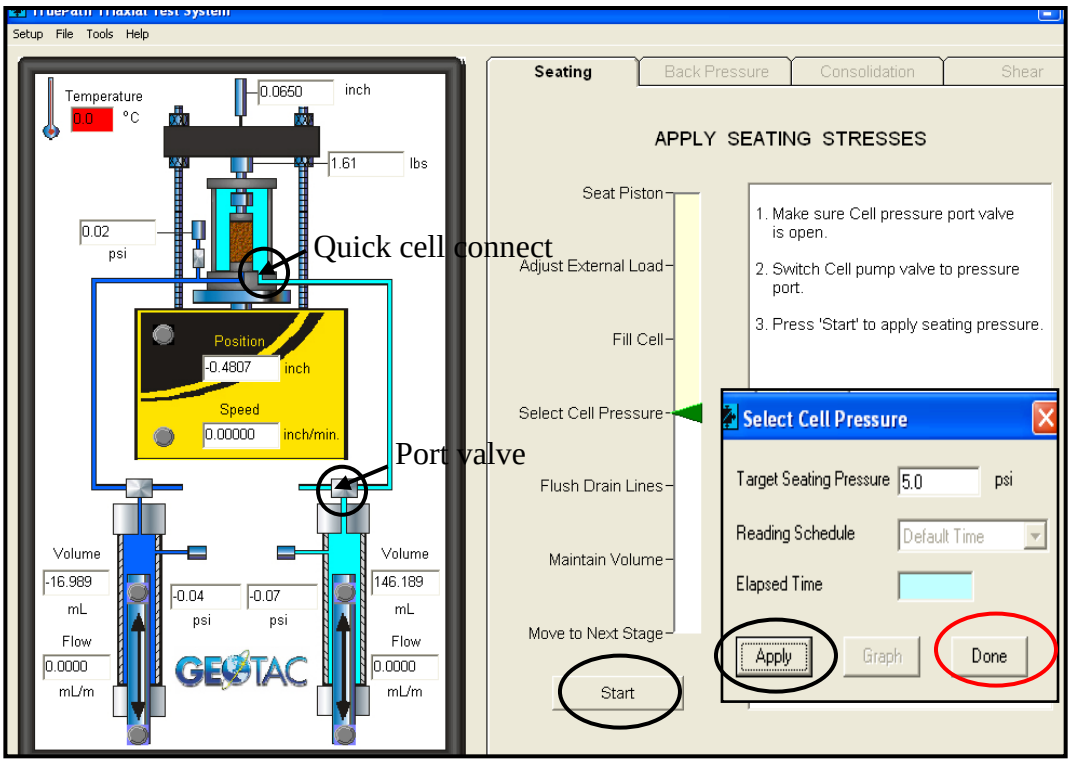

Figure 4.14. Application of initial confining pressure

4.4.5. Flushing the Drains

This technique is intended to force water to flow through the top and bottom drain lines using the bottom pump in order to expel air from these drain lines. First the bottom pump pressure line should be connected to the T fitting as shown in Figure 4.15. Then the bottom pump valve is switched to the pressure line and the top drain inlet valve#1 and the top drain vent valve#4 are opened. An overflow tube is then attached to valve#4 and the "Start" button is pressed. Water should flow from the bottom pump into the T fitting through valve#1 and into the container through valve#4. In order to dislodge completely the air bubbles from the drain lines, the flow can be stopped and restarted simultaneously; Moreover, closing the vent valve #4 for one or two seconds and reopening it again while water is flowing from the top drain line valve can help in

creating a pump pressure that speeds up the process of dislodging the air bubbles. After pressing the “Stop” button, valves#1 and 4 are closed and the bottom drain inlet valve #2 and bottom drain vent valve#3 are opened and the same procedure is repeated.

This technique is repeated until no more air bubbles are expelled through the drain lines. It is better to refill the bottom pump before completing the flushing step by switching the bottom pump to the refill container, pressing on “Tools” from the main menu, pressing “Manual Mode”, and selecting “Pore pump” (bottom pump). The “down” arrow is then clicked so that the bottom pump piston will move downward while water from the container will be drawn into the pump. The pore pump valve should then be returned to the pressure line, and flushing is continued if needed. Finally, the flushing stage should be terminated by closing valves#1 though 4 and pressing the “Done” button.

Figure 4.15. Flushing of the drains

4.4.6. Maintain the Volume

The final step is to apply a confining pressure of 14.5 Psi (100 kPa). First, the "Maintain Volume" tab should be pressed as shown in Figure 4.16. Next, the "Start" button is pressed and inlet drain valves #1 and 2 are opened. The required confining cell pressure is then typed in the appropriate space and the "Start" button is pressed. The time required for the seating stage for the clays tested in this study is around 2 to 3 hours. A graph can be displayed to show the variation of the confining pressure with time. Furthermore, a curve showing the volume of water that is drained from the specimen as a function of time can also be displayed on the screen. When water stops draining out from the sample under the specified confining pressure, the maintain volume stage can be terminated. This is done by clicking on the "Stop" button and then on the "Done" button to end the maintain volume stage.

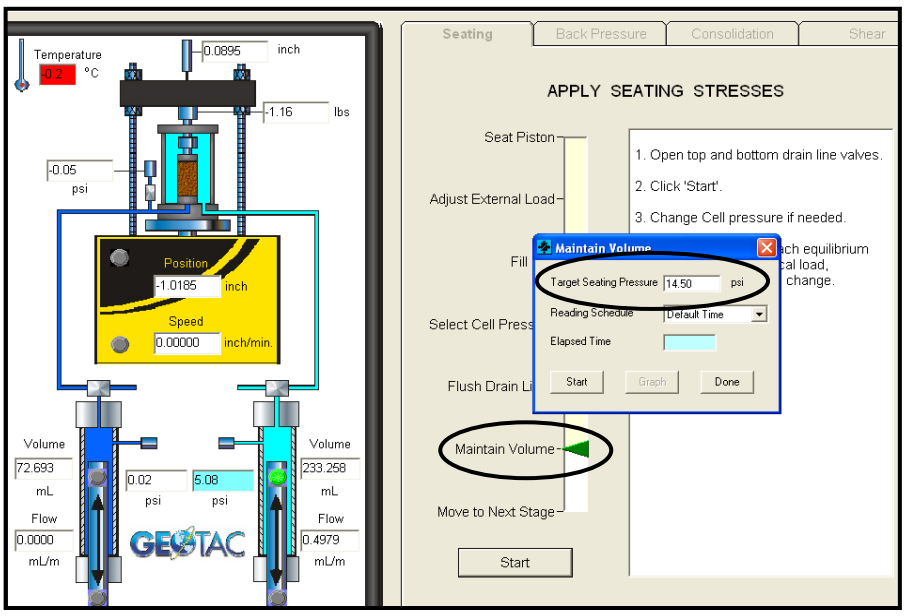

Figure 4.16. Application of confining pressure

4.5. Back Pressure Saturation Stage

To ensure full saturation of the slurry-consolidated Kaolin specimen, a back pressure/saturation pressure of 45 Psi is applied to the specimen using the back pump. The back pressure saturation stage consists of the following steps:

- Keep the bottom drain vent valve#3 closed, remove the drain line from bottom drain valve#3, and install in its place the pore pressure transducer and open drain vent valve#3.
- Check that inlet drain valves #1 and 2 are opened and make sure that the port valve of the bottom pump is opened, while drain valve #4 is closed.
- Input the value of the required saturation pressure (45 Psi), and initiate saturation by click on the "Start" button as shown in Figure 4.17.
- View the curve that shows the increase of back saturation pressure with time as shown in Figure 4.18. The value of the back pressure can be checked either by looking at the curve or by looking directly at the bottom pressure transducer that is displayed on the left side of the screen. Usually a period of 3 to 5 hours is needed to reach the back pressure value.
- Once the saturation pressure has reached its value, press on "Stop saturation", and check the B value. To do that, click on "Check B" and enter a small increment of cell pressure (5 Psi) as shown in Figure 4.19. Then, close drain inlet valves#1 and 2, and press on "Start". The cell pump will instantaneously increase the cell pressure by 5 Psi, and the pore water pressure should indicate a similar increase of pore water pressure if the sample is completely saturated. The software calculates the B-value and reports its value every 15

seconds on the screen. During this check, a B-value of 0.96 to 1 was generally obtained for tests conducted in this study.

- After an acceptable B-value is ensured, click on “Done” and wait till the window for the B value check disappears by itself. When this happens, re-open drain inlet valves#1 and 2, and press on “Done” to end the back pressure saturation stage. If saturation was not achieved using the initial specified back pressure of value 45 Psi, increase the saturation pressure by a certain increment and repeat the saturation process.

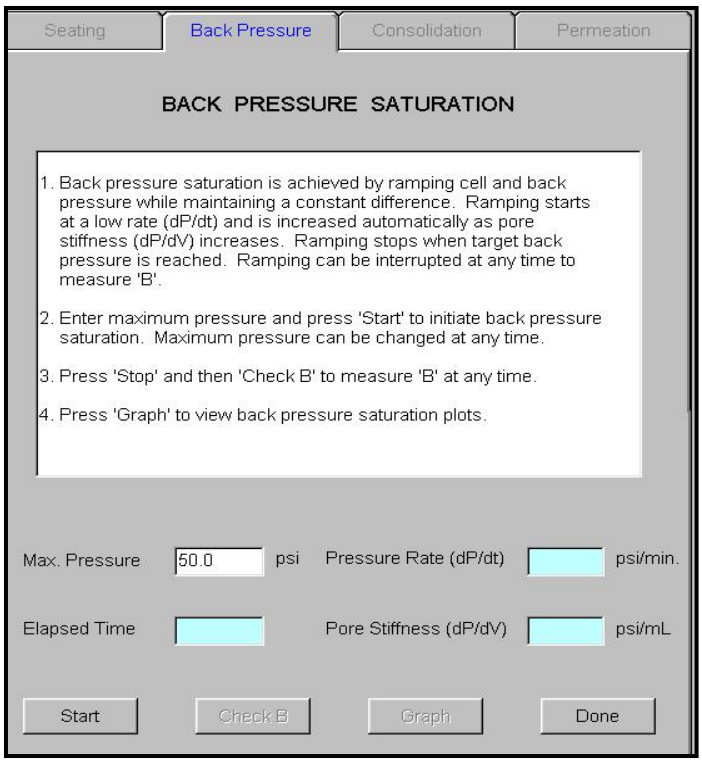

Figure 4.17. Window for back pressure saturation stage.

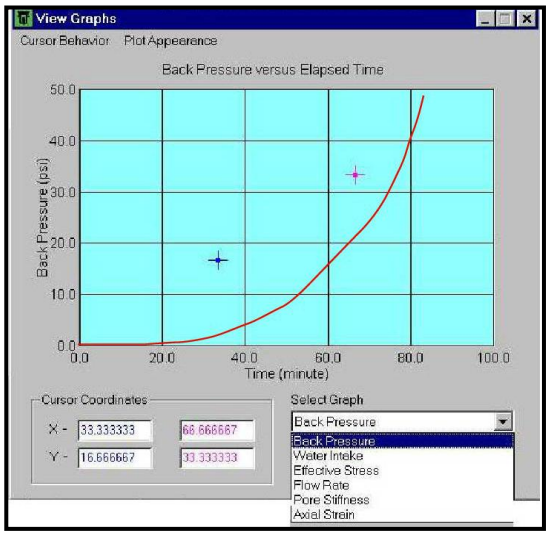

Figure 4.18. View the curve during the saturation process

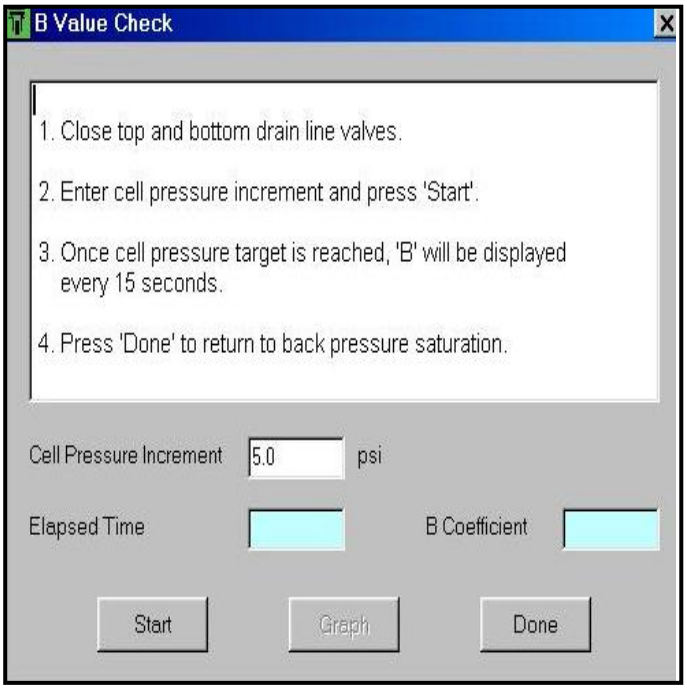

Figure 4.19. Window for “B” value check.

4.6. Isotropic Consolidation Stage

The consolidation stage is initiated by clicking on the “Consolidation” tab. First, the relevant data which includes the effective confining pressures and the stress rate that have been previously entered during the creation of the data test file should be

checked. The activated window for isotropic consolidation is shown in Figure 4.20. In this stage, the user can still change the target effective stress and the vertical stress rate, but cannot change the type of consolidation. Once all the input data is verified and consolidation is initiated, consolidation continues until the reading of the pore water volume intake for the pore pump becomes a constant. At this time, the isotropic consolidation stage can be assumed to be completed. A period of 1 hour, 2 hours, and 6 hours is usually needed to consolidate the Kaolin specimens at confining pressures of 14.5 Psi, 21.75 Psi, and 29 Psi respectively.

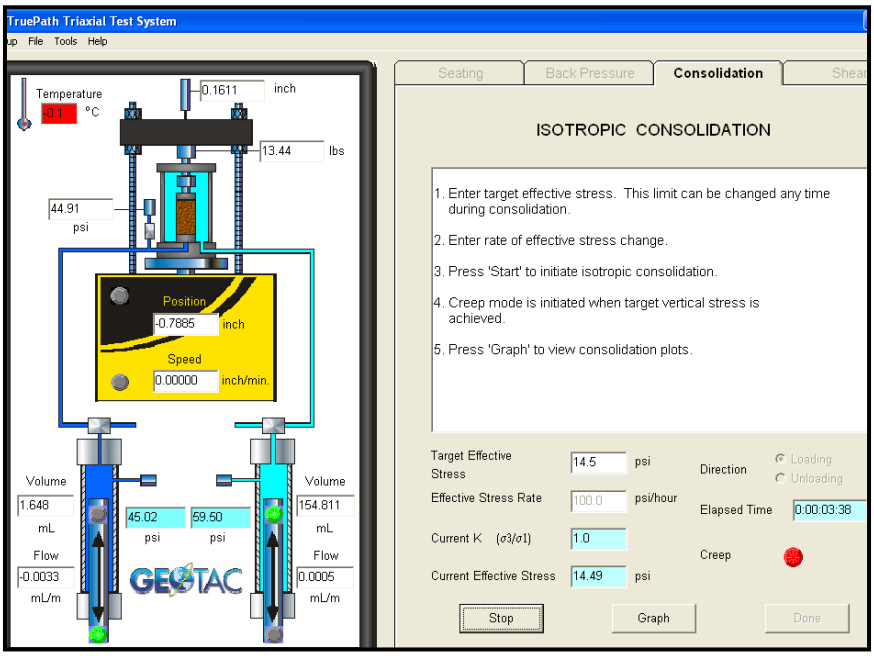

Figure 4.20. Window for isotropic consolidation

4.7. Drained/Partially Drained/Undrained Shearing Stage

At the end of the isotropic consolidation stage, a gap will form between the top cap of the specimen and the bottom of the loading piston. The user has to use the manual controls to close the gap and reestablish contact before starting the shearing

stage. Once the window for the “Drained shear” or “Undrained Shear” is activated, the user is required to enter the strain rate. In this research, a value of 0.25%/hour is used for the strain rate when doing a drained shear tests, a value between 3.5%/hour and 120%/hour for partially drained tests, and a value of 1%/hour for undrained test.

Once the strain rate is chosen, cell valves#1 and 2 that are connected to the pore pump could have 3 different statuses depending on the drainage conditions. If the tests is fully drained, then cell valve #1 and 2 are opened, while if the tests are partially drained, then only cell valve#1 is opened and cell valve#2 is closed. Finally, if the tests are undrained, then both cell valves# 1 and 2 must be closed. In any of the above mentioned drainage conditions, valve#3 between the pore pressure sensor and the pore pump should be checked to be open. The “Start” button is then clicked as shown in Figure 4.21 to initiate shearing. Different curves can be viewed while the test is in progress.. When the strain reaches a percentage of 15-16%, click on the “End test” tab to terminate the test and to close the software.

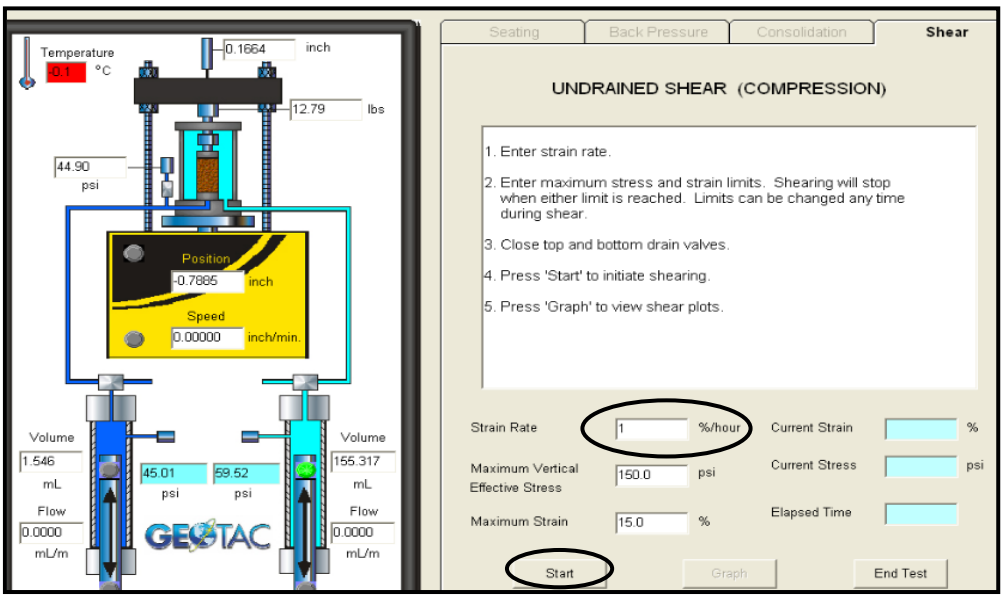

Figure 4.21. Window for undrained shear test

4.8. Test Tear Down

Test tear down process involves removing pressures from the specimen and the triaxial chamber and the load frame. This can be accomplished as follows:

- Enter the True Path software and lock the cell piston.
- Select the manual controls, and choose cell pump. After that, choose "Pressure control" as shown in Figure 4.22 and record a value of 0 Psi for the cell pressure and press start. Water will drain out from the cell chamber into the cell pump to reduce the cell pressure to zero.
- Use the manual control and reduce the pore pump pressure to zero.
- Use the manual control to lower the loading frame platen.
- Connect the top air vent valve and remove the hose from the bottom cell connect and replace it with a tube that discharges water into a container.
- After the water is drained out from the cell, remove the triaxial chamber from the loading frame, and dismantle the cell parts, wash them, and prepare them for another test.

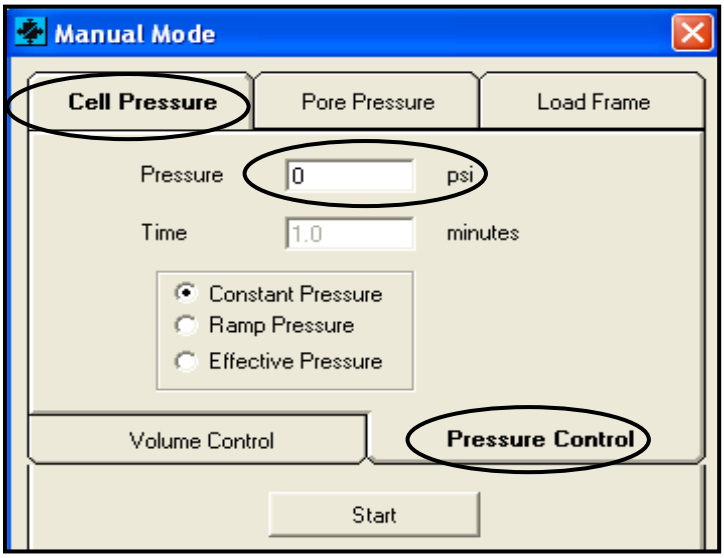

Figure 4.22. Window for unloading stage

4.9. Summary

A comprehensive description for operating the automated triaxial equipment "TruePath" was presented in this chapter in a simple way which includes a step by step procedure with figures and charts that facilitate the understanding of the testing process. The information presented in this chapter will make it easier for any future user to work and operate the "TruePath" equipment. However, reading the manual of the "TruePath" system is crucial and vital in order to complete all the required information that the user should know prior to operating the system.

CHAPTER 5

TEST RESULTS AND ANALYSIS FOR DRAINED TESTS

5.1. Introduction

The automated triaxial test setup "TruePath" by Geotac was used to conduct CD tests on control and reinforced clay specimens saturated with a back pressure of 310 kPa. The samples were then isotropically consolidated under confining pressure of 100, 150 and 200 kPa and sheared drained at a strain rate of 0.25%/hr, while measuring volume change through drain lines connected to the porous stones at the top and bottom of the sample. The measured volume change reflects a global change in the composite sample and do not provide information on local changes in the water content in the sand column and the surrounding clay. Throughout the tests, the total confining pressure was kept constant as the vertical stress was increased in compression.

The test results of consolidated drained tests conducted on 15 Kaolin specimens are presented in this chapter which includes the results of control or unreinforced specimens, specimens reinforced with ordinary sand columns, and specimens reinforced with encased sand columns. These results are then combined and compared with 24 tests conducted by Maalouf (2012). The results include a description of the modes of failure that characterize the behavior of the different test specimens and a detailed analysis of the parameters which are known to affect the load response of clay specimens that are reinforced with sand columns. The effect of these parameters which include the area replacement ratio, column penetration depth, geotextile encasement,

and confining pressure on the drained shear strength, stiffness, volume change, and effective shear strength parameters of the Kaolin specimens is investigated and highlighted in this chapter. Furthermore, the test results corresponding to Kaolin specimens reinforced with ordinary and encased sand columns are compared and analyzed to isolate and investigate the effect of geotextile fabric on the degree of improvement in the mechanical properties of reinforced specimens.

5.2. Test Results

The test results are presented in the form of deviatoric stress versus axial strain curves and volumetric strain versus axial strain curves. Since no peaks were exhibited in the deviatoric stresses (σ_d) in the majority of the tests, failure was defined at an axial strain of 15%, unless a peak was observed at smaller strain levels.

5.2.1. Unreinforced/Control Kaolin Specimens

Curves showing the variation of the deviatoric stress and the volumetric strain versus axial strain at confining pressures of 100 kPa, 150 kPa, and 200 kPa for the control Kaolin specimens are presented in Figure 5.1. For all confining pressures, the deviatoric stress continued to increase with axial strain, even at strains exceeding 14% to 15%, which were the maximum strains measured in the control tests. However, it could be observed that the rate of increase in deviatoric stress appears to decrease appreciably at strains exceeding 6% to 8%. The same applies to the variation of the volumetric strain with axial strain.

The Mohr Coulomb effective stress failure envelope for the control specimens is shown on Figure 5.2. The effective cohesion (c') and the effective angle of internal friction (Ø') for the control specimen were determined to be 0 kPa and 21.8º respectively.

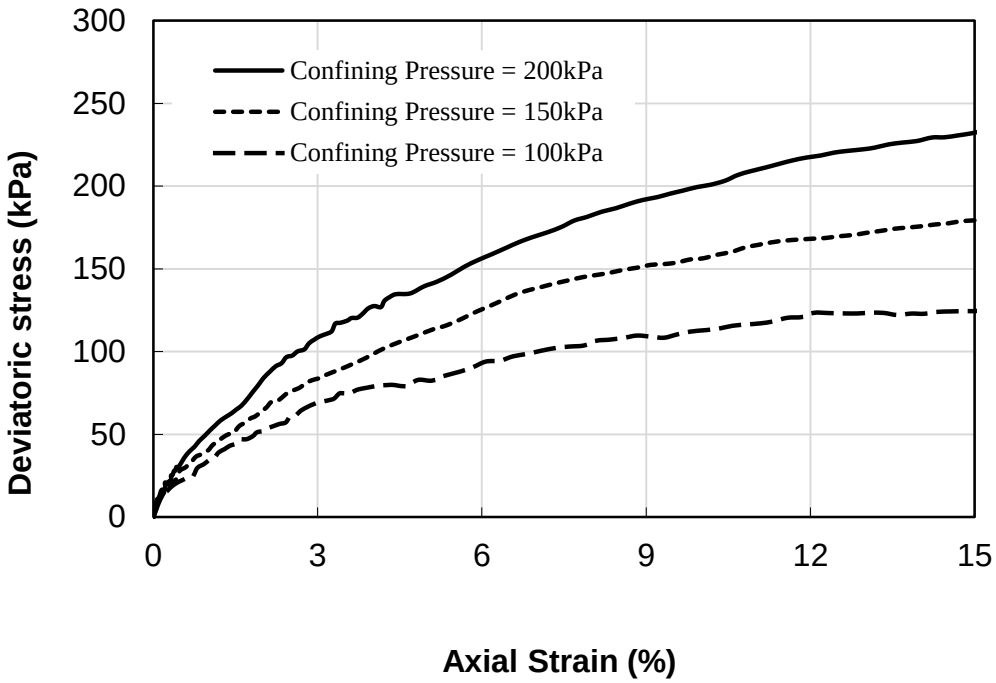

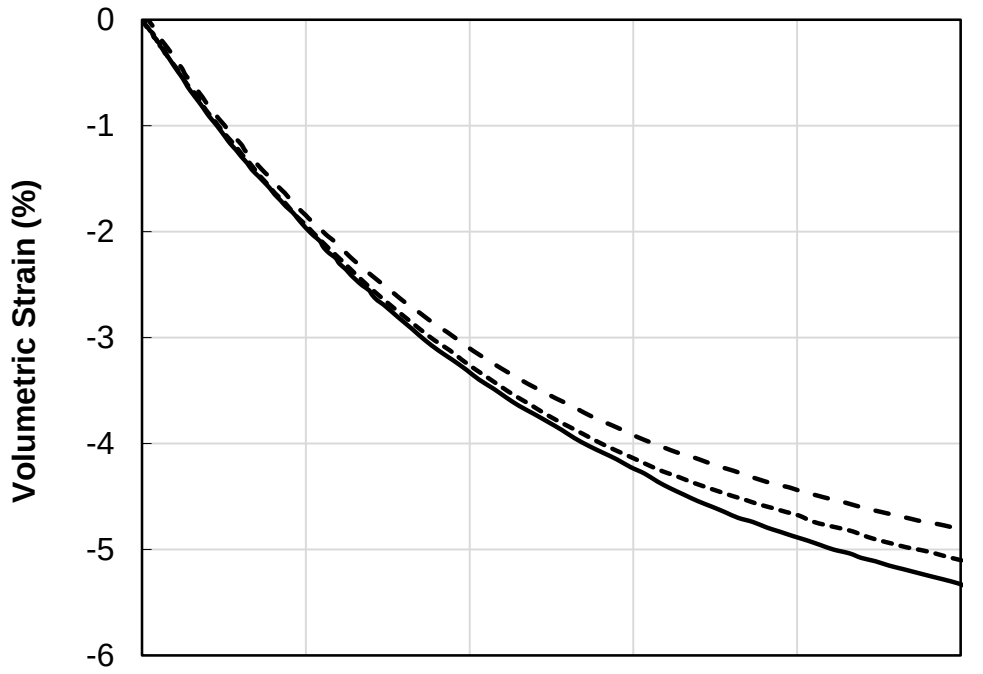

Figure 5.1. Deviatoric stress and volumetric strain versus axial strain for unreinforced/control specimen at confining pressures of 100 kPa, 150 kPa, and 200kPa

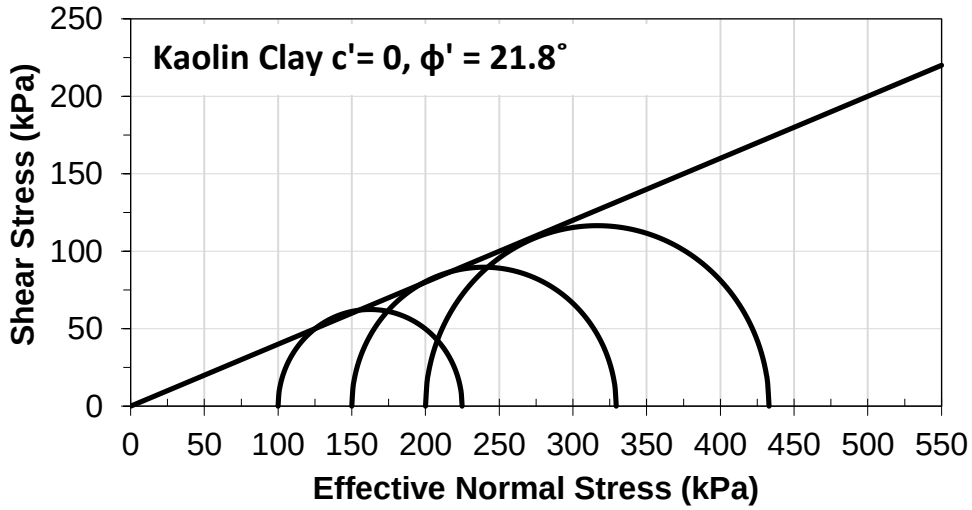

Figure 5.2. Mohr Coulomb effective stress failure envelope for control/unreinforced Kaolin specimens

5.2.2. Kaolin Specimens Reinforced with Sand Columns

Results obtained from the triaxial tests conducted on kaolin specimens reinforced with partially and fully penetrating encased and ordinary sand columns are presented in Table 5.1 and in Figures 5.3 to 5.11, which include pictures of the modes of failure and graphs showing the variation of the deviatoric stress and volumetric strain with axial strain. Figures 5.3 to 5.7 represent the results for an area replacement of 31.7%, while Figs.5.8 to 5.11 illustrate the superposition of results of all the area replacement ratios (7.9%, 17.8%, and 31.7%). The results were analyzed to investigate the effect of relevant parameters such as column penetration ratio H_c/H_s, area replacement ratio A_c/A_s, and confining pressure on the improvement in the drained shear strength and the effective strength parameters of the clay. It should be noted that in all the discussion presented below, it was assumed that the sand column and the

surrounding clay act as a single element with homogeneous distributions of stresses and strains.

5.2.2.1. Modes of Failure

For samples that were reinforced with partially penetrating columns, the mode of failure was characterized by bulging of the clay specimen. The bulging was slight along the height with some concentration happening under the sand column in samples reinforced with ordinary columns. Furthermore a slight bulging of the columns was observed. For partially penetrated encased columns, the bulging was significant and concentrated in the lower-half of the clay specimen with a shear plane passing just under the sand column. However, the encased columns did not suffer any bulging due to the confining effect of the geotextile. As an illustration, photographs showing the degree of bulging in samples with partially penetrating 4-cm ordinary columns at different confining pressures are shown on Figure 5.5. The bulging is evident in the samples tested at all confining pressures, and a shear plane passing at the lower section of the specimen was observed for the 200kPa confining pressure. The concentration of bulging at the lower half of the sample for samples reinforced with encased partially penetrating 4-cm sand columns is shown on Figure 5.4 for the three confining pressures respectively.

Table 5.1. Test Results for Kaolin specimens reinforced with ordinary and encased sand columns

Test No.	Confining pressure σ_3, (kPa)	Diameter of sand column (mm)	Area replacement ratio: A_c/A_s (%)	Column Penetration Ratio: H_c/H_s	Height of Sand Hs (cm)	Deviatoric stress @ failure (kPa)	Volume strain (%)	E_{sec} @ 1% axial strain (kPa)	Increase in deviatoric stress (%)	Reduction in Volumetric Strain (%)
1	100	0	0.00	0.00	-	124.80	-4.82	3387.18	-	-
2		20	7.90	0.75	10.65	124.70	-5.00	3800.00	-0.08	-3.75
3		20	7.90	1.00	14.20	134.10	-4.09	4050.00	7.45	15.07
4		20 (ESC)	7.90	0.75	10.65	119.57	-4.22	3420.00	-4.19	12.46
5		20 (ESC)	7.90	1.00	14.20	171.00	-4.01	2580.00	37.02	16.74
6		30	17.80	0.75	10.65	138.23	-3.76	3754.00	10.76	21.92
7		30	17.80	1.00	14.20	169.75	-2.33	7630.00	36.02	51.66
8		30 (ESC)	17.80	0.75	10.65	148.30	-3.72	4230.00	18.83	22.91
9		30 (ESC)	17.80	1.00	14.20	210.14	-3.11	5300.00	68.38	35.41
10		40	31.70	0.75	10.65	154.96	-2.43	4527.09	24.17	49.68
11		40	31.70	1.00	14.20	210.66	-0.75	6170.26	68.80	84.50
12		40 (ESC)	31.70	0.75	10.65	134.93	-2.22	3918.59	8.12	54.00
13		40 (ESC)	31.70	1.00	14.20	204.64	-1.10	7274.29	63.97	77.21
14	150	0	0.00	0.00	-	179.36	-5.10	4044.08	-	-
15		20	7.90	0.75	10.65	175.10	-5.17	3190.00	-2.38	-1.26
16		20	7.90	1.00	14.20	183.44	-4.57	4360.00	2.27	10.45
17		20 (ESC)	7.90	0.75	10.65	173.86	-4.27	4380.00	-3.07	16.38
18		20 (ESC)	7.90	1.00	14.20	225.15	-4.21	4150.00	25.53	17.55
19		30	17.80	0.75	10.65	193.07	-3.97	3765.00	7.64	22.17
20		30	17.80	1.00	14.20	238.45	-3.59	8580.00	32.94	29.60
21		30 (ESC)	17.80	0.75	10.65	197.52	-4.15	4469.00	10.12	18.57
22		30 (ESC)	17.80	1.00	14.20	258.61	-3.02	8100.00	44.18	40.88
23		40	31.70	0.75	10.65	219.00	-2.76	6096.42	22.10	45.97
24		40	31.70	1.00	14.20	292.40	-1.35	9822.88	63.02	73.63
25		40 (ESC)	31.70	0.75	10.65	191.40	-3.02	4443.58	6.71	40.82
26		40 (ESC)	31.70	1.00	14.20	279.60	-1.50	8200.00	55.89	70.55
27	200	0	0.00	0.00	-	233.00	-5.36	5075.26	-	-
28		20	7.90	0.75	10.65	217.92	-5.48	4725.00	-6.47	-2.20
29		20	7.90	1.00	14.20	233.40	-5.54	3600.00	0.17	-3.30
30		20 (ESC)	7.90	0.75	10.65	236.92	-4.99	6220.00	1.68	6.85
31		20 (ESC)	7.90	1.00	14.20	282.09	-5.33	5480.00	21.07	0.63
32		30	17.80	0.75	10.65	260.60	-3.70	6100.00	11.85	31.07
33		30	17.80	1.00	14.20	311.94	-3.23	7030.00	33.88	39.80
34		30 (ESC)	17.80	0.75	10.65	243.84	-4.28	7932.00	4.65	20.18
35		30 (ESC)	17.80	1.00	14.20	326.25	-2.91	7320.00	40.02	45.79
36		40	31.70	0.75	10.65	290.00	-3.04	8358.80	24.46	43.25
37		40	31.70	1.00	14.20	369.70	-1.40	11833.08	58.67	73.91
38		40 (ESC)	31.70	0.75	10.65	254.80	-4.39	6357.03	9.36	18.10
39		40 (ESC)	31.70	1.00	14.20	349.13	-1.10	14716.55	49.84	79.56

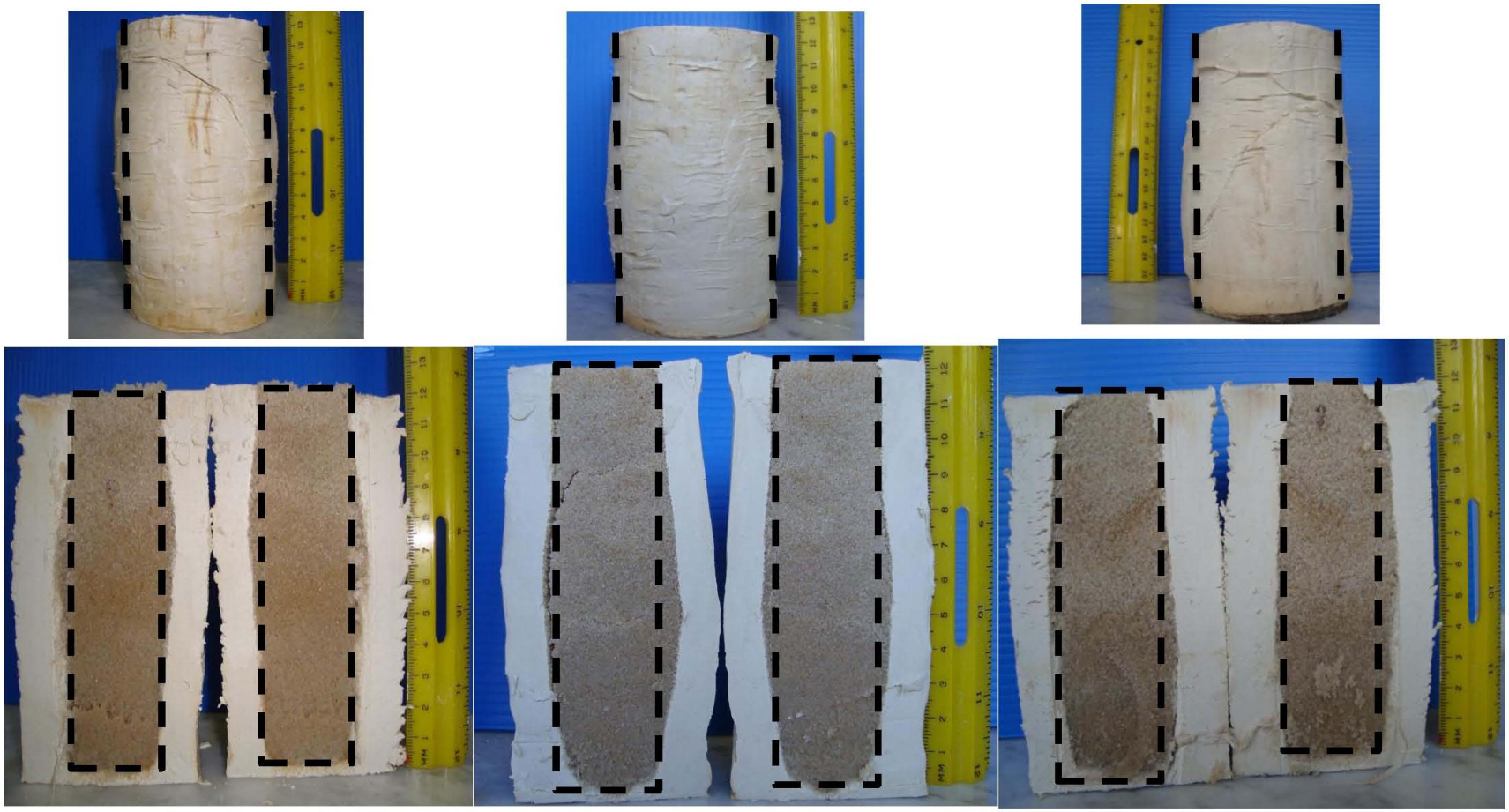

Figure 5.3. Example of external and internal modes of failure of test specimens (Hc/Hs = 1 and Ac/As = 31.7%, Ordinary)

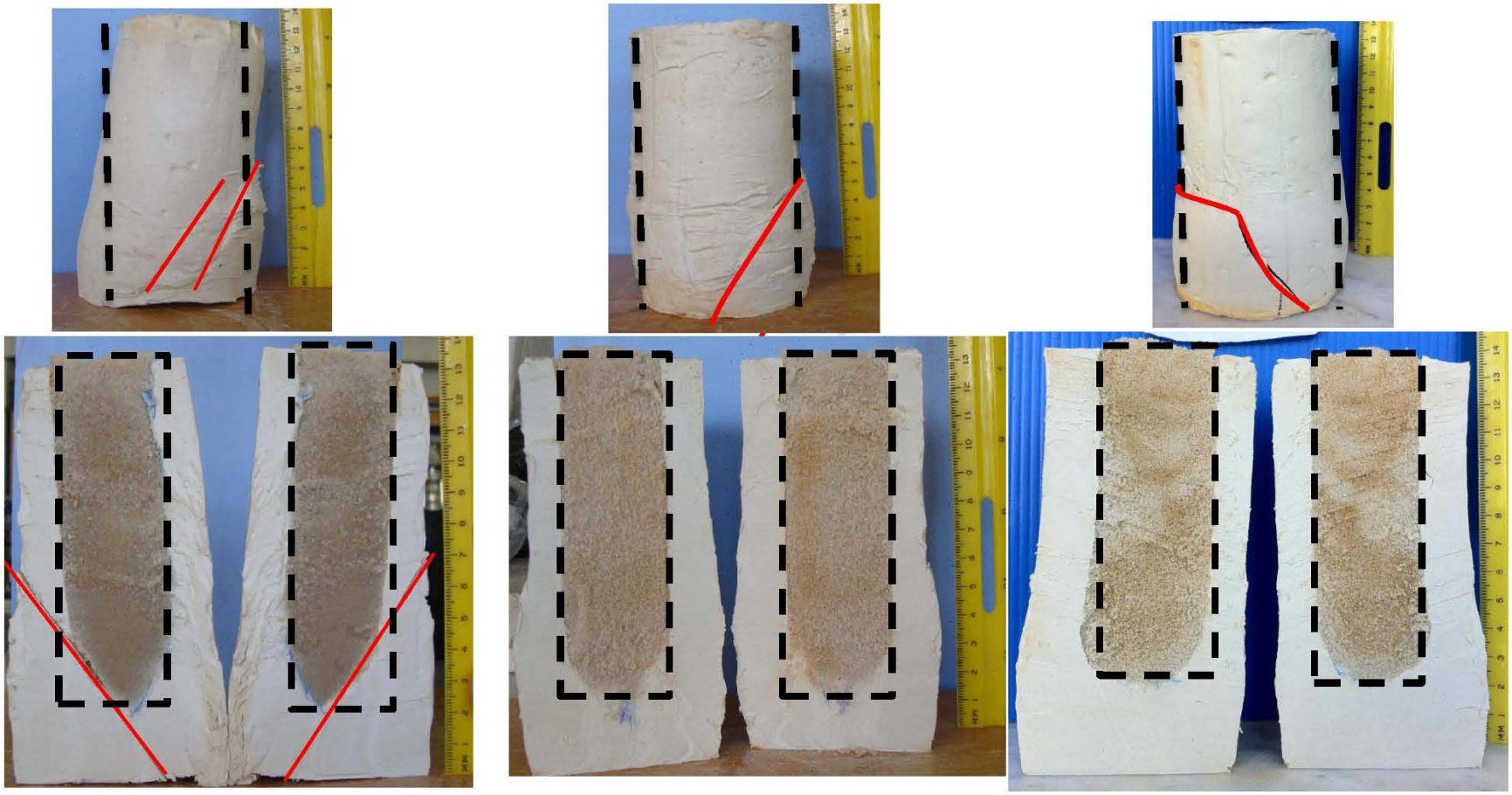

Figure 5.4. Example of external and internal modes of failure of test specimen (Hc/Hs = 0.75 and Ac/As = 31.7% Encased).

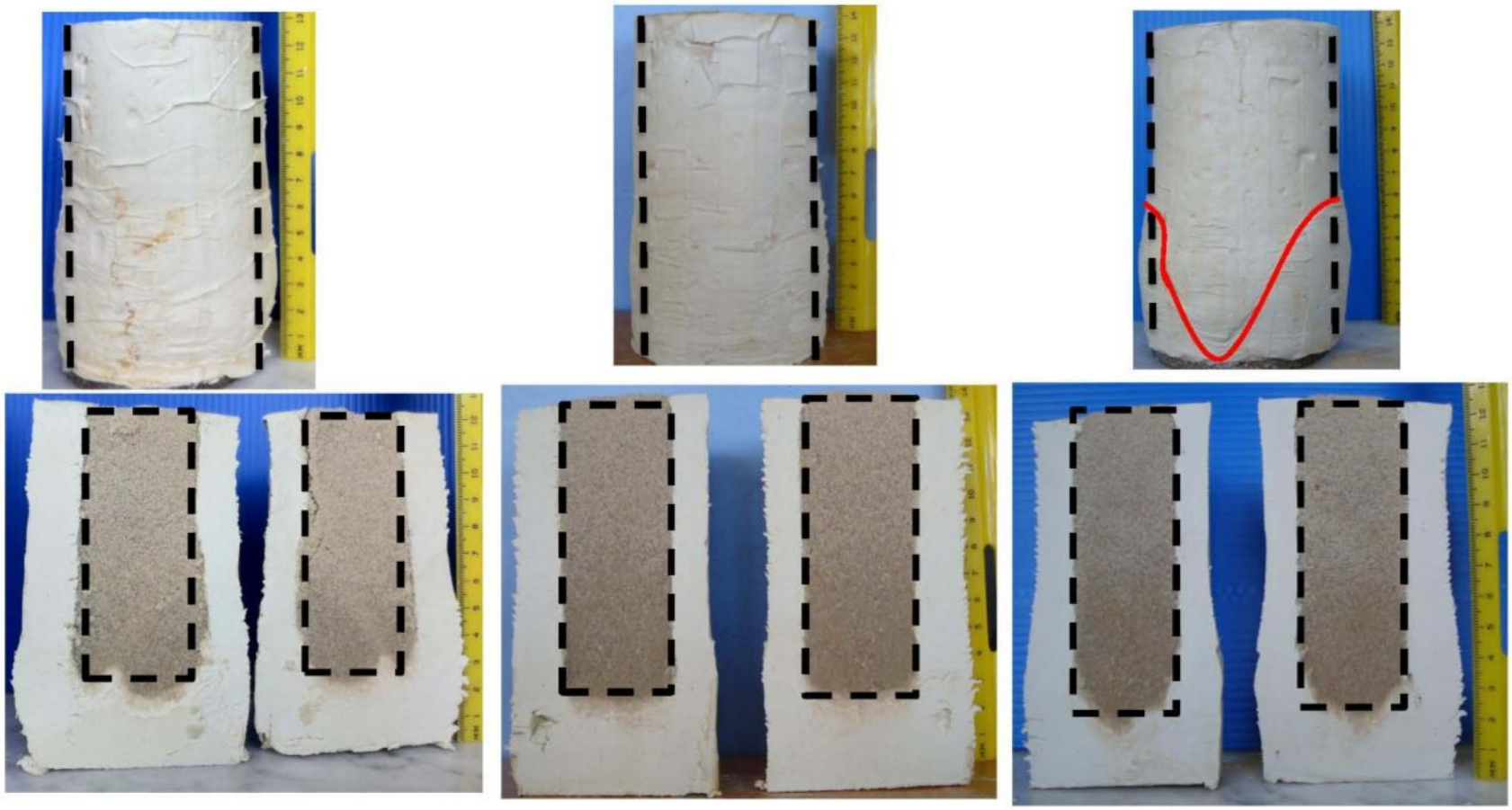

Figure 5.5. Example of external and internal modes of failure of test specimen (Hc/Hs = 0.75 and Ac/As = 31.7% Ordinary).

These observations agree with findings from previous studies (Hughes and Withers 1974, Sivakumar et al. 2004 and Najjar et al. 2010) which indicate that for partially penetrating columns of short lengths, the stresses at the base of the column generally exceed the bearing capacity of the soil leading to a premature bearing capacity failure in the unreinforced lower portion of the specimen. For samples reinforced with fully penetrating columns, bulging was more concentrated in the upper half of the sample, (Figure 5.3) with the degree of bulging decreasing significantly for encased columns.

To investigate the mode of failure of sand columns, the same test specimens were split along their vertical axes to expose the columns and the surrounding clay (Figures 5.3, 5.4, and 5.5). For samples reinforced with ordinary partially penetrating sand columns, the sections shown in Figure 5.5 indicate that the lower portion of the sand columns (length of about 1.5 times the column diameter) exhibited bulging of different levels, with the sample tested at 100 kPa exhibiting the most noticeable bulge. When partially penetrating columns were encased, the sand columns did not exhibit any noticeable bulging despite the fact that the clay specimens bulged in the lower half during drained shear (Figure 5.4). For samples reinforced with fully penetrating ordinary columns, the bulging of the column was in line with the bulging observed for the corresponding clay specimens with the most severe bulging occurring at about 2 to 3 column diameters from the top of the sample.(Figure 5.3). It is also worth noticing that as the confining pressure increases, the severity of the bulging decreases.

5.2.2.2. Stress-Strain Behavior

Figure 5.7 illustrates the results of the tests with area replacement ratio of 31.7% for the different conditions of reinforcement. The variation of the deviatoric stress and volumetric strain with the axial strain is presented in Figure 5.6 for tests conducted with area replacement ratio of 31.7% at 100, 150 and 200kPa. The stress-strain curves exhibited consistent increases in deviatoric stresses with strains as the samples were sheared towards critical state conditions. To define failure, the deviatoric stresses will be considered to have leveled out at an axial strain of 15%, which is the maximum strain that was measured in the drained tests.

The measured volumetric strains were all contractive. For all confining pressures, the negative volumetric strains were reduced significantly when 3 and 4-cm diameter sand columns (A_c/A_s=17.8% A_c/A_s=31.7%) were inserted in the soft clay (see Table 5.1). As expected, this reduction in contractive behavior was more significant for tests involving fully penetrating sand columns, which are expected to be more dilative compared to partially penetrating columns, and for tests involving higher replacement ratios. For tests involving the smaller area replacement ratio (A_c/A_s=7.9%), the measured volumetric strains for samples that were reinforced with partially penetrating sand columns were generally equal to or slightly smaller than those measured in the control specimens, indicating that the inclusion of sand columns did not have a significant impact on the tendency for volume change as shown in Figures 5.8 and 5.9..

The variation of the deviatoric stress and volumetric strain with axial strain is shown on Figure 5.8 to 5.11 for area replacement ratios ranging from 0% to 100%. These curves allow for a better understanding of the impact of the area replacement ratio on the drained response of the sand column-reinforced clay specimens. An

investigation of the curves on Figures 5.8 to 5.11 indicate that: (1) as the area replacement ratio increases, the sand columns become more efficient at improving the deviatoric stresses at failure and reducing contractive behavior, (2) as the area replacement ratio increases, the stress-strain curves of the composite clay specimens approach the stress-strain curve of the sand specimen at a faster rate, and (3) as the area replacement ratio increases, the stress-strain response as indicated by the shape of the stress-strain curves shifts from the strain hardening behavior that is witnessed in the unreinforced control clay specimens (0% replacement) to the strain softening behavior with a clear peak that is characteristic of the pure sand specimens (100% replacement). This shift is seen as the area replacement ratio reaches 31.7% and is clearer for fully penetrating columns as shown in Figures 5.10 and 5.11.

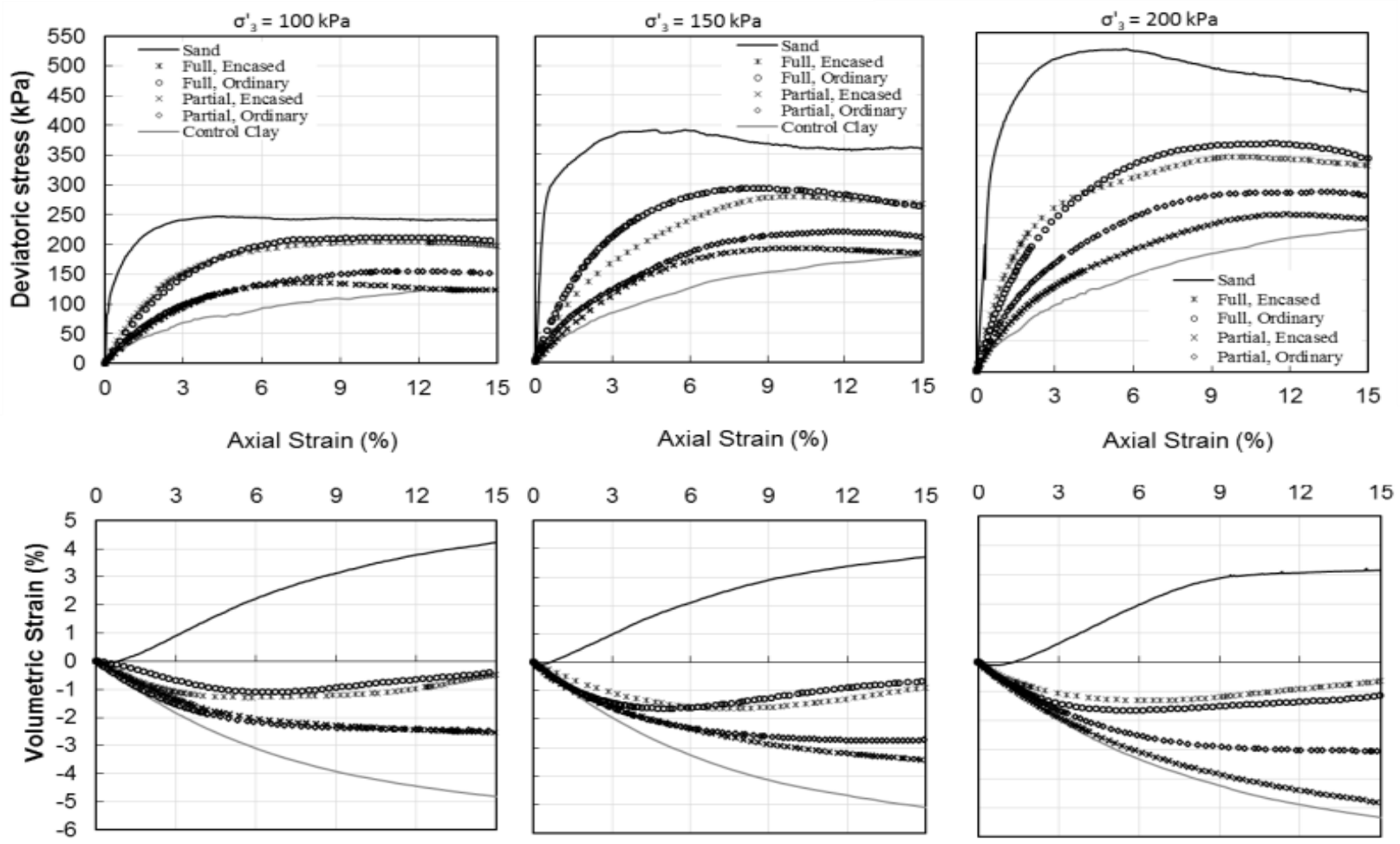

Figure 5.6. Deviatoric stress and volumetric strain versus axial strain for reinforced specimens at confining pressures of 100 kPa, 150 kPa, and 200kPa (As/Ac=31.7%)

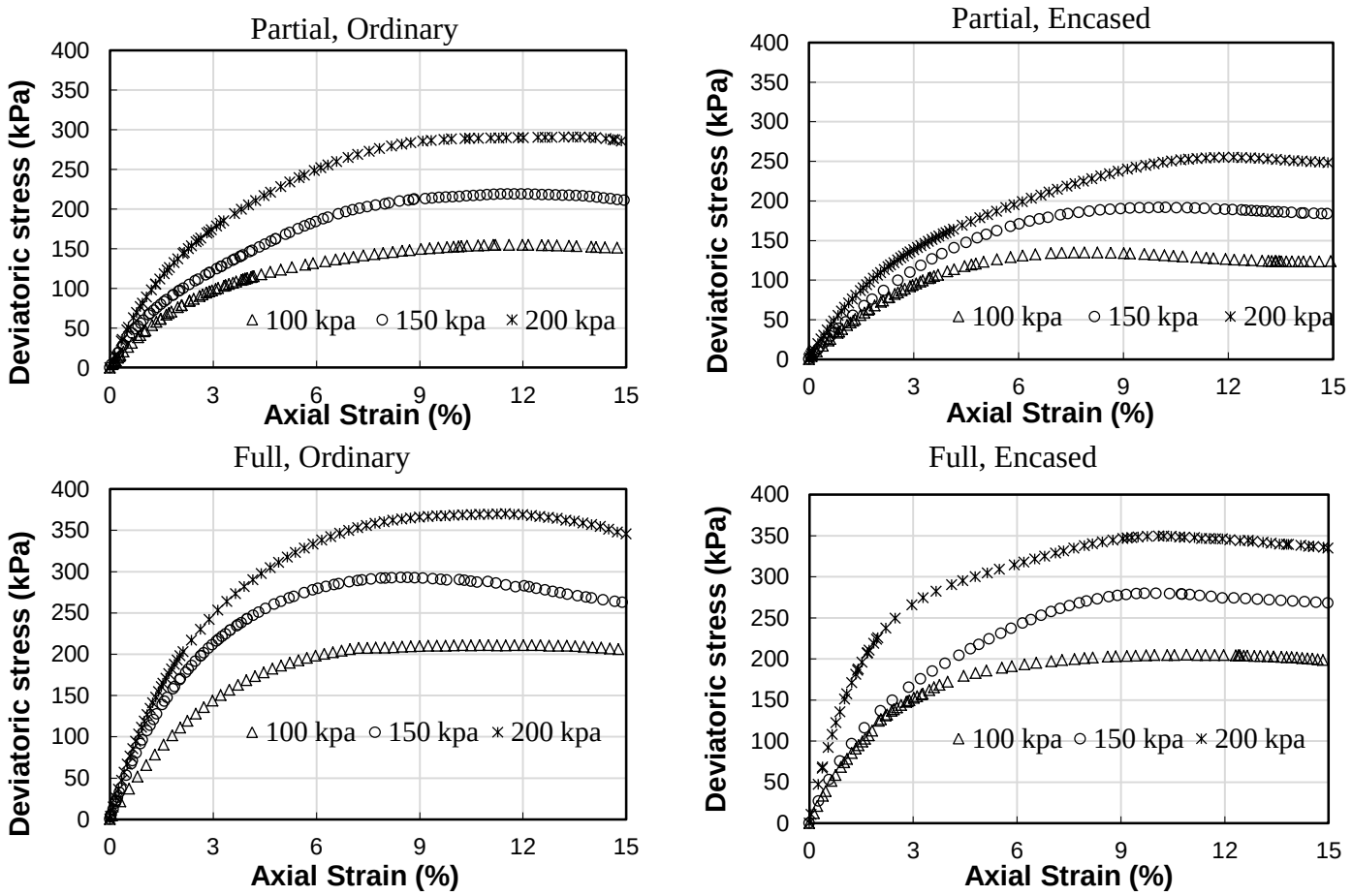

Figure 5.7. Deviatoric stress versus axial strain for all cases of reinforced specimens at confining pressures 100kPa, 150kPa,200kPa (As/Ac=31.7%)

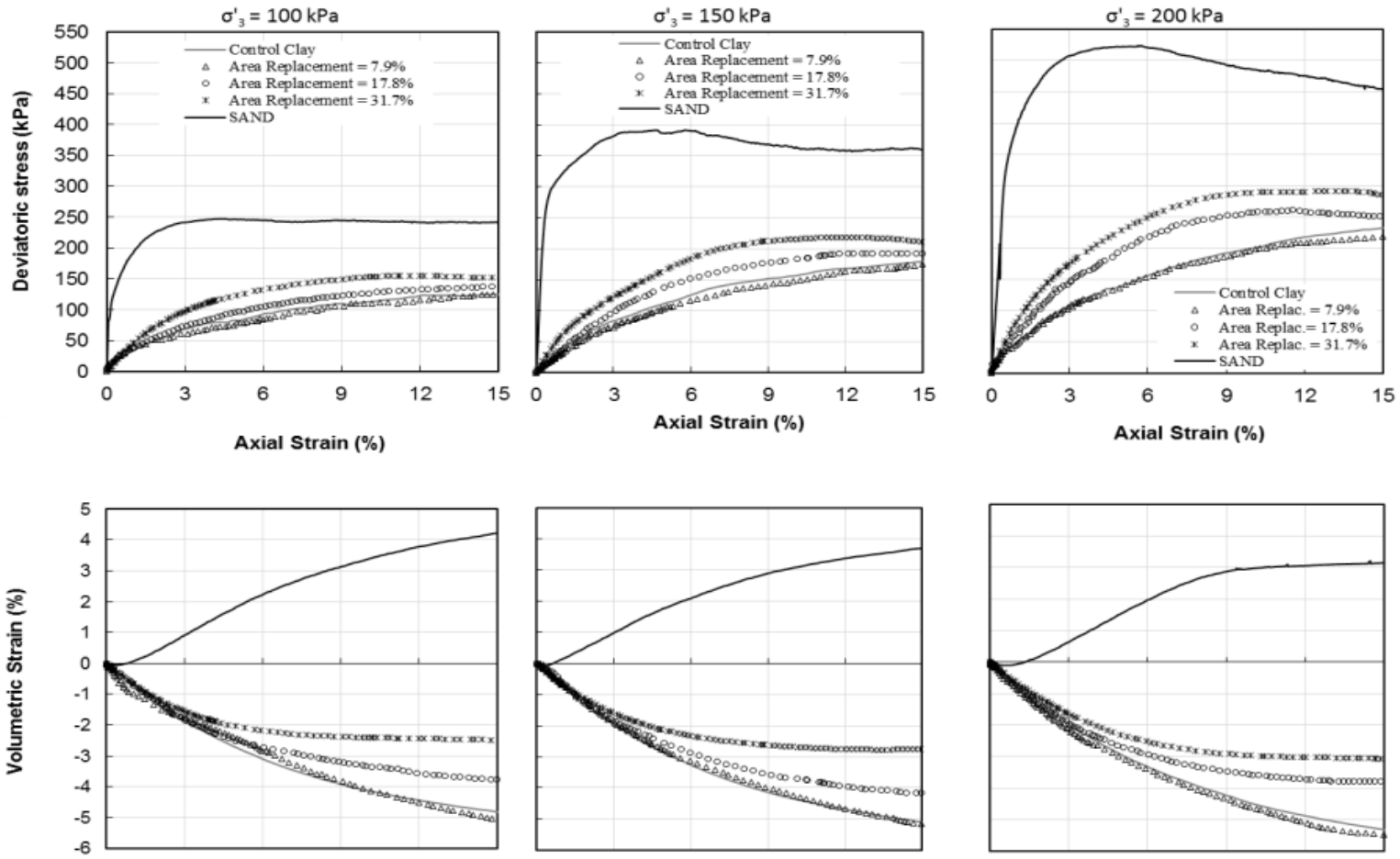

Figure 5.8. Deviatoric stress versus axial strain for specimens reinforced with partially penetrating ordinary columns at confining pressures 100kPa, 150kPa and 200kPa (As/Ac=7.9%, 17.8%, 31.7%)

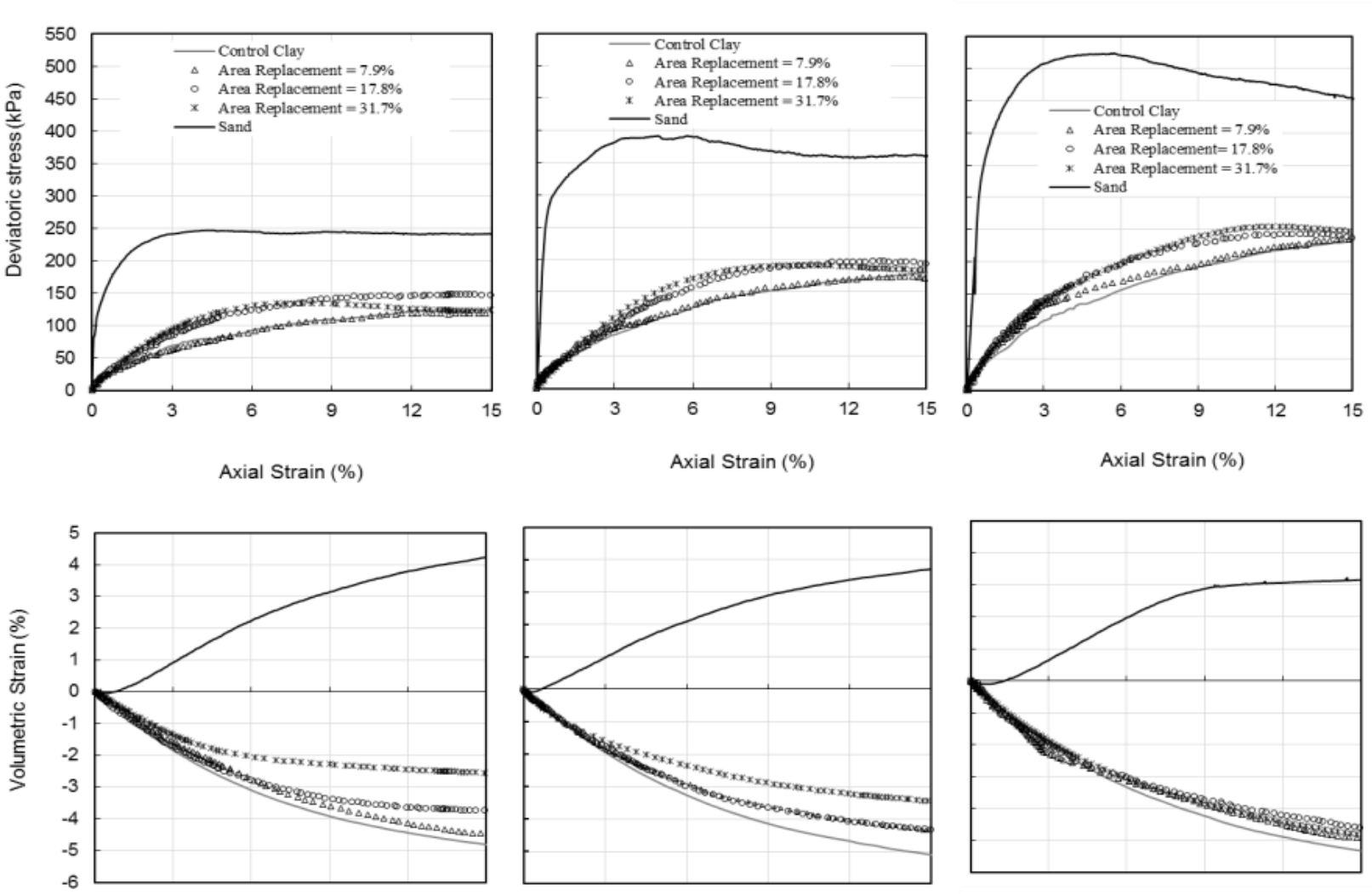

Figure 5.9. Deviatoric stress versus axial strain for specimens reinforced with partially penetrating encased columns at confining pressures 100kPa, 150kPa and 200kPa (As/Ac=7.9%, 17.8%, 31.7%)

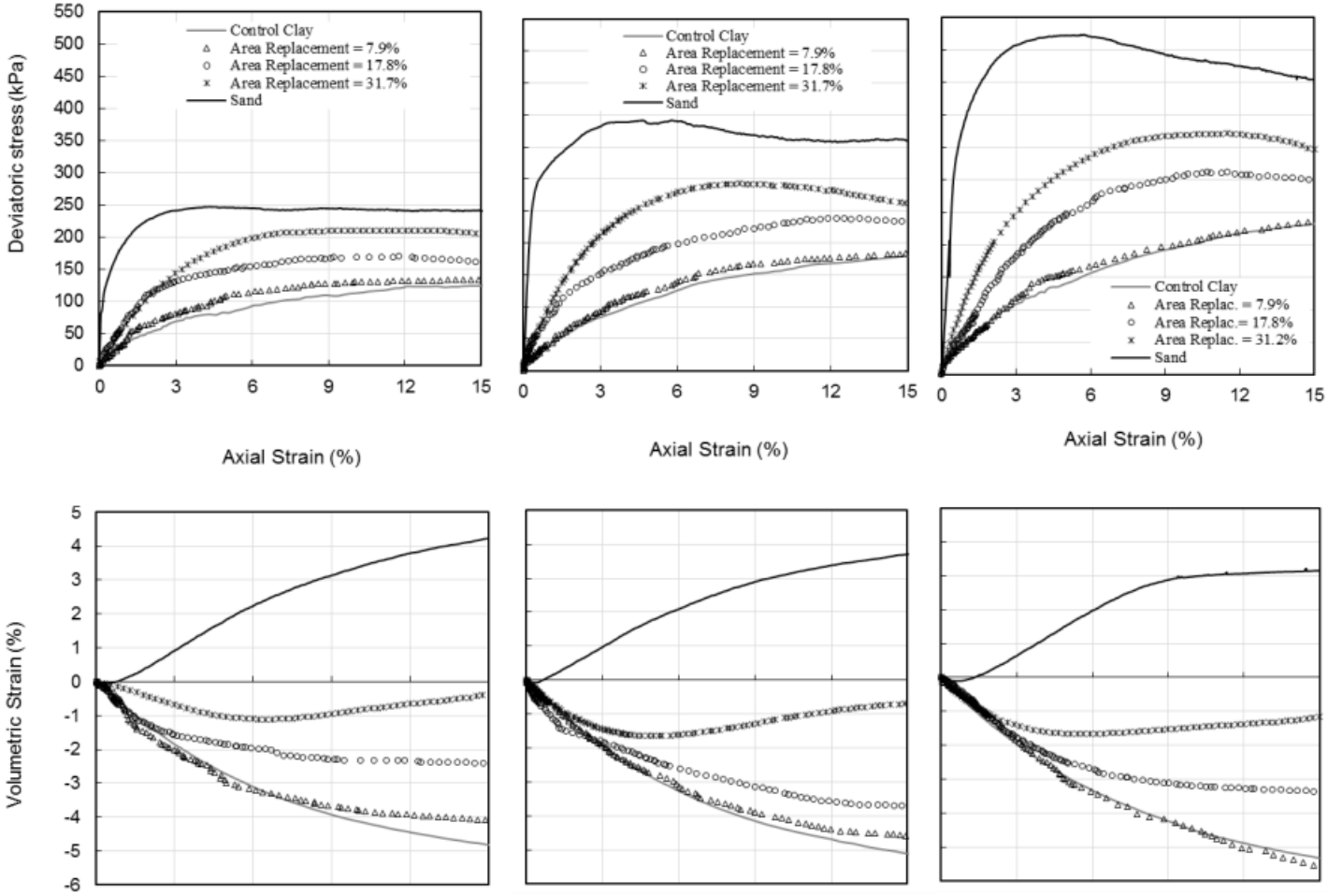

Figure 5.10. Deviatoric stress versus axial strain for specimens reinforced with fully penetrating ordinary columns at confining pressures 100kPa, 150kPa and 200kPa (As/Ac=7.9%, 17.8%, 31.7%)

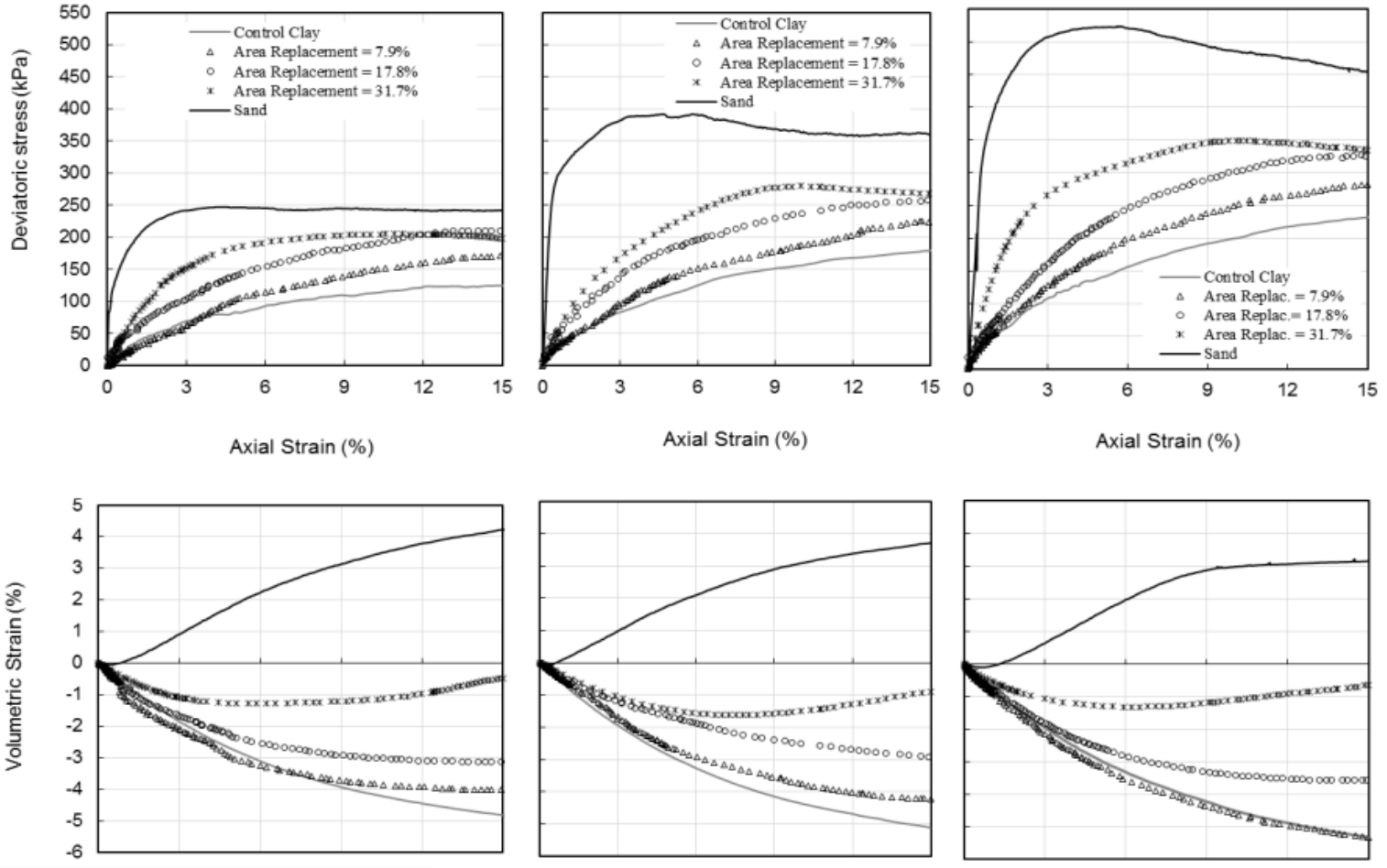

Figure 5.11. Deviatoric stress versus axial strain for specimens reinforced with fully penetrating encased columns at confining pressures 100kPa, 150kPa and 200kPa (As/Ac=7.9%, 17.8%, 31.7%)

5.2.2.3. Effect of Sand Columns on Deviatoric Stress at Failure

The percent improvement in the deviatoric stress at failure for the series of tests involving an area replacement ratio of 31.7% is presented in Table 5.1 and plotted versus the initial effective confining pressure in Figure 5.12.

For the high area replacement ratio of 31.7%, the improvement in the deviatoric stress at failure was found to range from 58.67% to 68.8% for samples reinforced with fully penetrating ordinary columns and from 22.1% to 24.46% for samples reinforced with partially penetrating ordinary columns. For the fully penetrating columns, encasing the 4-cm columns with a geosynthetic fabric did not lead to any improvement in the load-carrying capacity as indicated by the slightly reduced improvements in the deviatoric stresses at failure and which were found to range from 49.84% to 63.97%. For partially penetrating encased 4-cm columns, significant reductions in the percent improvement in the deviatoric stress at failure were observed with measured improvements ranging from 6.71% to 9.36% for partially penetrating encased columns. This reduced performance of the encased 4-cm columns could be due to the coupled effect of the relatively large diameter of the sand column used (4-cm column in a 7.1cm clay specimen) and nature of the geotextile used in this study. Murugesan and Rajagopal (2008) state that the additional confinement provided by the encasement is generally inversely proportional to the diameter of the column and is thus expected to be small for the large diameter 4-cm columns.

An investigation of the variation of the percent improvement in the deviatoric stress at failure with effective confining pressure (Figure 5.12) indicates that for the drained tests conducted in this study using encased columns, the percent improvement in the deviatoric stress at failure decreased as the initial effective confining pressure was

increased from 100 kPa to 200 kPa. These findings could be explained by the results of triaxial tests conducted by Wu and Hong (2009) on geotextile-encased and ordinary quartz sand specimens with diameters of 7cm and a height of 14cm compacted at 60% and 80% relative density. Three types of geotextile sleeves were used to encase the columns. Tests were conducted using dry sand at confining pressures of 20, 50, 100, 200, and 500 kPa. Test results indicated that the increase in the deviatoric stress of the sand specimen due to the encasement decreases with increases in confining pressure. The highest increase in deviatoric stress (13.8 times higher than the non-encased sand specimen for the strongest geotextile at 30% strain) was at 20 kPa pressure. At the highest confining pressure of 500 kPa, the increase was only 1.5 times that of the non-encased specimen.

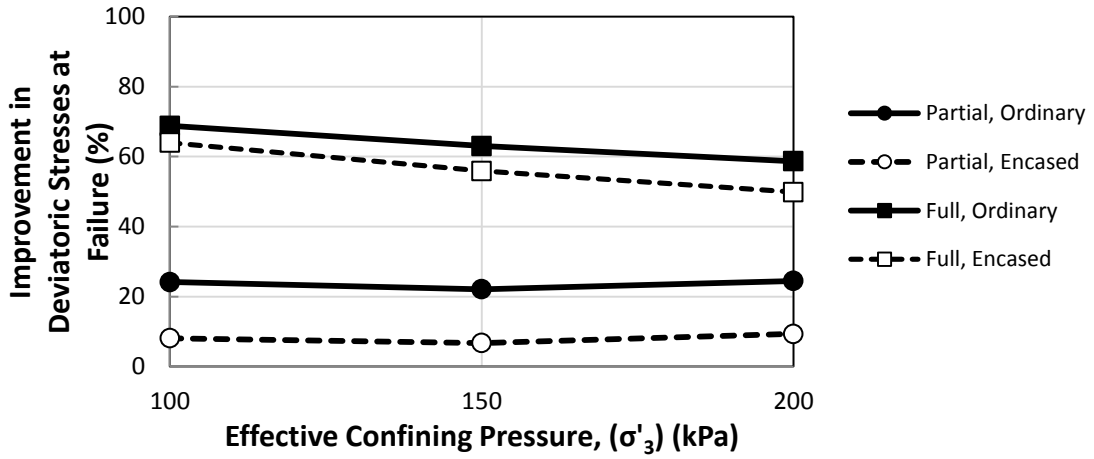

Figure 5.12. Variation of improvement in deviatoric stress at failure with confining pressure (As/Ac=31.7%)

The improvements that were witnessed in the clay specimens that were reinforced with 4-cm columns (area replacement ratio of 31.7%) were compared to the

improvements that were reported by Maalouf (2012) for samples reinforced with 2-cm (area replacement ratio of 7.9%) and 3-cm sand columns (area replacement ratio of 17.8%).

The comparisons for partially penetrating ordinary and encased columns are presented in Figures 5.13 and 5.14, respectively. The comparisons indicate that improvements in the deviatoric stresses for ordinary columns were only observed for area ratios of 17.8% (average improvement of about 10%) and 31.7% (average improvement of about 23%). For the intermediate area ratio of 17.8%, encasement with a geosynthetic did not affect the improvement while for the high area ratio of 31.7%, encasement had a negative impact on the improvement as indicated in the previous discussion.

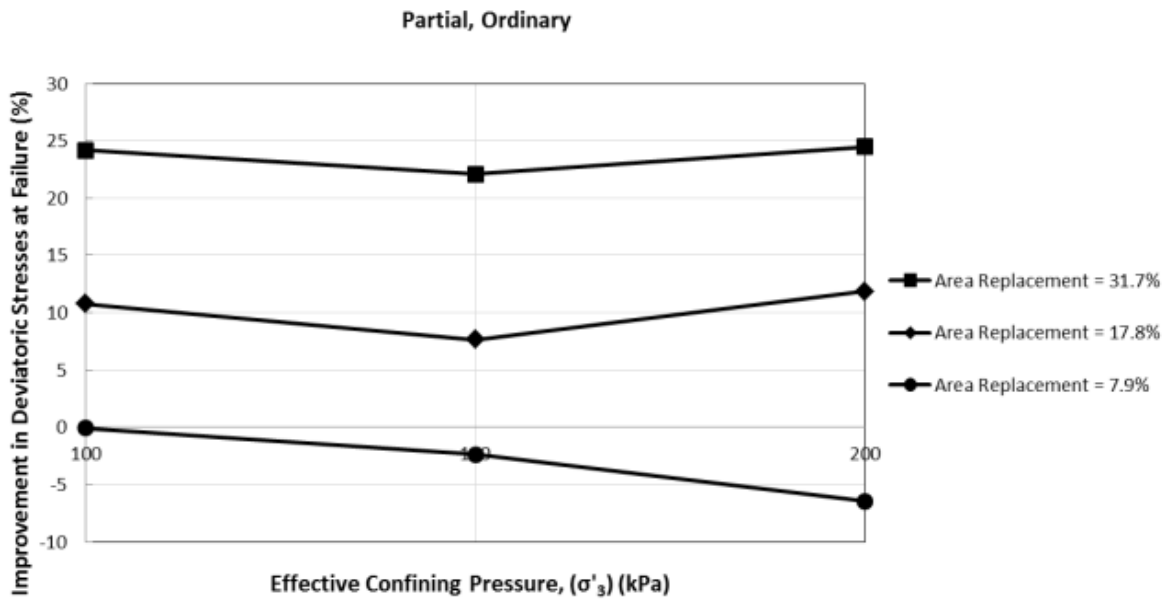

Figure 5.13. Variation of improvement in deviatoric stress at failure with confining pressure (Hc/Hs= 0.75, As/Ac=7.9%%, 17.8%, 31.7%, Ordinary)

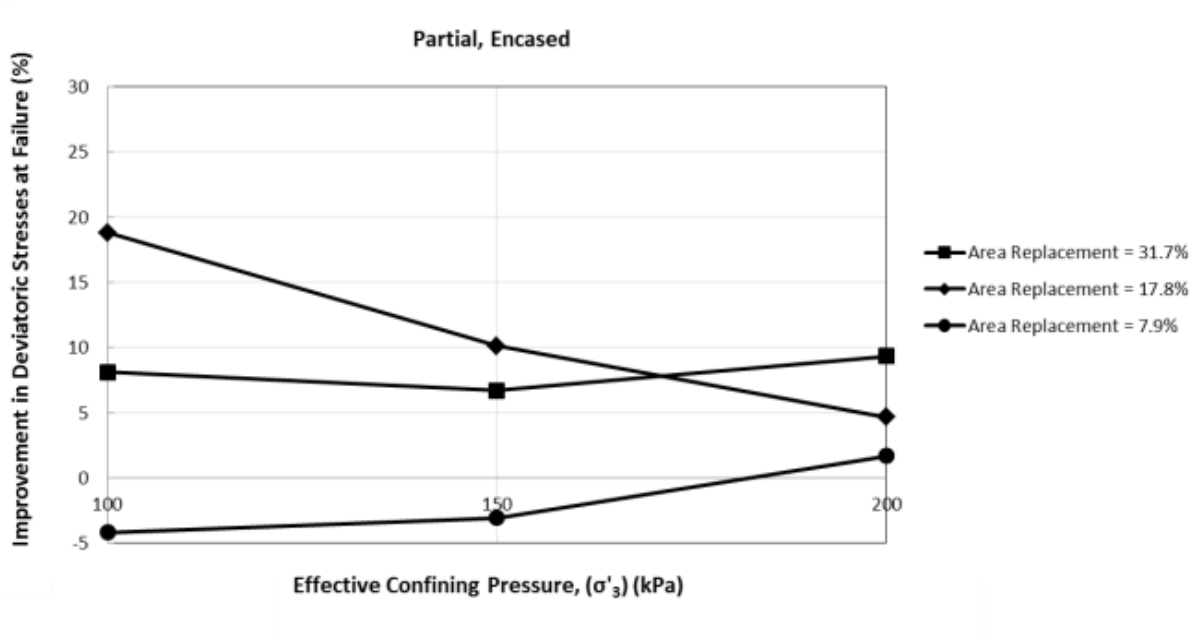

Figure 5.14. Variation of improvement in deviatoric stress at failure with confining pressure (Hc/Hs= 0.75, As/Ac=7.9%, 17.8%, 31.7%, Encased)

The comparisons for fully penetrating ordinary and encased columns are presented in Figures 5.15 and 5.16, respectively. The comparisons indicate that improvements in the deviatoric stresses for ordinary columns were observed for all area ratios with average improvements increasing from about 4% to 35% to 60% (please check) as the area ratio increased from 7.9% to 17.8% to 31.7%. For all area ratios, the percent improvement appeared to be decreasing slightly as the effective confining pressure increased from 100 kPa to 200 kPa. For the fully penetrating encased columns, results on Figure 5.16 indicated that samples reinforced with the smallest diameter column (2-cm) seemed to benefit the most from the encasement with a geotextile (average improvement of about 27% compared to 4% for ordinary columns), while samples reinforced with the largest diameter columns (4-cm) suffered from a slight

decrease in the percent improvement in strength compared to the ordinary columns as previously mentioned. Samples reinforced with the intermediate column diameter of 3-cm showed an increase in the percent improvement (average improvement of about 50%) compared to the ordinary columns (average improvement of about 34%).

The trends observed in the results exhibited in Figures 5.13 to 5.16 are consistent with the results presented in Murugesan and Rajagopal (2008, 2010) and Wu and Hong (2009). These investigators reported that the pressures developed in encased columns were found to decrease as the diameter of the columns increased, since the additional confinement provided by the encasement is inversely proportional to the diameter of the columns. They also reported that the improvement brought by the column encasement decreases as the effective confining pressure increases. These findings explain the lower values of improvement when using an encased column compared to ordinary columns for the highest area replacement ratio of 31.7% and the largest confining pressures.

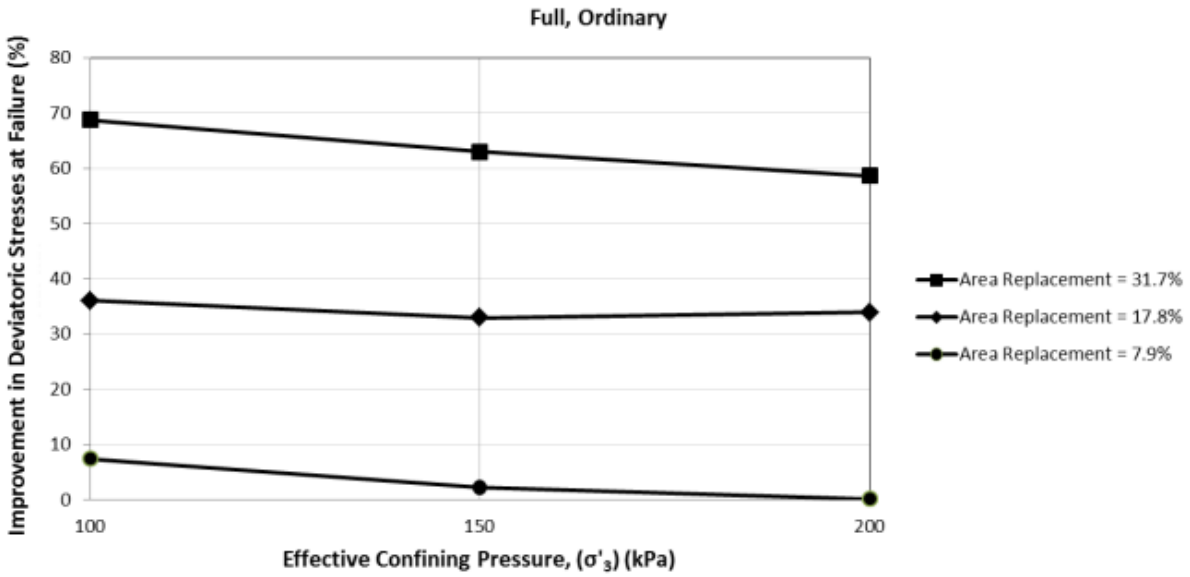

Figure 5.15. Variation of improvement in deviatoric stress at failure with confining pressure (Hc/Hs= 1, As/Ac=7.9%, 17.8%, 31.7%, Ordinary)

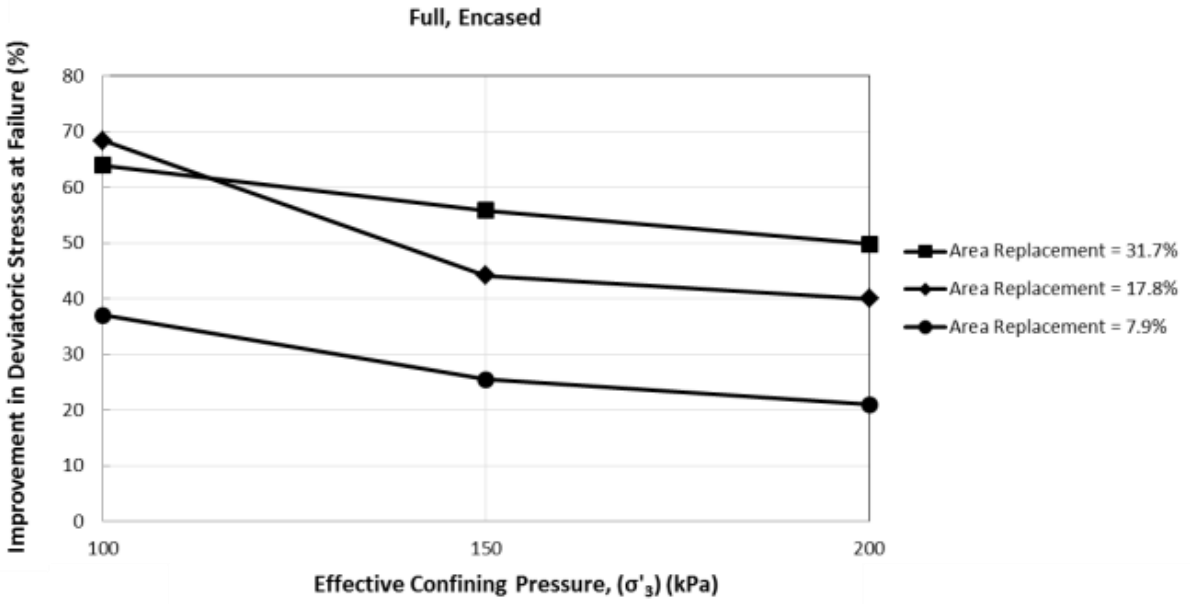

Figure 5.16. Variation of improvement in deviatoric stress at failure with confining pressure (Hc/Hs= 1, As/Ac=7.9%, 17.8%, 31.7%, Encased)

5.2.2.4. Effect of Sand Columns on Volume Change

Measurements of the volumetric strains at failure were made for all tests and reported in Table 5.1. Figure 5.17 shows the percent reduction in volumetric strains versus percent improvement in deviatoric stress for tests conducted with area replacement ratio of 31.7% (4-cm sand columns). Results on Figure 5.17 indicate that the percent reduction in volumetric strains was significantly high, spanning a range of about 43% to 85%. More importantly, the reductions in volumetric strains due to the significant dilative tendency of the sand columns was found to be correlated positively with the improvement that was observed in the load-carrying capacity of the composite.

Figures 5.18 and 5.19 illustrate the superposition of results of percent reduction in volumetric stress at failure versus percent improvement in deviatoric stress for all the area replacement ratios (7.9%, 17.8%, and 31.7%). Results pertaining to partially penetrating columns are presented in Figure 5.18 while results pertaining to fully penetrating columns are presented in Figure 5.19.

Results indicate that the reductions in volumetric strains for samples that were reinforced with partially and fully penetrating ordinary sand columns were correlated with the area replacement ratio used. The reductions in volumetric strain were found to be the smallest for an area replacement ratio of 7.9% and the largest for an area replacement ratio of 31.7%. In addition, for cases with ordinary columns, the reductions observed in the volumetric strains were associated with increases in the percent improvement in the deviatoric stress at failure. This direct correlation between area replacement ratio, reduction in volumetric strain, and increase in the percent improvement in deviatoric stress at failure was not found to hold for cases involving encased columns. For example, relatively large improvements in strength were observed

for some cases involving encased columns although these cases were not associated with higher reductions in volumetric strains. Such cases (which were more relevant to the 2cm and 3cm columns) indicate that the additional improvement in strength due to the encasement is correlated more with the additional confinement brought by the encasement to the column and not to improvements in the tendency for volume change.

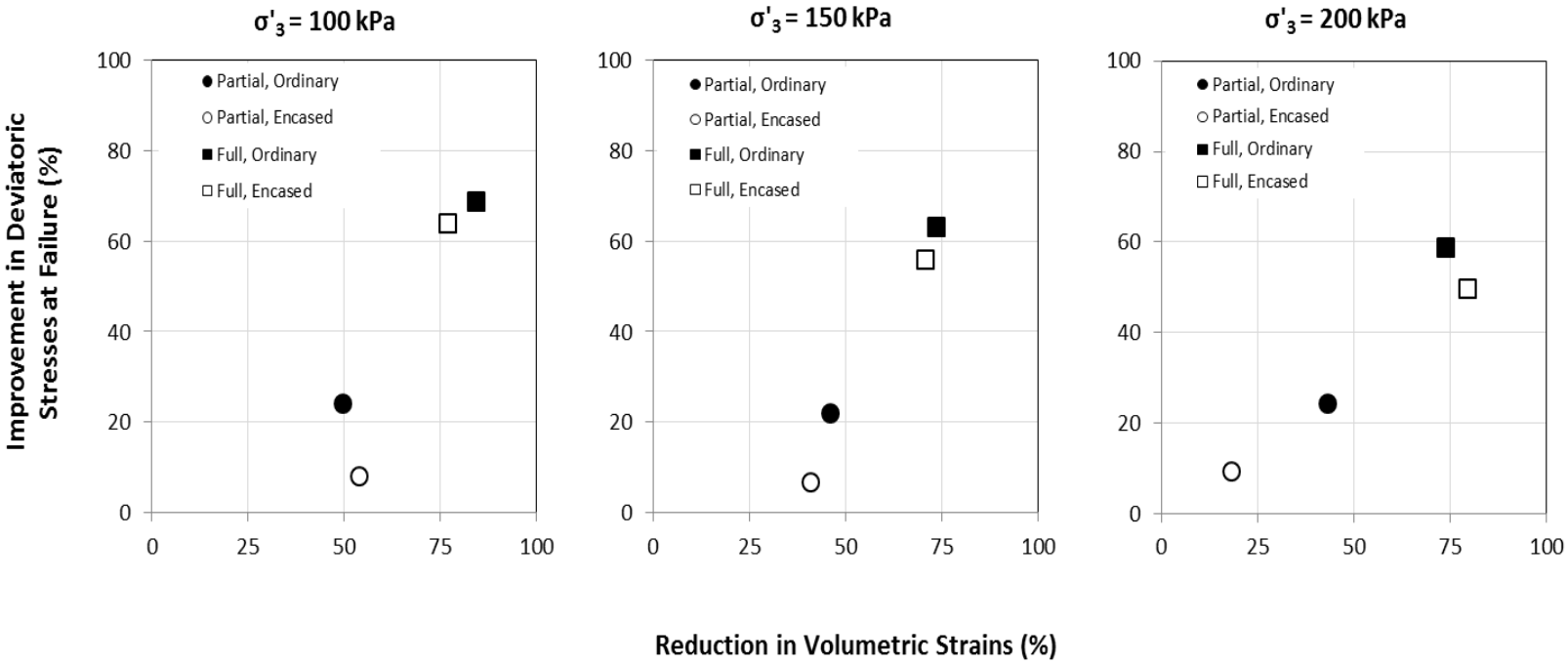

Figure 5.17. Relationship between improvements in deviatoric stress and reduction in volumetric strains at failure (Ac/As= 31.7%)

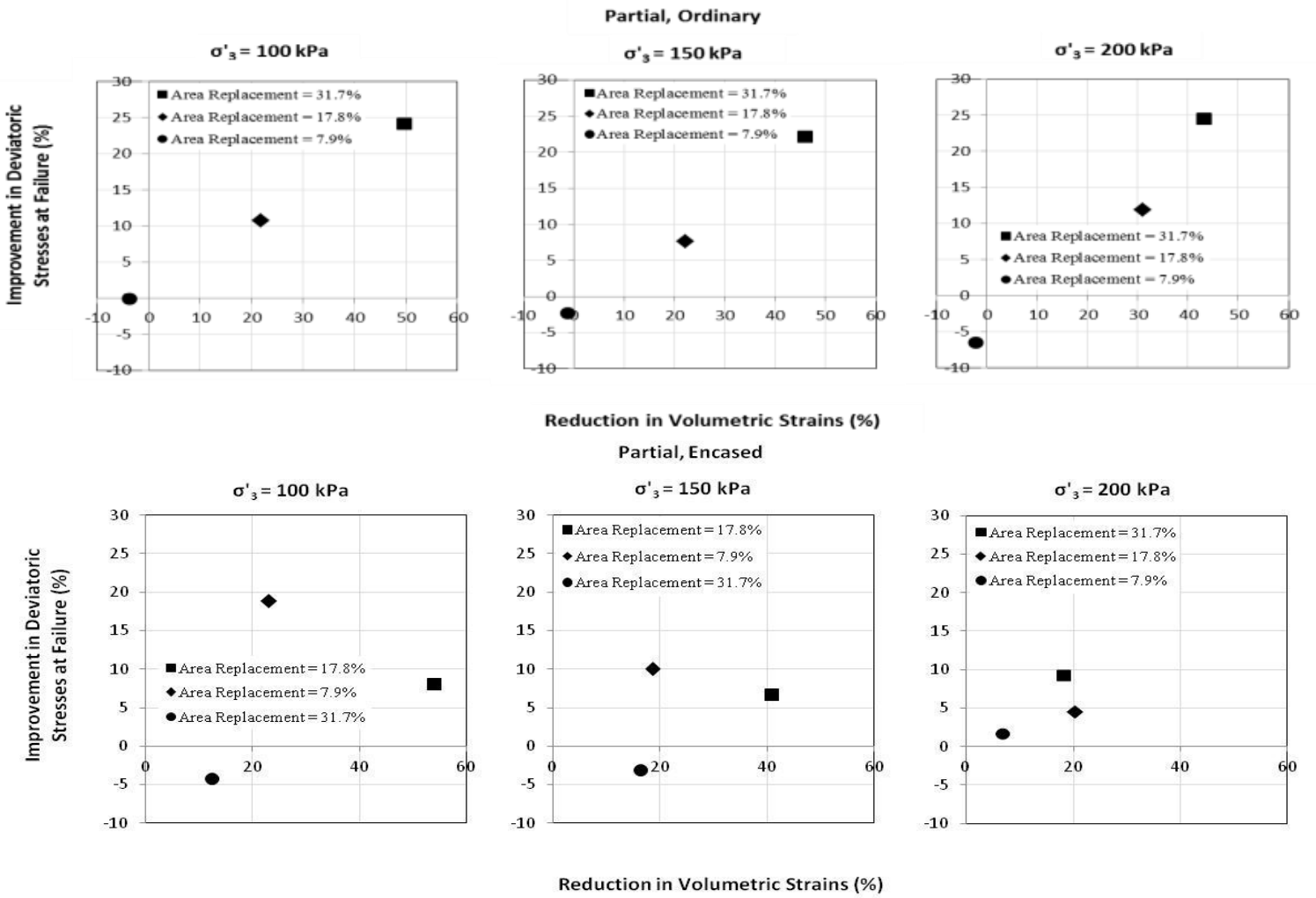

Figure 5.18. Relationship between improvements in deviatoric stress and reduction in volumetric strains at failure (Hc/Hs=0.75, Ac/As= 7.9%, Ac/As= 17.8%,Ac/As= 31.7%, Ordinary and Encased)

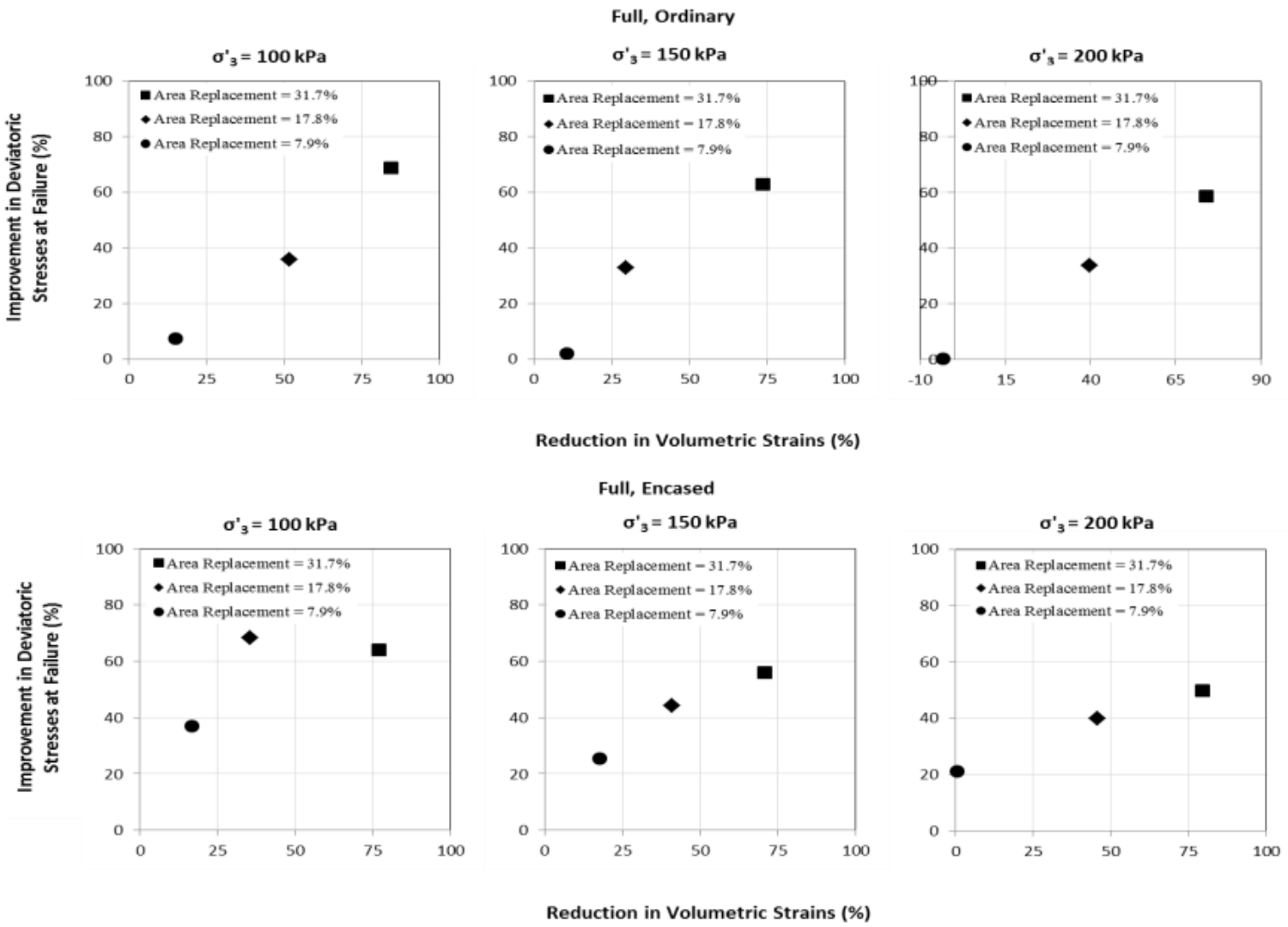

Figure 5.19. Relationship between improvements in deviatoric stress and reduction in volumetric strains at failure (Hc/Hs=1, Ac/As= 7.9%, Ac/As= 17.8%,Ac/As= 31.7%, Ordinary and Encased)

5.2.2.5. Effect of Sand Columns on the Drained Secant Modulus

A drained secant modulus $(E_{sec})_{1\%}$ defined at an axial strain of 1% was calculated for each test by dividing the deviatoric stress measured at an axial strain of 1% by the corresponding strain. Results of the calculated values of $(E_{sec})_{1\%}$ are presented in Table 5.1 for the samples reinforced with 4-cm columns. Also presented in Table 5.1 are the $(E_{sec})_{1\%}$ values corresponding to the specimens reinforced with the 2-cm and 3-cm sand columns (Maalouf 2012) for comparison.

The variation of the calculated $(E_{sec})_{1\%}$ with initial effective confining pressure for tests conducted using an area replacement ratio of 31.7% is shown in Figure 5.20. Also shown on Figure 5.20 are the $(E_{sec})_{1\%}$ values for the control clay specimens. The curves on Figure 5.20 indicate that $(E_{sec})_{1\%}$ increases relatively linearly with effective confining pressure for control and reinforced specimens. Specimens that were reinforced with partially and fully penetrating ordinary columns exhibited average increases of about 50% and 120% in the value of $(E_{sec})_{1\%}$, respectively. When the columns were encased, the average increase in $(E_{sec})_{1\%}$, dropped to about 17% for partially penetrating columns and remained relatively constant at about 130% for the fully penetrating columns.

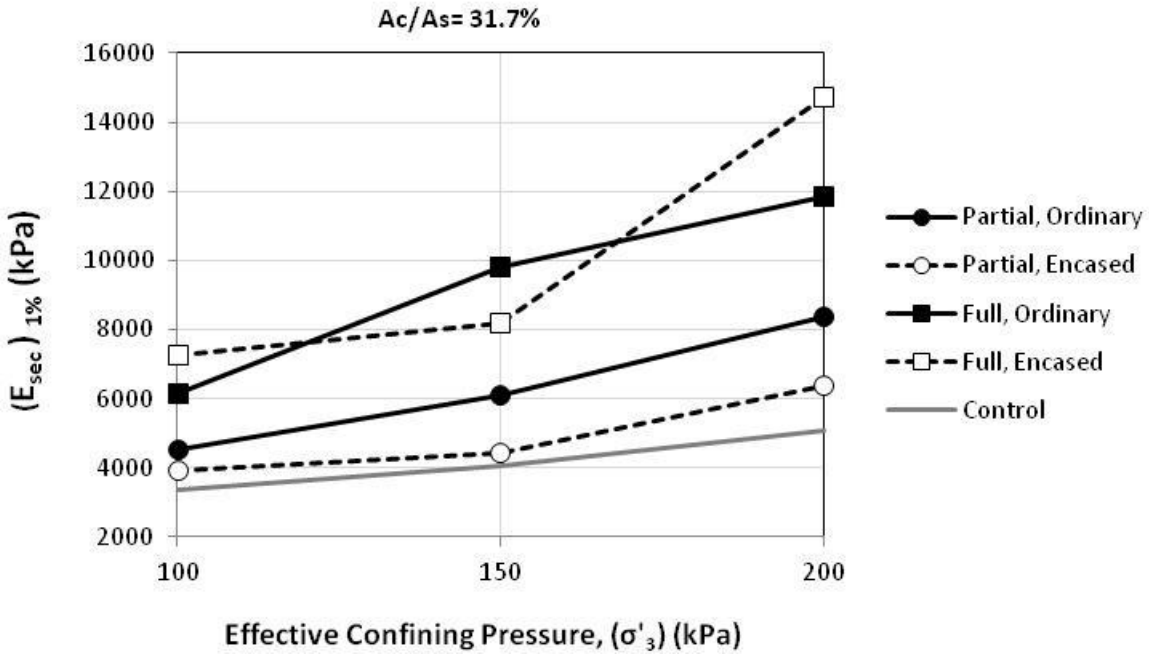

Figure 5.20. Variation of $(Esec)_{1\%}$ with effective confining pressure (Ac/As=31.7%)

The calculated values of $(E_{sec})_{1\%}$ for cases involving area replacement ratios of 7.9%, 17.8%, and 31.7% are plotted versus confining pressure on Figures 5.21 to 5.24 to illustrate the effect of the area replacement ratio on $(E_{sec})_{1\%}$ for both partially penetrating and fully penetrating ordinary and encased columns. In general, results indicate very small increases and some reductions in $(E_{sec})_{1\%}$ for partially and fully penetrating 2-cm sand columns compared to the control clay specimens. For tests conducted with partially penetrating 3-cm columns, no significant increases in $(E_{sec})_{1\%}$ were observed except for a confining pressure of 200 kPa where the increase in $(E_{sec})_{1\%}$ was found to be about 51% for the ordinary column and about 96% for the encased column. For tests conducted with fully penetrating 3-cm columns, consistent increases in $(E_{sec})_{1\%}$ were observed at all confining pressures with average increases of about 104% for ordinary columns and about 79.6% for encased columns. For comparison, the

average increases in $(E_{sec})_{1\%}$ for the fully penetrating ordinary and encased 4-cm diameter columns were 120% and 130%, respectively.

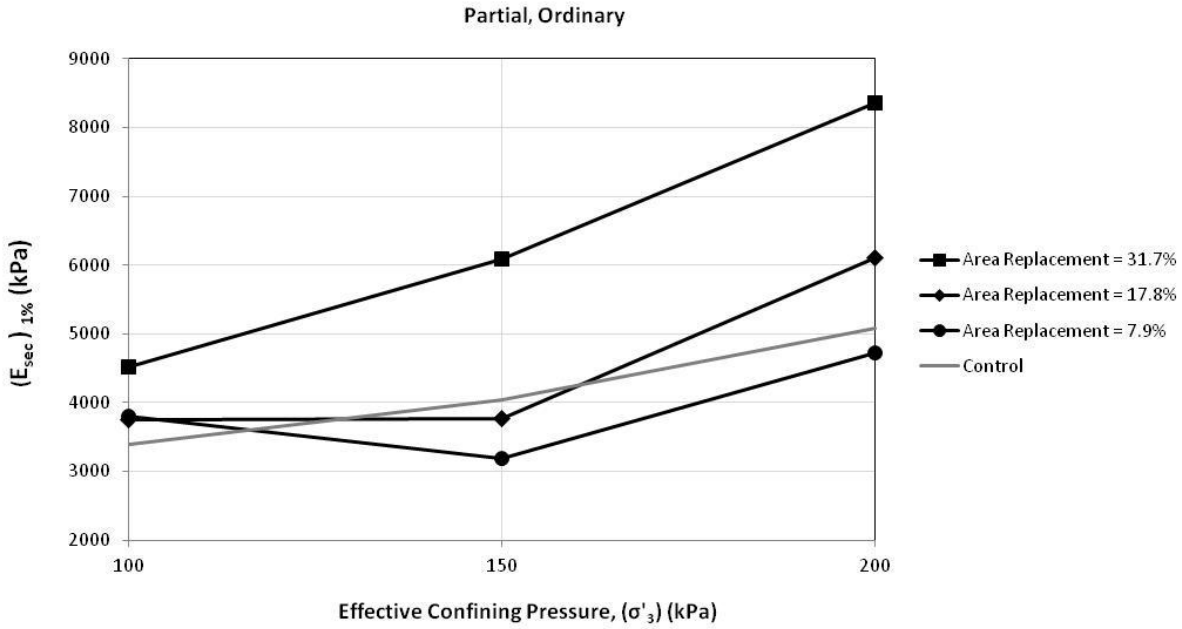

Figure 5.21. Variation of $(Esec)_{1\%}$ with effective confining pressure (Hc/Hs=0.75, Ac/As=7.9%, 17.8%, 31.7%, Ordinary)

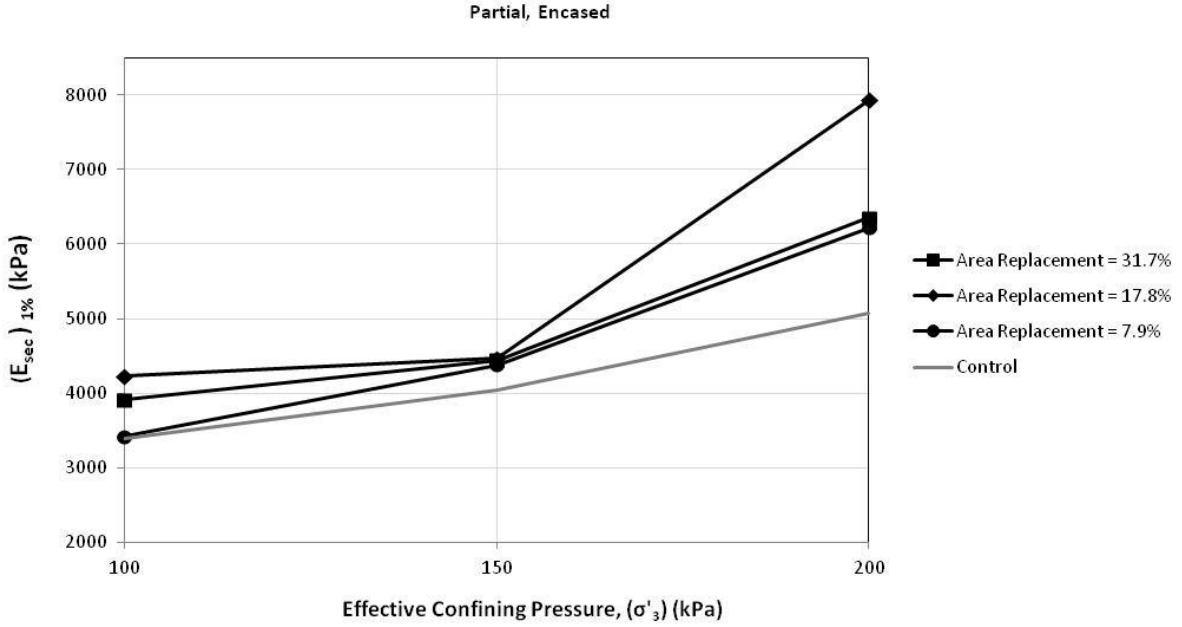

Figure 5.22. Variation of $(Esec)_{1\%}$ with effective confining pressure (Hc/Hs=0.75,Ac/As=7.9%, 17.8%, 31.7%, Encased)

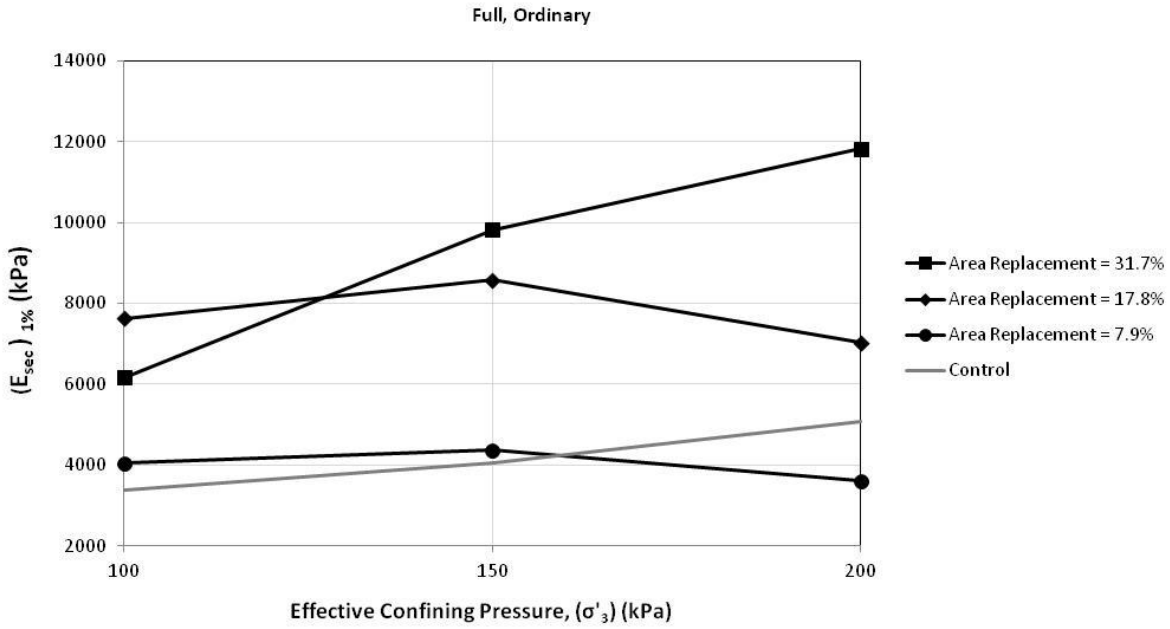

Figure 5.23. Variation of $(Esec)_{1\%}$ with effective confining pressure (Hc/Hs=1,Ac/As=7.9%, 17.8%, 31.7%, Ordinary)

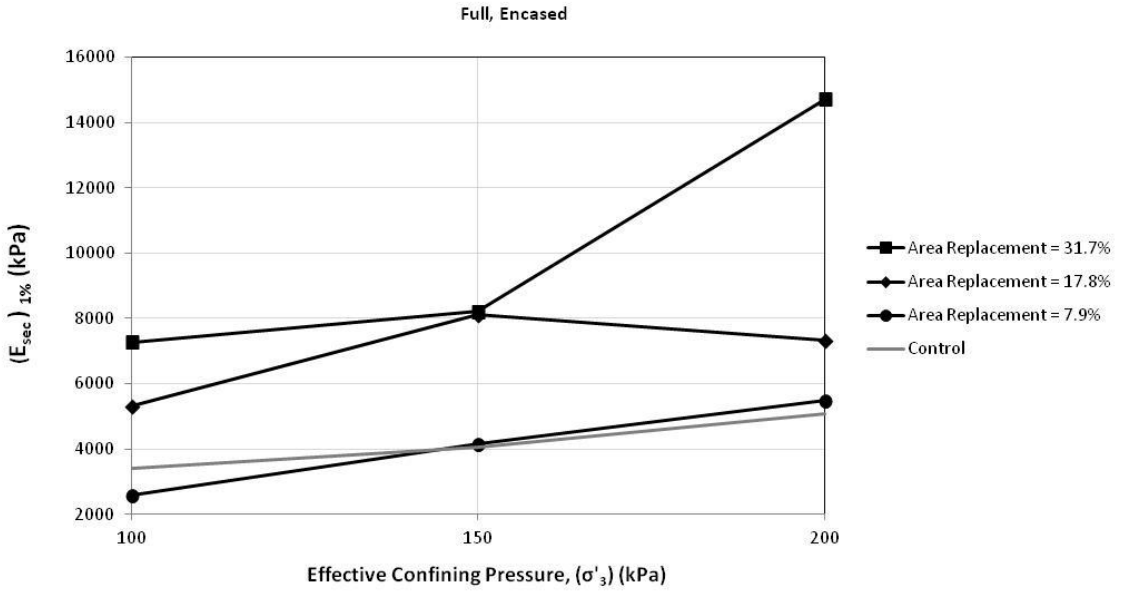

Figure 5.24. Variation of $(Esec)_{1\%}$ with effective confining pressure (Hc/Hs=1,Ac/As=7.9%, 17.8%, 31.7%, Encased)

The response observed in Figures 5.21 to 5.24 for clay/sand composites at low strain levels (as reflected in $(E_{sec})_{1\%}$) is quite complex, particularly with regards to the reduction observed in $(E_{sec})_{1\%}$ and the roles that partial penetration, presence of encasement, and confining pressure could have played with this regard. The installation of the sand column could also have contributed to the reduction in (E_{sec}) at small strains, where the response of the sand column could be affected negatively by any reduction in the contact stresses (confinement) between the column material and the surrounding clay due to column installation. These effects are more critical for partially penetrating columns (reduced contact at the column tip) and relatively small effective confining pressures (lack of full contact at small strains). More importantly, the different stress–strain properties of the clay and the sand could also influence (E_{sec}), particularly at the early stages of loading where sharing of load between the column and the clay initiates, and where the dilation of the column could result in a rapid loss of stiffness. The contrast in stiffness between the columns and the clay is expected to decrease as the column dilates and transfers more of its load to the clay.

The dependency of the drained secant modulus on strain level was investigated by plotting the variation of E_{sec} with strain for specimens reinforced with an area replacement ratio of 31.7% at effective confining pressures of 100, 150, and 200 kPa (see Figure 5.25). The results indicated that the secant modulus for reinforced and control specimens decreases as the axial strain increases, reflecting the nonlinearity in the stress-strain response. Specimens that are reinforced with sand columns exhibit a sharp drop in the secant stiffness for strains that are less than 1% to 2%. After a strain of

2%, the stiffness decreases with strain at a decreasing rate. Similar results are obtained for the smaller diameter sand columns.

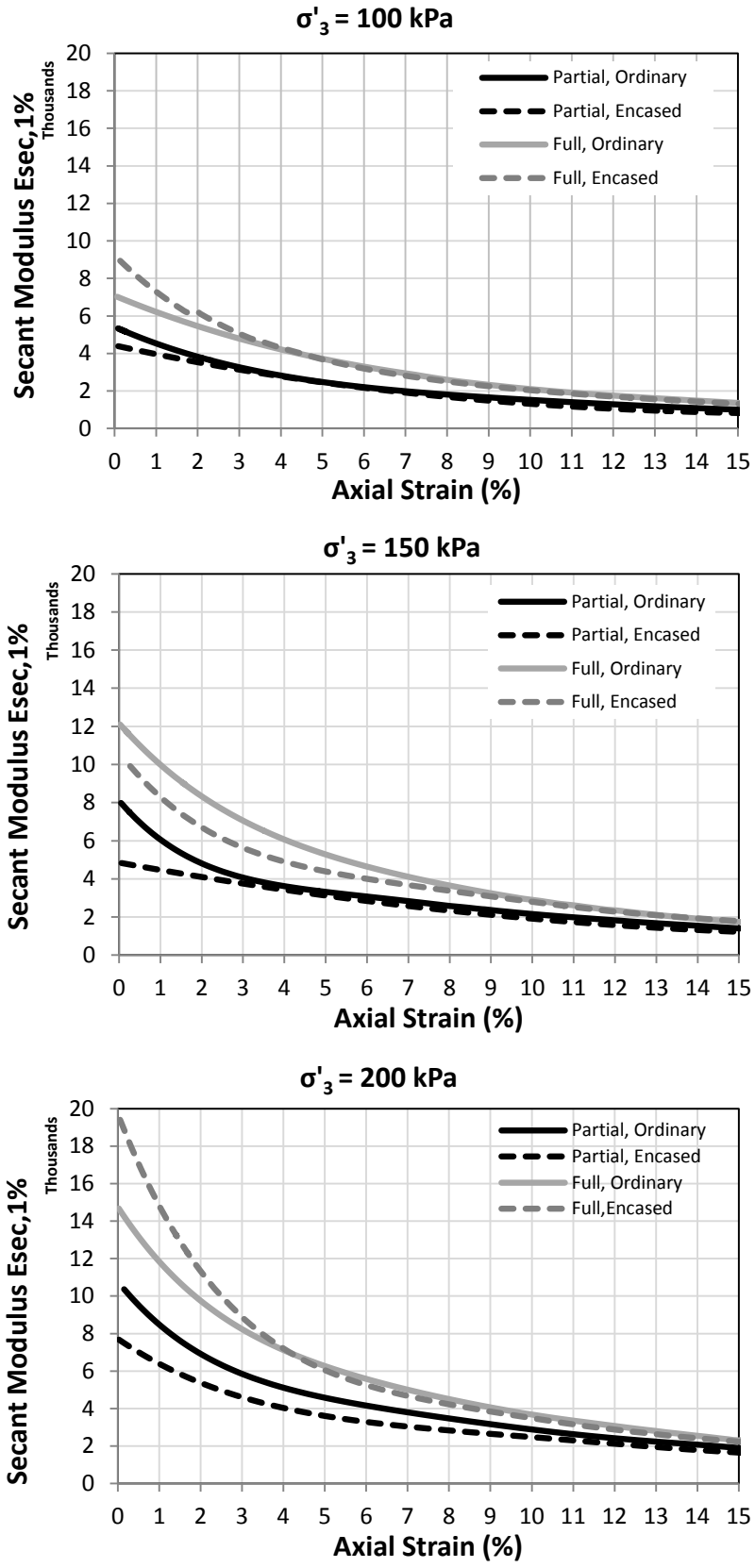

Figure 5.25. Variation of $(Esec)_{1\%}$ with strain for control and composite specimens (Ac/As=31.7%)

5.2.2.6. Effect of sand columns on the Drained Shear Strength

Figures 5.26 to 5.31 show the effective Mohr-Coulomb envelops corresponding to each combination of area replacement ratio and column penetration ratio analyzed in the present study and in the study conducted by Maalouf (2012), for ordinary and encased columns, respectively. The resulting shear strength parameters c' and ϕ' are summarized in Table 5.2.

The data in Table 5.2 indicates that the insertion of partially penetrating 2-cm sand columns didn't lead to a noticeable change/increase in the effective friction angle ϕ' and only an increase in the cohesion intercept c' to 12kPa for the ordinary column. For fully penetrating 2-cm columns, non-zero effective cohesion intercepts c' of 10 kPa and 18 kPa, with associated effective friction angles ϕ' of 20^o and 21.6^o, were observed for ordinary and encased columns respectively. For the case involving ordinary columns, the non-zero c' and the reduced ϕ' reflect the improvement observed in the deviatoric stress at the lower confining pressure of 100 kPa and the lack of improvement at higher confining pressures. On the other hand, the non-zero c' of 18 kPa and the unimproved ϕ' of 21.6^o are expected given previous research which shows that encasing sand columns with geosynthetics of different strengths results in non-zero cohesive intercepts which increase as the strength of the fabric increases (Wu and Hong 2009), with the increases in c' being associated with no improvements in the friction angle ϕ'.

For samples reinforced with 3-cm ordinary columns, the friction angle ϕ' was found to increase to 22.5^o and 24.5^o (compared to 21.8^o for the control clay) for cases involving partially penetrating and fully penetrating sand columns, respectively. The increases in ϕ' were associated with small increases in the effective cohesion intercept c' found to be 5 and 10 for partially and fully penetrating sand columns, respectively.

On the other hand, samples that were reinforced with 3-cm encased columns showed no improvements in the friction angle compared to the control specimens, but were associated with non-zero *c'* values of 15 kPa and 30 kPa for cases involving partially penetrating and fully penetrating sand columns, respectively. The envelops for the ordinary columns showed consistent increases in the friction angle, while the envelops for the encased columns were parallel to, but higher than, the envelop of the control clay specimens

For samples reinforced with 4-cm ordinary columns, the friction angle ϕ' was found to increase to 23.8^{o} and 26^{o} for cases involving partially penetrating and fully penetrating sand columns, respectively. The increases in ϕ' were associated with increases in the effective cohesion intercept *c'* found to be 7 and 19 for partially and fully penetrating sand columns, respectively. On the other hand, samples reinforced with partially penetrating encased columns showed no improvement in the friction angle but were associated with a non-zero *c'* of 7. Furthermore, samples reinforced with fully penetrating encased columns showed an improvement over the control clay in the friction angle ϕ' which increased from 21.8° to 24.8°. This increase in the friction angle was associated with a non-zero *c'* of 22.5 kPa.

Add a graph showing the Mohr-Coulomb envelops on top of each other on the same graph. Draw the lines only in the range of the failure stresses for each test without drawing the actual Mohr Circle (only the tangent points). Draw one graph for the ordinary tests and one graph for the encased tests.

Table 5.2. Effective shear stress failure parameters

Column Diameter (cm)	Column Penetration Ratio	c' (kPa)	ϕ' (deg)
0	0	0	21.8
2	0.75	12	18.8
2	1	10	20
2(ESC)	0.75	0	21.5
2(ESC)	1	18	21.6
3	0.75	5	22.5
3	1	10	24.5
3(ESC)	0.75	15	20.2
3(ESC)	1	30	21.8
4	0.75	7	23.8
4	1	19	26
4(ESC)	0.75	7	21.8
4(ESC)	1	22.5	24.8

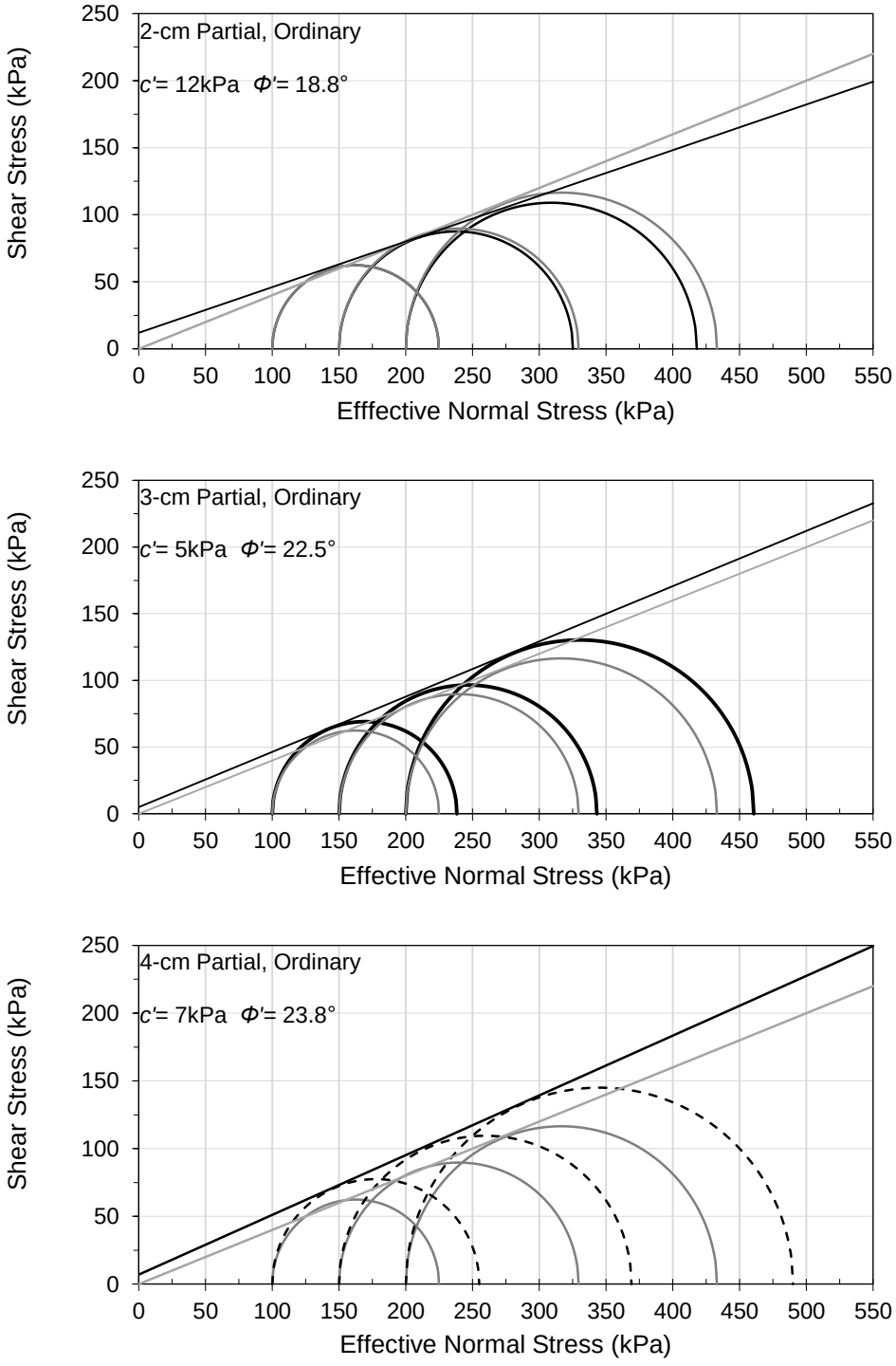

Figure 5.26. Drained failure envelopes for reinforced and control kaolin specimens (Hc/Hs=0.75, Ac/As= 7.9%, 17.8%, 31.7%, Ordinary)

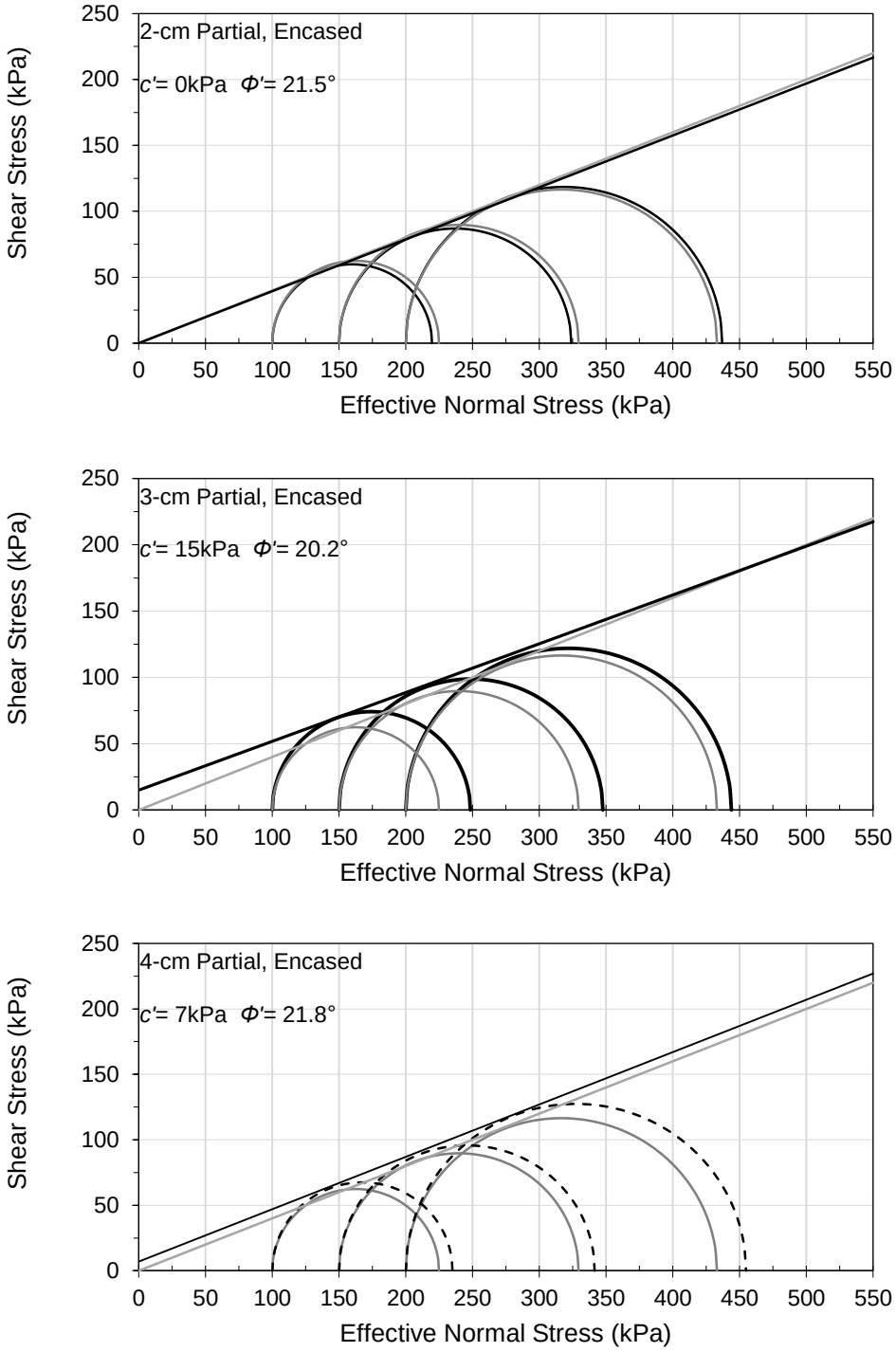

Figure 5.27. Drained failure envelopes for reinforced and control kaolin specimens (Hc/Hs=0.75, Ac/As= 7.9%, 17.8%, 31.7%, Encased)

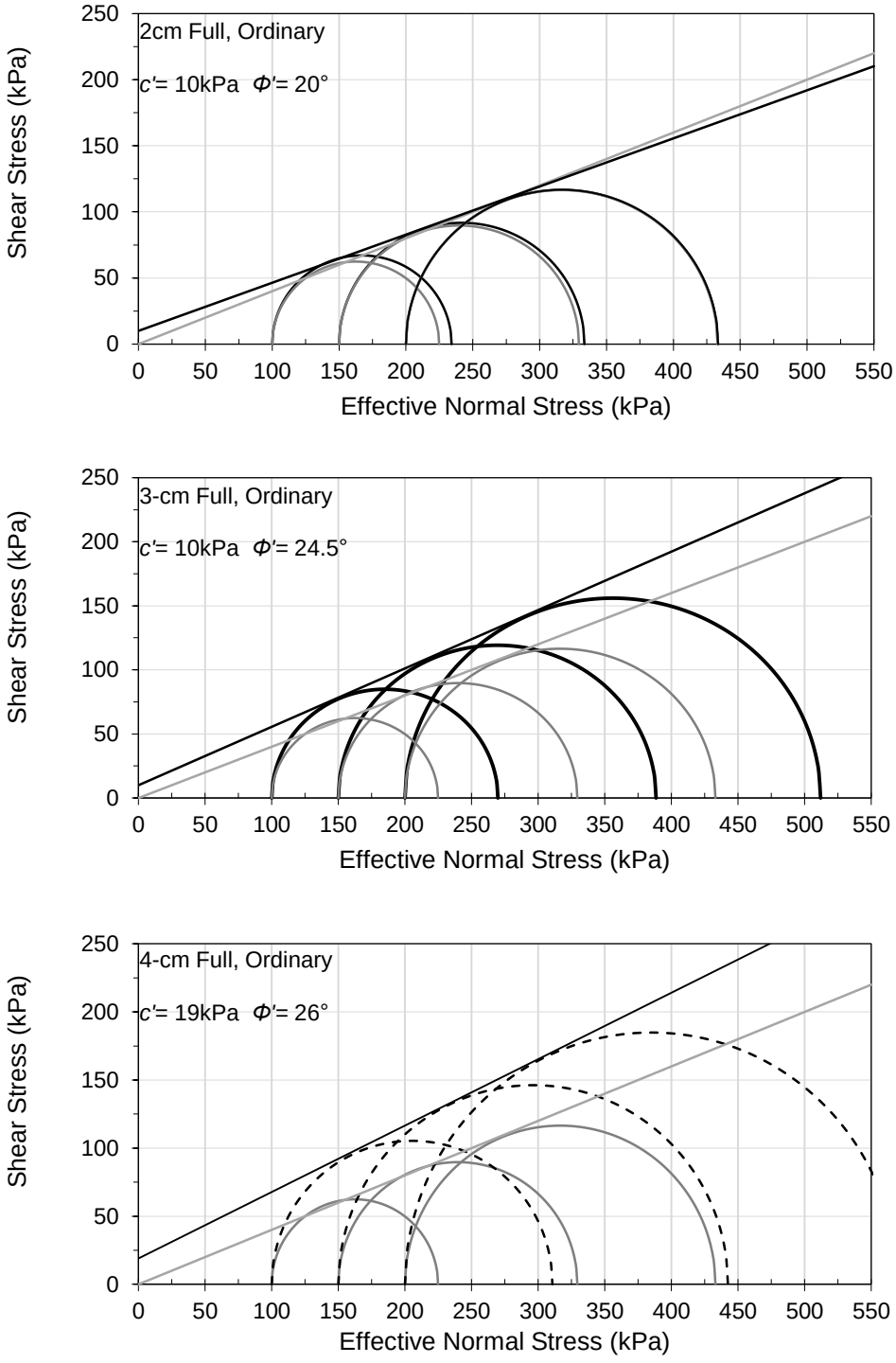

Figure 5.28. Drained failure envelopes for reinforced and control kaolin specimens (Hc/Hs=1, Ac/As= 7.9%, 17.8%, 31.7%, Ordinary)

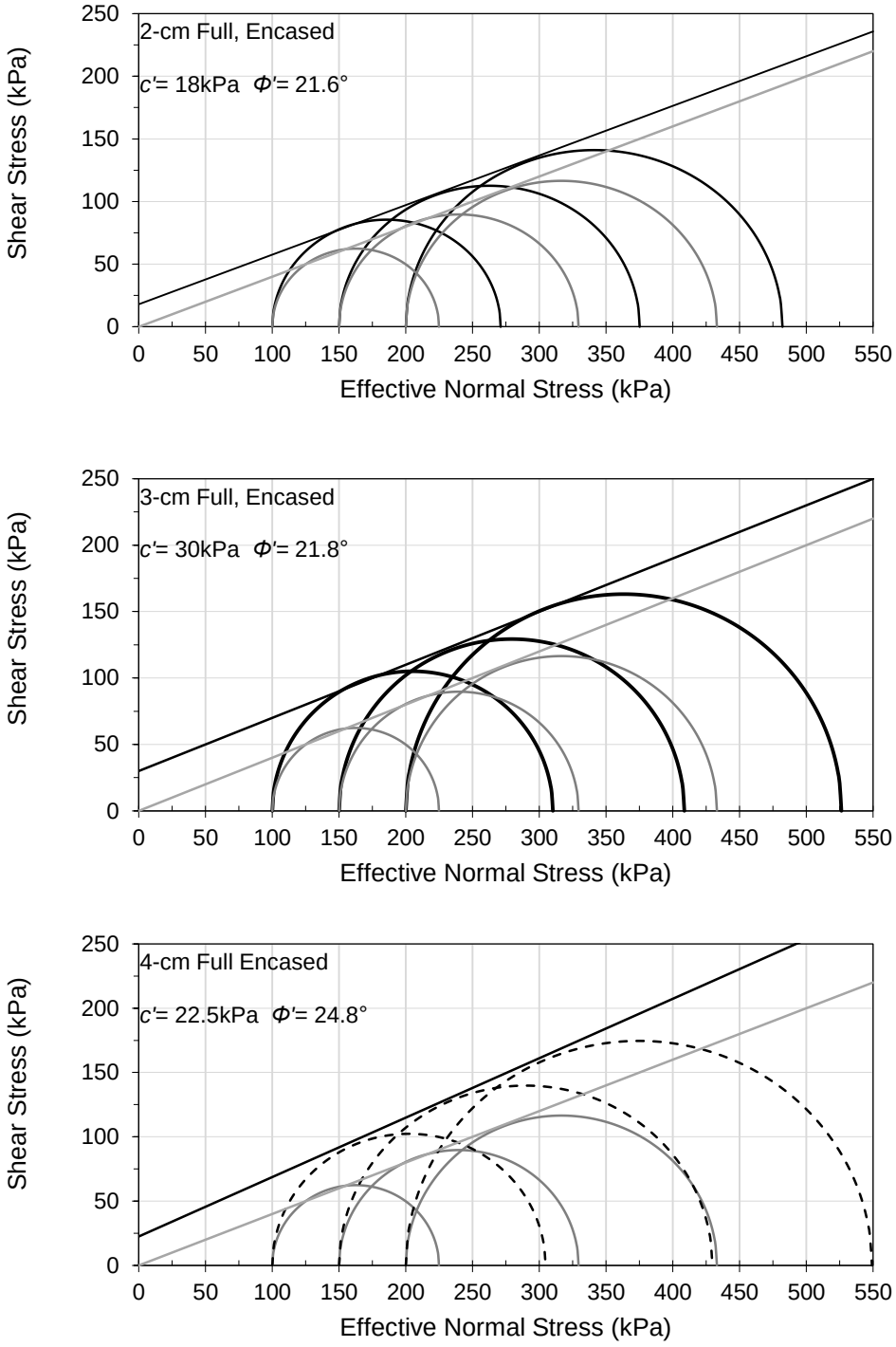

Figure 5.29. Drained failure envelopes for reinforced and control kaolin specimens (Hc/Hs=1, Ac/As= 7.9%, 17.8%, 31.7%, Encased)

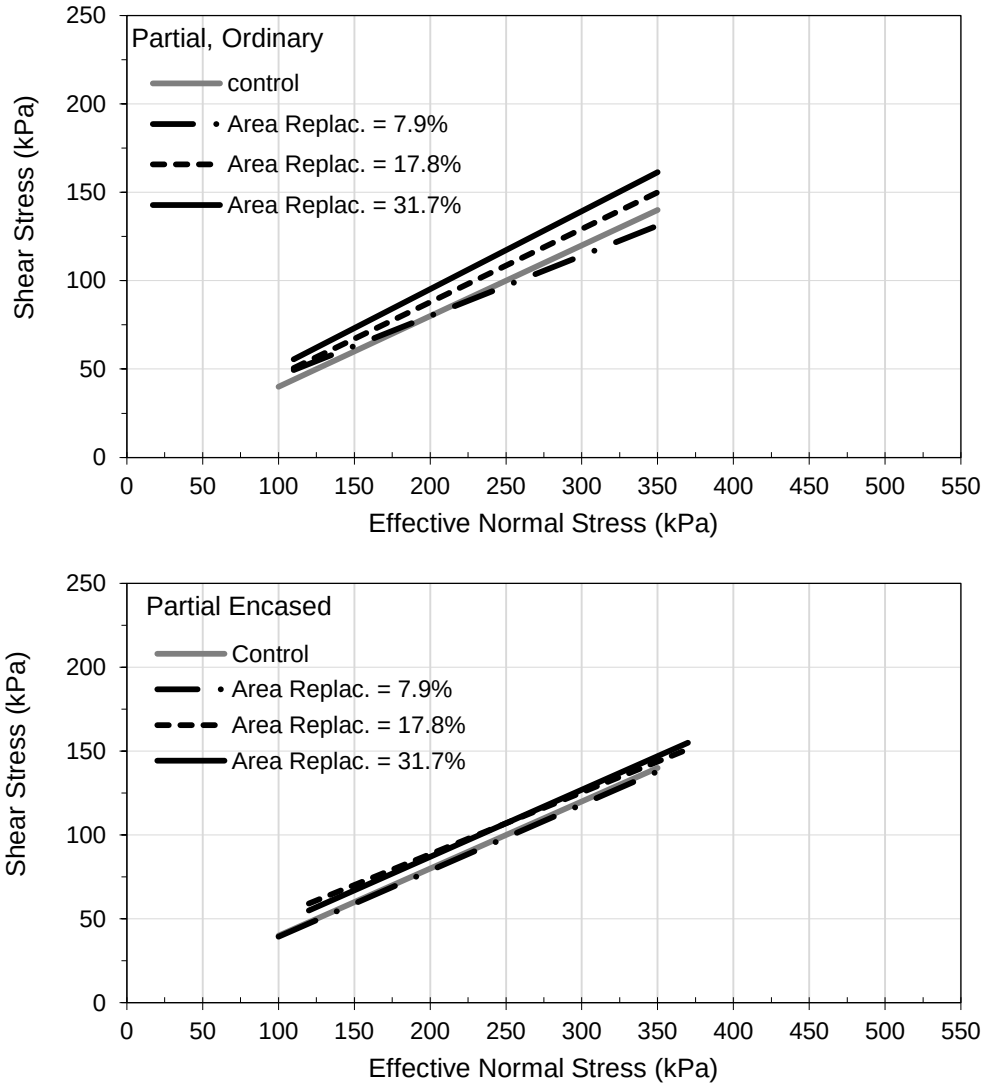

Figure 5.30. Drained failure envelopes for reinforced and control kaolin specimens (Hc/Hs=0.75, Ac/As= 7.9%, 17.8%, 31.7%, Ordinary & Encased)

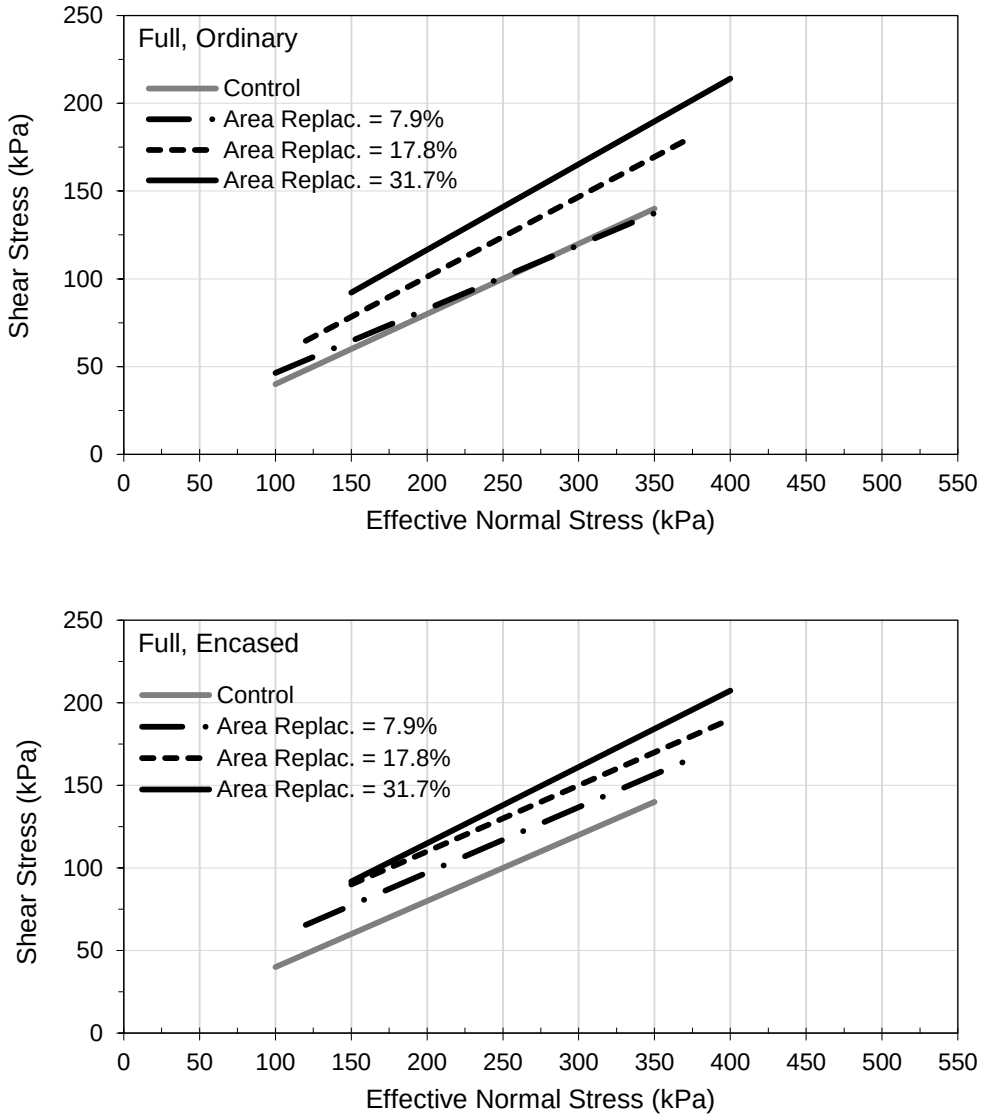

Figure 5.31. Drained failure envelopes for reinforced and control kaolin specimens (Hc/Hs=1, Ac/As= 7.9%, 17.8%, 31.7%, Ordinary & Encased)

5.3. Summary of Main Findings

Based on the results of 15 consolidated drained triaxial tests that were conducted in this experimental research study and complemented with 24 tests done by Maalouf

(2012), the following conclusions can be drawn with regards to the effect of sand columns on the drained response of soft clay:

1. Reinforcing normally consolidated soft kaolin specimens with sand columns at an area replacement ratio of 7.9% resulted in reductions in $(Esec)_{1\%}$, with the only exceptions being tests conducted with encased columns at a confining pressure of 200 kPa. For tests conducted using area replacement ratios of 17.8%, increases in $(Esec)_{1\%}$ were observed for fully penetrating columns at all confining pressures and for partially penetrating columns at a confining pressure of 200 kPa. For tests conducted using area replacement ratios of 31.7%, increases in $(Esec)_{1\%}$ were observed for all cases and at all confining pressures. Interestingly, in the case of the 4-cm fully penetrating ordinary column at 100kPa the $(Esec)_{1\%}$ was found to be to be lower than for the 17.8% area replacement ratio, which contradicts the trend, but further proves that the installation effects can significantly affect the results particularly at low confining pressures.

2. The inclusion of 3-cm and 4-cm sand columns in the clay reduced appreciably the contractive volumetric strains of the clay specimens, with the reduction being more significant for tests involving fully penetrating sand columns, which are expected to be more dilative compared to partially penetrating columns. No significant reductions in volumetric strains were observed for samples reinforced with the 2-cm columns. For tests with 4-cm sand columns, a correlation between tendency with volume change and the penetration depth was observed, which also dictates the failure mode. Partially penetrating columns would tend to fail by punching rather than bulging and since the encasement and high confining pressure further restrict bulging, a decrease in the reduction in volumetric strain is measured compared to fully penetrating encased columns. This observation is more easily seen in high area replacement ratio due to the

dilative effect of the sand column which becomes more dominant as the replacement ratio increases.

3. The use of ordinary 2-cm diameter sand columns did not result in notable increases in the deviatoric stress at failure with the maximum improvement being 7.45% for the case of fully penetrating columns with a confining pressure of 100 kPa. When the 2-cm columns were encased, the improvement at 100 kPa increased to 37.02%, while improvements of about 25% and 21% were observed for confining pressures of 150 and 200 kPa, respectively. For the average area replacement ratio of 17.8%, improvements ranging from about 33% to 36% were observed for samples reinforced with fully penetrating ordinary columns and from about 7% to 12% for partially penetrating ordinary columns. For samples with encased columns, additional improvements in the deviatoric stress at failure were observed due to the encasement, with the improvement ranging from about 40% to 68% for specimens reinforced with fully penetrating columns and from about 5% to 19% for partially penetrating columns. For the higher area replacement ratio of 31.7%, improvements ranging from about 59% to 69% were observed for samples reinforced with fully penetrating ordinary columns and from about 22% to 24% for partially penetrating ordinary columns. For samples with encased columns, the improvement ranged from about 50% to 64% for specimens reinforced with fully penetrating columns and from about 7% to 9% for partially penetrating columns.

4. For clay specimens that were reinforced with partially penetrating 2-cm sand columns, the effective friction angle ϕ' and the apparent cohesion c’ were not significantly affected by the presence of the sand columns. For fully penetrating 2-cm columns, non-zero c’ values were observed and were associated with unchanged or

slightly reduced ϕ ' values compared to the control clay specimens. The non-zero c' values reflect the improvements in deviatoric stresses at failure at the lower confining pressure of 100 kPa compared to the higher confining pressures of 150 and 200 kPa.

5. For the average and high area replacement ratios of 17.8% and 31.7% improvements in ϕ ' were observed for ordinary columns, while improvements in c' were observed for encased columns. These results of encased columns are in line with previous research which shows that encasing sand columns with geosynthetics results in non-zero cohesive intercepts (Wu and Hong 2009), with the increases in c' being associated with no improvements in the friction angle ϕ '. The effective friction angle ϕ 'improved from 21.8° (control) to 22.5°(partially penetrating) and 24.5°(fully penetrating) for ordinary 3cm columns (17.8% area replacement ratio). For the case of 4cm ordinary columns (31.7% area replacement ratio) the effective friction angle was found to be 23.8° and 26° for partially and fully penetrating columns, respectively. The apparent cohesion *c'* increased from 0 (control) to 15 (partially penetrating) and 30 kPa (fully penetrating) for encased 3cm columns (17.8% area replacement ratio). For the case of 4cm ordinary columns (31.7% area replacement ratio) the apparent was found to be 7° and 22.5° for partially and fully penetrating encased columns, respectively.

CHAPTER 6

TEST RESULTS AND ANALYSIS FOR UNDRAINED TESTS

6.1. Introduction

The results of consolidated undrained tests conducted on 9 Kaolin specimens that were reinforced with 4-cm sand columns are presented in this chapter and compared with the results of 15 tests conducted by Maakaroun (2009). The results include a description of the modes of failure that characterize the behavior of the different test specimens and a detailed analysis of the parameters which are known to affect the load response of clay specimens that are reinforced with sand columns. The effects of these parameters which include the area replacement ratio, column penetration depth, and confining pressure on the undrained shear strength, stiffness, generation of excess pore water pressure, and effective shear strength parameters of the Kaolin specimens are investigated and highlighted in this chapter.

6.2. Test Results

The test results are presented in the form of deviatoric stress and excess pore pore pressure versus axial strain curves. In the analysis of the test results, failure was defined at an axial strain of 15%, unless a peak was observed at smaller strain levels.

6.2.1. Unreinforced/Control Kaolin Specimens

Curves showing the variation of the deviatoric stress and excess pore water pressure versus axial strain at confining pressures of 100 kPa, 150 kPa, and 200 kPa for the control Kaolin specimens are presented in Figure. 6.1. In addition, the variation of the deviatoric stress, normalized with initial effective confining pressure, is plotted against axial strain and presented on Figure. 6.2.

The deviatoric stresses at failure for the control specimens were 64.6 kPa, 84.2 kPa, and 110.2 kPa, corresponding to Su/σ3 ratios of 0.32, 0.28, and 0.27 respectively, where Su is the undrained shear strength. These Su/σ3 ratios are typical of normally consolidated clays prepared from slurry that are sheared in undrained conditions (example Han Lin and Penumadu (2005) and Prashant and Penumadu 2005). The excess pore water pressures at failure were 61.3 kPa, 95.1 kPa, and 130.9 kPa at confining pressures of 100 kPa, 150 kPa, and 200 kPa respectively. The Skempton's pore pressure parameter "A", defined as the ratio of the excess pore water pressure at failure to the deviatoric stress at failure, was equal to 0.95, 1.12, and 1.19 at confining pressures of 100 kPa, 150 kPa, and 200 kPa respectively, indicating normally consolidated clay behavior.

For all confining pressures, the deviatoric stress increased with axial strain and reached a maximum value at a strain of 6% to 7% after which the curve leveled out with further increase in the axial strain. Similarly, excess pore water pressure increased with axial strain and reached a maximum value at a strain of 10%.

The secant modulus of elasticity (Esec) of Kaolin specimens at an axial strain of 1% was determined at confining pressures of 100 kPa, 150 kPa, and 200 kPa. The

modulus of elasticity increased as the confining pressure increased and was equal to 4150 kPa, 6092 kPa, and 7637 kPa, respectively.

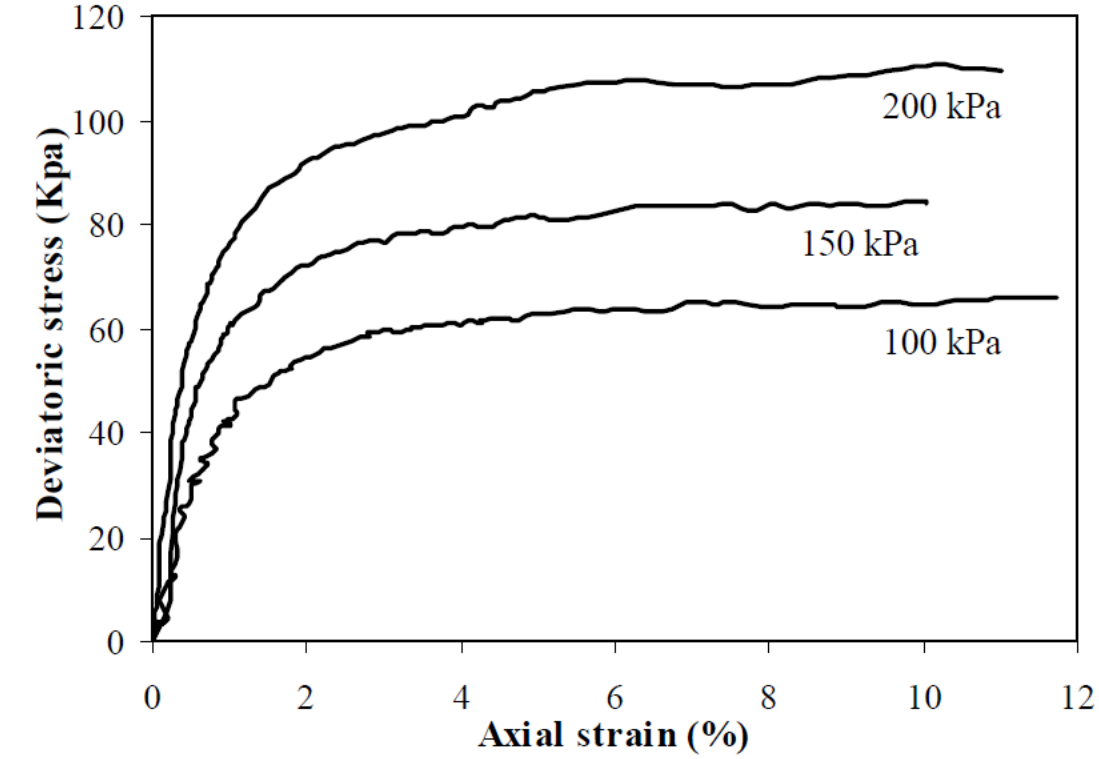

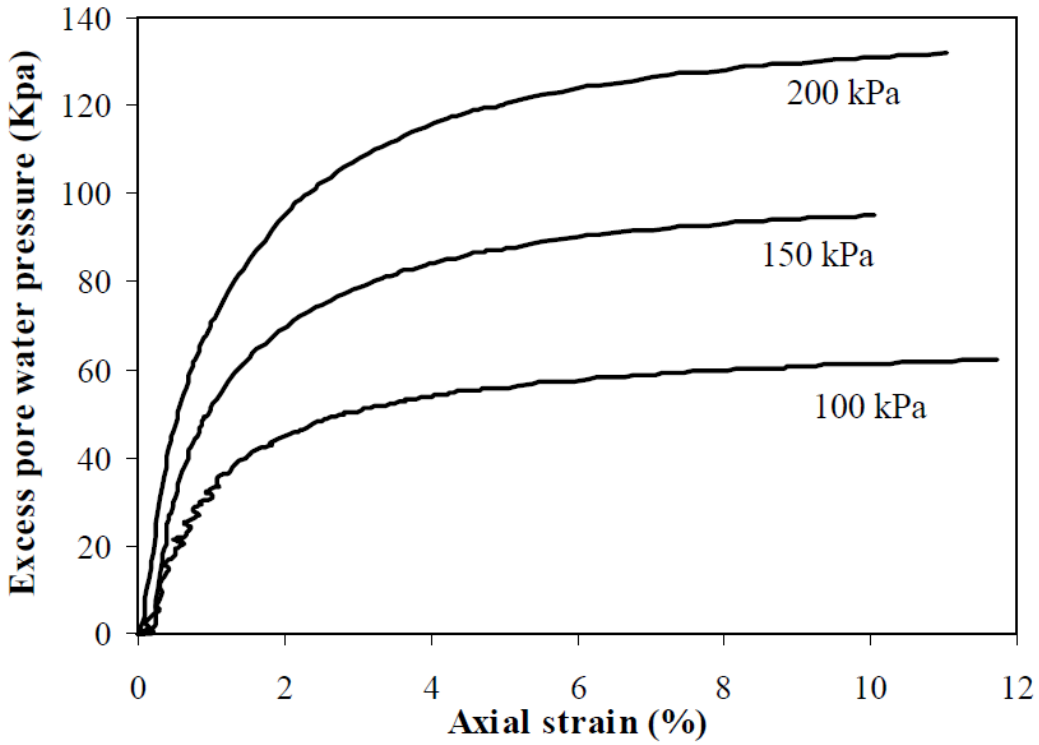

Figure 6.1. Deviatoric stress and excess pore water pressure versus axial strain for unreinforced/control specimen at confining pressures of 100 kPa, 150 kPa, and 200kPa

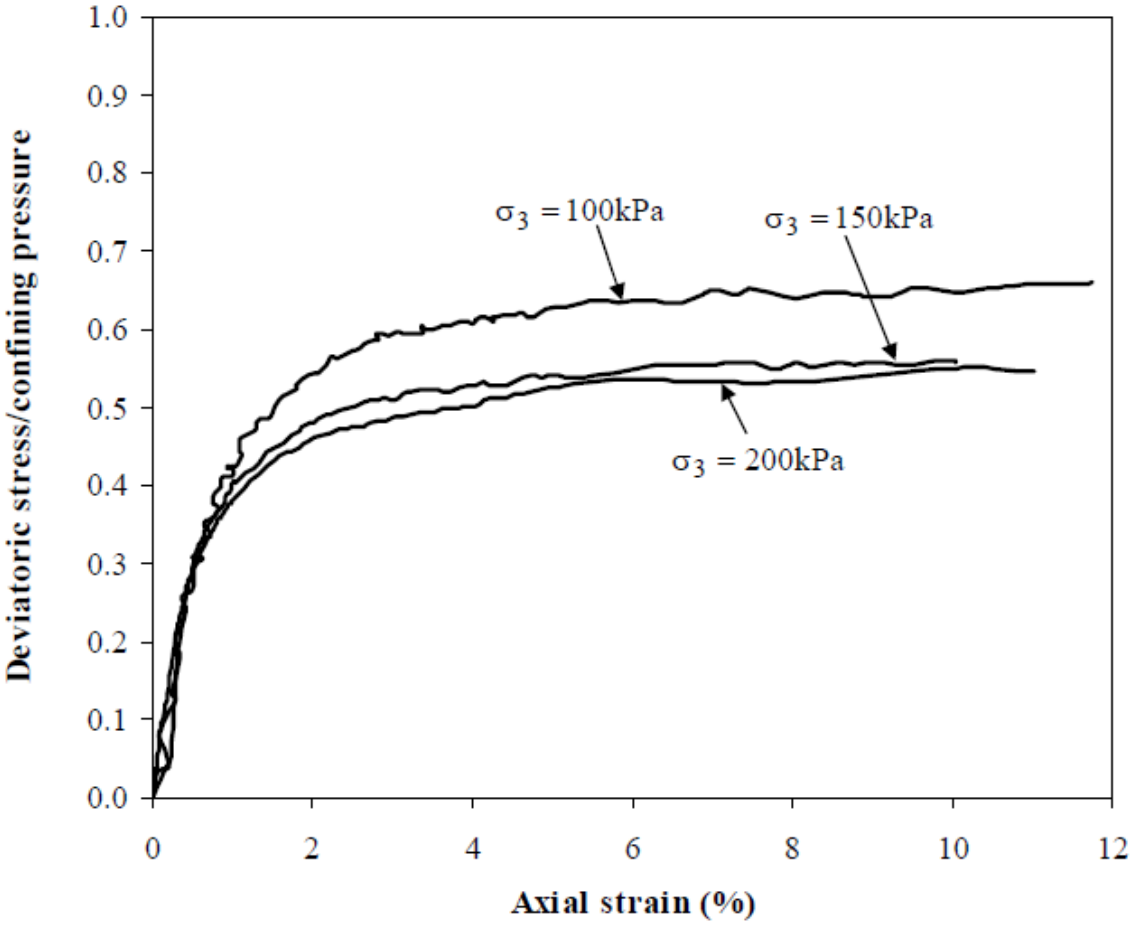

Figure 6.2. Normalized deviatoric stress with confining pressure versus axial strain for unreinforced Kaolin specimens

The Mohr Coulomb effective stress failure envelop for the control specimens is shown on Figure. 6.3. The apparent effective cohesion (c') and the effective angle of internal friction (Ø') for the control specimen were 0 kPa and 26.3º respectively. These effective values (c') and (Ø') are in line with results from CU- triaxial test results conducted on normally consolidated Kaolin specimens prepared from slurry as reported in Lin and Penumadu (2005).

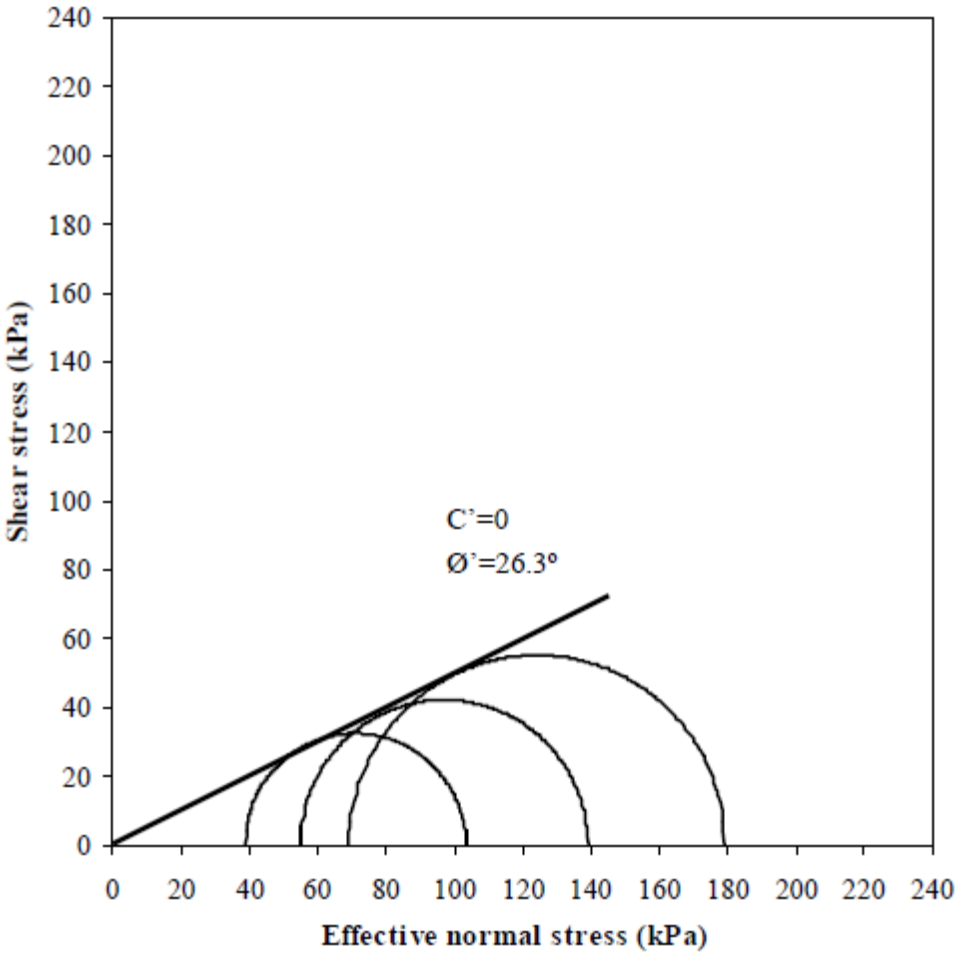

Figure 6.3. Mohr Coulomb effective stress failure envelop for control/unreinforced Kaolin specimens

6.2.2. Kaolin Specimens Reinforced with Sand Columns

Results obtained from the triaxial tests conducted on kaolin specimens reinforced with partially and fully penetrating ordinary sand columns are presented in Table 6.1 and in Figures. 6.4 to 6.9, which include pictures of the modes of failure and graphs showing the variation of the deviatoric stress and excess pore pressure with axial strain. The results were analyzed to investigate the effect of relevant parameters such as column penetration ratio H_c/H_s, area replacement ratio A_c/A_s, and confining pressure on the improvement in the undrained shear strength and the apparent effective strength

parameters of the clay. It should be noted that in all the discussion presented below, it was assumed that the sand column and the surrounding clay act as a single element with homogeneous distributions of stresses and strains.

6.2.2.1. Modes of Failure

For samples that were reinforced with partially penetrating 4-cm diameter columns, the mode of failure was characterized by bulging of the clay specimen. The bulging was concentrated at the lower portions of the specimens. Furthermore, no bulging of the sand columns was observed. As an illustration, photographs showing the degree of bulging in samples with partially penetrating 4-cm ordinary columns at different confining pressures are shown on Figure. 6.4. The bulging severity decreases with increasing confining pressure. This bulging was therefore more evident in the samples tested at confining pressures of 100 kPa and 150 kPa, but was less severe for the higher confining pressure of 200 kPa.

These observations agree with findings from previous studies (Hughes and Withers 1974, Sivakumar et al. 2004 and Najjar et al. 2010) which indicate that for partially penetrating columns of short lengths, the stresses at the base of the column generally exceed the bearing capacity of the soil leading to a premature bearing capacity failure in the unreinforced lower portion of the specimen.

Table 6.1. Test Results for Kaolin specimens reinforced with ordinary sand columns

Test No.	Confining pressure σ_3, (kPa)	Drainage	Diameter of sand column (mm)	Area replacement ratio: A_c/A_s (%)	Column Penetration Ratio: H_c/H_s	Undrained Shear Strength (kPa)	Excess pore water pressure (kPa)	E_{sec} @ 1% axial strain (kPa)	Increase in Undrained Shear Strength (%)	Reduction in Excess Pore Pressure (%)
1	100	Undrained	0	0	0	32.3	61.3	4150	-	-
2		Undrained	20	7.9	0.75	35.2	57.3	4220	9	6.5
3		Undrained	20	7.9	1	36.6	51.2	4390	13.3	16.5
6		Undrained	30	17.8	0.75	38.9	48.9	4597	20.4	20.2
7		Undrained	30	17.8	1	56.7	42.7	5853	75.5	30.3
9		Undrained	40	31.7	0.75	43	35.8	4451	33.1	41.6
10		Undrained	40	31.7	1	86.7	2.9	7019	168.4	95.3
11	150	Undrained	0	0	0	42.1	95.1	6092	-	-
12		Undrained	20	7.9	0.75	48.2	88.9	6100	14.5	6.5
13		Undrained	20	7.9	1	50.3	87.8	6368	19.5	7.7
14		Undrained	30	17.8	0.75	56.8	78.1	6697	34.9	17.9
15		Undrained	30	17.8	1	73.9	65.2	8624	75.5	31.4
15		Undrained	40	31.7	0.75	69.2	59.13	6976	65	37.8
17		Undrained	40	31.7	1	129	-0.27	11046	206.4	100.28
18	200	Undrained	0	0	0	55.1	130.9	7637	-	-
19		Undrained	20	7.9	0.75	60.1	120.3	7904	9.1	8.1
20		Undrained	20	7.9	1	65.8	112.1	7996	19.4	14.4
21		Undrained	30	17.8	0.75	71.2	107.8	8983	29.2	17.6
22		Undrained	30	17.8	1	92.3	89.4	10103	67.5	31.7
23		Undrained	40	31.7	0.75	77.8	93.33	7062	41.2	28.7
24		Undrained	40	31.7	1	150.2	24.1	14074	172.5	81.6

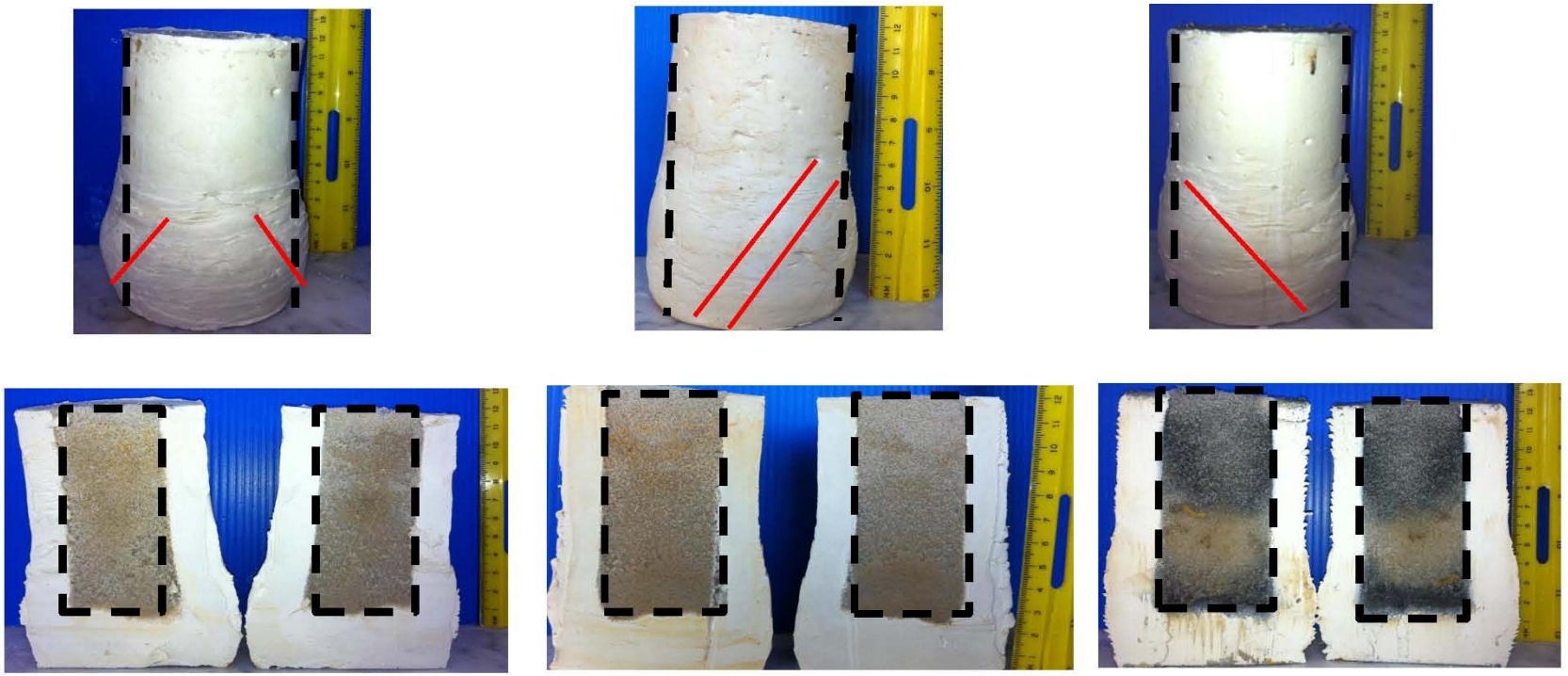

Figure 6.4 Example of external and internal modes of failure of test specimens (H_c/H_s = 0.75 and A_c/A_s = 31.7%, Ordinary)

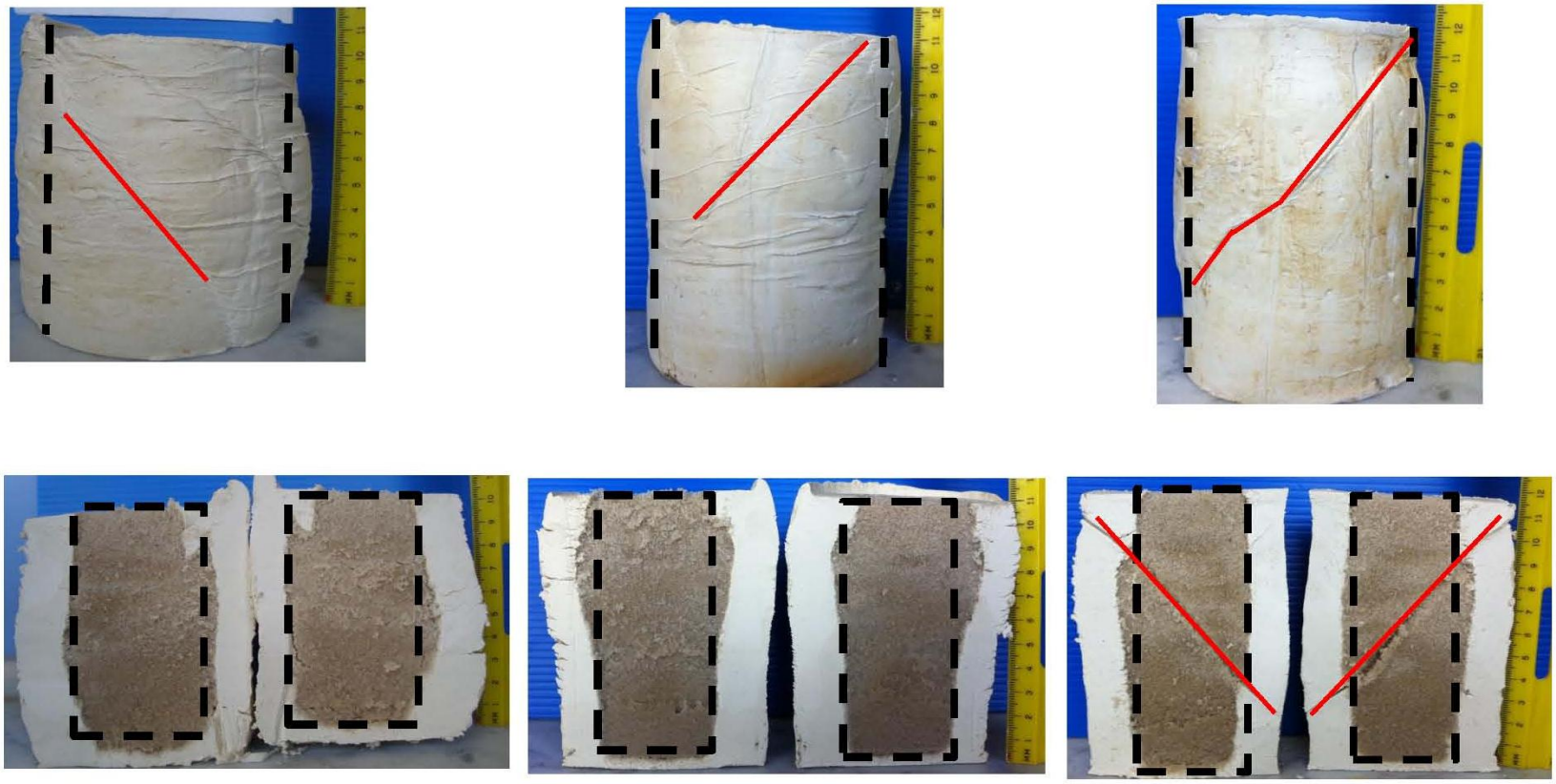

Figure 6.5 Example of external and internal modes of failure of test specimen ($H_c/H_s = 1$ and $A_c/A_s = 31.7\%$, Ordinary).

For samples reinforced with fully penetrating columns, the mode of failure was also characterized by the bulging of the specimens with mobilized shear planes. However, the bulging was uniform along the length of the specimen for the 100kPa confining pressure tests, but appeared to be more concentrated in the middle and upper half of the samples for confining pressures of 150kPa and 200kPa respectively.

To investigate the mode of failure of sand columns, the same test specimens were split along their vertical axes to expose the columns and the surrounding clay (Figures. 6.4, 6.5). For samples reinforced with ordinary partially penetrating sand columns, the sections shown in Figure. 6.4 indicate that the lower portion of the sand columns (length of about 1.5 times the column diameter) exhibited bulging of different levels, with the sample tested at 100 kPa exhibiting the most noticeable bulge. For samples reinforced with fully penetrating ordinary columns, the bulging of the column was in line with the bulging observed for the corresponding clay specimens with bulging occurring at the top and middle of the samples (Figure. 6.5). It is also worth noticing that as the confining pressure increases, the severity of the bulging decreases. It is also interesting to note that the shear plane mobilized in the 200kPa test passed through the sand column and shifted it laterally as it went further down the length of the sample. This behavior indicates that fully penetrating columns are more effective in reinforcing the sample than for partially penetrating columns which fail by punching through the underlying clay.

6.2.2.2. Stress-Strain Behavior

The variation of the deviatoric stress and pore water pressure with the axial strain is presented in Figs. 6.6 and 6.7 for tests conducted with an area replacement ratio of 31.7% with partial and full penetrating columns respectively. For partially penetrating columns, the stress-strain curves exhibited consistent increases in deviatoric stresses with strains as the samples were sheared towards critical state conditions, which were not reached at the maximum strain of 15%. To define failure, the deviatoric stresses will be considered to have leveled out at an axial strain of 15%, which is the maximum strain that was measured in the undrained tests with area replacement ratio of 31.7%. For the samples reinforced with fully penetrating columns, a peak was observed in all specimens at a strain that is less than 15%. For these tests, failure was defined at the measured peak stress.

In all the cases tested, pore water pressures initially increased as the deviatoric stresses reached their maximum values. At larger strain levels, the generation of negative pore pressure in the sand columns during shearing resulted in a reduction in the excess pore pressure of the composite samples. The decrease in excess pore water pressures during shear can be attributed to the higher stiffness and to the dilatational tendency of the sand columns, which are expected to increase as the area replacement ratios and the penetration depths increase. As expected, samples reinforced with the fully penetrating 4-cm columns exhibited the sharpest reduction in excess pore pressures at larger strains. At strains exceeding 12%, the excess pore pressure generation leveled out and this was associated with the leveling out of the deviatoric stresses as the samples approached critical state conditions.

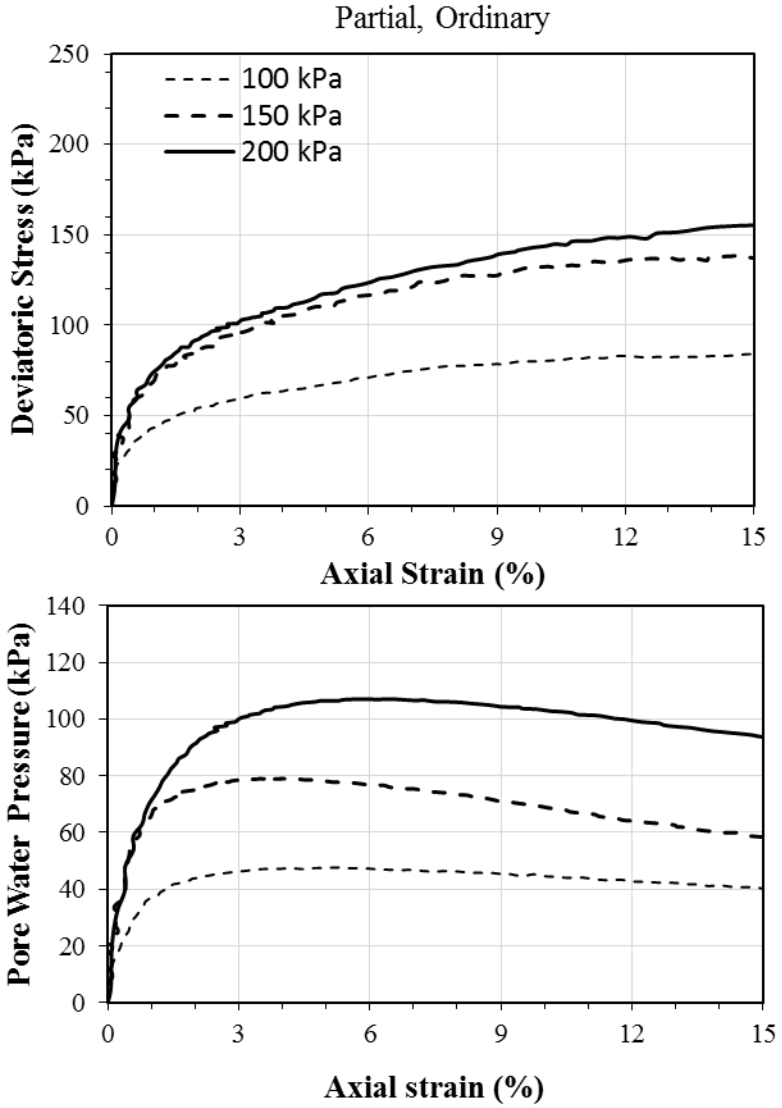

Figure 6.6. Deviatoric stress and pore water pressure versus axial strain for reinforced specimen at confining pressures of 100 kPa, 150 kPa, and 200kPa (Hs/Hc=0.75, As/Ac=31.7%, Ordinary)

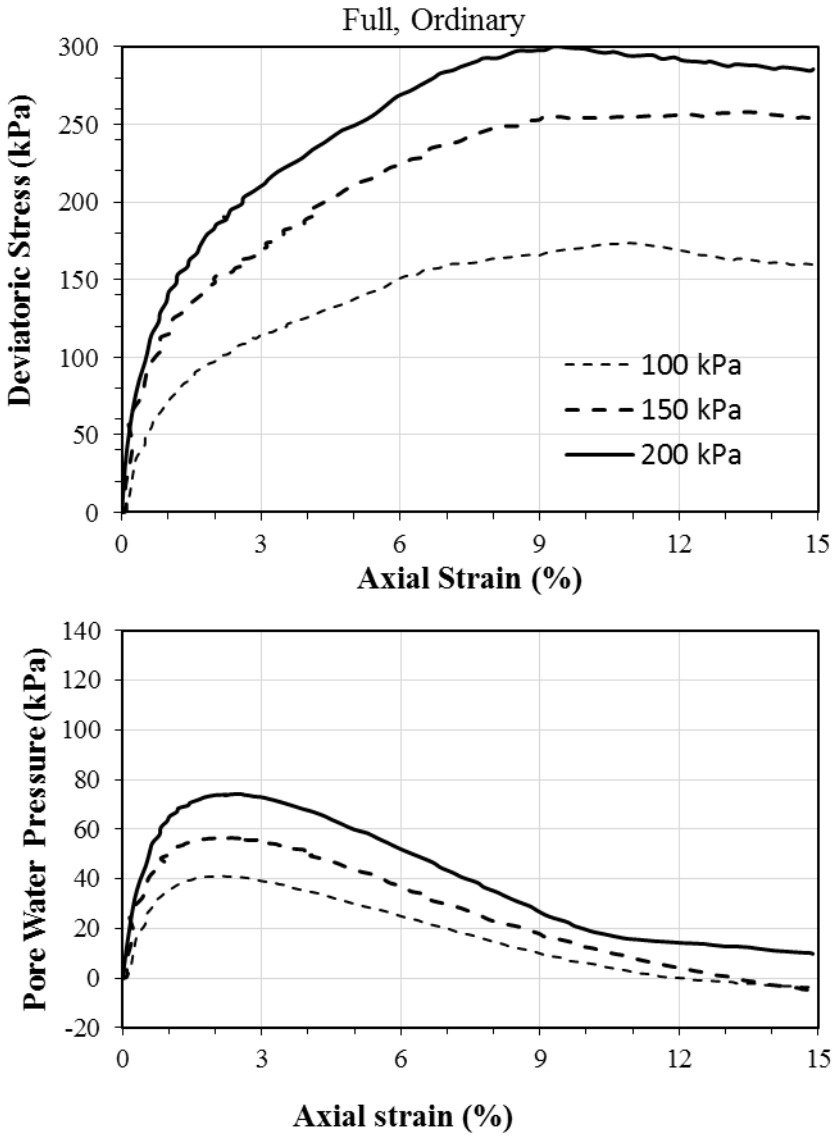

Figure 6.7. Deviatoric stress and pore water pressure versus axial strain for reinforced specimen at confining pressures of 100 kPa, 150 kPa, and 200kPa (Hs/Hc=1, As/Ac=31.7%, Ordinary)

Figures 6.8 and 6.9 show a compilation of deviatoric stress and excess pore pressure curves for area replacement ratios of 0%, 7.9%, 17.8%, and 31.7% for partially penetrating and fully penetrating columns, respectively. Results on these figures indicate that for partially penetrating columns, increasing the area ratio does not lead to effective improvements in load-carrying capacity. This could be explained by the

observed mode of failure of these specimens which showed that the failure for partially penetrating columns is governed by the unreinforced portion of the clay specimen. The finding that the unreinforced clay governs the load-carrying capacity is supported by the shape of the stress-strain curves for samples reinforced with partially penetrating columns, where the reinforced samples did not exhibit any clear peak (similar to control clay specimens). For fully penetrating samples on the other hand, results indicate that significant improvements in the undrained load response were observed particularly for the higher area replacement ratios of 17.8% and 31.7%, where the pore pressure response showed a significant tendency for generation of excess negative pore pressures in the reinforced specimens. The generation of negative pore pressures resulted in increases in the effective confining pressure on the specimens reinforced with 3-cm and 4-cm columns compared to the specimens reinforced with 2-cm columns and the control clay specimens.

6.2.2.3. Effect of Sand Columns on Undrained Shear Strength at Failure

The percent improvement in the undrained shear strength at failure for the series of tests involving an area replacement ratio of 31.7% along with the previous results from the work of Maakaroun (2009) are presented in Table 5.1 and plotted versus the initial effective confining pressure in Figures. 6.10, 6.11 and 6.12. Results indicate that the use of ordinary 4-cm diameter sand columns (area replacement ratio=31.7%) resulted in significant increases in the undrained shear strength at failure with the highest improvement being 206.4% for fully penetrating columns at 150kPa confining pressure. Furthermore, the results of this higher replacement ratio showed

higher improvements for fully penetrating ordinary columns than for partially penetrating ordinary columns.

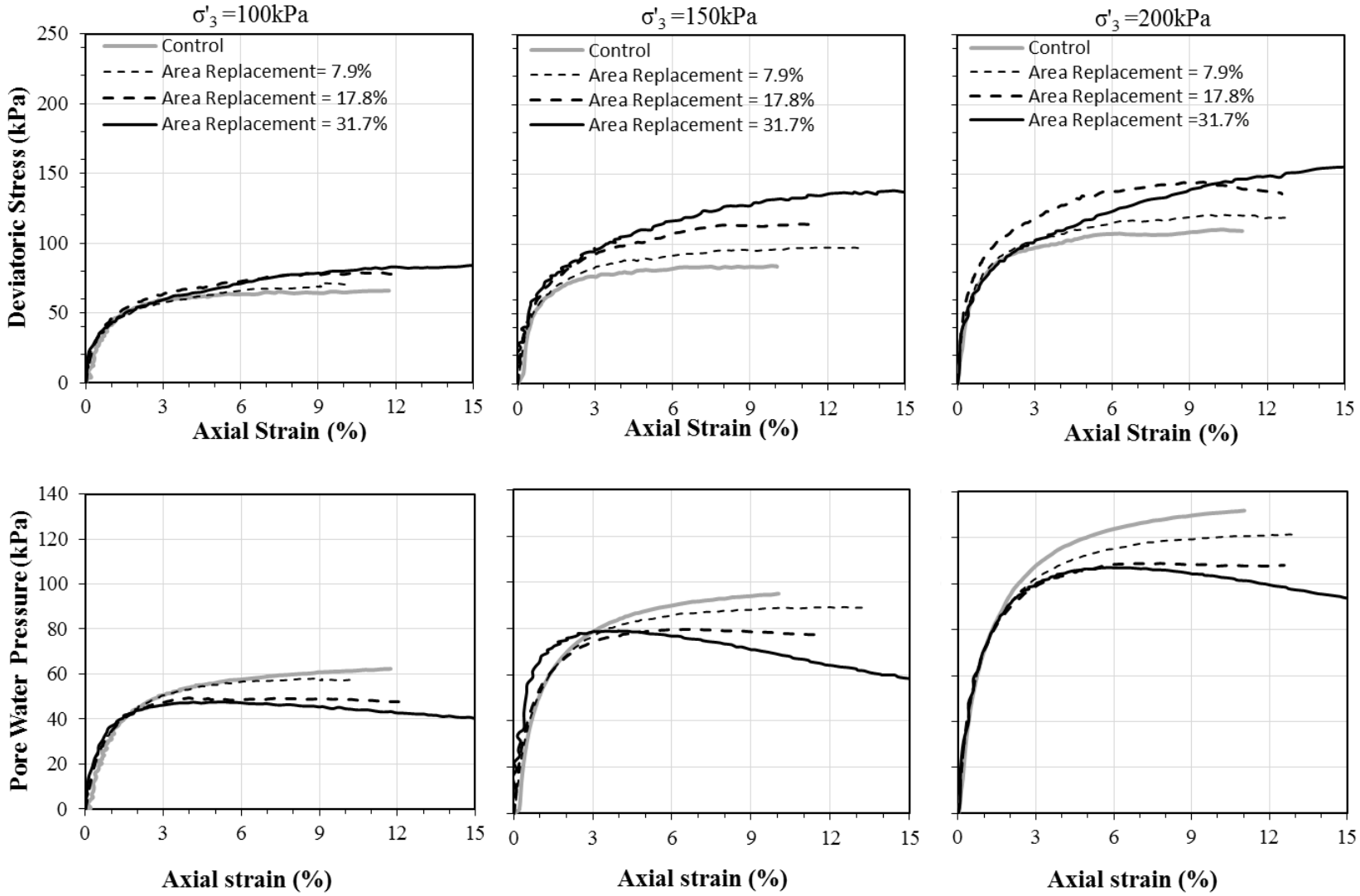

Figure 6.8. Deviatoric stress and pore water pressure versus axial strain for specimens reinforced with partially penetrating ordinary columns at confining pressures 100kPa, 150kPa and 200kPa (As/Ac=7.9%, As/Ac=17.8%,As/Ac=31.7%)

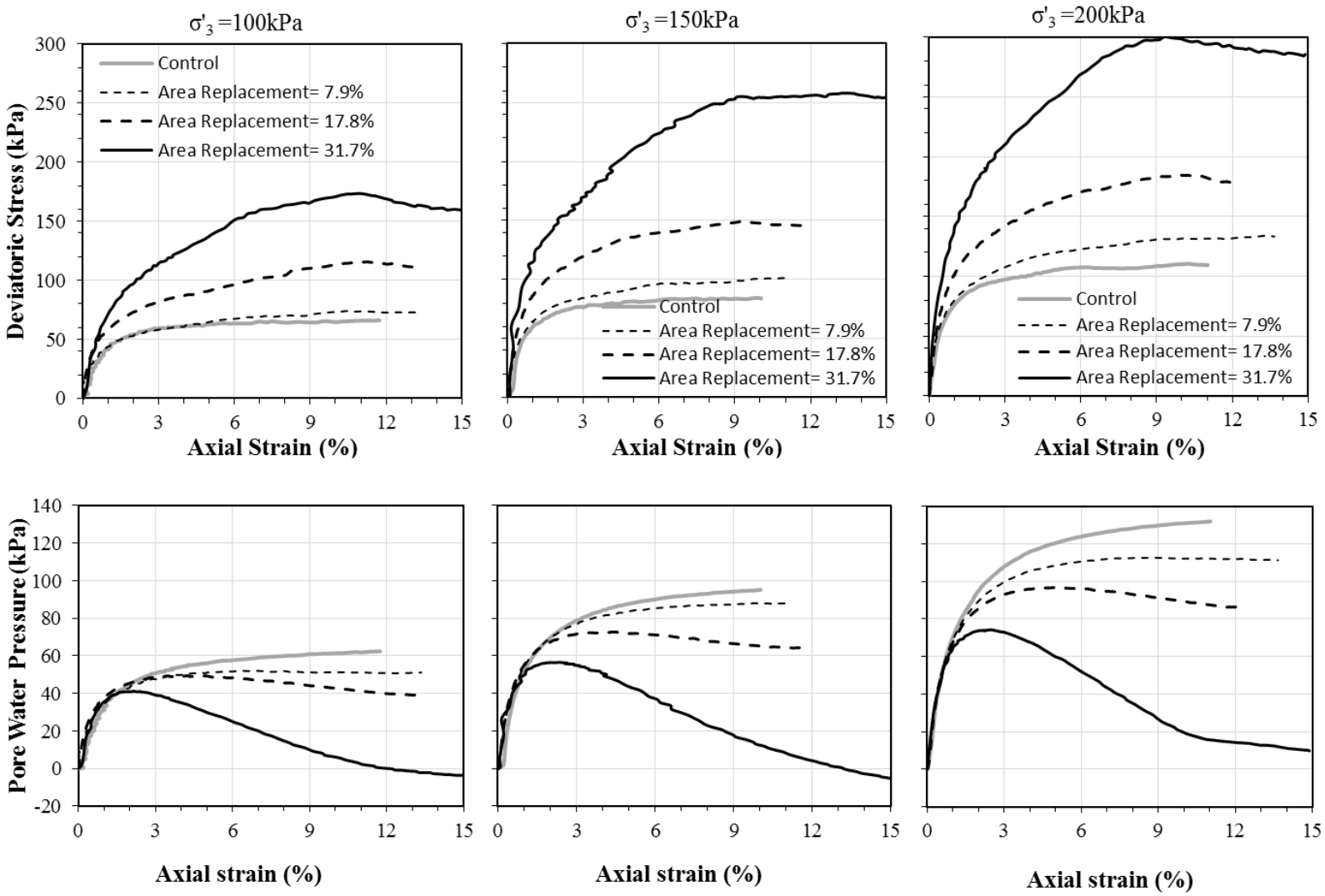

Figure 6.9. Deviatoric stress and pore water pressure versus axial strain for specimens reinforced with fully penetrating ordinary columns at confining pressures 100kPa, 150kPa and 200kPa (As/Ac=7.9%, As/Ac=17.8%,As/Ac=31.7%)

The improvements ranged from 33.1% to 65% for partially penetrating ordinary columns and 168.4% to 206.4% for fully penetrating ordinary columns. In comparison with the smaller area replacement ratios of 7.9% and 17.8%, the 31.7% area replacement ratio resulted in significant and unproportional improvements in the undrained shear strength. Although this is true across the whole range of tests, the most notable increase in load-carrying capacity was for the tests conducted with fully penetrating columns at a confining pressure of 150 kPa where the magnitude of the improvement increased from as little as 19.5%, to an intermediate value of 75.5% and finally to a significant improvement of 206.4% for area replacement ratios of 7.9%, 17.8% and 31.7%, respectively. Furthermore, Figures 6.11 and 6.12 show results that are consistent with what Maakaroun (2009) and Najjar et al (2010) have analyzed. These results show that the improvement in undrained shear strength was relatively independent of the effective confining pressure. This result is important because it indicates that for normally consolidated clay layers that exhibit an increase in the undrained shear strength with depth, the presence of ordinary sand columns will increase the undrained shear strength of the clay with the same percentage irrespective of the embedment depth in the clay

An analysis of the results in Table 1 for test specimens that were reinforced with ordinary sand columns indicates that the relative increase in the undrained strength when comparing partially penetrating columns (Hc /Hs=0.75) to fully penetrating columns was much more pronounced as the area replacement ratio increased. For a confining pressure of 150kPa, in the case where the area replacement ratio was 31.7% an increase from 65% to 206.4% was measured compared to the case where the area replacement ratio was equal to 17.8% and the measured increase was 34.9% to 75%.

This disproportionate increase in strength indicates that the improvement in undrained shear strength may not only be a function of the column penetration ratio *Hc* /*Hs*, but also of the ratio of the column height to the column diameter. This dependence has been studied by other researchers (example Narasimha Rao et al. 1992) who proposed the idea of the critical column length beyond which the column will not have any positive effect on improvements in capacity. Narasimha Rao et al. (1992) suggested that a column length greater than five column diameters may no longer participate in increasing the load carrying capacity of soft cohesive clays.

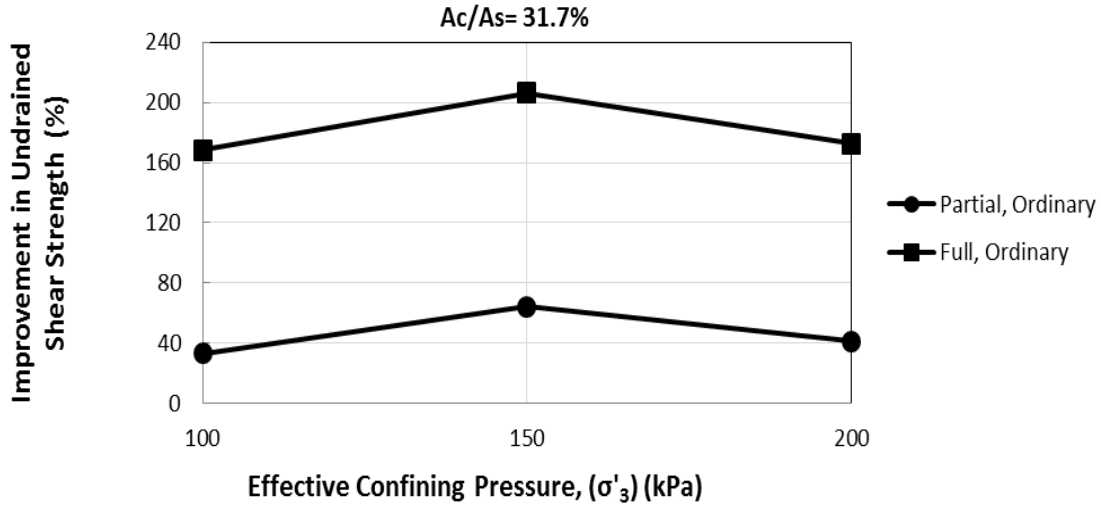

Figure 6.10. Variation of improvement in undrained shear strength with confining pressure (As/Ac=31.7%)

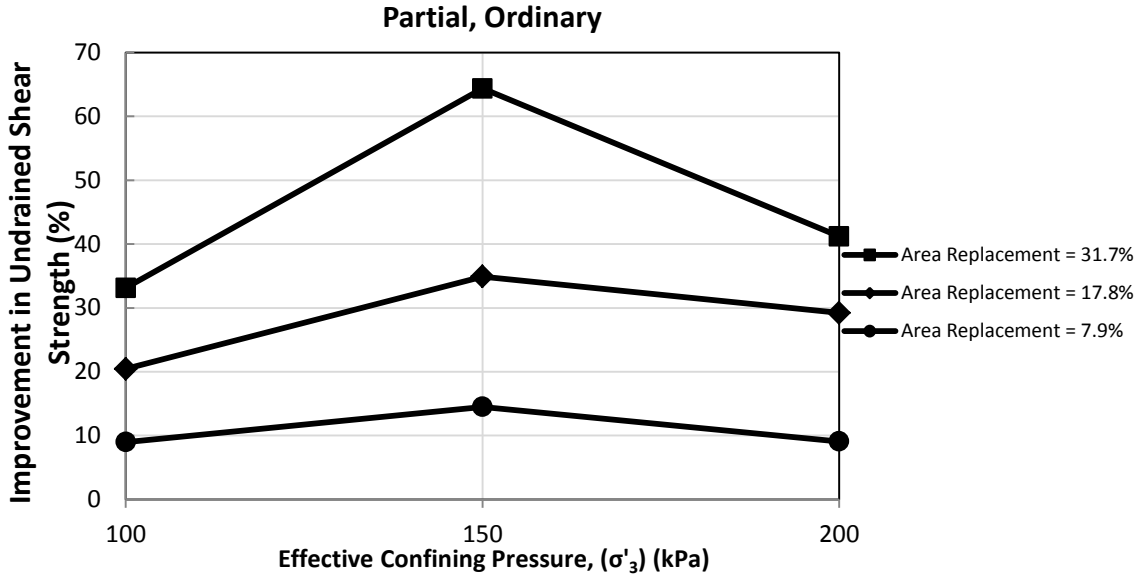

Figure 6.11. Variation of improvement in undrained shear strength with confining pressure (Hc/Hs= 0.75, As/Ac=7.9%%, As/Ac=17.8%,As/Ac=31.7%, ordinary)

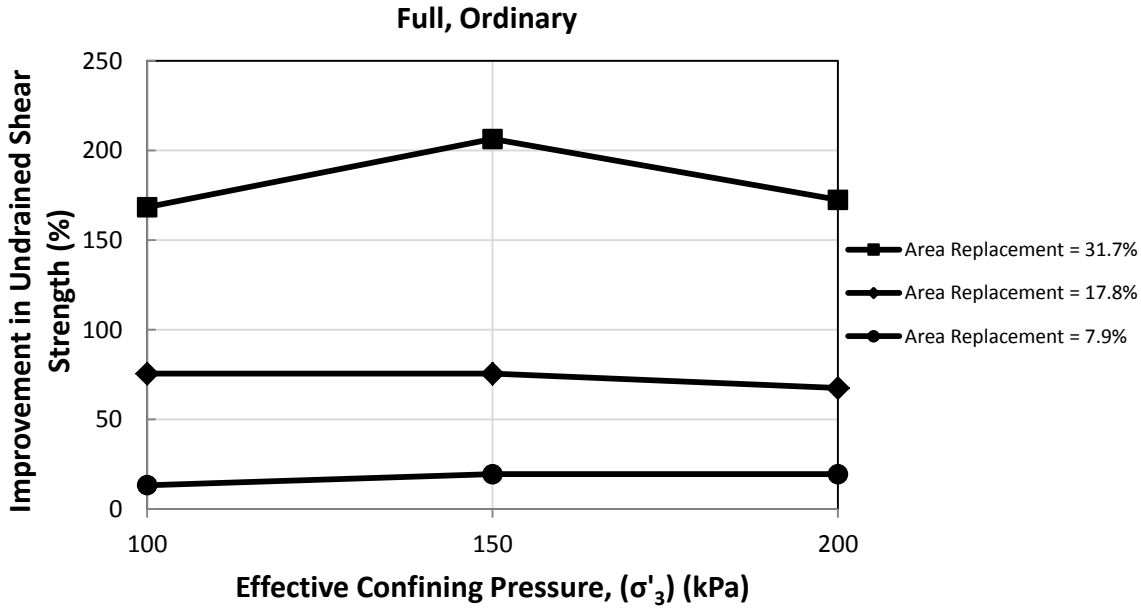

Figure 6.12. Variation of improvement in undrained shear strength with confining pressure (Hc/Hs= 1, As/Ac=7.9%%, As/Ac=17.8%,As/Ac=31.7%, ordinary)

To investigate the possible dependency of the increase in undrained strength on the ratio of the column height to column diameter, the percent increase in undrained strength was plotted on Figure. 6.13 against the ratio of the column height to diameter for the tests conducted in this study and the study done by Maakaroun (2009) and for all confining pressures. Average trend lines or curves were plotted through the data for the three area ratios used. In addition, data points from tests conducted by Sivakumar et al. (2004) and which show improvements in undrained shear strength due to the inclusion of 3.2-cm diameter sand columns in Kaolin clay are also plotted on the same figure for comparison.

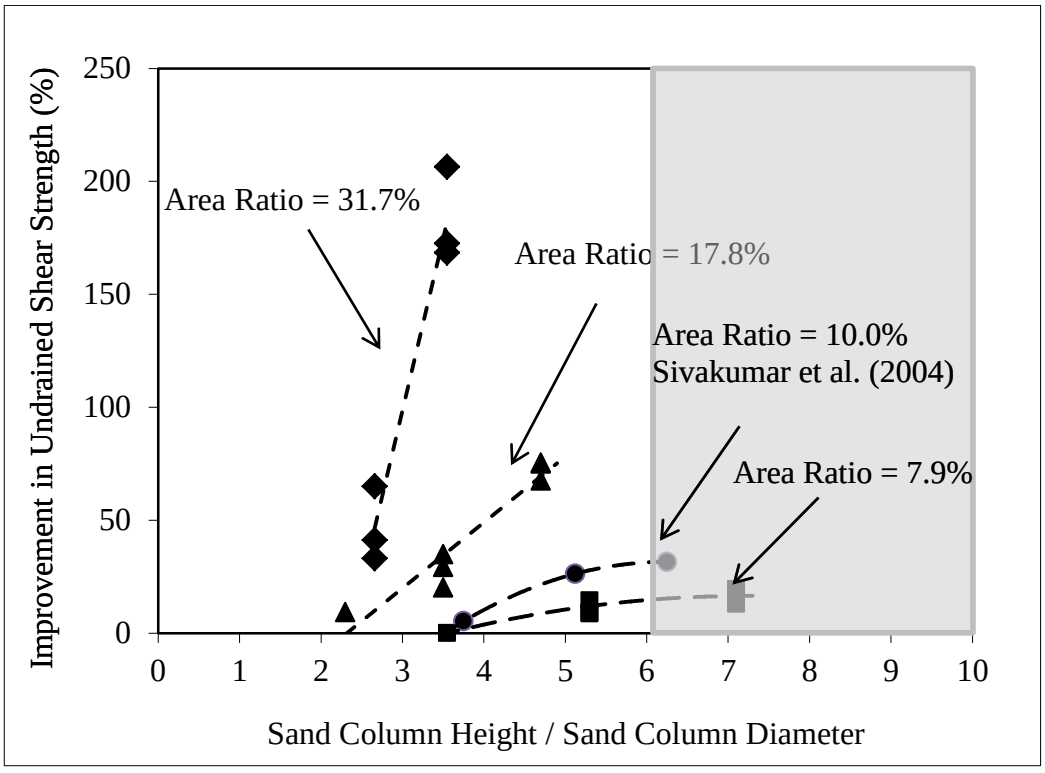

Figure 6.13. Effect of ratio of column height to diameter on undrained shear strength

The data presented on Figure. 6.13 support the hypothesis of a "critical column length" beyond which the increase in undrained shear strength becomes relatively negligible. This "critical column length" is greater than six column diameters as indicated by the grey area in Figure 6.13. The existence of this critical column length provides a plausible explanation for the large relative increase in strength that was observed when the height of the sand column was increased from 10.65 cm (Hc/Hs=0.75) to 14.2 cm (Hc/Hs=1) for specimens that were reinforced with an area ratio of 31.7%. In these tests, the maximum ratio of the column height to column diameter was 3.55 for the fully penetrating column, a ratio which is still smaller than the expected critical column ratio of about 6. In comparison, the ratio of the column height to column diameter was equal to 7.1 and 5.3 respectively for the fully penetrating and partially penetrating columns (Hc/Hs=0.75) for specimens reinforced with an area ratio of 7.9%. The improvement in undrained shear strength in these specimens leveled out at a maximum improvement of about 17%.

6.2.2.4. Effect of Sand Columns on Excess Pore Pressure Generation

An analysis of the results on Table 5.1 indicates that for fully penetrating sand columns with area replacement ratios of 7.9%, 17.8%, and 31.7%, the average reduction in the excess pore water pressure at different confining pressures was 12.9%, 31.3%, and 92.4% respectively. For partially penetrating columns with Hc/Hs=0.75, the average reductions of excess pore water pressures at different confining pressures are about 7%, 17% and 36% for area replacement ratios of 7.9%, 17.8% and 31.7% respectively. Hence, insertion of sand columns reduces the excess pore water pressure during undrained loading, and their effectiveness in reducing the water pressure

increases with increasing the column length and area replacement ratio. Figures 6.14 to 6.16 show the reduction in excess pore water pressure with the improvement in undrained shear strength for the 31.7% replacement ratio (this study) and for the area ratios of 7.9% and 17.8% studied by Maakaroun (2009). These figures further capture the positive effect of reducing pore water pressure which results in an increased undrained shear strength. This decrease in pore water pressure is associated with the behavior of the sand columns which tend to dilate and generate negative pore pressures.

6.2.2.5. Effect of Sand Columns on the Drained Secant Modulus

A drained secant modulus $(E_{sec})_{1\%}$ defined at an axial strain of 1% was calculated for each test by dividing the deviatoric stress measured at an axial strain of 1% by the corresponding strain. Results of the calculated values of $(E_{sec})_{1\%}$ are presented in Table 6.1 along with the previously calculated values by Maakaroun (2009) for area replacement ratios of 7.9% and 17.8% and plotted in Figures. 6.17 to 6.20. As indicated by the test results of Table 6.1, the insertion of fully penetrating 4cm sand columns increased the stiffness of the unreinforced Kaolin specimens from 4150 to 7019, from 6092 to 11046 and from 7637kPa to 14074kPa for confining pressures of 100kPa, 150kPa and 200kPa respectively. The stiffness of the reinforced Kaolin specimens was also improved as the column length increased. This indicates that for longer columns, more stresses will be distributed along the column length, and consequently less settlement will result. These observations are in line with the analysis done by Maakaroun (2009). Thus it is recommended to extend the column to the full depth of the soft clay layer..

The dependency of the drained secant modulus on strain level was investigated by plotting the variation of E_{sec} with strain for specimens reinforced with an area replacement ratio of 31.7% at effective confining pressures of 100, 150, and 200 kPa as shown in Figure 6.20. The results indicated that the secant modulus for reinforced and control specimens decreases as the axial strain increases, reflecting the nonlinearity in the stress-strain response. The specimens exhibited a sharp drop in the secant stiffness for strains that are less than 1% to 2%. After a strain of 2%, the stiffness decreases with strain at a decreasing rate.

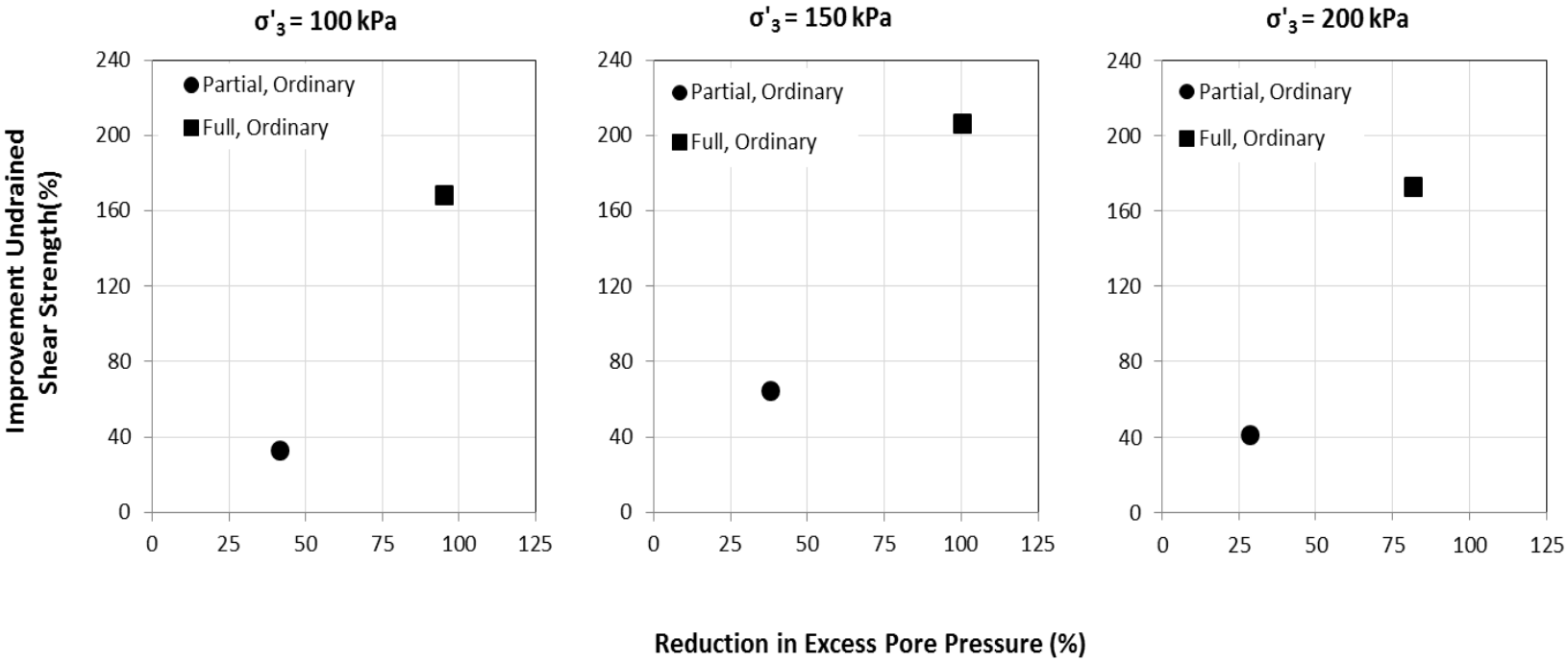

Figure 6.14. Relationship between improvements in undrained shear strength and reduction in excess pore pressure at failure (Ac/As= 31.7%)

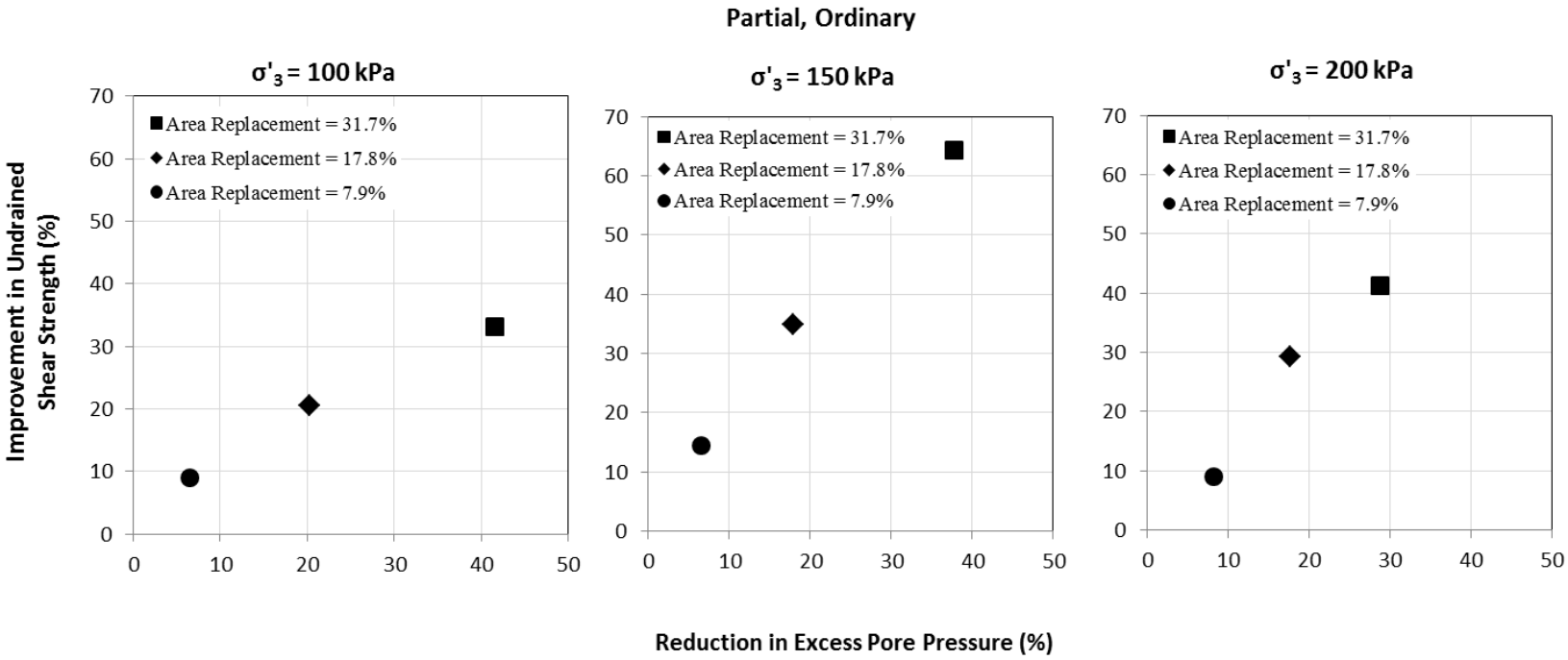

Figure 6.15. Relationship between improvements in undrained shear strength and reduction in excess pore pressure at failure (Hc/Hs=0.75, Ac/As= 7.9%, Ac/As= 17.8%,Ac/As= 31.7%, ordinary)

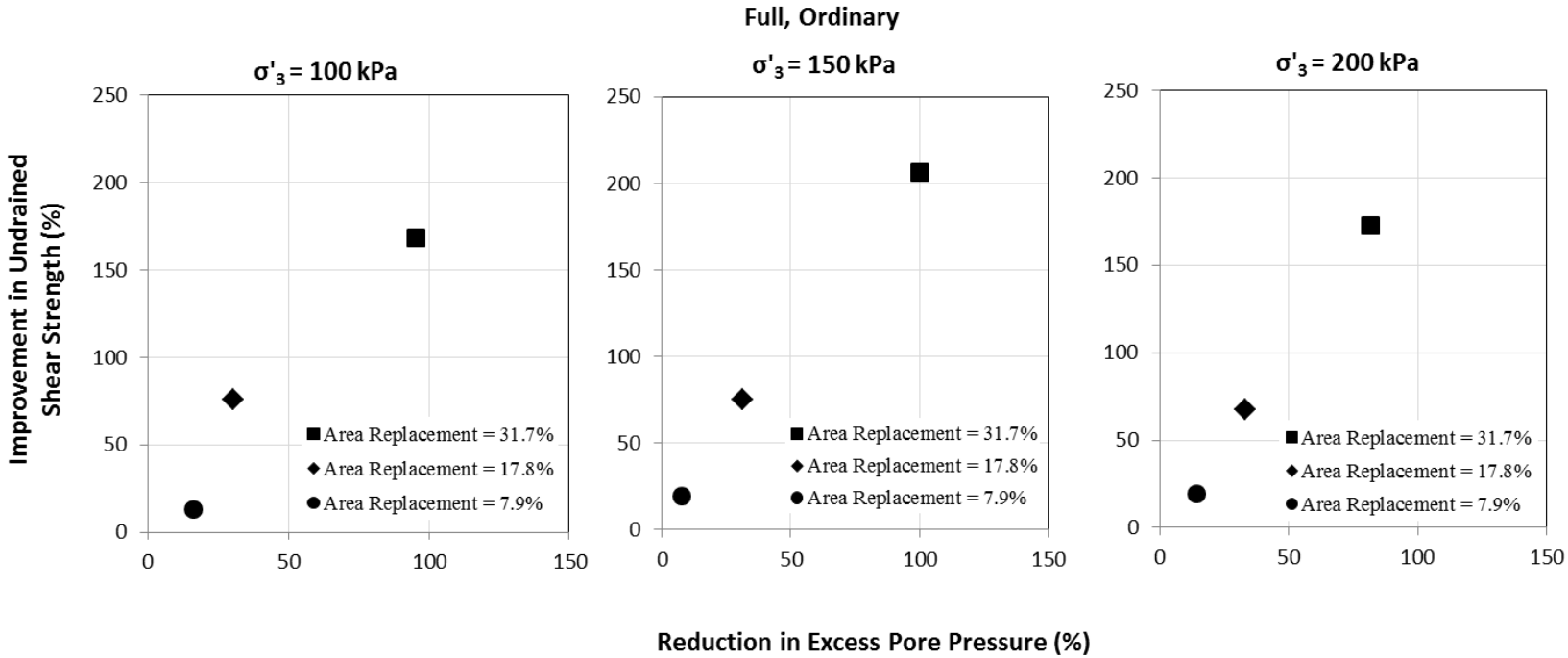

Figure 6.16. Relationship between improvements in undrained shear strength and reduction in excess pore pressure at failure (Hc/Hs=1, Ac/As= 7.9%, Ac/As= 17.8%,Ac/As= 31.7%, ordinary)

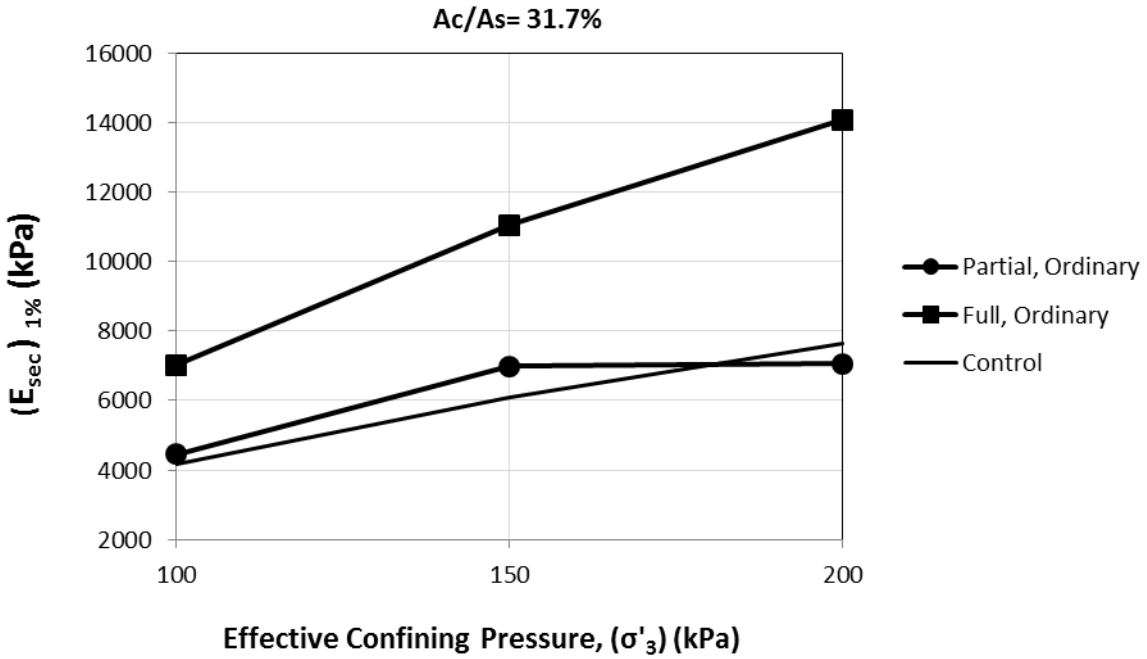

Figure 6.17. Variation of $(E_{sec})_{1\%}$ with effective confining pressure (Ac/As=31.7%)

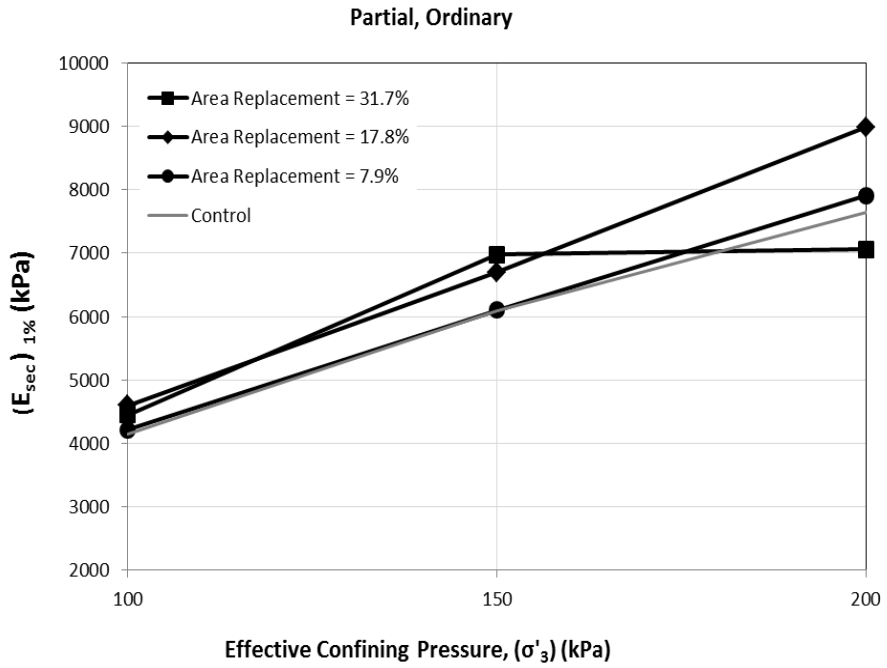

Figure 6.18. Variation of $(E_{sec})_{1\%}$ with effective confining pressure (Hc/Hs=0.75, Ac/As=7.9%, Ac/As=17.8%,Ac/As=31.7%, ordinary)

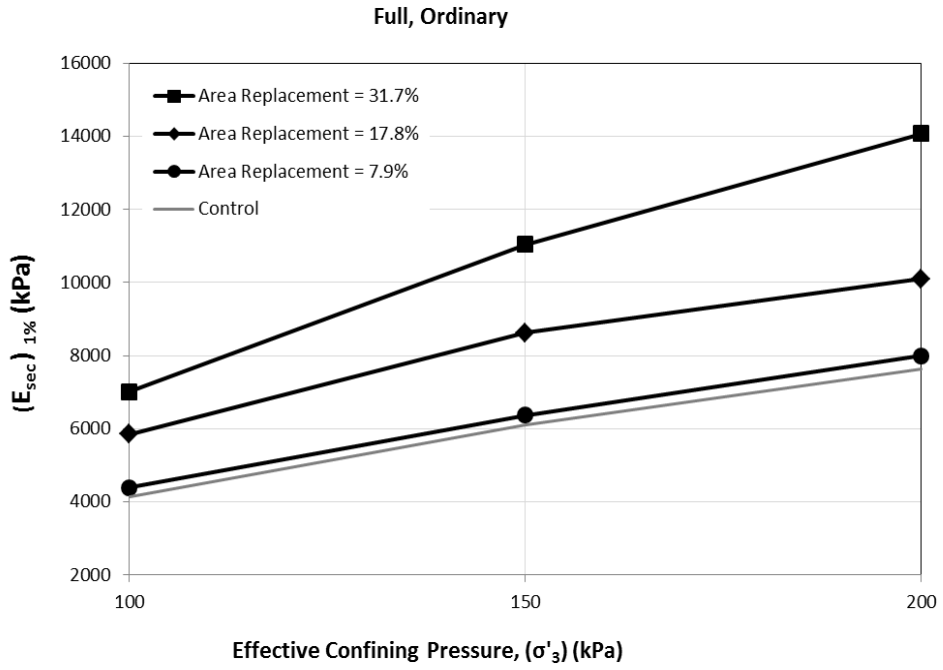

Figure 6.19. Variation of $(E_{sec})_{1\%}$ with effective confining pressure (Hc/Hs=1,Ac/As=7.9%, Ac/As=17.8%,Ac/As=31.7%, ordinary)

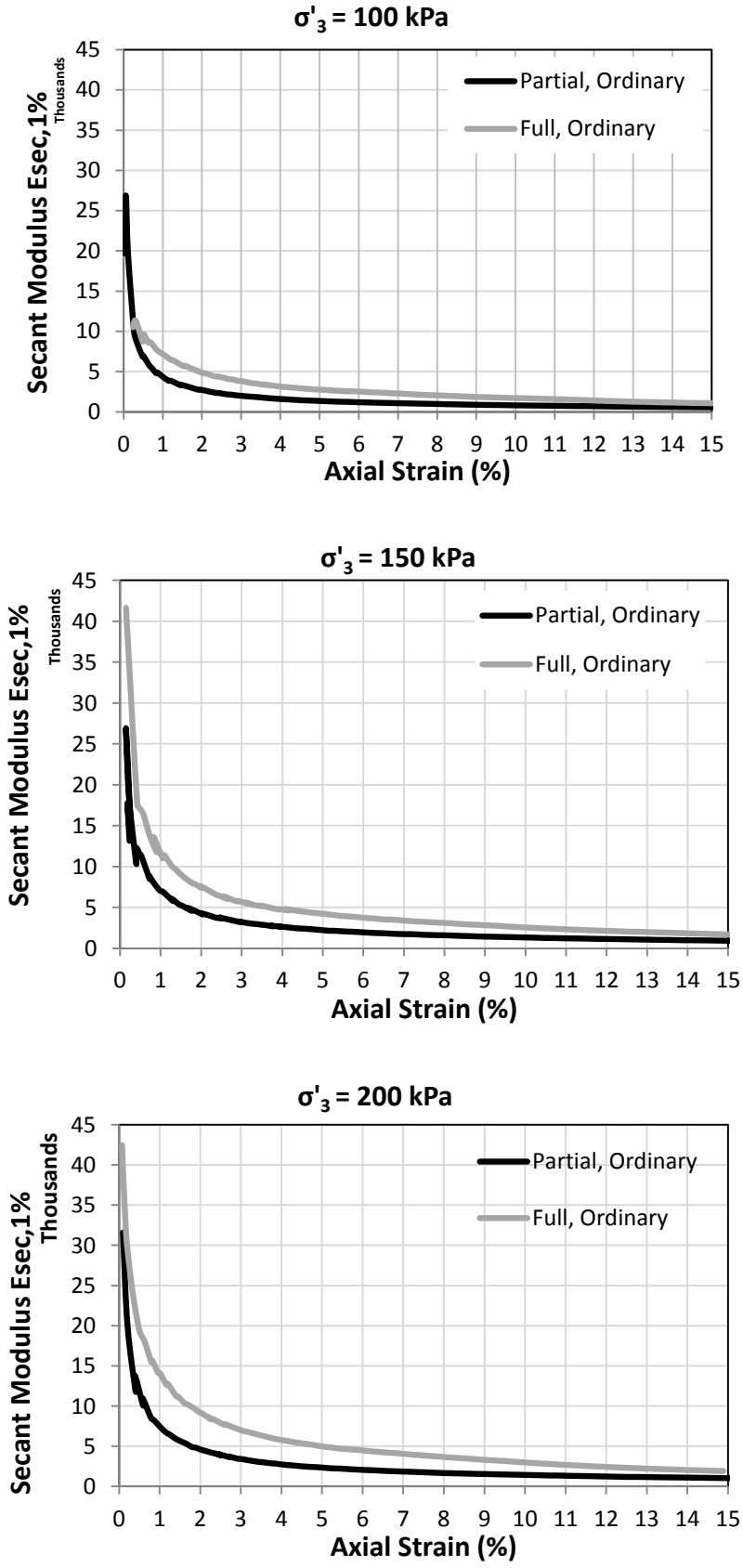

Figure 6.20. Variation of (E_{sec}) with strain for composite specimens (Ac/As=31.7%)

6.2.2.6. Effect of sand columns on the "Effective" Shear Strength Parameters

Figure 6.21 shows the effective Mohr-Coulomb envelops corresponding to unreinforced/control specimens and specimen reinforced with 4cm (Ac/As= 31.7%) partially and fully penetrating columns. Figure 6.22 shows the effective Mohr-Coulomb envelops corresponding to unreinforced/control specimens and specimen reinforced with 2cm, 3cm, and 4cm (Ac/As= 7.9%, 17.8% and 31.7%, respectively) partially and fully penetrating columns. The resulting shear strength parameters c' and ϕ' are summarized in Table 6.2.

As indicated by the data shown in Table 6.2, the insertion of sand columns with different depths and diameters didn't lead to a noticeable change/increase in the drained angle of internal friction (Ø') of the composite sand column Kaolin material. In fact, the drained friction angles decreased slightly in some cases, and up to 2.5˚ for the partially penetrating 4cm diameter column (see Table 6.2). However, this decrease in the friction angle was generally accompanied by an increase in the drained cohesion (c'). The increase in the drained cohesion (c') for partially penetrating column with an area replacement ratio of 31.7% was 7kPa. The effective cohesion increased from 0 kPa for unreinforced Kaolin specimen to 7 kPa for the Kaolin specimens that were reinforced with partially penetrating columns with a diameter of 4cm.

Table 6.2. Effective shear stress failure parameters

Column Diameter (cm)	Column Penetration Ratio	c' (kPa)	ϕ' (deg)
0	0	0	26.3
2	0.75	4.4	23.7
2	1	1	25.3
3	0.75	0	25.9
3	1	12	23.6
4	0.75	7	23.8
4	1	8	26

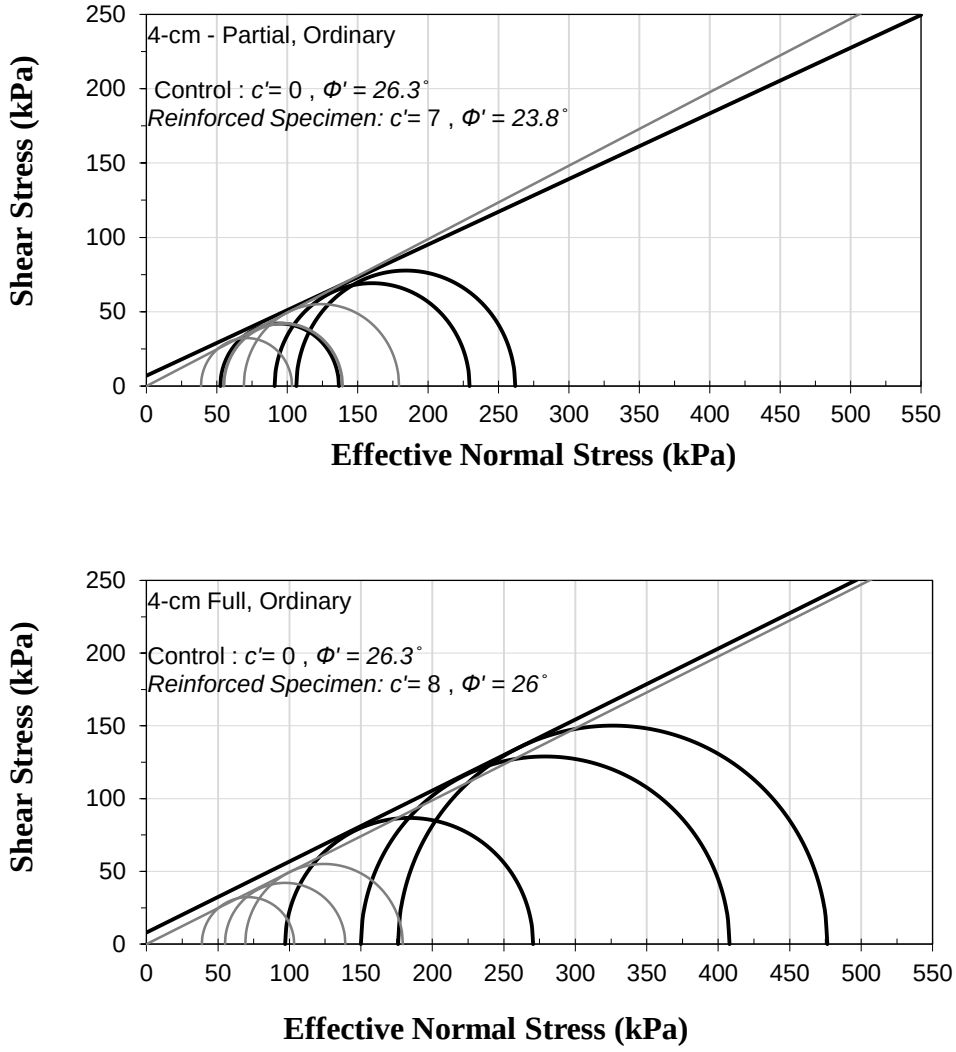

Figure 6.21. Drained failure envelopes for unreinforced and reinforced kaolin specimens (Ac/As= 31.7%)

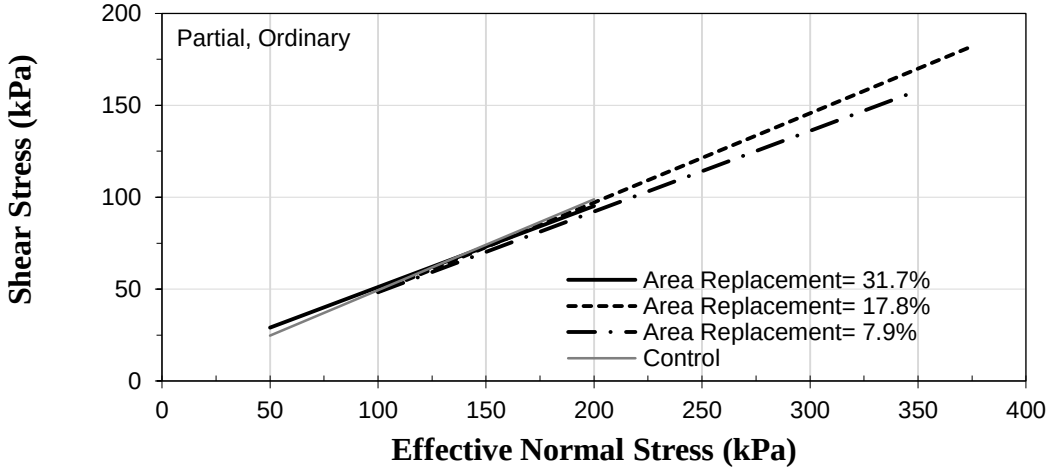

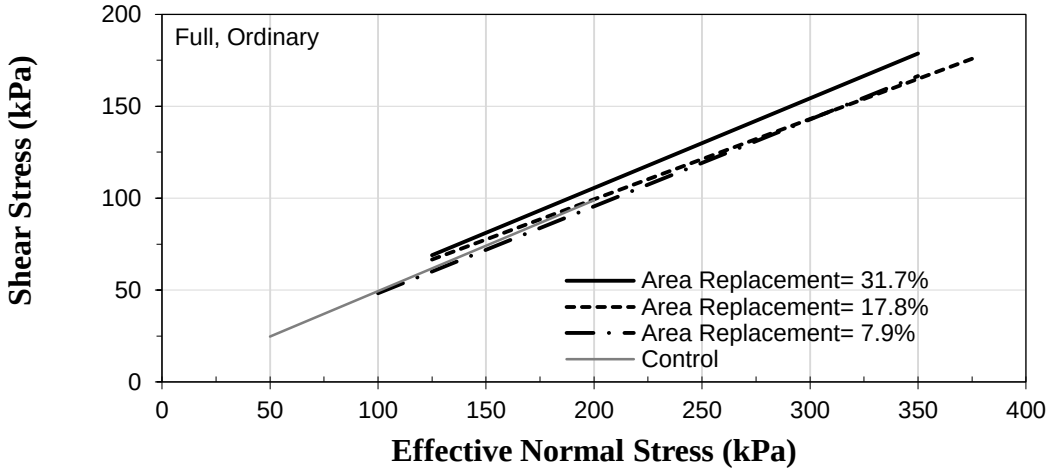

Figure 6.22. Drained failure envelopes for partial and full penetrating ordinary columns (Ac/As= 7.9%, Ac/As= 17.8%, Ac/As= 17.8%)

6.3. Summary of Main Findings

Based on the results of 9 consolidated undrained triaxial tests that were conducted in this experimental study and combined with 15 consolidated undrained triaxial tests done by Maakaroun (2009), the following conclusions can be drawn regarding the effect of sand columns on the undrained load response of soft clay, generation of excess pore water pressure during undrained loading, stiffness of reinforced clay, and effective shear strength parameters::

1. The presence of fully penetrating sand columns reduces significantly the bulging of the Kaolin specimen. Moreover, bulging of the reinforced Kaolin composite is reduced with increasing the column length. The bulging severity decreases with

increasing confining pressure. Specimens reinforced with partially penetrating columns failed by premature bearing failure in the unreinforced lower portion of the specimen

2. It was interesting to observe a shear plane passing through the sand column and shifting it laterally in the case of the 200kPa fully penetrating column. This shows that fully penetrating columns are more effective than partially penetrating columns since in the latter case failure occurs in the soft clay.

3. For fully penetrating ordinary sand columns, the stiffness of the reinforced clay increased by about 1.8 times when increasing the area replacement ratio from 7.9% to 31.7%. Moreover, extending the column length has a positive effect on increasing the stiffness of the reinforced Kaolin composite.

4. Insertion of fully penetrating ordinary sand columns with different area replacement ratios reduces significantly the generation of excess pore water pressure during undrained shearing. Moreover, the effectiveness of the sand column in reducing the excess pore water pressure increases with increasing the column length and area replacement ratio.

5. For fully penetrating ordinary sand columns and for area replacement ratio of 31.7%, the increase in undrained shear strength ranged from 168.4% to 206.4%. In comparison with smaller area replacement ratios of 7.9% and 17.8%, the 31.7% area replacement ratio resulted in a jump in the improvement of undrained shear strength. For partially penetrating ordinary sand columns and for area replacement ratio of 31.7%, the increase in undrained shear strength ranged from 33.1% to 65%

6. For Kaolin specimens that were reinforced with sand columns, the data did not show any clear indication of the effect of the confining pressure on the improvement in undrained shear strength

7. The data collected for samples that were reinforced with sand columns supports the hypothesis of a “critical column length” which is greater than about six column diameters, beyond which the increase in undrained shear strength due to the presence of the sand columns becomes negligible

8. The insertion of sand columns with different area replacement ratios and different column penetration depths didn’t cause an improvement in the drained friction angle (Ø’) of the reinforced clay; however, for fully penetrating sand column with area replacement ratio of 31.7%, the drained cohesion (c’) of the composite sand column kaolin material was increased from 0 kPa (for unreinforced specimen) to 8 kPa. However, this increase in the drained cohesion was complemented by a slight decrease in the drained friction angle from 26.3˚ (for unreinforced specimens) to 26˚

9. Finally combining the analysis done by Maakaroun (2009) for area replacement ratios of 7.9% and 17.8% with a higher area replacement ratio of 31.7%, have led to a higher reliability in the results and the conclusions reached.

CHAPTER 7

COMPARISON BETWEEN DRAINED AND UNDRAINED TESTS

7.1. Introduction

This chapter explores the effects of drainage and rate of loading on the load response of soft clays that are reinforced with sand columns. To achieve this objective, part of the results of the current comprehensive laboratory testing program that consisted of 9 consolidated drained (CD) triaxial tests will be compared to their 9 consolidated undrained (CU) triaxial tests counterparts, which had an area replacement ratio of 31.7%. Furthermore, the results will then be compared to the results reported in Najjar et al. (2010) and which were based on a series of consolidated undrained (CU) tests and the results reported in Maalouf (2012) and which were based on a series of consolidated drained (CD) tests which had lower area replacement ratios (7.9%, 17.8%). The clay specimens had diameters of 7.1 cm and heights of 14.2 cm and were reinforced with ordinary sand columns with diameters of 2, 3 or 4cm and were constructed as fully or partially penetrating in the clay specimen. Tests were conducted at effective confining pressures of 100, 150, and 200 kPa.

7.2. Test Results

The results for the drained and undrained test cases are compiled and presented in Table 7.1. These results are analyzed in this chapter to determine the effect of the drainage condition on the load response of the soft clay. In the analysis, emphasis is placed on the improvement in the deviatoric stress at failure, generation of excess pore pressure and its relation to the tendency for volume change, and on the improvement in stiffness and shear strength parameters.

Table 7.1. Comparison between Drained and Undrained (this study) and, Drained (Maalouf 2012) with Undrained (Najjar et al. 2010) Results

Test No.	Confining pressure σ_3, (kPa)	Drainage	Diameter of sand column (mm)	Area replacement ratio: A_c/A_s (%)	Column Penetration Ratio: H_c/H_s	Deviatoric stress @ failure (kPa)	Excess pore water pressure (kPa)	Volume strain (%)	E_{sec} @ 1% axial strain (kPa)	Increase in deviatoric stress (%)	Reduction in Excess Pore Pressure (%)	Reduction in Volumetric Strain (%)
1	100	Undrained	0	0.0	0.00	64.6	61.3	-	4150	-	-	-
2		Undrained	20	7.9	0.75	70.4	57.3	-	4220	9.0	6.5	-
3		Undrained	20	7.9	1.00	73.2	51.2	-	4390	13.3	16.5	-
4		Undrained	30	17.8	0.75	77.8	48.9	-	4597	20.4	20.2	-
5		Undrained	30	17.8	1.00	113.4	42.7	-	5853	75.5	30.3	-
6		Undrained	40	31.7	0.75	86.0	35.8	-	4451	33.1	41.6	-
7		Undrained	40	31.7	1.00	173.4	2.9	-	7019	168.4	95.3	-
8		Drained	0	0.0	0.00	124.8	-	-4.8	3387	-	-	-
9		Drained	20	7.9	0.75	124.7	-	-5.0	3800	-0.1	-	-3.8
10		Drained	20	7.9	1.00	134.1	-	-4.1	4050	7.5	-	15.1
11		Drained	30	17.8	0.75	138.2	-	-3.8	3754	10.8	-	21.9
12		Drained	30	17.8	1.00	169.8	-	-2.3	7630	36.0	-	51.7
13		Drained	40	31.7	0.75	155.0	-	-2.4	4527	24.2	-	49.7
14		Drained	40	31.7	1.00	210.7	-	-0.7	6170	68.8	-	84.5
15	150	Undrained	0	0.0	0.00	84.2	95.1	-	6092	-	-	-
16		Undrained	20	7.9	0.75	96.4	88.9	-	6100	14.5	6.5	-
17		Undrained	20	7.9	1.00	100.6	87.8	-	6368	19.5	7.7	-
18		Undrained	30	17.8	0.75	113.6	78.1	-	6697	34.9	17.9	-
19		Undrained	30	17.8	1.00	147.8	65.2	-	8624	75.5	31.4	-
20		Undrained	40	31.7	0.75	138.4	59.1	-	6976	65.0	37.8	-
21		Undrained	40	31.7	1.00	258.0	-0.3	-	11046	206.4	100.3	-
22		Drained	0	0.0	0.00	179.4	-	-5.1	4044	-	-	-
23		Drained	20	7.9	0.75	175.1	-	-5.2	3190	-2.4	-	-1.3
24		Drained	20	7.9	1.00	183.4	-	-4.6	4360	2.3	-	10.5
25		Drained	30	17.8	0.75	193.1	-	-4.0	3765	7.6	-	22.2
26		Drained	30	17.8	1.00	238.5	-	-3.6	8580	32.9	-	29.6
27		Drained	40	31.7	0.75	219.0	-	-2.8	6096	22.1	-	46.0
28		Drained	40	31.7	1.00	292.4	-	-1.3	9823	63.0	-	73.6
29	200	Undrained	0	0.0	0.00	110.2	130.9	-	7637	-	-	-
30		Undrained	20	7.9	0.75	120.2	120.3	-	7904	9.1	8.1	-
31		Undrained	20	7.9	1.00	131.6	112.1	-	7996	19.4	14.4	-
32		Undrained	30	17.8	0.75	142.4	107.8	-	8983	29.2	17.6	-
33		Undrained	30	17.8	1.00	184.6	89.4	-	10103	67.5	31.7	-
34		Undrained	40	31.7	0.75	155.6	93.3	-	7062	41.2	28.7	-
35		Undrained	40	31.7	1.00	300.4	24.1	-	14074	172.5	81.6	-
36		Drained	0	0.0	0.00	233.0	-	-5.4	5075	-	-	-
37		Drained	20	7.9	0.75	217.9	-	-5.5	4725	-6.5	-	-2.2
38		Drained	20	7.9	1.00	233.4	-	-5.5	3600	0.2	-	-3.3
39		Drained	30	17.8	0.75	260.6	-	-3.7	6100	11.8	-	31.1
40		Drained	30	17.8	1.00	311.9	-	-3.2	7030	33.9	-	39.8
41		Drained	40	31.7	0.75	290.0	-	-3.0	8359	24.5	-	43.3
42		Drained	40	31.7	1.00	369.7	-	-1.4	11833	58.7	-	73.9

7.2.1. Analysis for Control Kaolin Specimens

The variations of the deviatoric stress, pore pressure, and volumetric strain with axial strain are plotted on Figure. 7.1 for the control clay specimens. The stress-strain curves for the undrained tests indicate that the deviatoric stresses reached their maximum values at axial strains that are generally less than 5%. On the other hand, the stress-strain curves for the drained tests exhibited consistent increases in deviatoric stresses with strains as the samples were sheared towards critical state conditions. Moreover, the deviatoric stresses at failure (assuming failure at 15% strain) were found to be consistently greater in drained tests compared to undrained tests (more than twice in magnitude), irrespective of the level of the confining pressure . On the other hand, the stress-strain response indicates that the undrained clay exhibited higher stiffness at the onset of loading compared to drained tests.

The differences in the observed stress-strain response could be explained by observing the variations in the pore water pressure (for undrained tests) and volumetric strain (for the drained tests) as shearing progressed. The measured volumetric strains in the drained tests were all contractive and consistent with the positive pore pressures witnessed in the corresponding undrained tests. The positive volumetric strains during shearing results in a decrease in the void ratio of the drained clay specimens leading to a strain hardening behavior. The positive pore water pressures on the other hand result in a decrease in the effective confining pressure of the undrained specimen resulting in an early peak in the deviatoric stress. These results are expected for normally consolidated clays that are sheared in a triaxial setup under drained and undrained conditions, respectively.

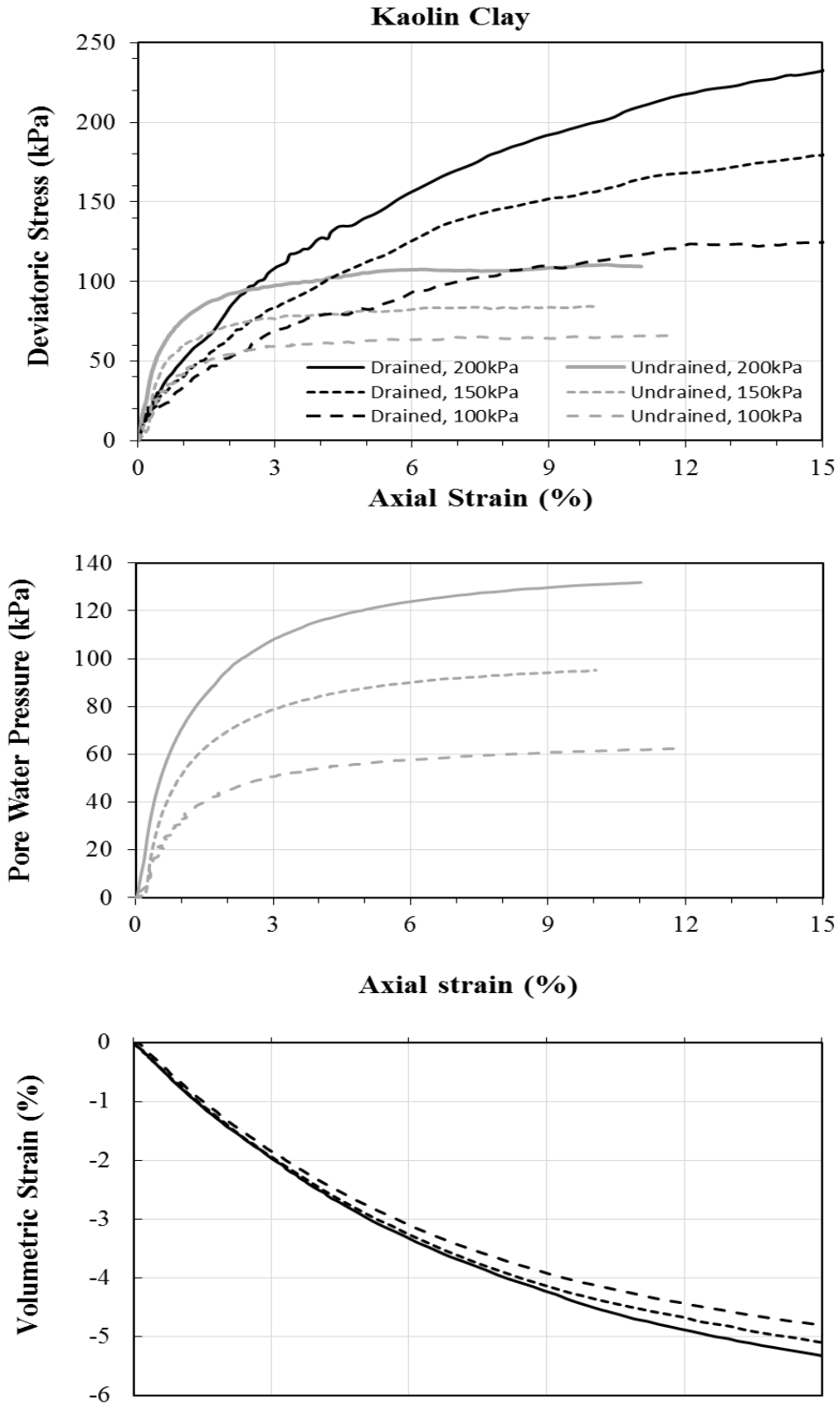

Figure 7.1. Deviatoric stress, excess pore pressure, and volumetric strain versus axial strain for control clay

The effective Mohr circles and the corresponding effective Mohr-Coulomb failure envelops for the drained and undrained tests are plotted on Figure. 7.2 for comparison. Interestingly, results on Figure 7.2 indicate that the effective friction angle ϕ' was 26.3° for the undrained tests and 21.8° for the drained tests, while the effective cohesive intercept c' was equal to zero for both types of tests. The difference in the calculated friction angles from the CD tests and the CU tests with pore pressure measurement could be considered to be significant and is attributed to two main issues: (1) The difference in the mean effective confining pressure at failure between the drained and undrained tests (about 3 to 4 times greater in drained tests compared to undrained tests), and (2) the difference in the rate of loading between the drained and undrained tests (strain rate equal to 0.25% per hour for drained tests and 1% per hour for undrained). Although the two effects are expected to result in an increase in the effective friction angle for undrained tests compared to drained tests, the difference seems to be higher than expected and will lead to some complications in the analysis of the reinforced clay specimens as will be seen in later sections of this chapter.

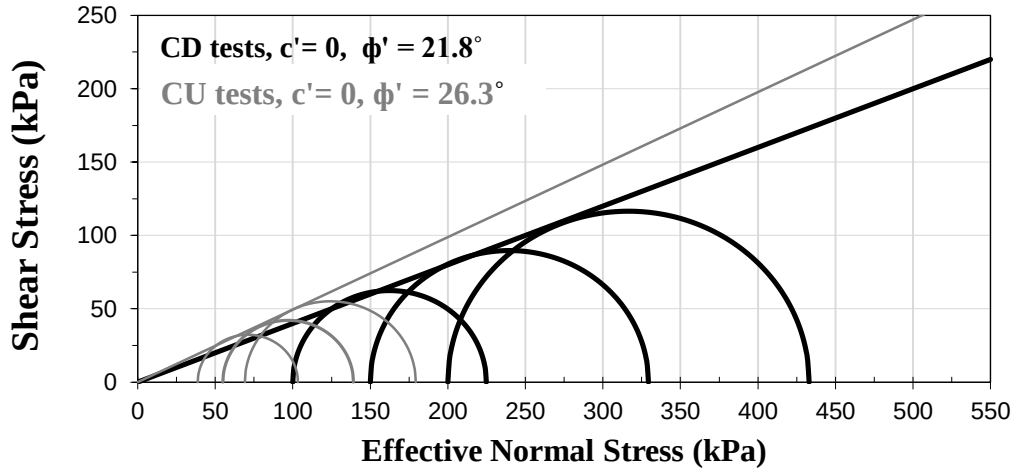

Figure 7.2. Comparison between Mohr-Coulomb failure envelops for control clay specimens from CD and CU triaxial tests.

7.2.2. Analysis for Ottawa Sand Specimens

The variations of the deviatoric stress, pore pressure, and volumetric strain with axial strain are plotted for the medium dense (relative density of about 44%) sand specimens on Figure. 7.3. The stress-strain curves for the drained tests indicate that the deviatoric stresses reached their maximum values at relatively small axial strains (about 2%) as the specimens dilated significantly during shearing. On the other hand, the stress-strain curves for the undrained tests exhibited consistent increases in deviatoric stresses with strains up to an axial strain of about 6% where the deviatoric stresses leveled out. The stress-strain behavior of the undrained tests were associated with the generation of negative pore pressures which increased in magnitude significantly at the onset of loading and leveled out at an axial strain of about 6%. The relatively large negative pore pressures that were generated in the undrained tests coupled with the dilative response that was observed in the drained tests reflect the significant dilative nature of the Ottawa sand at a relative density of 44%, which is the density used to construct the columns in the testing program.

The effective Mohr circles and the corresponding effective Mohr-Coulomb envelops for the drained and undrained tests for Ottawa sand are plotted on Figure. 7.4 for comparison. Results on Figure. 7.4 indicate that the effective friction angle ϕ' was about 33° for the undrained tests and 35° for the drained tests and the effective cohesive intercept c' was equal to zero for both types of tests. The difference between the measured effective friction angles could be attributed to the mean effective stresses at failure which were an order of magnitude greater for the undrained tests (due to the generation of negative excess pore pressures in the undrained specimens as indicated in Figure. 7.4).

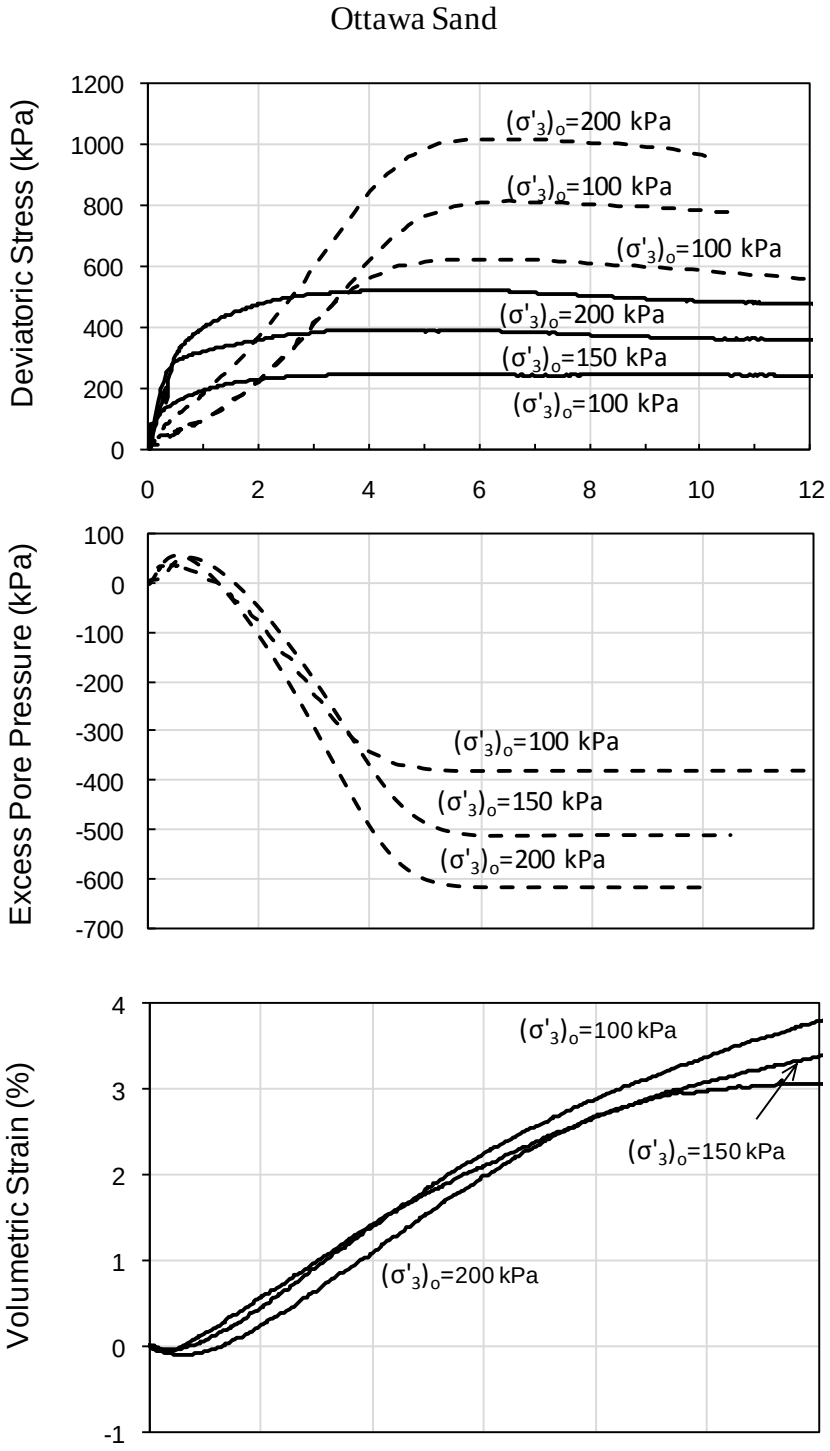

Figure 7.3. Deviatoric stress, excess pore pressure, and volumetric strain versus axial strain for Ottwa sand (Dotted lines indicate undrained tests and solid lines indicate drained tests).

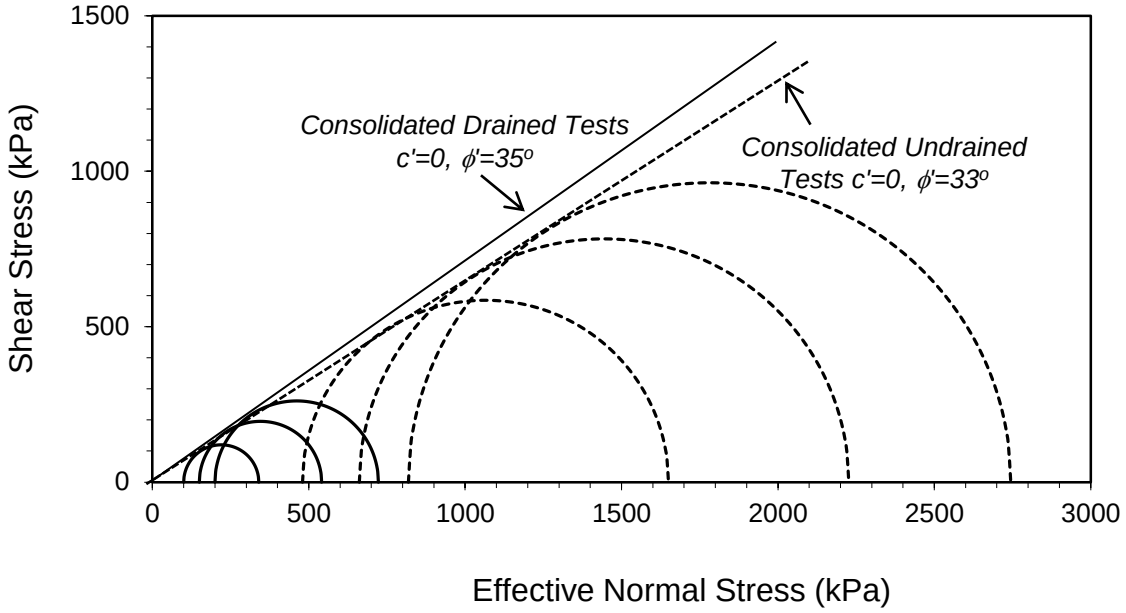

Figure 7.4. Comparison between Mohr-Coulomb failure envelops for Ottawa sand specimens from CD and CU triaxial tests.

7.2.3. Undrained and Drained Response for Clay Reinforced with Ordinary Sand Columns

7.2.3.1. Comparison between the Stress Strain Behavior

The variation of the deviatoric stress, excess pore pressure, and volumetric strain with axial strain is presented in Figures. 7.5 and 7.6 for clay samples that were reinforced with partially penetrating and fully penetrating ordinary sand columns, respectively. Results are presented for drained and undrained tests on the same figures to allow for a direct comparison between the load response at initial effective confining pressures of 100, 150, and 200 kPa.

Results for specimens reinforced with partially penetrating columns (Figure. 7.5) indicate that for the small area replacement ratio A_c/A_s of 7.9%, no improvements

in the load-carrying capacity were observed in the drained tests, while slight improvements were observed for undrained tests. On the other hand, results pertaining to the medium and large area replacement ratios of 17.8% and 31.7% indicated improvements in the load-carrying capacity of the clay specimens for both drained and undrained tests.

The lack of any improvement in the load response in the drained tests for samples with A_c/A_s of 7.9% was associated with no change in the volumetric strain in reference to the control clay specimens. On the other hand, test specimens with an A_c/A_s of 17.8% and 31.7% exhibited reductions in the magnitude of the contractive volumetric strains in association with the improvements observed in the drained load response. For the undrained tests, the improvement that was observed in the load response for all area replacement ratios was associated with a reduction in the excess positive pore pressure in comparison to the control clay specimens. This reduction in positive pore pressures was found to be higher for samples reinforced with a higher area replacement ratio of 31.7% and was associated with larger improvements in the load response.

It is worth noting that for all samples with reinforced with partially penetrating columns and at all initial effective confining pressures, the load-carrying capacities that were observed in the drained tests were higher than the load-carrying capacities that were observed for the undrained counterparts. This is related to the fact that the control clay specimens in the drained tests exhibited a higher load capacity compared to the control undrained tests as indicated in Figure 7.1.

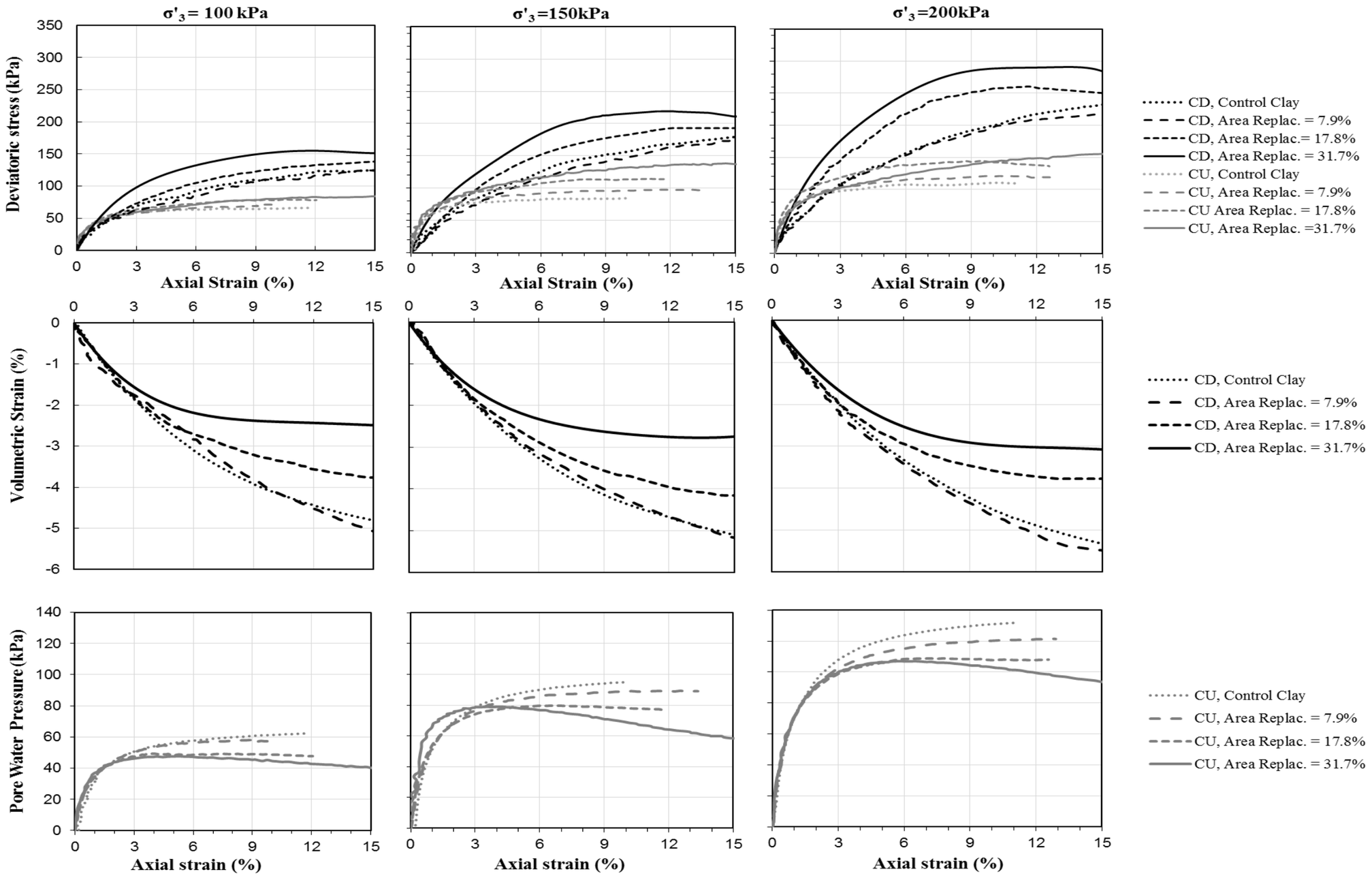

Figure 7.5. Comparison between the variation of the deviatoric stress, excess pore pressure, and volumetric strain with axial strain for drained and undrained loading conditions (ordinary sand columns, partial penetration).

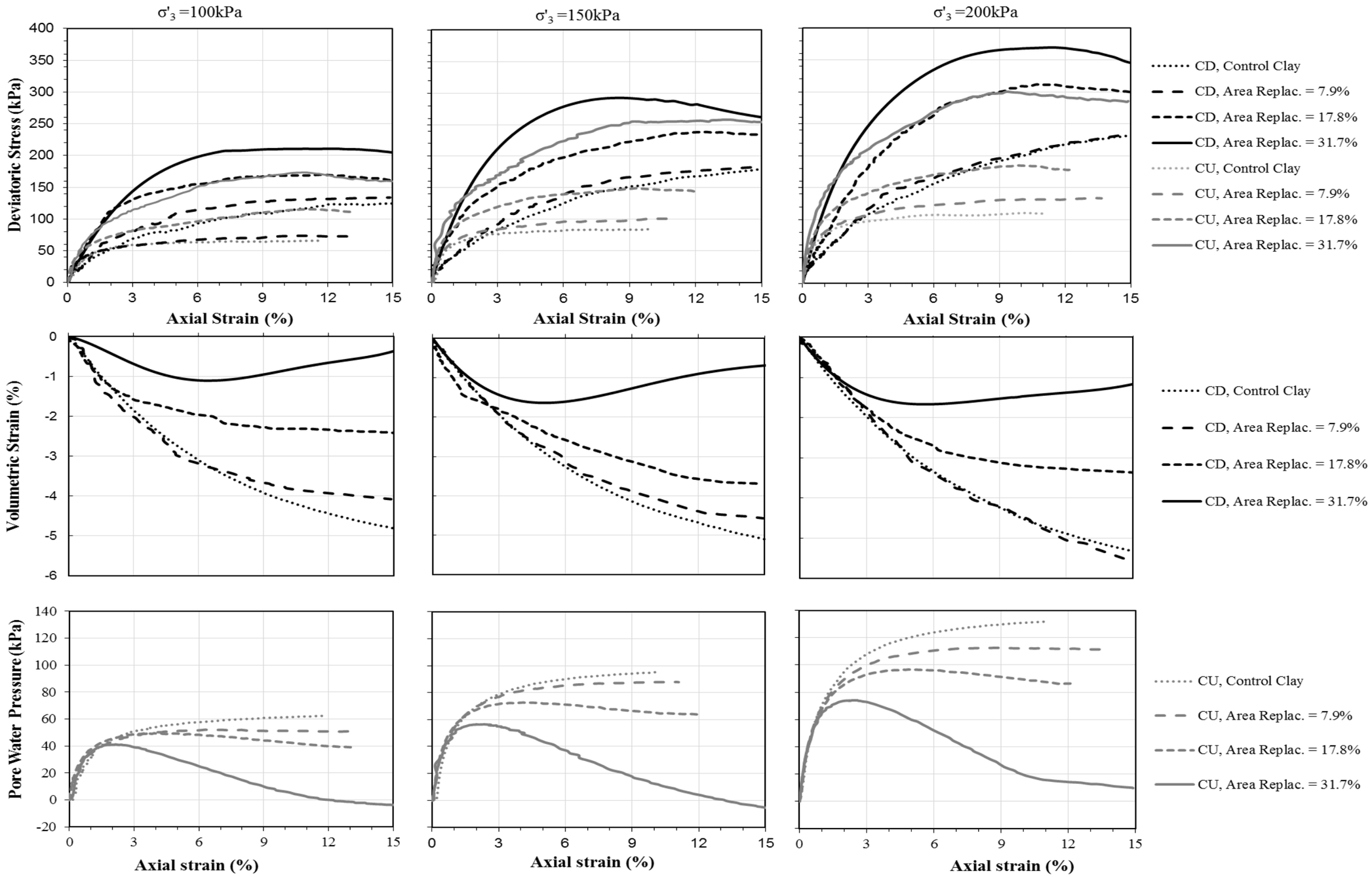

Figure 7.6. Variation of deviatoric stress and volumetric strain with axial strain (ordinary sand columns, full penetration).

Results for specimens reinforced with fully penetrating columns (Figure 7.6) indicated similar tendencies to those witnessed for partially penetrating columns for the small and medium area replacement ratios. For example, almost no improvements in the load-carrying capacity and no changes in the volumetric strains were observed in the drained tests for A_c/A_s of 7.9%. For the undrained tests with an A_c/A_s of 7.9%, slight improvements in the load-carrying capacity were observed and were associated with decreases in the generation of excess positive pore pressures.

On the other hand, results pertaining to the higher area replacement ratio of 17.8% indicated significant improvements in the load-carrying capacity of the clay specimens for both drained and undrained tests, with the improvements being clearly associated with decreases in the magnitudes of the volumetric strains in drained tests and in the excess positive pore pressures in the undrained tests. The decrease in the excess positive pore water pressure and contractive volumetric strains during shear could be attributed to the significant tendency for dilation in the 3-cm diameter sand column compared to the 2-cm diameter sand columns and the control specimen. However, and as seen in Figure 7.6, both the reduction in volumetric strains and positive pore pressures still follow the same trend as the control drained and undrained tests. This shows that even though the sand columns are significantly improving the load carrying capacity of the specimens, the behavior is still strongly affected by the clay part of the composite material.

The results for the tests conducted on specimens that were reinforced at an area replacement ratio of 31.7% clearly show that the sand column at this relatively high area replacement ratio is starting to significantly affect the behavior of the composite. This is clearly indicated in the results of the undrained tests in which almost all of the positive

pore pressures that were initially generated were dissipated after 12% strain leading to relatively large improvements in load carrying capacity. The significant reduction in excess pore pressures in these tests is a result of (1) the generation of negative pore pressures in the sand column and (2) the dissipation of some of the positive pore pressures in the clay part of the specimen due to internal exchange of water between the 4-cm sand columns and the surrounding clay. The net effect of the above 2 phenomenon is a significant increase in the deviatoric stress of the undrained specimen which almost approached the load carrying capacity of the drained 31.7% test.

It should be noted that for all the tests analyzed in this chapter and for any given combination of area replacement ratio and column penetration ratio, the deviatoric stresses at failure for drained conditions constitute an upper bound for the strength of the clay-sand column composite, while the undrained tests resulted in lower-bound strengths. The difference in the load response due to the drainage condition decreases as the area replacement ratio increases.

7.2.3.2. Comparison between the Deviatoric Stress at Failure

The percent improvements in the deviatoric stress at failure for both drained and undrained tests are plotted versus the initial effective confining pressure in Figure 7.7 for clay samples that were reinforced with partially penetrating and fully penetrating ordinary sand columns.

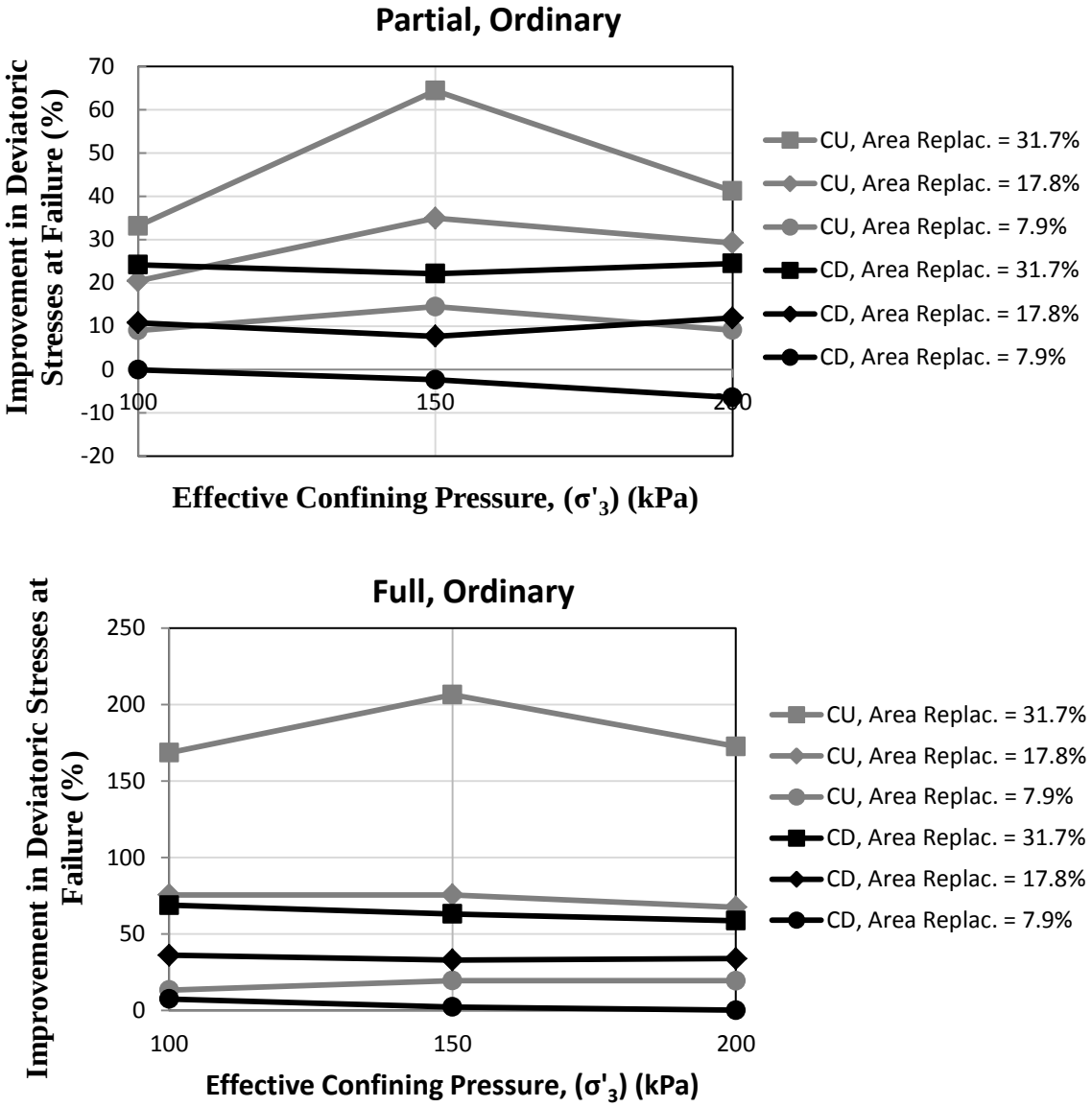

Figure 7.7. Improvement in the deviatoric stress at failure for partially penetrating ordinary sand columns and fully penetrating ordinary sand columns for drained and undrained tests.

For the undrained tests, results in Figure 7.7 indicate that the increase in the deviatoric stress at failure for partially penetrating columns ranged from 9 to 15% for A_c/A_s=7.9%, from 20 to 35% for A_c/A_s=17.8% and from 33 to 65% for A_c/A_s=31.7%. For the corresponding drained tests, the respective improvements ranged from -6 to 0% for A_c/A_s=7.9%, from 8 to 12% for A_c/A_s=17.8% and from 17 to 25% for A_c/A_s=31.7%.

For samples reinforced with fully penetrating columns, the results of the undrained tests indicated that the increase in the deviatoric stress at failure ranged from 13 to 20% for A_c/A_s=7.9%, from 67 to 75% for A_c/A_s=17.8% and from 168 to 206% for A_c/A_s=31.7%. For the corresponding drained tests, the respective improvements ranged from 0 to 7.5% for A_c/A_s=7.9%, from 33 to 35% for A_c/A_s=17.8%, and from 58 to 69% for A_c/A_s=31.7%.

An analysis of the results presented in Figure 7.7 indicates that the percent improvement in the deviatoric stress at failure for the undrained tests was consistently higher than the improvement observed for the drained tests. This observation could lead to the conclusion that sand columns are more efficient at increasing the load-carrying capacity of soft clays in an undrained setting than in a drained setting. It should be noted though that the percent improvement in the deviatoric stress at failure was calculated for the drained and undrained tests on reinforced specimens in reference to the drained and undrained response of the control clay, respectively. Results in Figures. 7.5 and 7.6 indicate that although the percent improvement in the deviatoric stress at failure was higher for undrained tests, the absolute values of the deviatoric stress at failure were still much higher for drained tests at low and medium area replacement ratio (7.9 and 17.8%) and slightly higher for the high area replacement ration (31.7%), signifying that the drained load response could likely represent an upper bound in the shear strength of the reinforced clay specimens up until a certain area replacement ratio which would be higher than 31.7%. For a given area replacement ratio, the drained strength of the clays was found to be consistently greater in magnitude than the undrained strength. This indicates that in field applications involving the use of sand columns in soft clays, it is expected that the drained shear strength which will govern the behavior of the

reinforced clay for long-term conditions would likely be greater than the undrained shear strength which governs the stability of the reinforced clay in the short term. This of course will depend on the area replacement ratio as discussed previously.

7.2.3.3. Comparison between the Effective Shear Strength Parameters

The effective shear strength parameters that were obtained from drained and undrained tests on samples tested at effective confining pressures of 100, 150 and 200 kPa are presented in Table 7.2 for comparison. The corresponding Mohr coulomb failure envelopes are shown in Figures. 7.8, 7.9 and 7.10 for clay specimens reinforced with ordinary 2-cm, 3-cm and 4-cm diameter sand columns, respectively.

For specimens that were reinforced with partially penetrating 2-cm ordinary sand columns, no improvements in the load carrying capacity were observed compared to control clay specimens. This translated into effective shear strength parameters (c' and ϕ') that were relatively similar to the control specimens (see Table 7.2 and Figure. 7.8). For specimens that were reinforced with fully penetrating 2-cm ordinary sand columns (see Table 7.2 and 7.8), c' and ϕ' resulting from the undrained tests were also similar to the parameters of the undrained control clay, despite the fact that average improvements in the order of 17.5% were observed in the deviatoric stresses at failure. This could be explained by the fact that the improvements in deviatoric stresses at failure were offset by decreases in excess pore pressure at failure for the reinforced specimen, resulting in c' and ϕ' that were more or less unchanged compared to the undrained control specimens. Finally, results of the drained tests that were conducted on fully penetrating 2-cm sand columns indicated a reduction in the effective friction

angle ϕ' and an increase in c' in comparison to the control clay specimen (ϕ' decreased from 21.8^{o} to 20^{o} and c' increased from 0 kPa to 10 kPa). These results reflect the decreasing trend in the percent improvement in deviatoric stress at failure with increasing effective confining pressure as indicated for drained fully penetrating 2-cm specimens in Figure 7.7.

Table 7.2. Comparison between effective shear strength parameters for clay specimens reinforced with ordinary sand columns and tested under drained and undrained conditions.

Drainage Condition	Type of Column	Column Penetration Ratio	Area Replacement Ratio (%)	c' (kPa)	ϕ' (deg)
Drained	-	-	-	0	21.8
Drained	Ordinary	0.75	7.9	12	18.8
Drained	Ordinary	1	7.9	10	20
Drained	Ordinary	0.75	17.8	5	22.5
Drained	Ordinary	1	17.8	10	24.5
Drained	Ordinary	0.75	31.7	7	23.8
Drained	Ordinary	1	31.7	18	26
Undrained	-	-	-	0	26.3
Undrained	Ordinary	0.75	7.9	4.4	23.7
Undrained	Ordinary	1	7.9	1	25.3
Undrained	Ordinary	0.75	17.8	0	25.9
Undrained	Ordinary	1	17.8	12	23.6
Undrained	Ordinary	0.75	31.7	7	23.8
Undrained	Ordinary	1	31.7	8	26

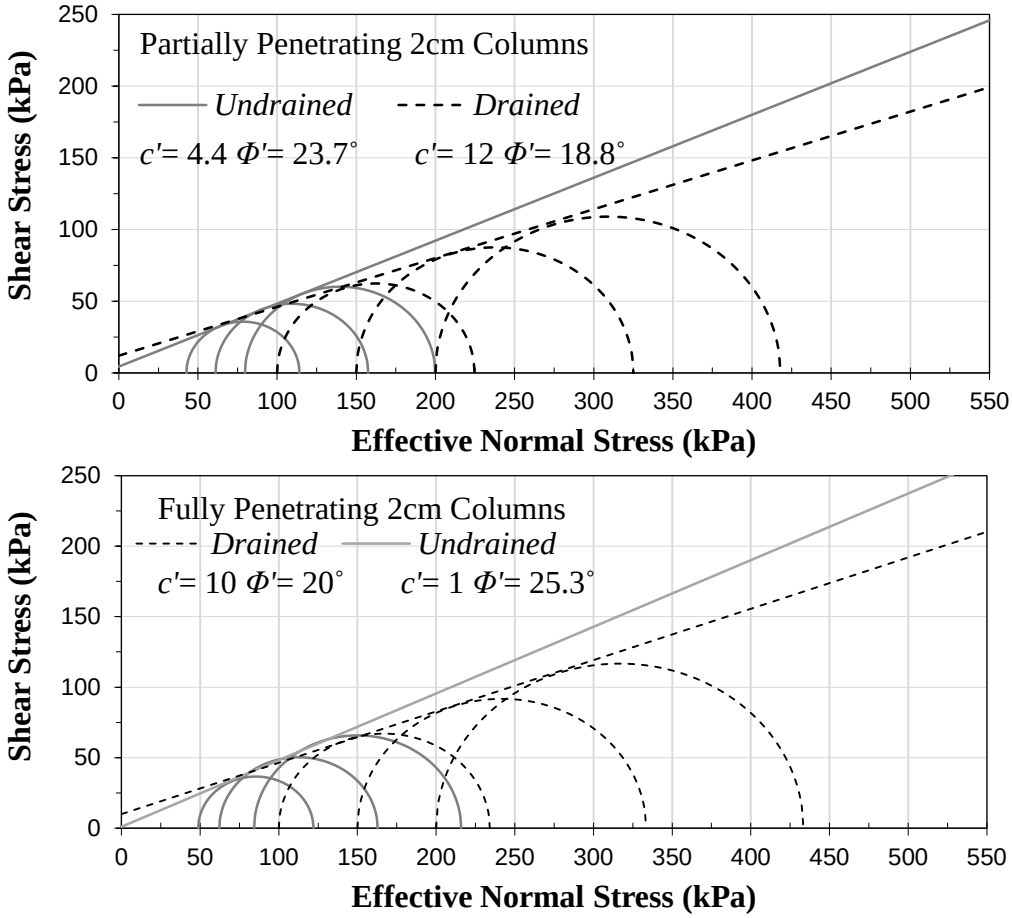

Figure 7.8. Mohr-Coulomb failure envelopes (samples with ordinary 2-cm sand columns).

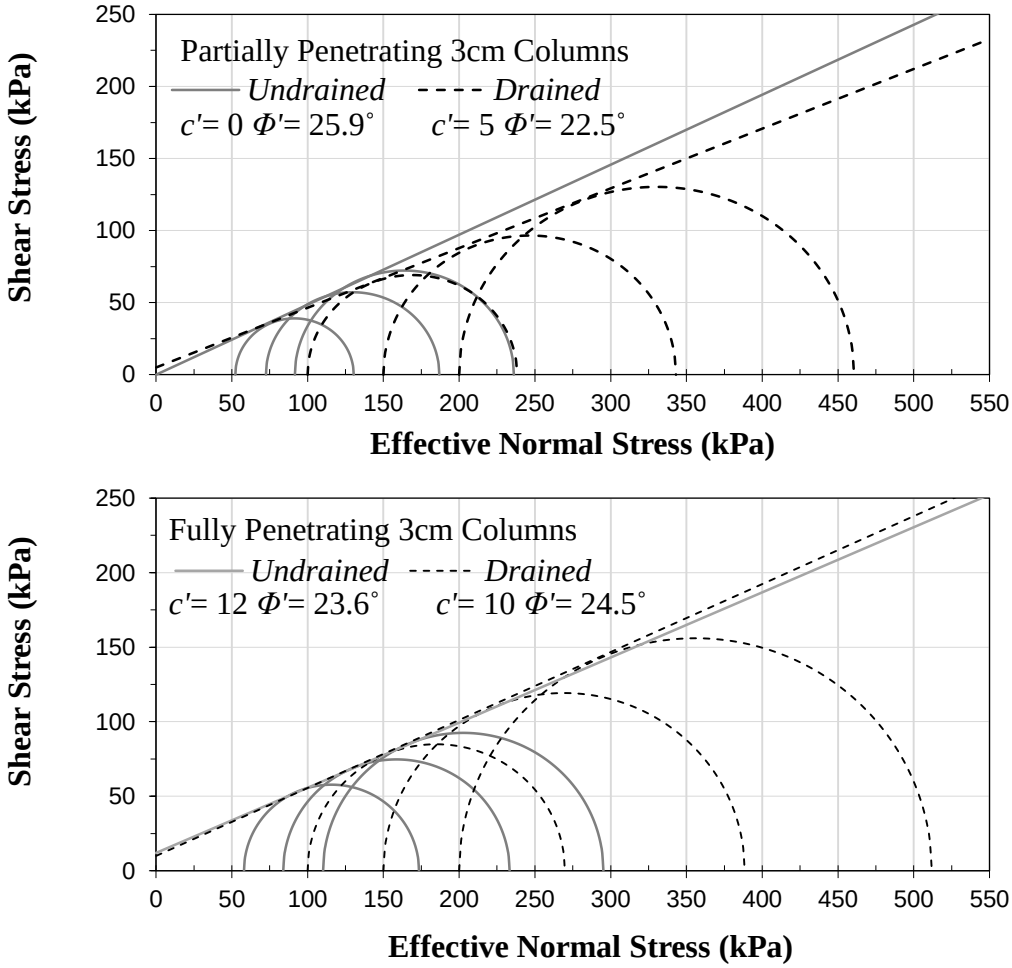

Figure 7.9. Mohr-Coulomb failure envelopes (samples with ordinary 3-cm sand columns).

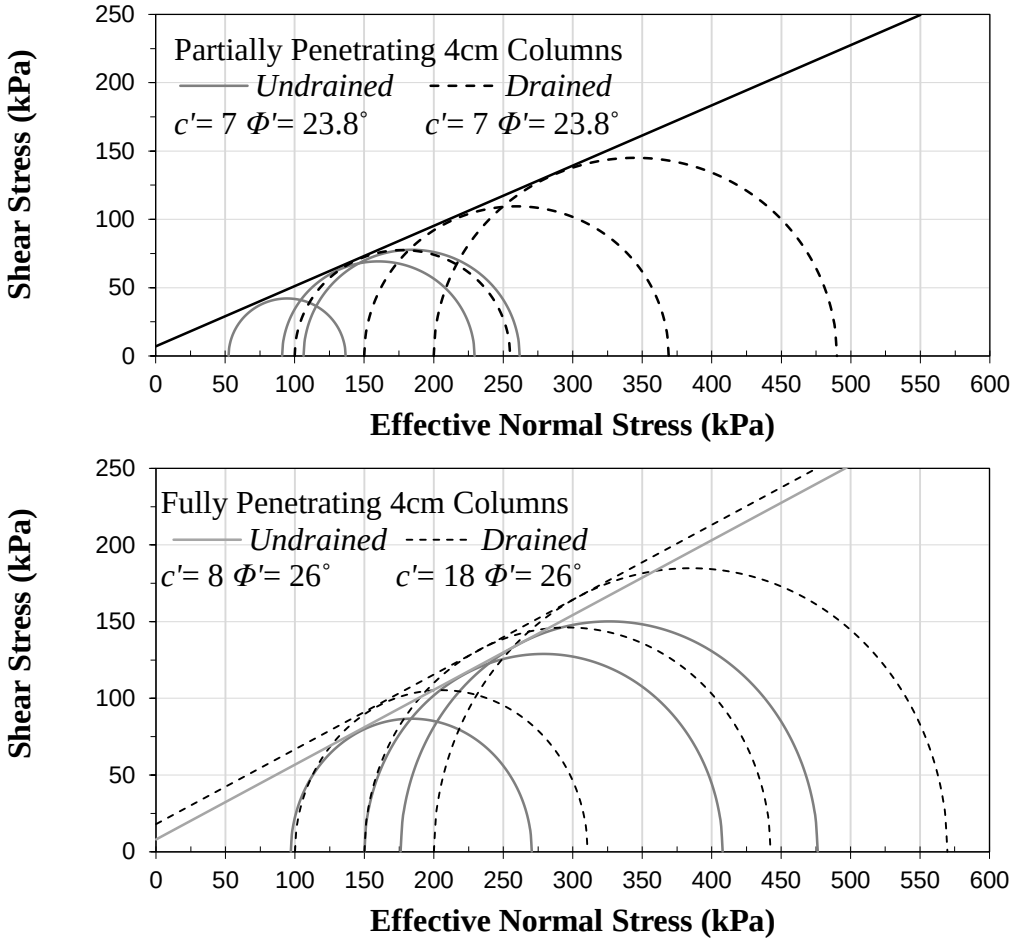

Figure 7.10. Mohr-Coulomb failure envelopes (samples with ordinary 4-cm sand columns).

For specimens that were reinforced with partially penetrating 3-cm ordinary sand columns, no improvements were observed in c' and ϕ' for the undrained tests (c' = 0, $\phi' = 26^{o}$), and slight improvements were observed in c' (c' increased from 0 in control to 5kPa) and ϕ' for drained tests ($\phi' = 22.5^{o}$ compared to $\phi' = 21.8^{o}$ for control clay). The lack of improvement in c' and ϕ' for the undrained tests does not reflect the 30% average improvement in the deviatoric stress at failure that was observed in Figure 7.7, the reason being the associated reduction in pore pressure witnessed in these tests.

For specimens that were reinforced with fully penetrating 3-cm sand columns, an increase in *c'* (from 0 to 12 kPa) and a slight reduction in ϕ' (from 26^o to 24^o) were observed in the undrained tests. For the drained tests, *c'* increased to 19kPa and ϕ' increased appreciably (from 21^o to 26^o).

For specimens that were reinforced with partially penetrating 4-cm ordinary sand columns, slight improvement was observed in *c'* (*c'* increased from 0 in control to 18kPa), and ϕ' decreased by 4.7˚ for undrained tests. On the other hand, for drained tests ϕ' decreased by 0.2˚ and improvement was observed in *c'* (*c'* increased from 0 in control to 18kPa). The lack of improvement in *c'* and ϕ' for the undrained tests which was observed by Maalouf (2012) for the 3-cm columns and attributed to the associated reduction in pore pressure does not apply to this high 31.7% area replacement ratio. The results might be affected by the 200kPa undrained test which didn't have the same degree of improvements of the 100 and 150kPa tests, and thus reduced ϕ. Furthermore, For specimens that were reinforced with fully penetrating 4-cm sand columns, an increase in *c'* (from 0 to 8 kPa) and a very slight reduction in ϕ' (from 26.3^o to 26^o) were observed in the undrained tests. For the drained tests, *c'* increased to 18kPa and ϕ' increased appreciably (from 21.8^o to 26^o). It is interesting to note that unlike the smaller area replacement ratios, this higher 31.7% ratio yielded results which indicate that drained and undrained tests will have the same ϕ' and slightly different *c'* with the drained test having the higher *c'*.

A thorough analysis of the results in Table 7.2 and in Figures. 7.8 to 7.10 leads to the following observations with regards to the difference between the effective shear

strength parameters that were inferred from drained and undrained tests on identical samples:

1. The major difference in the inferred values of ϕ' for the control clay specimens from drained ($\phi' = 21.8^o$) and undrained tests ($\phi' = 26.3^o$) adds a level of complexity to the analysis of the effective strength envelops of the reinforced clay.
2. Irrespective of the difference in the ϕ' of the control clay, the utilization of c' and ϕ' solely (ex. Table 7.2) as a basis for comparing the effective shear strength envelops from drained and undrained tests might not be indicative of the differences in the results. This is due to the fact that the resulting c' and ϕ' from drained and undrained tests in identical samples are not derived from the same range of effective stress, with the range of mean stresses in undrained tests being 2 or 3 times smaller than the range of the stresses in the drained tests for the 7.9% and 17.8% area replacement ratios. The above analysis which was done by Maalouf (2012) is confirmed by the results of the 31.7% area replacement ratio tests conducted in this study. Since the range of mean stresses in the undrained tests started to approach the drained tests, the same ϕ' was observed for both drainage conditions with c' being higher for the drained test.
3. Based on point 2 above, it is observed that differences in the failure envelops from drained and undrained tests tend to become smaller as the differences in the mean effective stresses between drained and undrained tests become smaller. This is shown clearly in the tests

conducted using 4-cm columns (Figure. 7.10) where the increase in the deviatoric stresses and the decrease in the excess pore pressures at failure in the undrained tests were significant enough to push the Mohr circles to higher stresses. For these tests (especially the fully penetrating 4-cm column), the difference between the drained and undrained Mohr-Coulomb failure envelops becomes smaller for a wide range of effective normal stresses.

7.2.3.4. Comparison between Secant Young's Modulus

A secant Young's modulus $(E_{sec})_{1\%}$ defined at an axial strain of 1% was calculated for each test by dividing the deviatoric stress measured at an axial strain of 1% by the corresponding strain. Results of the calculated values of $(E_{sec})_{1\%}$ for drained and undrained tests are presented in Table 7.1 and plotted in Figures.7.11 and 7.12 versus the initial effective confining pressure for comparison. For the undrained tests involving partially penetrating 2-cm (A_c/A_s=7.9%), 3-cm (A_c/A_s=17.8%) and 4-cm (A_c/A_s=31.7%) columns, no improvements were observed in the values of $(E_{sec})_{1\%}$ for all confining pressures. For fully penetrating columns, results indicate that the average improvement in the secant undrained Young's modulus $(E_{sec})_{1\%}$ for effective confining pressures of 100 kPa, 150 kPa, and 200 kPa was about 5% for an area replacement ratio of 7.9%, about 38% for area replacement ratios of 17.8% and about 78% for area replacement ratios of 31.7%.

Interestingly, results of the drained tests conducted with an area replacement ratio of 7.9% exhibited a reduction in $(E_{sec})_{1\%}$ at 150 and 200kPa confining pressures for partially penetrating columns and at 200kPa confining pressure for fully penetrating

columns. Similarly, samples that were reinforced with an area replacement ratio of 17.8% using partially penetrating columns also exhibited a reduction in $(E_{sec})_{1\%}$ confining pressure of 150 kPa. On the other hand, results of tests conducted on fully penetrating columns exhibited a consistent increase in $(E_{sec})_{1\%}$, reaching about 125% for confining pressure of 100 kPa, 112% for confining pressure of150 kPa, and about 38% for a confining pressure of 200 kPa. The reduced efficiency of the sand columns in providing improvement in stiffness at high confining pressures (200 kPa) is not clear at this time, but could be due to a possible reduction in the lateral confinement of the sand column during shear at the initial stage of loading of the composite specimens. On the other hand, samples reinforced with the higher 31.7% area replacement ratio exhibited constant increase in $(E_{sec})_{1\%}$, for both partially and fully penetrating columns and for all confining pressures, with an average improvement of 50% for partially penetrating columns and 120% for fully penetrating columns.

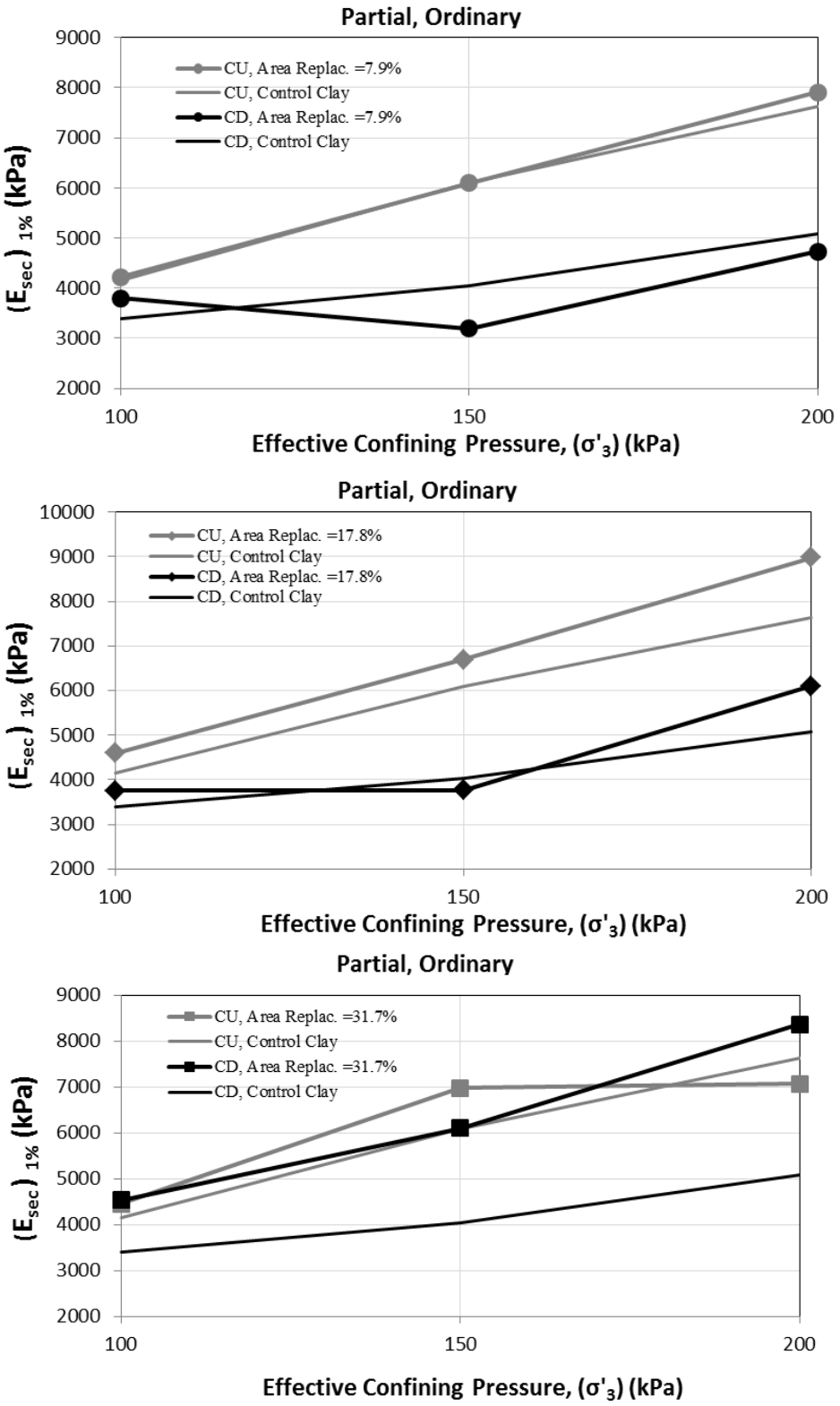

Figure 7.11. Variation of $(E_{sec})_{1\%}$ with effective confining pressure for samples reinforced with partially penetrating ordinary sand columns

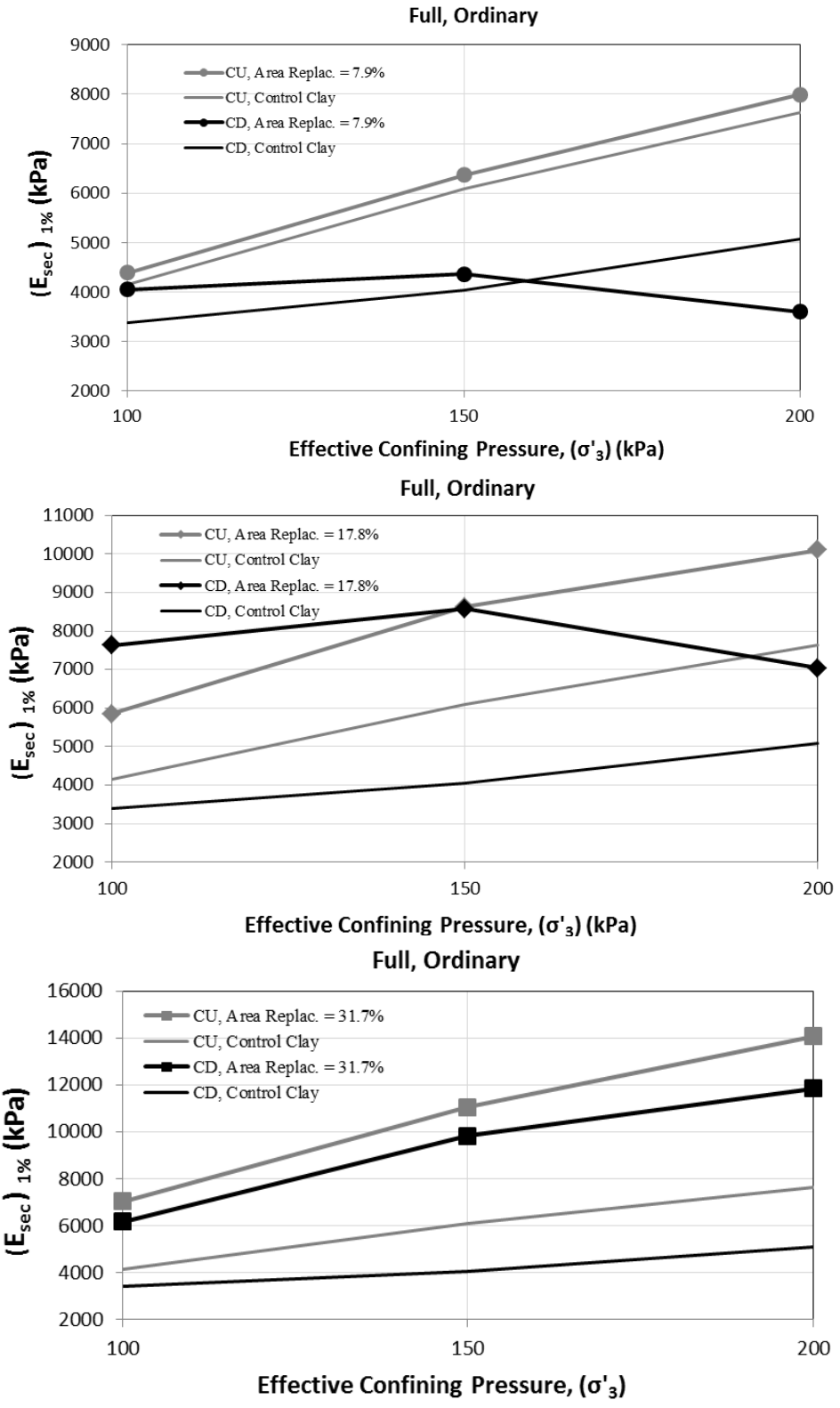

Figure 7.12. Variation of $(E_{sec})_{1\%}$ with effective confining pressure for samples reinforced with fully penetrating ordinary sand columns

A comparison between $(E_{sec})_{1\%}$ values that are obtained from identical drained and undrained tests indicates that except for test cases with partially penetrating 4-cm column at a confining pressure of 200 kPa and with fully penetrating 3-cm column at a confining pressure of 100kPa, the stiffness of the specimens as indicated by $(E_{sec})_{1\%}$ was larger for the undrained tests. The results can be explained by noting that the dependency of $(E_{sec})_{1\%}$ of the control clay tests on the initial effective confining pressure in the undrained tests was much stronger than the dependency of $(E_{sec})_{1\%}$ in the control drained tests on confining pressure. As the effective confining pressure increased from 100 kPa to 200 kPa, $(E_{sec})_{1\%}$ in the undrained control tests increased from 4150 kPa to 7637 kPa, whereas the corresponding increase in the drained control tests was from 3387 kPa to 5075 Kpa.

7.3. Summary of Main Findings

Based on a comparison between the 18 consolidated drained and undrained triaxial tests that were conducted in this experimental research study (9 CD, 9 CU) and 24 consolidated undrained and drained triaxial tests that were reported in Najjar et al. (2010) and Maalouf (2012), respectively, the following conclusions can be drawn with regards to the difference in the drained and undrained load response of the composite clay:

1. For the control clay, a significant difference was observed in the effective friction angle ϕ' obtained from the CD tests ($\phi' = 21.8^o$) and the CU tests with pore pressure measurement ($\phi' = 26.3^o$). The difference could be attributed to the significant difference in the mean effective confining pressures at failure and the rate of loading

between the drained and undrained tests. This difference was higher than expected and lead to some complications in the analysis of results of the reinforced clay specimens.

2. Based on a thorough analysis of the variation of the deviatoric stress, pore pressure, and volumetric strain with axial strain for ordinary columns, and based on a quantitative analysis of the percent improvement in the deviatoric stresses at failure, it is concluded that:

- The percent improvement in the deviatoric stress at failure for the undrained tests was consistently higher than the improvement observed for the drained tests. This observation could lead to the conclusion that sand columns are more efficient at increasing the load-carrying capacity of soft clays in an undrained setting than in a drained setting.
- Although the percent improvement in the deviatoric stress at failure was higher for undrained tests, the absolute values of the deviatoric stress at failure were still much higher for drained tests, signifying that the drained load response could likely represent an upper bound in the shear strength of the reinforced clay specimens analyzed in this study. This was however contrasted by the fact that at high area replacement ratio (31.7%), the maximum deviatoric stress of the undrained tests approached those of the drained tests, indicating a shift in the governing behavior from the clay to the sand column.
- This indicates that in field applications involving the use of sand columns in soft clays with small and medium area replacement ratio (less than 30%), it is expected that the drained shear strength which will govern the behavior of the reinforced clay for long-term conditions

would likely be greater than the undrained shear strength which governs the stability of the reinforced clay in the short term.

3. An analysis of the effective Mohr-Coulomb failure envelops from drained and undrained tests indicated that:

- The use of 2-cm columns (partially and fully penetrating) does not generally result in any improvement in the effective failure envelops in reference to the control specimens. The effective friction angle ϕ' was consistently smaller than the control specimen, and was complemented with an increase in *c'* which was more significant for in the drained test results.
- The use of 3-cm columns (partially and fully penetrating) resulted generally in improvements in the Mohr-Coulomb failure envelops, with the improvements being the most evident with fully penetrating columns.
- The use of 4-cm columns (partially and fully penetrating) resulted in improvements in the failure envelops, except for the case of partially penetrating undrained test which had a low friction angle compared to the control specimen. This was explained to be caused by the low strength of the 200kPa confining pressure test.
- The utilization of c' and ϕ' solely as a basis for comparing the effective shear strength envelops from drained and undrained tests might not be indicative of the differences in the results, since c' and ϕ' from drained and undrained tests are not derived from the same range of effective stress.

- It is observed that differences in the failure envelops from drained and undrained tests tend to become smaller as the differences in the mean effective stresses between drained and undrained tests become smaller. This was most evident in the case of the 31.7% area replacement ratio, in which drained and undrained tests had comparable maximum deviatoric stress value (especially in fully penetrating columns).

4. A secant Young's modulus $(E_{sec})_{1\%}$ defined at an axial strain of 1% was used as a basis for comparing the effect of drainage on the stiffness of the reinforced clay specimens. Results indicated that for specimens with a given area replacement ratio and a column penetration ratio, the undrained $(E_{sec})_{1\%}$ was generally found to be larger in magnitude than the drained $(E_{sec})_{1\%}$. In addition, the undrained $(E_{sec})_{1\%}$ exhibited consistent increases in reinforced specimens compared to control specimens. This was not the case for the small and medium area replacement ratios of 7.9 and 17.8% , in which the drained $(E_{sec})_{1\%}$ was found to decrease compared to the control specimens, especially for tests conducted at smaller confining pressures where the effects of column installation could have played a role in the reduction in $(E_{sec})_{1\%}$. The high area replacement ratio of 31.7% has proven to improve stiffness in both drained and undrained drainage condition consistently with increasing confining pressure.

CHAPTER 8

TEST RESULTS AND ANALYSIS FOR PARTIALLY DRAINED TESTS

8.1. Introduction

The drained and undrained response of soft clays reinforced with sand columns has been the main focus of researchers and studies for the last 30yrs. Although these studies have been essential for the development of design parameters and relationships, the fact that they do not model the real field behavior persists. Hence, there is a need to understand the effect of the partial drainage that occurs through the sand columns. Juran and Guermazi (1988), and Andreou et al (2008), published results of partially drained tests which prove that partial drainage might have an effect on the measured strength, volumetric strains, and pore water pressures. The objective of tests reported in this chapter is to conduct partially drained tests with volumetric strain and pore pressure measurements in an effort to understand the real field behavior.

The automated triaxial test setup "TruePath" by Geotac was used to conduct PD tests on reinforced clay specimens saturated with a back pressure of 310 kPa. The samples were then isotropically consolidated under confining pressure of 100, 150 and 200 kPa and sheared drained at different rates of strain ranging from 3.5%/hr to 80%/hr, while measuring volume change through drain lines connected to the porous stones at the top of the sample and measuring pore water pressures through the drain valve at the bottom of sample. In other words, the sample was allowed to drain only from the top while shearing it under fast strain rates, which allowed for the simulation of a partially

drained setup in which pore water pressures were generated and volume changes occur. The measured volume change reflects a global change in the composite sample and does not provide information on local changes in the water content in the sand column and the surrounding clay. Throughout the tests, the total confining pressure was kept constant as the vertical stress was increased in the compression.

The test results of consolidated partially drained tests conducted on 12 Kaolin specimens are presented in this chapter which includes the results of unreinforced specimens, and specimens reinforced with ordinary 3-cm diameter fully penetrating sand columns. The results include a description of the modes of failure that characterize the behavior of the different test specimens and a detailed analysis of the parameters which are known to affect the load response of clay specimens that are reinforced with sand columns. These parameters include the confining pressure, volume change, and generation of excess pore water pressure.

Furthermore, the test results were analyzed to establish a relationship between the degree of consolidation that was observed during any given partially drained test and the measured load-carrying capacity. The degree of consolidation was established from the recommendations provided in Henkel and Gibson (1954) who studied the influence of duration of test at constant rate of strain on the measured shear strength. This will be further explained in the following sections of this chapter. In addition to Henkel and Gibson (1954), the results published by Andreou et al (2008) and Juran and Guermayzi (1988) which also deal with partially drained setups will be compared with the results of this study.

8.2. Test Results

The test results are presented in the form of deviatoric stress versus axial strain curves, volumetric strain versus axial strain curves, and pore water pressure versus axial strain curves. Failure was defined at an axial strain of 12%, unless a peak was observed at smaller strain levels.

8.2.1. Kaolin Specimens Reinforced with Sand Columns

Results obtained from the triaxial tests conducted on kaolin specimens reinforced with fully penetrating 3-cm sand columns are presented in Table 8.1 and in Figures. 8.1 to 8.3, which include pictures of the modes of failure and graphs showing the variation of the deviatoric stress, volumetric strain, and pore water pressure with axial strain. The results were analyzed to investigate the effect of drainage conditions on the shear strength and the degree of volumetric strain in relation with the excess pore water pressures generated.

8.2.1.1. Modes of Failure

For samples sheared at the relatively small strain rate of 3.5%/hr, the mode of failure was characterized by bulging of the clay specimen, which was more concentrated at the top of the specimen. This bulging is identical to the bulging observed for fully drained conditions.

For samples sheared at a strain rate of 40%/hr, the mode of failure was also characterized by bulging of the specimen, which was concentrated towards the middle of the specimen as shown in Figure 8.1 (100kPa and 200kPa from left to right

respectively). To investigate the mode of failure of sand columns, the same test specimens were split along their vertical axes to expose the columns and the surrounding clay. The sand columns showed slight bulging along the same location as the bulging of the clay. This is shown in Figure 8.1, where for the 100kPa case, the column bulged at the same degree of the clay, whereas for the 200kPa case, a shear plane passed through the column and shifted it laterally as it went further down the height of the specimen. This was also observed for the undrained case at 200kPa confining pressure (see chapter 6).

Samples sheared at 80%/hr strain rate had similar if not identical modes of failure at 100kPa and 200kPa confining pressure as the modes of failures observed for the 40%/hr strain rate. This is shown in Figure 8.2, where for the 100kPa case both the specimen and the sand column suffered bulging around the middle of the sample, whereas for the 200kPa case a shear plane passed through the column and shifted it laterally.

These modes of failure seem to indicate that at low strain rates, the behavior of the partially drained sample will resemble the behavior of the fully drained sample, and that for high strain rates and especially at high confining pressure, the behavior of the partially drained sample will resemble the behavior of the undrained sample.

Table 8.1. Test Results for Partially Drained Kaolin specimens inserted with frozen sand columns

Test	Confining pressure σ_3,	Diameter of sand column (cm)	Rate of loading (%strain	Drained/Partially drained/ Undrained	Area replacement ratio: A_c/A_s (%)	Height of sand column (cm)	Column height penetration ratio, (H_c/H_s)	Deviatoric stress @ failure (kPa)	Volume Strain (%)	Excess pore water pressure (kPa)	Reduction in Volumetric Strain (%)	Reduction in Excess Pore Pressure (%)
1	100	0	0.25	D	0	0	-	124.8	-4.82	-	-	-
2		0	1	U	0	0	-	64.6	-	61.3	-	-
3		3	0.25	D	17.8	14.2	1	169.7	-2.33	-	51.66	-
4		3	1	U	17.8	14.2	1	115.5	-	42.7	-	30.34
5		3	3.5	PD	17.8	14.2	1	167.4	-2.25	1.64	53.38	97.32
6		3	40	PD	17.8	14.2	1	159.4	-1.72	14.07	64.28	77.05
7		3	80	PD	17.8	14.2	1	149.6	-1.026	34.97	78.72	42.95
8		3	80	U	17.8	14.2	1	104.7		45.55		25.69
9	150	0	0.25	D	0	0	-	179.36	-5.1	-	-	-
10		0	1	U	0	0	-	84.2	-	95.1	-	-
11		3	0.25	D	17.8	14.2	1	216.4	-3.45	-	30.5	-
12		3	1	U	17.8	14.2	1	188.3	-	65.2	-	31.44
13		3	3.5	PD	17.8	14.2	1	209.7	-3.08	-0.86	39.65	100.9
14		3	40	PD	17.8	14.2	1	199.5	-2.49	18.39	51.18	80.66
15		3	80	PD	17.8	14.2	1	187.2	-1.65	40.1	67.65	57.84
16		3	80	U	17.8	14.2	1	137.6	-	77.2	-	18.82
17	200	0	0.25	D	0	0	-	233	-5.36	-	-	-
18		0	1	U	0	0	-	110.2	-	130.9	-	-
19		3	0.25	D	17.8	14.2	1	312	-3.23	-	39.8	-
20		3	1	U	17.8	14.2	1	185	-	87.4	-	33.23
21		3	3.5	PD	17.8	14.2	1	309.5	-3.1	0.24	43.23	99.82
22		3	40	PD	17.8	14.2	1	291.3	-2.11	5.7	60.62	96.64
23		3	80	PD	17.8	14.2	1	256.3	-1.4	40.49	73.94	69.07
24		3	80	U	17.8	14.2	1	181.8	-	97	-	25.9

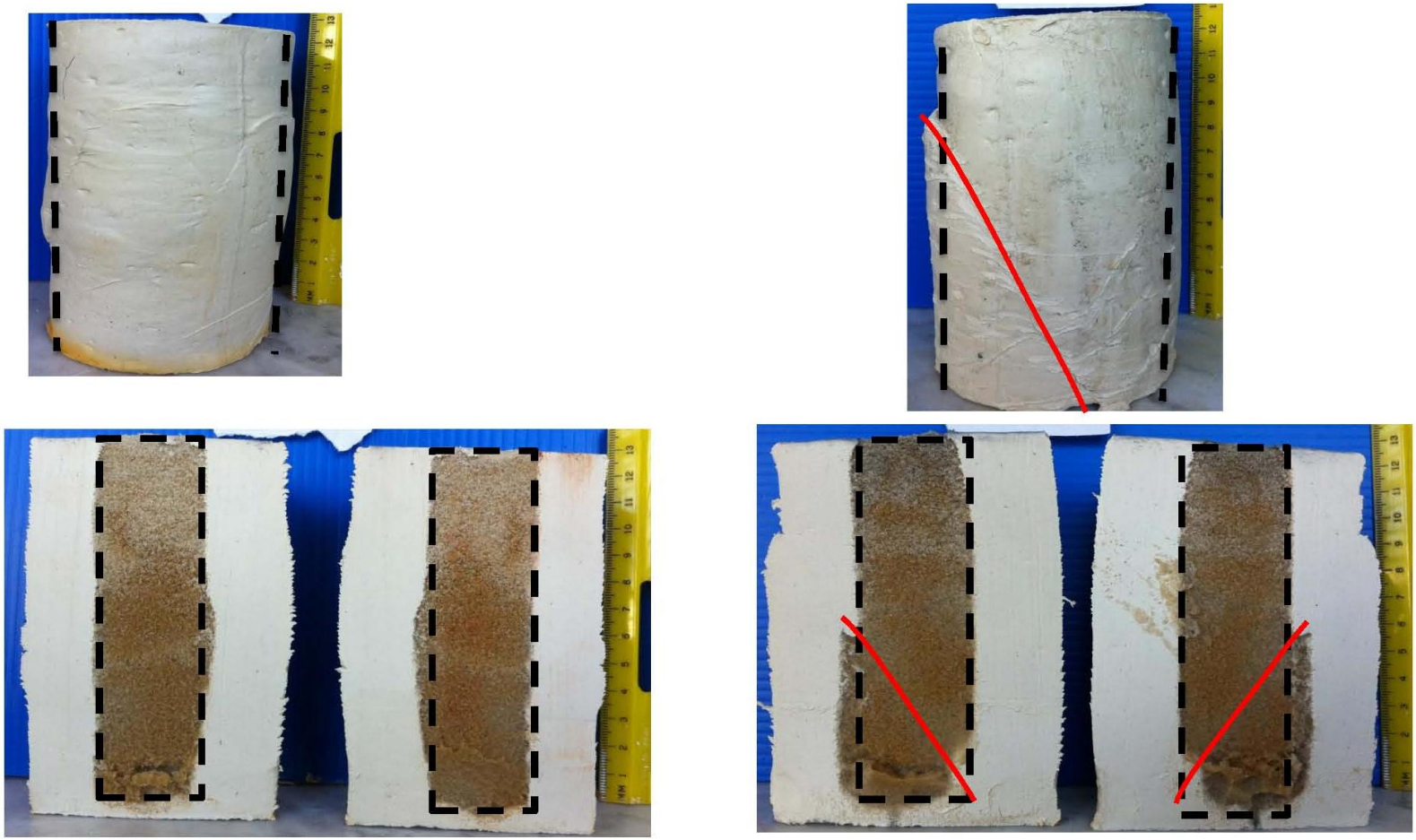

Figure 8.1. Example of external and internal modes of failure of test specimens, (H_c/H_s = 1, strain rate of 40%/hr)

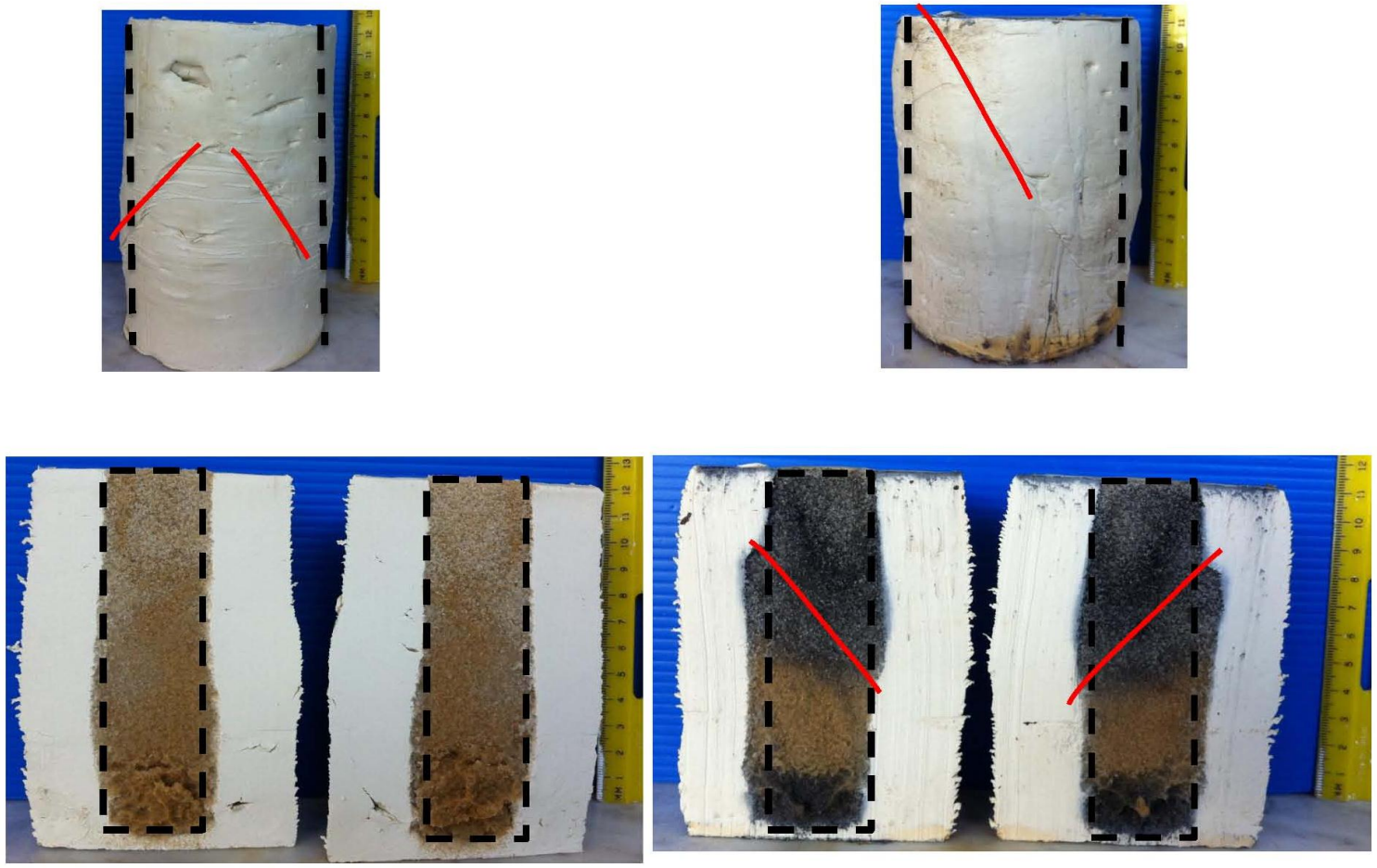

Figure 8.2. Example of external and internal modes of failure of test specimens, (H_c/H_s = 1, strain rate of 80%/hr)

8.2.1.2. Stress-Strain Behavior

The variation of the deviatoric stress, pore water pressure, and volumetric strain with the axial strain is presented in Figure. 8.3 at 100,150 and 200kPa confining pressure. The stress-strain curves exhibited consistent increases in deviatoric stresses with strains as the samples were sheared towards critical state conditions. To define failure, the deviatoric stresses will be considered to have leveled out at an axial strain of 12%, which is the maximum strain that was measured in the tests. The measured volumetric strains (partially drained and drained tests) were all contractive. The pore water pressures (partially drained and undrained tests) increased as the deviatoric stresses reached their maximum values. After reaching a maximum value, the pore pressures decreased for all tests except for the control clay test. This decrease in excess pore water pressures during shear can be attributed to the higher stiffness and to the possible dilatational tendency of the sand columns. For all confining pressures, the negative volumetric strains were reduced significantly when 3cm diameter sand columns (A_c/A_s=17.8%) were inserted in the soft clay (see Table 8.1). As expected, this reduction in contractive behavior was more significant for tests with faster shearing rates. This higher reduction in contractive behavior for the specimens sheared at a fast strain rate is complemented with higher pore pressures which did not have enough time to dissipate and induce volumetric strains.

The deviatoric stress versus axial strain curves show that all the partially drained specimens lay between two boundaries, the higher boundary being the fully drained 3cm test and the lower boundary being the undrained 3cm test. These results are consistent with the findings of Andreou et al (2008). Furthermore, as the shearing rate decreases, the partially drained curves become closer to the fully drained curve. Even

though the 3.5%/hr strain rate test had favorable conditions to develop positive pore pressures (14 times faster than normal drained tests) which would decrease its strength, it still yielded an almost identical result to the fully drained tests at all confining pressure. This can be explained by the radial drainage that was allowed from the clay to the sand column and up through the upper porous stone in the partially drained tests.

The results on Figure 8.3 indicate that even at the highest strain rate of 80% per hour, the stress-strain curves and the volumetric strain show that an appreciable degree of drainage has occurred in the tested specimens, irrespective of the confining pressure. These results could be surprising given the very fast rate of shearing involved. However, the presence of the sand columns which acted as drainage boundaries and the relatively high permeability of the kaolinite clay used in this study (more permeable than typical natural clays) may explain the observed behavior. The positive volumetric strains that were observed in the fast tests could explain the observed improvement exhibited in the stress-strain response of these partially drained specimens in comparison to the stress-strain responses their equivalent undrained counterparts.

In an effort to investigate whether there was any rate effect that could have affected the measured stress strain response of the partially drained tests due to the relatively fast shear rates (80%/hr), undrained tests were done at 100, 150, and 200kPa confining pressure at a strain rate of 80% per hour. The results of these tests were compared with the results of the undrained tests that were sheared at 1%/hr strain. As shown in Figure 8.3, the effect of strain rate is almost negligible, since an 80 times faster test only yielded slightly lower values of deviatoric stress (see Table 8.1). The same applies for the pore pressures which were almost identical for both strain rates, with the pore pressures corresponding to 80%/hr being slightly higher.

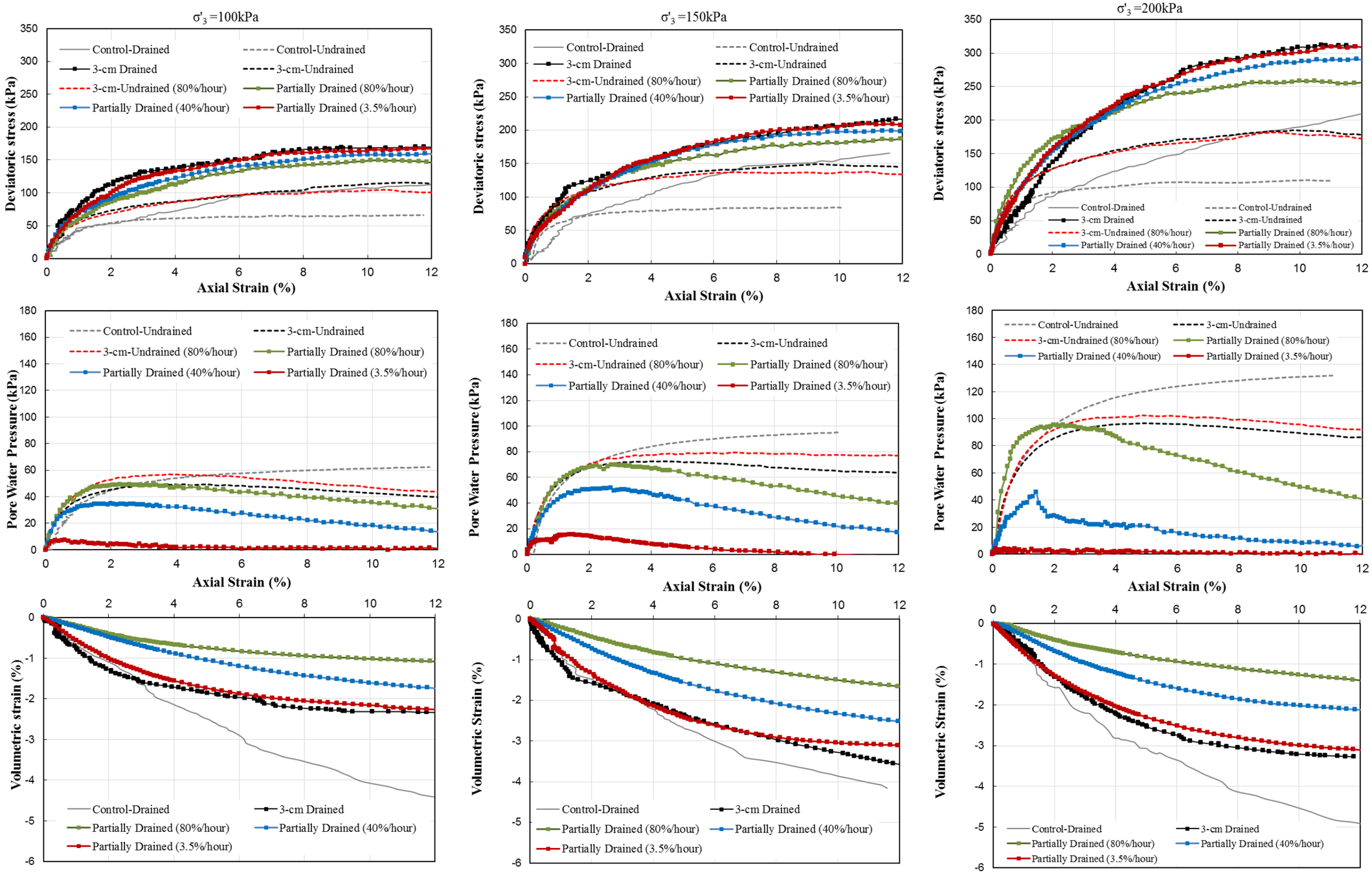

Figure 8.3. Deviatoric stress, pore water pressure, and volumetric strain versus axial strain for reinforced specimens at confining pressures of 100 kPa, 150 kPa, and 200kPa

8.2.1.3. Effect of Strain Rate and Drainage Conditions on Volume Change and Pore Pressure

Measurements of the volumetric strains at failure were made for partially drained and drained tests and reported in Table 8.1. Figure 8.4 shows the percent reduction in volumetric strains versus strain rate for tests with an area replacement ratio of 17.8%. Similarly, pore pressures were measured at the bottom of the samples for partially drained and undrained tests and reported in Table 8.1. Figure 8.5 shows the percent reduction in excess pore water pressure versus strain rate for tests with an area replacement ratio of 17.8%. Figure 8.6 illustrates the superposition of results of percent reduction in volumetric stress at failure and percent reduction in excess pore water pressure.

The percent reduction in volumetric strains for partially drained tests ranged from about 53 to 79%, with specimens sheared at slower rates having the lower improvements. This is expected, since the faster the shearing rate, the less time the specimens have to drain. On the other hand, the percent reduction in excess pore pressure ranged from 43 to 97%, with specimens sheared at slower rates having the highest improvements. This is also expected due to the fact the slower the shear rate, the more time the specimens have to dissipate the excess pore water pressure. It is important to note that the 0.25%/hr strain rate test shown in Figure 8.4 is a fully drained test, and the 1%/hr strain rate test shown in Figure 8.5 is an undrained test. As a result, comparison between the two is not viable. Figure 8.6 shows how the results complement each other in terms of volumetric strains and pore pressures for the partially drained tests. The results clearly show that as the strain rate decreases, the reduction in excess pore pressure increases and the reduction in volumetric strains

decreases. These findings are consistently recurrent for the 100, 150, and 200kPa confining pressures.

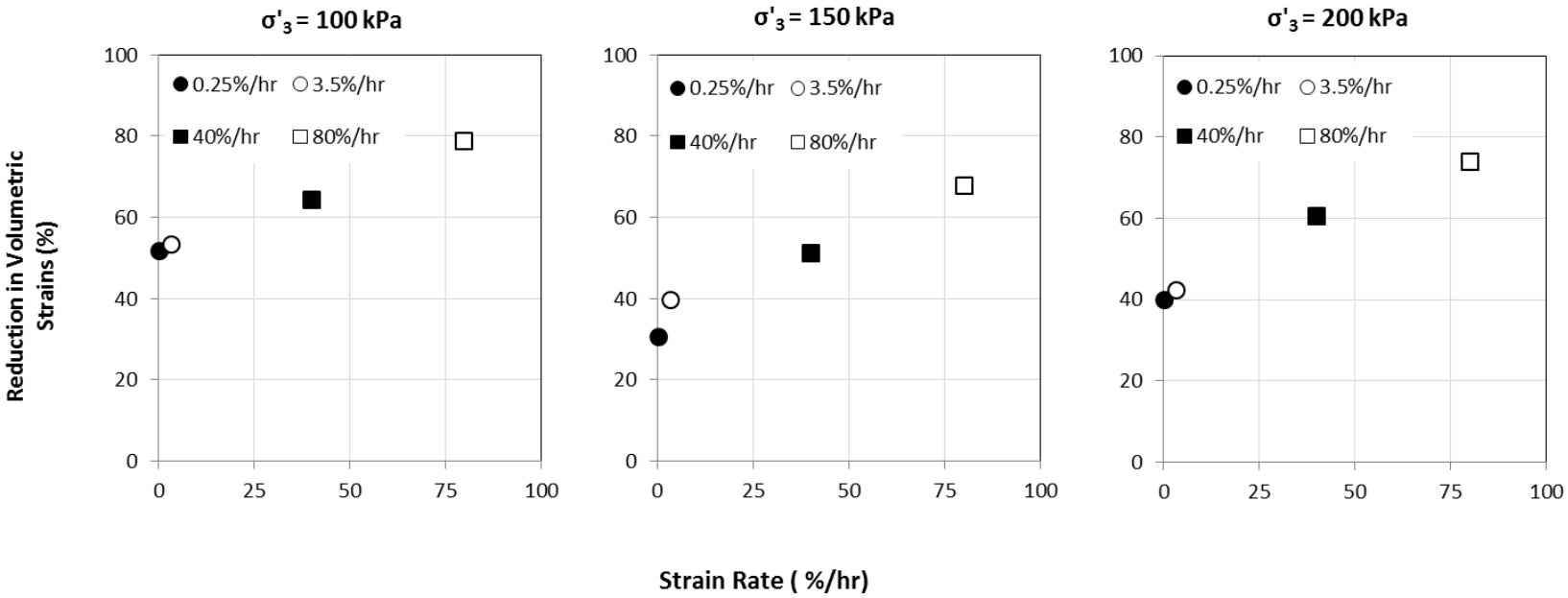

Figure 8.4. Relationship between reduction in volumetric strains at failure and strain rate (Ac/As= 17.8%)

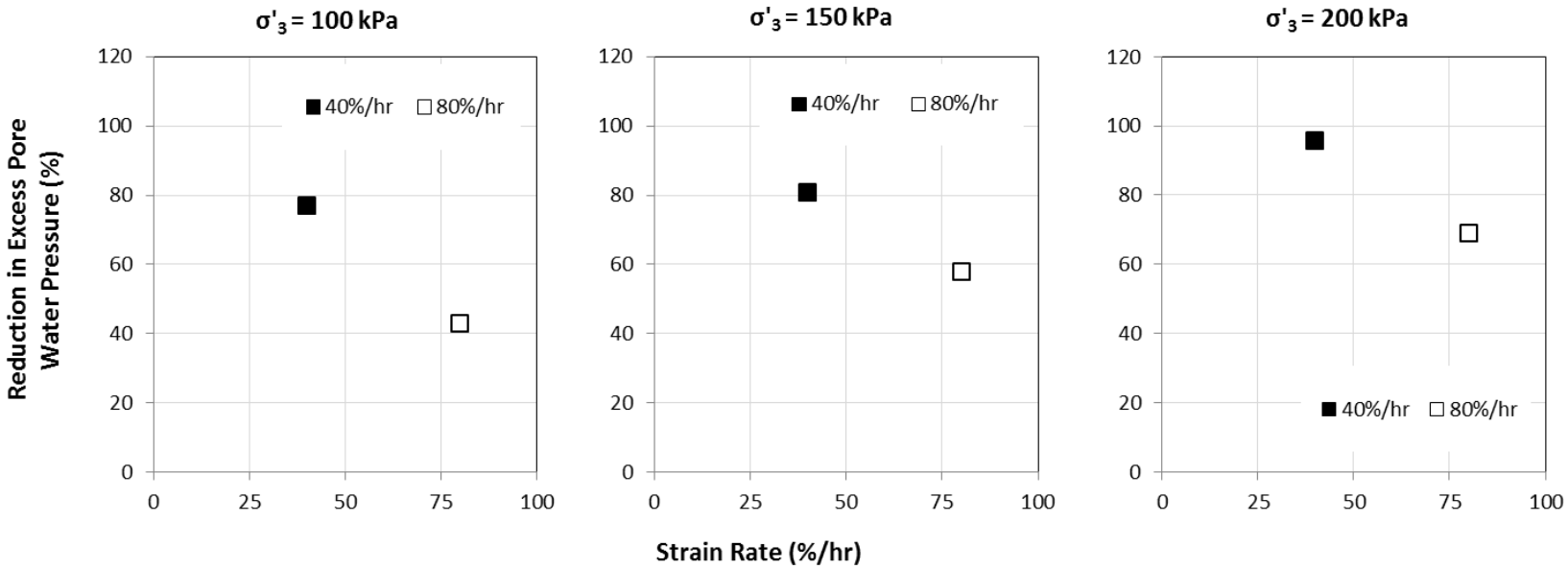

Figure 8.5. Relationship between reduction in excess pore water pressure and strain rate (Ac/As= 17.8%)

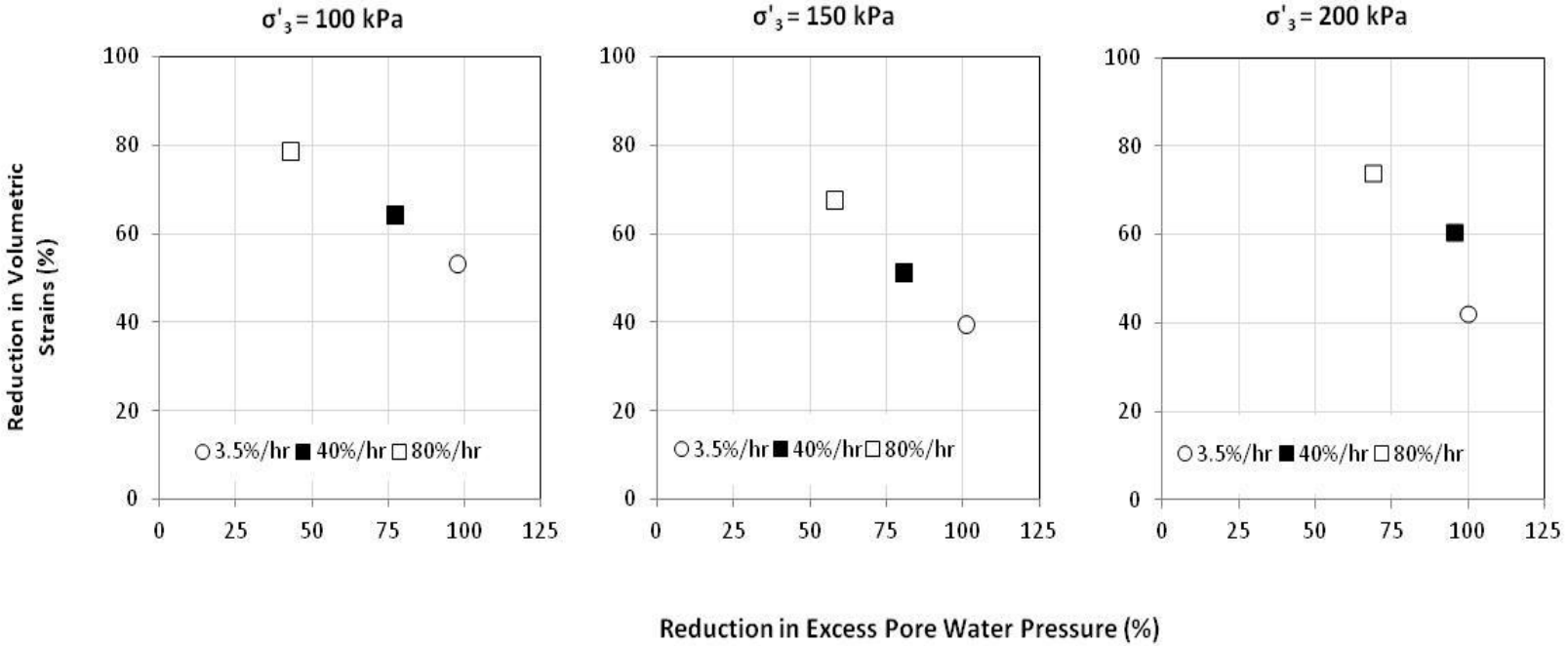

Figure 8.6. Relationship between reduction in volumetric strain and reduction in excess pore water pressure (Ac/As= 17.8%)

8.2.1.4. Effect of Partial Drainage on the Measured Strength

In order to investigate the effect of partial drainage on the measured strength of the specimens, several parameters must be defined and analyzed. These parameters are presented in Table 8.2 which will serve as reference for all the calculated values. Previously, failure has been defined at 12% axial strain unless a peak was observed at lower strains. Therefore, the time to failure will be derived as the duration of the tests until a peak stress is reached, or at 12% strain. Furthermore, in order to normalize this time to failure, it will be normalized with respect to the time needed for 50% consolidation to occur (t_{50}) during the consolidation phase for a given sample. This ratio of $t_{failure}$ to t_{50} is a term that is typically used to determine the shearing rates required for drained conditions to occur in a typical consolidated drained tests (generally $t_{failure}/t_{50}$ is taken at least as 80) and for pore pressures to equalize in an undrained test (generally $t_{failure}/t_{50}$ is taken at 10).

In previous sections, it was observed that as the shearing rate decreases, the behavior of partially drained specimens becomes closer to that of fully drained specimens. This is linked to the degree of consolidation (U_f) that the sample undergoes at failure in a partially drained test, and which is expected to increase as the shearing rate decreases or as $t_{failure}/t_{50}$ increases. The process of calculating the degree of consolidation after a certain time (dictated by the shearing rate) must account for the radial drainage occurring through the central sand column. Henkel and Gibson (1954) in their paper entitled “Influence of Duration of Tests at Constant Rate of Strain on Measured Drained Strength”, proposed the following relationship for calculating the degree of consolidation:

$$\overline{U}_f = 1 - \frac{H^2}{\eta c_t t_f} \quad (8.1)$$

Where H is half the height of the sample, η is a numerical factor depending on the extent and location of drainage surfaces (32 for radial drainage), c_t is the coefficient of consolidation, and finally t_f is the time to failure. The coefficient c_t in equation 8.1 is the radial coefficient of consolidation which could be estimated from the horizontal coefficient of consolidation as indicated in Equation 8.2. The horizontal coefficient of consolidation that is back calculated from the time required for 100% consolidation to occur during the consolidation phase of the test assuming radial drainage through the central sand columns. The horizontal coefficient of consolidation is affected by the radius of the sand column (r_w), the radius of the specimen (r_e) and the ratio between the two.

$$c_h = \frac{d_e^2 \times F(n) \times \ln(\frac{1}{1-U_h})}{8 \times t_{100}} \quad (8.2)$$

Where d_e is the diameter of the specimen, F(n) a factor depending on n , U_h is the degree of consolidation (assumed to be equal 95% since vertical consolidation is neglected), and t_{100} is the time to achieve 100% consolidation.

$$n = \frac{r_e}{r_w} \quad (8.3)$$

$$F(n) = \left[\left(\frac{n^2}{n^2-1}\right) \times \ln(n)\right] - \frac{3n^2-1}{4n^2} \quad (8.4)$$

The use of Equations 8.1 to 8.4 allows for estimating the degree of consolidation that a partially drained sample undergoes at the time at which failure occurs.

Table 8.2. Test Results for Partially Drained Kaolin specimens and analysis of drainage conditions

Test	Confining pressure σ_3 (kPa)	Diameter of sand column (cm)	Rate of loading (%strain/hr)	Drained/ Partially Drained/ Undrained	Area replacement ratio: A_c/A_s (%)	Column height diameter ratio, (H_c/D_c)	t_{50} from Consolidation (min)	t_{100} from Consolidation (min)	n=re/rw (cm2/min)	F(n)	C_h (cm2/min)	Uf(%) shear	Time to Peak Failure (min)	Time to 12% strain (min)	Time to 12%Failure/t50	Time to peak%/ t50	Volumetric Strain @ failure	Deviatoric Stress @ failure	(Dev. Stress - Undrained) / (Drained-Undrained)	(Volumetric Strain PD) / (Volumetric Strain D)
1	100	3	0.25	D	17.8	3.55	3.5	18	2.4	0.3	0.36	99.8	2880	2880	823	823	2	170	1	1
2		3	3.5	PD	17.8	3.55	3.5	18	2.4	0.3	0.36	97.9	205.71	205.71	58.78	58.78	2.26	167.39	1.00	0.97
3		3	40	PD	17.8	3.55	3.5	18	2.4	0.3	0.36	75.3	17.70	18.00	5.14	5.06	1.71	159.40	0.80	0.73
4		3	80	PD	17.8	3.55	3.5	18	2.4	0.3	0.36	45.5	8.03	9.00	2.57	2.29	1.06	149.55	0.70	0.45
5		3	80	U	17.8	3.55	3.5	18	2.4	0.3	0.36	0.0	7.94	9.00	2.57	2.27	0.00	104.70	0.00	0.00
6		3	1%	U	17.8	3.55	-	-	-	-	-	-	-	-	-	-	0.0	115.5	-	-
7	150	3	0.25	D	17.8	3.55	4	18.5	2.4	0.3	0.35	99.8	2784	2880	720	696	4	216	1	1
8		3	3.5	PD	17.8	3.55	4	18.5	2.4	0.3	0.35	97.6	187	205.71	51.43	46.71	3.09	209.69	0.90	0.87
9		3	40	PD	17.8	3.55	3.9	18.5	2.4	0.3	0.35	74.3	17.475	18.00	4.62	4.48	2.50	199.50	0.80	0.70
10		3	80	PD	17.8	3.55	4.5	19	2.4	0.3	0.34	48.7	9	9.00	2.00	2.00	1.66	187.20	0.60	0.46
11			1%	U	17.8	3.55	-	-	-	-	-	0.0	-	-	-	-	0	149.36	0.00	0.00
12		3	80	U	17.8	3.55	3.8	16.5	2.4	0.3	0.39	-	8.0	9.00	2.12	2.12	0.00	137.58	-	-
13	200	3	0.25	D	17.8	3.55	5	20	2.4	0.3	0.32	99.8	2784	2880	576	557	3	312	1	1
14		3	3.5	PD	17.8	3.55	5	20	2.4	0.3	0.32	97.6	206	205.71	41.14	41.20	3.10	309.50	0.98	0.96
15		3	40	PD	17.8	3.55	5	20	2.4	0.3	0.32	72.5	17.7	18.00	3.60	3.54	2.11	291.30	0.84	0.66
16		3	80	PD	17.8	3.55	5	20	2.4	0.3	0.32	46.0	9	9.00	1.80	1.80	1.26	256.34	0.57	0.39
17		3	80	U	17.8	3.55	5	20	2.4	0.3	0.32	0.0	6.9	9.00	1.80	1.39	0.00	181.80	0.00	0.00
18		3	80	U	17.8	3.55	-	-	-	-	-	-	-	-	-	-	0.0	185.0	-	-

The measured deviatoric stresses at failure are reported in Table 8.2, and plotted against $t_{failure}/t_{50}$ in Figure 8.7. Results for a given effective confining pressure indicate that as $t_{failure}$ increases (as the strain rate decreases), the measured deviatoric stresses increase until they reach a plateau at a value of $t_{failure}$ equal to about $50t_{50}$, irrespective of the confining pressure used.

Since the analysis in the previous sections showed that the stress-strain curves for partially drained tests are bracketed by the curves of the fully drained and undrained tests (Figure 8.3), a normalized strength improvement index is defined as the ratio of $(\sigma_{d,\,PD} - \sigma_{d,U})$ to $(\sigma_{d,\,PD} - \sigma_{d,D})$, where $\sigma_{d,\,PD}$ is the deviatoric stress measured for the partially drained tests, $\sigma_{d,U}$ is the deviatoric stress of the undrained tests (assumed to be a lower-bound strength for the composite) and $\sigma_{d,D}$ is the deviatoric stress of the drained tests (assumed to be an upper-bound strength for the composite). This strength improvement index is analogous to the liquidity index for soils, in the sense that it provides a relative measure of the magnitude of strength that could be mobilized in a partially drained test in relation to the minimum and maximum strengths that could be obtained assuming undrained and drained conditions, respectively.

The strength improvement index $(\sigma_{d,\,PD} - \sigma_{d,U}) / (\sigma_{d,\,PD} - \sigma_{d,D})$ is plotted on Figure 8.8 against $t_{failure}/t_{50}$ for all test. The results on Figure 8.8 indicate that the normalized stress improvement index that was calculated for all the partially drained tests is strongly correlated to the ratio $t_{failure}/t_{50}$. The relationship indicates a strength improvement index of about 60% at a relatively low $t_{failure}/t_{50}$ of about 1.0, increasing to about 80% for $t_{failure}/t_{50}$ of about 5.0. After a $t_{failure}/t_{50}$ of about 5.0, the strength index levels out and approaches a value of 100% (indicating mobilization of the fully drained

strength) at $t_{failure}/t_{50}$ of about 40 to 60. It should be noted that the relationship between the strength improvement index and $t_{failure}/t_{50}$ does not depend on the effective confining pressure used in the different tests.

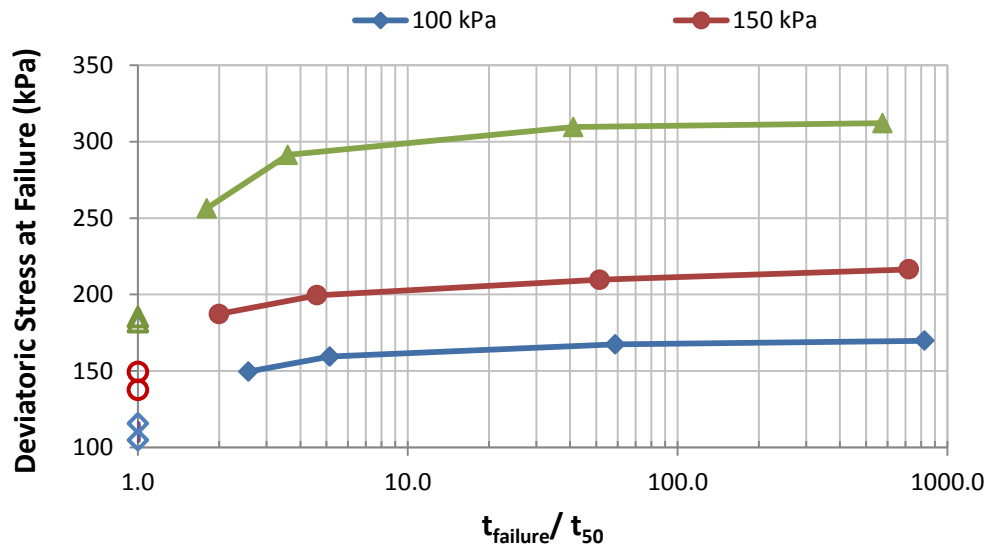

Figure 8.7. Deviatoric stress versus $t_{failure}/t_{50}$

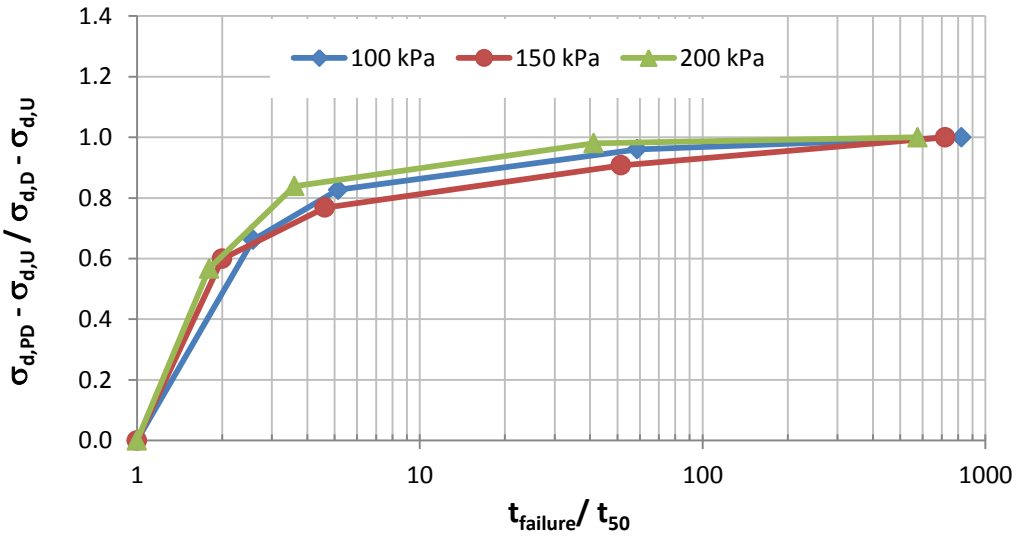

Figure 8.8. Strength Improvement Index $(\sigma_{d,\,PD} - \sigma_{d,U})/(\sigma_{d,\,D} - \sigma_{d,U})$ versus $t_{failure}/t_{50}$

8.2.1.5. Relation between the theoretical degree of consolidation (Henkel & Gibson, 1954) and the mobilization of partially drained strength

The relationship proposed by Henkel and Gibson (1954) predicts the degree of consolidation that occurs during shearing based on the time of failure, the height of the specimen, and the coefficient of consolidation (Equation 8.1). This equation was used to predict the degree of consolidation for all the partially drained tests conducted in the study (Table 8.1). From a theoretical perspective, it is expected that the degree of consolidation as calculated from the model proposed by Henkel and Gibson (1954) could provide a stronger indication of the degree of partial drainage in comparison to the ratio of $t_{failure}/t_{50.}$ To tests this hypothesis, the strength improvement index for the partially drained tests was plotted versus the computed degree of consolidation. The results are shown on Figure 8.9 and confirm the above hypothesis. The curves on Figure 8.9 indicate that for an average degree of consolidation at failure of 50% (PD tests at strain rate of 80% per hour), the strength improvement index was about 60%, indicating that the partially drained strength was more than half the way between the undrained strength and the drained strength. For an average degree of consolidation at failure of about 75% (PD tests at strain rate of 40% per hour), the strength improvement index was about 80%. The slowest partially drained tests (3.5% per hour) resulted in a theoretical degree of consolidation of about 98%. The strength improvement index for these cases was about 95% indicating more or less complete mobilization of the fully drained strength of the composite.

Another measure of the degree of consolidation that occurred during the partially drained tests is the volumetric strain that was measured during the partially drained tests. The ratio of the volumetric strain for the partially drained test to the

volumetric strain measured for the fully drained sample provides a relative indication of the amount of water that was drained out from the sample during the partially drained tests compared to the fully drained tests. This ratio is indicative of the degree of consolidation that was achieved in the partially drained tests. The strength of this ratio is that it could be computed from the results of the triaxial test and is not calculated from a theoretical model.

The variation of the strength improvement index for the partially drained tests with the ratio of the volumetric strain measured in PD tests to the volumetric strain measured in the fully drained tests is plotted on Figure 8.10. A comparison between Figs. 8.9 and 8.10 shows a remarkable similarity between the two curves, indicating that the strength improvement index could be correlated to the ratio of the volumetric strains. This finding is important because it indicates that simple measurements of volumetric strains from a triaxial test could provide valuable feedback on the degree of consolidation that has occurred during shear and could be used as a basis for predicting the relative mobilization of shear strength for the partially drained tests relative to the drained and undrained strengths through the strength improvement index in Figure 8.10.

As a final confirmation of the above findings, the degree of consolidation as predicted by the model of Henkel and Gibson (1954) was plotted versus the ratio of the volumetric strain of the partially drained test to the volumetric strain of the fully drained test as shown in Figure 8.11. The results on Figure 8.11 show an almost perfectly linear one to one relationship between the degree of consolidation and the volumetric improvement ratio. This provides explanation for the close resemblance between Figures 8.9 and 8.10.

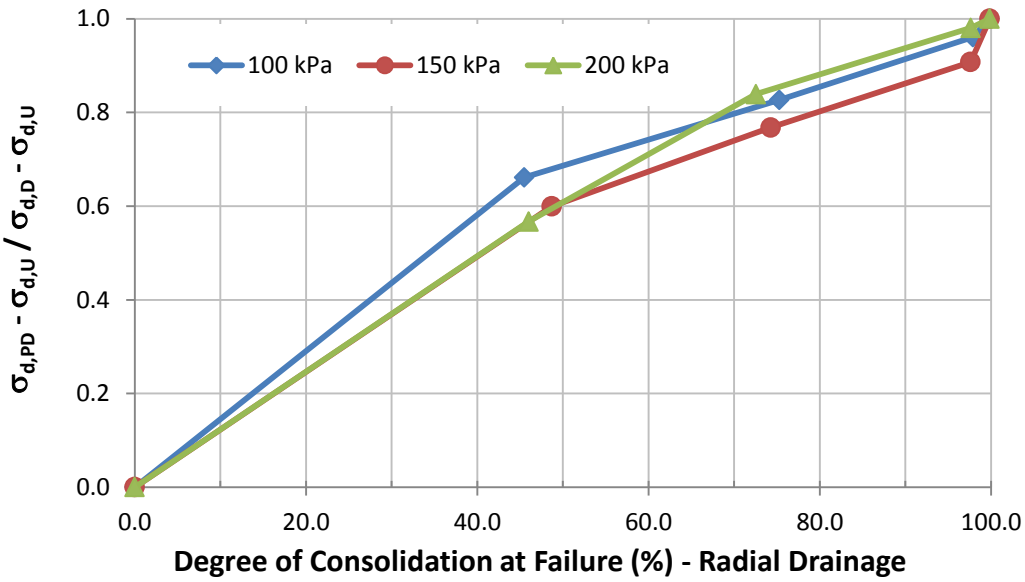

Figure 8.9. Strength improvement index versus degree of consolidation at failure

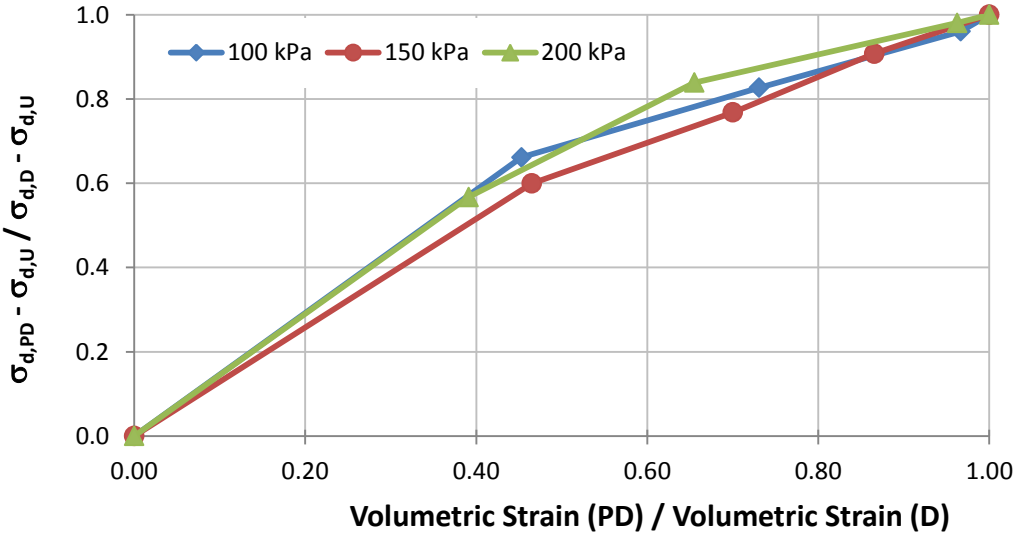

Figure 8.10. Stress improvement ratio versus volumetric improvement ratio

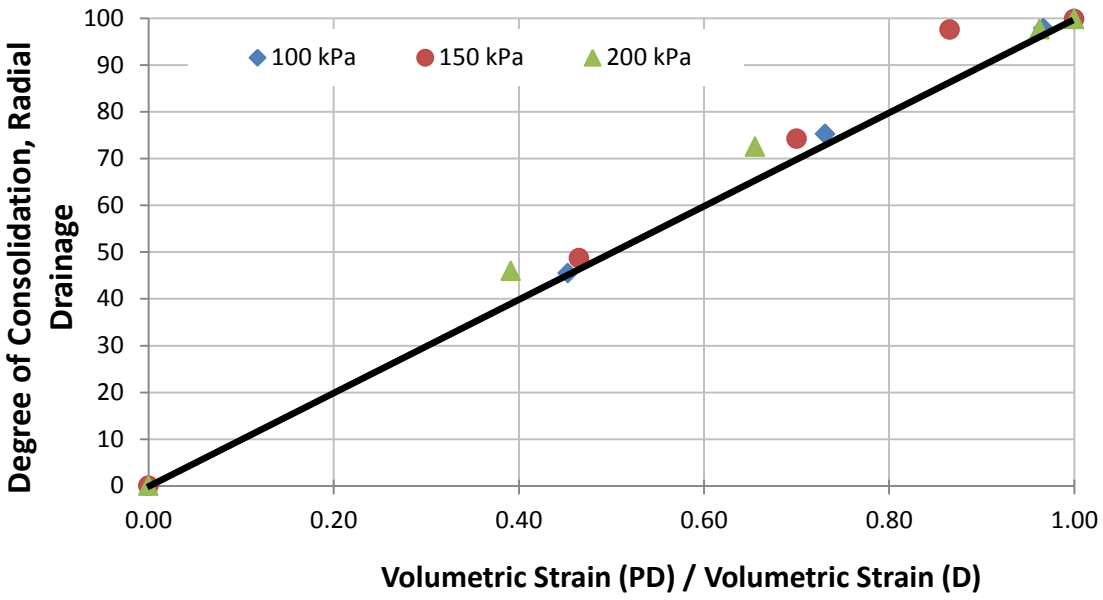

Figure 8.11. Degree of consolidation versus the volumetric improvement ratio.

8.3. Summary of Main Findings

Based on the results of 13 consolidated partially drained triaxial tests that were conducted in this experimental study, the following conclusions can be drawn regarding the effect of drainage conditions and shearing rates on the drained load response of soft clay, generation of excess pore water pressure, induced volumetric strains, modes of failure, and the validity of the proposed formula by Henkel and Gibson (1954).

1. The modes of failure indicate that at low strain rates (3.5%/hr), the behavior of the partially drained sample will resemble the behavior of the fully drained sample which consists of bulging of the specimen, and that for high strain rates (40%/hr and 80%/hr) especially at high confining pressure, the behavior of the partially drained sample will resemble the behavior of the undrained sample, which also consists of bulging, however with a shear plane passing through the sand column and shifting it laterally.

2. For all confining pressures, the negative volumetric strains were reduced significantly when 3cm diameter sand columns (Ac/As=17.8%) were inserted in the soft clay. As expected, this reduction in contractive behavior was more significant for tests with faster shearing rates. This higher reduction in contractive behavior for the specimens sheared at a fast strain rate is complemented with higher pore pressures which did not have enough time to dissipate.
3. The deviatoric stress versus axial strain curves show that all the partially drained specimens lie between two boundaries, the higher boundary being the fully drained test and the lower boundary being the undrained test. This is consistent with the findings of Andreou et al (2008). Furthermore, as the shearing rate decreases, the partially drained curves become closer to the fully drained curve.
4. Results of partially drained samples showed that as the strain rate decreases, the reduction in excess pore pressure increases and the reduction in volumetric strains decreases. These findings are consistently recurrent for the 100, 150, and 200kPa confining pressures.
5. As the $t_{failure}$ increases, the measured deviatoric stress increases until reaching a constant value at $t_{failure}$ equal to about $50t_{50}$ for all three confining pressures 100, 150, and 200kPa. The biggest jump in improvements in the deviatoric stresses happens before $5t_{50}$. After $5t_{50,}$ the partially drained tests mobilize 80% of the available range of improvement (undrained tests being the lower bound of the range and drained tests being the upper bound of the range), while after $50t_{50}$ almost all the range is mobilized

6. A strength improvement index was defined to represent a relative measure of the strength mobilized in the partially drained tests compared to the undrained and drained strengths. Results show that both the degree of consolidation as predicted by the model by Henkel and Gibson (1954) and the volumetric improvement ratio as computed from the volumetric strain measurements of the partially drained and drained triaxial test could be utilized to predict the strength improvement index for partially drained tests.

CHAPTER 9

CONCLUSIONS, RECOMMENDATIONS, AND FURTHER RESEARCH

9.1. Introduction

This chapter includes the main concluding remarks and observations resulting from the drained, undrained, and partially drained triaxial testing programs conducted on 37 Kaolin specimens that were prepared from slurry, consolidated in a prefabricated 1-dimensional consolidometer, and reinforced with either ordinary or encased sand columns with different column penetration ratios (H_c/H_s= 0.75, and 1) and different area replacement ratios (A_c/A_s=17.8% and 31.7%). The data collected from the CD and CU tests highlighted the effect of sand columns on the stiffness, drained shear strength, and the volumetric strain for the reinforced clay, while the PD tests highlighted the effect of shearing rate and drainage conditions on the volumetric strain and pore pressure generation. An effort was also made to compare the load response of the drained and undrained tests conducted in this study with the response observed by Najjar et al. (2010) and Maalouf (2012) Recommendations and further research works are also discussed in this chapter.

9.2. Conclusions

Based on the results of 37 consolidated drained, undrained, and partially drained triaxial tests that were conducted in this experimental research study, the following conclusions can be drawn with regards to the reliability of the testing

procedure used and the effect of drainage conditions on the load response of soft clay, volumetric strains during drained loading, stiffness of reinforced clay, and effective shear strength parameters:

9.2.1. Drained Conditions

1. The specimen preparation method used in this study resulted in repeatable test specimens with acceptable variations in density for the clay specimens and the sand columns. The average and standard deviation of the bulk density of the clay were 16.13 kN/m^3 and 0.08 kN/m^3, respectively corresponding to an average void ratio of 1.34 and a standard deviation of 0.03. The average bulk density for the sand columns was found to be 19.4 kN/m^3 with a standard deviation of 0.12 kN/m^3. The relatively small variations observed in the densities of the kaolin clay and the sand columns indicated that friction in the 1-D consolidometers was minimal and that the specimen preparation procedure and the column preparation method were generally repeatable.

2. Reinforcing normally consolidated soft kaolin specimens with sand columns at an area replacement ratio of 7.9% resulted in reductions in $(Esec)_{1\%}$, with the only exceptions being tests conducted with encased columns at a confining pressure of 200 kPa. For tests conducted using area replacement ratios of 17.8%, increases in $(Esec)_{1\%}$ were observed for fully penetrating columns at all confining pressures and for partially penetrating columns at a confining pressure of 200 kPa. For tests conducted using area replacement ratios of 31.7%, increases in $(Esec)_{1\%}$ were observed for all cases and at all confining pressures. Interestingly, in the case of the 4-cm fully penetrating ordinary column at

100kPa the $(Esec)_{1\%}$ was found to be to be lower than for the 17.8% area replacement ratio, which contradicts the trend, but further proves that the installation effects can significantly affect the results particularly at low confining pressures.

3. The inclusion of 3-cm and 4-cm sand columns in the clay reduced appreciably the contractive volumetric strains of the clay specimens, with the reduction being more significant for tests involving fully penetrating sand columns, which are expected to be more dilative compared to partially penetrating columns. No significant reductions in volumetric strains were observed for samples reinforced with the 2-cm columns. For tests with 4-cm sand columns, a correlation between tendency with volume change and the penetration depth was observed, which also dictates the failure mode. Partially penetrating columns would tend to fail by punching rather than bulging and since the encasement and high confining pressure further restrict bulging, a decrease in the reduction in volumetric strain is measured compared to fully penetrating encased columns. This observation is more easily seen in high area replacement ratio due to the dilative effect of the sand column which becomes more dominant as the replacement ratio increases.

4. The use of ordinary 2-cm diameter sand columns did not result in notable increases in the deviatoric stress at failure with the maximum improvement being 7.45% for the case of fully penetrating columns with a confining pressure of 100 kPa. When the 2-cm columns were encased, the improvement at 100 kPa increased to 37.02%, while improvements of about 25% and 21% were observed for confining pressures of 150 and 200 kPa, respectively. For the average area

replacement ratio of 17.8%, improvements ranging from about 33% to 36% were observed for samples reinforced with fully penetrating ordinary columns and from about 7% to 12% for partially penetrating ordinary columns. For samples with encased columns, additional improvements in the deviatoric stress at failure were observed due to the encasement, with the improvement ranging from about 40% to 68% for specimens reinforced with fully penetrating columns and from about 5% to 19% for partially penetrating columns. For the higher area replacement ratio of 31.7%, improvements ranging from about 59% to 69% were observed for samples reinforced with fully penetrating ordinary columns and from about 22% to 24% for partially penetrating ordinary columns. For samples with encased columns, the improvement ranged from about 50% to 64% for specimens reinforced with fully penetrating columns and from about 7% to 9% for partially penetrating columns.

5. For clay specimens that were reinforced with partially penetrating 2-cm sand columns, the effective friction angle ϕ' and the apparent cohesion c’ were not significantly affected by the presence of the sand columns. For fully penetrating 2-cm columns, non-zero c’ values were observed and were associated with unchanged or slightly reduced ϕ' values compared to the control clay specimens. The non-zero c’ values reflect the improvements in deviatoric stresses at failure at the lower confining pressure of 100 kPa compared to the higher confining pressures of 150 and 200 kPa.

6. For the average and high area replacement ratios of 17.8% and 31.7% improvements in ϕ' were observed for ordinary columns, while improvements in c’ were observed for encased columns. These results of encased columns are in

line with previous research which shows that encasing sand columns with geosynthetics results in non-zero cohesive intercepts (Wu and Hong 2009), with the increases in c' being associated with no improvements in the friction angle ϕ '. The effective friction angle ϕ 'improved from 21.8° (control) to 22.5°(partially penetrating) and 24.5°(fully penetrating) for ordinary 3cm columns (17.8% area replacement ratio). For the case of 4cm ordinary columns (31.7% area replacement ratio) the effective friction angle was found to be 23.8° and 26° for partially and fully penetrating columns, respectively. The apparent cohesion *c'* increased from 0 (control) to 15 (partially penetrating) and 30 kPa (fully penetrating) for encased 3cm columns (17.8% area replacement ratio). For the case of 4cm ordinary columns (31.7% area replacement ratio) the apparent was found to be 7° and 22.5° for partially and fully penetrating encased columns, respectively.

9.2.2. Undrained Conditions

1. The presence of fully penetrating sand columns reduces significantly the bulging of the Kaolin specimen. Moreover, bulging of the reinforced Kaolin composite is reduced with increasing the column length. The bulging severity decreases with increasing confining pressure. Specimens reinforced with partially penetrating columns failed by premature bearing failure in the unreinforced lower portion of the specimen.

2. It was interesting to observe a shear plane passing through the sand column and shifting it laterally in the case of the 200kPa fully penetrating column. This shows that fully penetrating columns are more effective than

partially penetrating columns since in the latter case failure occurs in the soft clay.

3. For fully penetrating ordinary sand columns, the stiffness of the reinforced clay increased by about 1.8 times when increasing the area replacement ratio from 7.9% to 31.7%. Moreover, extending the column length has a positive effect on increasing the stiffness of the reinforced Kaolin composite.

4. Insertion of fully penetrating ordinary sand columns with different area replacement ratios reduces significantly the generation of excess pore water pressure during undrained shearing. Moreover, the effectiveness of the sand column in reducing the excess pore water pressure increases with increasing the column length and area replacement ratio.

5. For fully penetrating ordinary sand columns and for area replacement ratio of 31.7%, the increase in undrained shear strength ranged from 168.4% to 206.4%. In comparison with smaller area replacement ratios of 7.9% and 17.8%, the 31.7% area replacement ratio resulted in a jump in the improvement of undrained shear strength. For partially penetrating ordinary sand columns and for area replacement ratio of 31.7%, the increase in undrained shear strength ranged from 33.1% to 65%.

6. For Kaolin specimens that were reinforced with sand columns, the data did not show any clear indication of the effect of the confining pressure on the improvement in undrained shear strength.

7. The data collected for samples that were reinforced with sand columns supports the hypothesis of a “critical column length” which is greater than about

six column diameters, beyond which the increase in undrained shear strength due to the presence of the sand columns becomes negligible.

8. The insertion of sand columns with different area replacement ratios and different column penetration depths didn't cause an improvement in the drained friction angle (Ø') of the reinforced clay; however, for fully penetrating sand column with area replacement ratio of 31.7%, the drained cohesion (c') of the composite sand column kaolin material was increased from 0 kPa (for unreinforced specimen) to 8 kPa. However, this increase in the drained cohesion was complemented by a slight decrease in the drained friction angle from 26.3˚ (for unreinforced specimens) to 26˚.

9. Finally combining the analysis done by Maakaroun (2009) for area replacement ratios of 7.9% and 17.8% with a higher area replacement ratio of 31.7%, have led to a higher reliability in the results and the conclusions reached.

9.2.3. Drained vs Undrained Conditions

1. For the control clay, a significant difference was observed in the effective friction angle ϕ' obtained from the CD tests ($\phi' = 21.8^{o}$) and the CU tests with pore pressure measurement ($\phi' = 26.3^{o}$). The difference could be attributed to the significant difference in the mean effective confining pressures at failure and the rate of loading between the drained and undrained tests. This difference was higher than expected and lead to some complications in the analysis of results of the reinforced clay specimens.

2. Based on a thorough analysis of the variation of the deviatoric stress, pore pressure, and volumetric strain with axial strain for ordinary columns, and based

on a quantitative analysis of the percent improvement in the deviatoric stresses at failure, it is concluded that:

- The percent improvement in the deviatoric stress at failure for the undrained tests was consistently higher than the improvement observed for the drained tests. This observation could lead to the conclusion that sand columns are more efficient at increasing the load-carrying capacity of soft clays in an undrained setting than in a drained setting.
- Although the percent improvement in the deviatoric stress at failure was higher for undrained tests, the absolute values of the deviatoric stress at failure were still much higher for drained tests, signifying that the drained load response could likely represent an upper bound in the shear strength of the reinforced clay specimens analyzed in this study. This was however contrasted by the fact that at high area replacement ratio (31.7%), the maximum deviatoric stress of the undrained tests approached those of the drained tests, indicating a shift in the governing behavior from the clay to the sand column.
- This indicates that in field applications involving the use of sand columns in soft clays with small and medium area replacement ratio (less than 30%), it is expected that the drained shear strength which will govern the behavior of the reinforced clay for long-term conditions would likely be greater than the undrained shear strength which governs the stability of the reinforced clay in the short term.

3. An analysis of the effective Mohr-Coulomb failure envelops from drained and undrained tests indicated that:

- The use of 2-cm columns (partially and fully penetrating) does not generally result in any improvement in the effective failure envelops in reference to the control specimens. The effective friction angle ϕ' was consistently smaller than the control specimen, and was complemented with an increase in *c'* which was more significant for in the drained test results.
- The use of 3-cm columns (partially and fully penetrating) resulted generally in improvements in the Mohr-Coulomb failure envelops, with the improvements being the most evident with fully penetrating columns.
- The use of 4-cm columns (partially and fully penetrating) resulted in improvements in the failure envelops, except for the case of partially penetrating undrained test which had a low friction angle compared to the control specimen. This was explained to be caused by the low strength of the 200kPa confining pressure test.
- The utilization of c' and ϕ' solely as a basis for comparing the effective shear strength envelops from drained and undrained tests might not be indicative of the differences in the results, since c' and ϕ' from drained and undrained tests are not derived from the same range of effective stress.
- It is observed that differences in the failure envelops from drained and undrained tests tend to become smaller as the differences in the mean effective stresses between drained and undrained tests become smaller. This was most evident in the case of the 31.7% area replacement ratio, in

which drained and undrained tests had comparable maximum deviatoric stress value (especially in fully penetrating columns).

4. A secant Young's modulus $(E_{sec})_{1\%}$ defined at an axial strain of 1% was used as a basis for comparing the effect of drainage on the stiffness of the reinforced clay specimens. Results indicated that for specimens with a given area replacement ratio and a column penetration ratio, the undrained $(E_{sec})_{1\%}$ was generally found to be larger in magnitude than the drained $(E_{sec})_{1\%}$. In addition, the undrained $(E_{sec})_{1\%}$ exhibited consistent increases in reinforced specimens compared to control specimens. This was not the case for the small and medium area replacement ratios of 7.9 and 17.8% , in which the drained $(E_{sec})_{1\%}$ was found to decrease compared to the control specimens, especially for tests conducted at smaller confining pressures where the effects of column installation could have played a role in the reduction in $(E_{sec})_{1\%}$. The high area replacement ratio of 31.7% has proven to improve stiffness in both drained and undrained drainage condition consistently with increasing confining pressure.

9.2.4. Partially Drained Conditions

1. The modes of failure indicate that at low strain rates (3.5%/hr), the behavior of the partially drained sample will resemble the behavior of the fully drained sample which consists of bulging of the specimen, and that for high strain rates (40%/hr and 80%/hr) especially at high confining pressure, the behavior of the partially drained sample will resemble the behavior of the undrained sample, which also consists of bulging, however with a shear plane passing through the sand column and shifting it laterally.

2. For all confining pressures, the negative volumetric strains were reduced significantly when 3cm diameter sand columns (Ac/As=17.8%) were inserted in the soft clay. As expected, this reduction in contractive behavior was more significant for tests with faster shearing rates. This higher reduction in contractive behavior for the specimens sheared at a fast strain rate is complemented with higher pore pressures which did not have enough time to dissipate.

3. The deviatoric stress versus axial strain curves show that all the partially drained specimens lie between two boundaries, the higher boundary being the fully drained test and the lower boundary being the undrained test. This is consistent with the findings of Andreou et al (2008). Furthermore, as the shearing rate decreases, the partially drained curves become closer to the fully drained curve.

4. Results of partially drained samples showed that as the strain rate decreases, the reduction in excess pore pressure increases and the reduction in volumetric strains decreases. These findings are consistently recurrent for the 100, 150, and 200kPa confining pressures.

5. As the $t_{failure}$ increases, the measured deviatoric stress increases until reaching a constant value at $t_{failure}$ equal to about $50t_{50}$ for all three confining pressures 100, 150, and 200kPa. The biggest jump in improvements in the deviatoric stresses happens before $5t_{50}$. After $5t_{50,}$ the partially drained tests mobilize 80% of the available range of improvement (undrained tests being the lower bound of the range and drained tests being the upper bound of the range), while after $50t_{50}$ almost all the range is mobilized.

6. A strength improvement index was defined to represent a relative measure of the strength mobilized in the partially drained tests compared to the undrained and drained strengths. Results show that both the degree of consolidation as predicted by the model by Henkel and Gibson (1954) and the volumetric improvement ratio as computed from the volumetric strain measurements of the partially drained and drained triaxial test could be utilized to predict the strength improvement index for partially drained tests.

9.3. Recommendations

Based on the test results reported in this study, it can be concluded that reinforcement of soft normally consolidated clays with sand columns can significantly increase the stiffness and shear strength of the soft clay. The degree of improvement in the stiffness and drained shear strength can be enhanced by increasing the area replacement ratio of the column and extending the column length to full penetration. Results also show that encasing the columns with geotextile fabrics can affect their performance and can lead to an increase in stiffness for the case of fully penetrating columns.

For practical cases that involve the use of sand columns with similar properties to the sand used in this study (friction angle of about 33 degrees) to improve the mechanical properties of normally consolidated clays that have similar index and strength properties to the Kaolin tested in this study ($S_u/\sigma'_v = 0.3$), it can be recommended based on the drained and undrained tests conducted in this study and based on the drained and undrained tests reported in Maalouf(2012) and Najjar et al. (2010) that the clay be improved with sand columns having a length to diameter ratio of

at least 6 at an area replacement ratio that is greater than 30% to ensure an improvement that is greater than 150% in the undrained shear strength. This high improvement in the undrained shear strength was attributed to a shifting of behavior from the clay to the sand. The improvement in the undrained shear strength at area replacement ratios of 17.8% and 31.7% can be relied on for improving the short term strength of the clay without compromising the long term drained strength of the unreinforced clay.

The limited tests that were conducted in this study on samples that were reinforced with sand columns that were encased with geotextile fabric did not allow for design recommendations to be specified. Several parameters which include the strength of the fabric, the confining pressure, the strengths of the sand and the clay, and the geometry of the column are expected to affect the detailed design of reinforced clay system. The determination of the effect of all these parameters on the design of encased sand columns will require more research as proposed in the following section.

The limited partially drained tests conducted in this study allowed for a basic understanding of the implications of partial drainage and shearing rate on the volumetric strains and pore pressures. The results of this series of tests proved that undrained behavior underestimates the strength of soft clay reinforced with sand columns, and that the partial drainage that occurs can significantly affect strength, volume change, and pore pressure generation. The determination of the effect of partial drainage on these parameters was hard due to the high coefficient of consolidation of the clay material used, and further research as proposed in the following section is needed.

9.4. Further Research

- The extension of the current study should entail the usage of a different clay

material that allows the specimens to be sheared at a rate that is close to real field conditions while allowing drainage of the clay through the sand columns. This model would represent the actual drainage conditions in the field while maintaining a representative stress state that is similar to that of the field.

- Since the strength of the sand column is expected to be dependent on the density and shear strength of the granular material, it will be valuable for any future researcher to use a higher angle of friction for the column material to study its effect on the mechanical properties of reinforced soft clay. The results of such tests can be combined with the test results obtained in this research study to isolate the effect of the friction angle of the sand column on the degree of improvement.
- Most of the previous research works addressed the "foundation loading" concept, where the load is directly applied to the column. Hence, an important research study can involve adjusting and modifying the available "TruePath" automated triaxial equipment to allow loading of the column directly instead of loading the entire area in "uniform loading" as was done in the current research study. In that case, the ultimate load carrying capacity of the column can be checked and compared with the available column prediction strength capacity equations (ex. Hughes and Withers 1974).
- The effect of geotextile confinement can be further studied by encasing the sand columns with geotextiles having different stiffnesses, so that the effect of the strength of the geotextile fabric can be studied and analyzed.

BIBLIOGRAPHY

Ambily, A.P., Gandhi, R. Shailesh (April 2007), "Behavior of stone columns based on experimental and FEM analysis". Journal of Geotechnical and Geoenvironmntal Engineering, ASCE, vol.133, No.4: pp 405-415 (2007)

Andreou P, Frikha W, Frank R, Canou J, Papadopoulos V, and Dupla J C (2008) Experimental study on sand and gravel columns in clay. Ground Improv 161(4):189-198

Ayadat, T. and Hanna, A. M. (2005). "Encapsulated stone columns as a soil improvement technique for collapsible soil." *Ground Improvement*, 9(4), 137-147.

Bachus R C and Barksdale R D (1984) Vertical and lateral behaviour of model stone columns. Proceedings of the International Conference on In Situ Soil and Rock Reinforcement, Paris: 99–104

Black, J., Sivakumar, V., Madhav, M. R., and McCabe, B. (2006). "An improved experimental set-up to study the performance of granular columns." *Geotechnical Testing Journal*, ASTM, 29(3), 193-199.

Black, J. V, Sivakumar, V., and McKinley, J.D. (February 2007), "Performance of clay samples reinforced with vertical granular columns". Canadian Geotechnical Journal, vol.44: pp 89-95 (2007)

Black J V, Sivakumar V and Bell A (2011) The settlement performance of stone column foundations. Geotechnique 61(11):909-922

Charles J A and Watts K A (1983) Compressibility of soft clay reinforced with granular columns. Proc. 8th Eur. Conf. Soil Mech. Found. Engng, Helsinki: 347–352

Chen J F, Han J, Oztoprak S and Yang X M (2009) Behavior of single rammed aggregate piers considering installation effects. Comp and Geotech 36:1191-1199

Elshazly H A, Elhafez D H and Mossaad M E (2008) Reliability of conventional settlement evaluation for circular foundations on stone columns. Geotech and Geol Eng J 26:323-334

Gibson, R. E. & Henkel, D. J. (1954). Influence of duration of tests at constant rate of strain on measured drained strength. Géotechnique (4), No. 1, 6-15.

Hughes, J.M.O., and Withers, N.J. (1974). “Reinforcing of soft cohesive soils with stone columns.” Ground Engineering 7(3): 42-49.

Juran, I. and Guermazi, A. (1988). “Settlement response of soft soils reinforced by compacted sand columns.” Journal of Geotechnical Engineering, ASCE, 114(8): 930-943.

Maalouf, Y. (2012). Effect of sand columns on the drained load response of soft clays. Master's thesis, American University of Beirut, Beirut, Lebanon.

Maakaroun, T., Najjar, S.S. and Sadek, S. (2009). “Effect of sand columns on the load response of soft clay.” Contemporary Topics in Ground Modification, Geotechnical Special Publication No. 187, ASCE, Orlando, Florida, 217-224.

McKelvey, D., Sivakumar, V., Bell, A., and Graham J. (July 2004), “Modeling vibrated stone columns in soft clay”. Journal of Geotechnical Engineering, vol.157, issue 3: pp 137-149 (2004)

Muir Wood, D., Hu, W., and Nash, D. F. T. (2000). “Group effects in stone column foundations: model tests.” *Geotechnique*, 50(6), 689-698.

Murugesan, S. and Rajagopal, K. (2006). “Geosynthetic-encased stone columns: numerical evaluation.” *Geotextiles and Geomembranes*, 24, 349-358.

Najjar, S.S., Sadek, S., and Maakaroun, T. (2010). “Effect of sand columns on the undrained load response of soft clays.” J. Geotechnical andGeoenvironmentalEngrg.in press (September 2010).

NarasimhaRao, S., Prasad, Y. V. S. N, and HanumantaRao, V. (1992). “Use of stone columns in soft marine clays.” *Proceedings of the 45thCanadian Geotechnical Conference*, Toronto, Canada, 9/1-9/7.

Sivakumar, V., McKelvey, D., Graham, J., and Hughus, D. (April 2004), “Triaxial tests on model sand columns in clay”. Canadian Geotechnical Journal, vol.41: pp 299-312 (2004).

Sivakumar V, Jeludine D K N M, Bell A, Glyn D T and Mackinnon P (2011), “The pressure distribution along stone columns in soft clay under consolidation and foundation loading”. Geotechnique 61(7):613-620